

Hayle Harbour Development

Hydraulic Studies Phase 2



Report EX 5569
Release 3.0
August 2007

Document Information

Project	Hayle Harbour Development
Report title	Hydraulic Studies Phase 2
Client	ING Real Estate Developments Ltd
Client Representative	Mr A Travers (Buro Happold)
Project No.	DDR3839
Report No.	EX 5569
Project Manager	Mr T J Chesher
Project Director	Mr T N Burt

Document History

Date	Release	Prepared	Approved	Authorised	Notes
05/07/07	1.0	wjf	tjc	tnb	Final report
27/07/07	2.0	wjf	tjc	tnb	Edits following first review
22/08/07	3.0	wjf	tjc	tnb	Mods to dispersion chapter

Prepared

Approved

Authorised

© HR Wallingford Limited

HR Wallingford accepts no liability for the use by third parties of results or methods presented in this report. The Company also stresses that various sections of this report rely on data supplied by or drawn from third party sources. HR Wallingford accepts no liability for loss or damage suffered by the client or third parties as a result of errors or inaccuracies in such third party data.

Summary

Hayle Harbour Development

Hydraulic Studies Phase 2

Report EX 5569

August 2007

ING Real Estate Developments, a real estate company wishes to develop the harbour area in Hayle, Cornwall, UK. Under the proposed scheme the main North Quay area will be developed to include a marina and adjacent to this, an improved fishing harbour with solid main breakwater to provide shelter from waves. The scheme will involve dredging a large part of Cockle Bank in the middle of the harbour area, and a small area adjacent to South Quay in order to re-establish this quayside. The two historical control structures on the Carnsew Pool are planned to be re-instated, so that sluicing through these gates, as well as the single gate on Copperhouse Pool will be possible. A gate on Penpol Creek is also proposed which will be used to impound water levels at mid-tide level in this Creek on occasions.

It was agreed that the work to consider the hydraulic aspects of the project would be undertaken in phases. In Phase 1, which was completed in March 2005, a review of the available data and previous study reports was undertaken and the potential issues regarding sediment and water quality arising from the scheme were considered.

The Phase 2 studies, described in this report, were aimed at applying numerical hydrodynamic and sediment transport models to assess the performance and impact of the scheme on the existing environment.

The Phase 2 studies were aimed at providing the following information:

- A detailed assessment of the present conditions at the site, in respect of hydrodynamic, sedimentological and water and sediment quality
- A quantitative assessment of the impact of the development under normal operating conditions
- A quantitative assessment of the impacts of the development during the construction phase.

Calibrated flow and sand transport models were established for this project, using site-specific measurements. Specific attention was required to reproduce the water exchange between the main estuary and the two former sluicing ponds (Carnsew and Copperhouse). Thereafter, spring and neap tide simulations were performed to establish a recent baseline regime against which the effects of the proposed development could be assessed.

The baseline scenarios confirmed that the sediment transport processes within the harbour are dominated by tidal effects. Waves and tides are responsible for the general morphology in the south of St Ives Bay. Whereas the tidal processes are quasi-steady and deterministic, wave energy will vary from season to season and year to year: as a consequence the morphology will also vary and this is consistent with the observed evidence for relatively large scale beach changes at the harbour entrance.

Historically, sluicing was carried out to sweep the harbour clear of sediment. Since sluicing stopped the harbour has accreted, suggesting net import of sediment. Even with the likely reduced storage volume of Copperhouse Pool (due to accretion) the simulations confirmed that sluicing would be effective in flushing sediment seawards.

Historical evidence indicates that Copperhouse Pool has accreted substantially over the past decades. Conversely, Carnsew Pool has not experienced the same degree of accretion: the north-eastern end of Carnsew still showing a deepened area which was dredged to create a cooling water pool for the power station which ceased operation years previously. This information suggests that Copperhouse pool has accreted due to sediment import from the Angarrack stream (there being no stream discharging into Carnsew Pool). That the accreted areas in Copperhouse Pool include areas of vegetation suggests finer, cohesive sediment which is also more likely to be derived from the Angarrack Stream rather than from marine sources.

Simulations including the proposed development were based on an initial design comprising:

- Removal of most of Cockle Bank (leaving the most easterly end where the historic turning post is located) to create a dredged area at the site of the proposed marina with new solid breakwater immediately seawards
- Reinstatement of the quay immediately outside the presently derelict sluice on South Quay.

For the final layout a half-tide weir on Penpol Creek was also included, in order to impound this area at approximately mean water level.

Flow simulations were performed for spring and neap tide conditions, and including the effects of sluicing. These tests indicated that the marina may experience some infill of marine-derived sand, and subsequent layouts involved the design of structured and a sand trap in order to minimise the amount of infill in the marina. Ultimately, a solution was obtained comprising a small sand trap immediately seaward of the marina. The amount of sedimentation in this sand trap and also in the marina will depend on whether or not impounding and sluicing is reinstated. Without sluicing the amount of infill is estimated to be of the order of 10-20,000m³/year. Regular sluicing from both Pools would tend to drive sediment back out of the estuary as occurred in the past, and in this case the degree of sedimentation in the sand trap would reduce.

Impounding and sluicing will alter the tidal regimes of the Pools, and water level information was extracted from the flow model and passed to Buro Happold for input into an analysis of the impact on the exposure/inundation of inter-tidal areas.

Under normal operating conditions (ie without sluicing), the modelling also indicated that the scheme would tend to have little overall effect on the sand flux at the entrance to the Harbour. At the entrance to The Lelant there is a small reduction in the flood flux, whilst the ebb flux is largely unchanged, giving rise to an overall small reduction in import into The Lelant. Sluicing would tend to drive sediment out of the estuary so that the import of sand into the Lelant (and Harbour) would tend to be further reduced.

Construction impacts were assessed by considering the dispersion of fine material released from the removal of Cockle Bank and associated dredging of the proposed marina area. The quantities of fine material released into the water column are likely to be relatively small (in comparison to the volume of fine sediment naturally entrained into the water column by the tide and wave action), and will depend on the type of dredging plant used. Dispersion pathways were investigated, and these indicated that there is the potential for the sediment released to be dispersed over a relatively wide area extending from the Pools to outside the estuary, with a

proportion of the material possibly settling out into the Pools and also into the Lelant area. The amount of material being dispersed into these areas could be reduced by specialist plant as well as by restricting the dredging to specific periods within the tidal cycle.

Water quality in the area focused on the potential effect of impounding water in Penpol Creek with a half-tide weir. Under present conditions, Penpol is readily flushed by the tide, and there are no known problems with water quality. The flow modelling results indicate that with the half-tide weir, the Penpol area will be very poorly flushed during neap tides, but will flush almost completely during two or three spring tides. This suggests that Penpol will effectively behave as a closed system during the neap part of the tidal cycle, when the tidal range is small, and then flush completely as springs are approached. The residence time between flushings will be approximately one week. This period is probably too short for any significant algal blooming to occur in the impounded Creek, even allowing for the possibility that small amounts of nutrients will be supplied by Penpol Creek. It is therefore considered that the water quality is likely to be acceptable in the Penpol area.

Contents

<i>Title page</i>	<i>i</i>
<i>Document Information</i>	<i>ii</i>
<i>Summary</i>	<i>iii</i>
<i>Contents</i>	<i>vii</i>
1. Introduction	1
1.1 Proposed developments in Hayle Harbour.....	1
1.2 Scope of HR Wallingford study.....	1
1.3 Structure of this report	1
2. Data Summary	2
2.1 Bathymetry.....	2
2.2 Tidal levels.....	2
2.3 Tidal flows	2
2.4 Freshwater inputs	3
2.5 Waves.....	3
2.6 Bed sediments	3
2.7 Sand flux measurements	4
3. Hydrodynamic modelling studies	4
3.1 Modelling approach	4
3.2 Flow model setup and calibration	4
3.2.1 Model Setup.....	4
3.2.2 Sluice gates and culverts	5
3.2.3 Model calibration.....	6
3.2.4 Model validation.....	6
3.3 Baseline simulations	7
3.3.1 Flow modelling.....	7
3.3.2 Sediment transport modelling.....	8
3.3.3 Wave-induced sediment transport	9
3.3.4 The effects of sluicing on the sediment transport.....	9
3.3.5 Summary of sediment transport regime.....	10
3.4 Simulations including the scheme.....	10
3.4.1 Scheme Layout 1	10
3.4.2 Scheme Layout 2	12
3.4.3 Scheme Layout 3	12
3.5 Hydrodynamic modelling conclusions.....	14
4. Dispersion of sediment arising from dredging during the construction phase	14
5. Desk assessment of water quality issues in Penpol Creek.....	17
5.1 Phase 1 assessment	17
5.2 Phase 2 assessment	18
6. Power generation on Penpol	19
7. Summary and conclusions	20
8. References and Bibliography.....	22

Contents continued

Figures

Figure 1.1	Location map
Figure 1.2	Proposed outline development at Hayle
Figure 2.1	Bathymetric survey transect positions (1983)
Figure 2.2	Locations of tidal level metering stations (1989 and 2005) and current meter stations (1989)
Figure 2.3	Locations of sediment samples (1983)
Figure 3.1	Model bathymetry (1983 data)
Figure 3.2	Model mesh
Figure 3.3	Comparison of modelled and observed water level at Location A 10-13 January 1989
Figure 3.4	Comparison of modelled and observed water level at Locations A,B,C 10 January 1989
Figure 3.5	Comparison of modelled and observed water level at Locations D,E,F 10 January 1989
Figure 3.6	Comparison of modelled and observed tidal currents at Locations 1,2,3 10-12 January 1989
Figure 3.7	Model baseline bathymetry (2005 data)
Figure 3.8	Comparison of modelled and observed water level at Locations A' and D' 6-8 July 2005
Figure 3.9	Comparison of modelled and observed water level at Locations E' and F' 6-8 July 2005
Figure 3.10	Highlighting variability in modelled tidal currents for identical tide conditions (10 Jan 1989) using 1983 and 2005 bathymetry
Figure 3.11	Baseline conditions spring tide flood currents (HW+9.5 Hours), Copperhouse sluice open (summer condition), single sluice operation on Carnsew Pool
Figure 3.12	Baseline conditions spring tide ebb currents (HW+4.5 Hours), Copperhouse sluice open (summer condition), single sluice operation on Carnsew Pool
Figure 3.13	Baseline conditions neap tide flood currents (HW+9.0 Hours), Copperhouse sluice open (summer condition), single sluice operation on Carnsew Pool
Figure 3.14	Baseline conditions neap tide ebb currents (HW+4.5 Hours), Copperhouse sluice open (summer condition), single sluice operation on Carnsew Pool
Figure 3.15	Baseline conditions spring tide flood currents (HW+9.5 Hours), Copperhouse sluice open (summer condition), double sluice operation on Carnsew Pool
Figure 3.16	Baseline conditions spring tide ebb currents (HW+4.5 Hours), Copperhouse sluice open (summer condition), double sluice operation on Carnsew Pool
Figure 3.17	Baseline conditions neap tide flood currents (HW+9.0 Hours), Copperhouse sluice open (summer condition), double sluice operation on Carnsew Pool
Figure 3.18	Baseline conditions neap tide ebb currents (HW+4.5 Hours), Copperhouse sluice open (summer condition), double sluice operation on Carnsew Pool
Figure 3.19	Baseline conditions spring tide peak ebb currents with impounding in Carnsew and Copperhouse Pools to HW + 3 hours, single sluice operation on Carnsew Pool
Figure 3.20	Baseline conditions spring tide peak ebb currents with impounding in Carnsew and Copperhouse Pools to HW + 3 hours, double sluice operation on Carnsew Pool
Figure 3.21	Comparison of modelled spring tide water levels
Figure 3.22	Comparison of modelled neap tide water levels
Figure 3.23	Sand transport algorithm
Figure 3.24	Baseline conditions spring tide net sand flux patterns
Figure 3.25	Baseline conditions neap tide net sand flux patterns

- Figure 3.26 Baseline conditions spring tide flood currents (HW+9.5 Hours), generated by 1m waves
- Figure 3.27 Baseline conditions spring tide ebb currents (HW+4.5 Hours), generated by 1m waves
- Figure 3.28 Baseline conditions spring tide flood currents (HW+9.5 Hours), generated by 2m waves
- Figure 3.29 Baseline conditions spring tide ebb currents (HW+4.5 Hours), generated by 2m waves
- Figure 3.30 Baseline conditions spring tide with 1m waves, net sand flux patterns
- Figure 3.31 Baseline conditions spring tide with 2m waves, net sand flux patterns
- Figure 3.32 Baseline conditions spring tide net sand flux patterns, impounding in Carnsew and Copperhouse Pools to HW + 3 hours, double sluice operation on Carnsew Pool
- Figure 3.33 Model bathymetry, Scheme 1
- Figure 3.34 Scheme 1 conditions spring tide peak flood currents (HW+9.5 Hours), Copperhouse sluice open (summer condition), single sluice operation on Carnsew Pool
- Figure 3.35 Scheme 1 conditions spring tide ebb currents (HW+4.5 Hours), Copperhouse sluice open (summer condition), single sluice operation on Carnsew Pool
- Figure 3.36 Scheme 1 conditions spring tide peak flood currents (HW+9.5 Hours), Copperhouse sluice open (summer condition), double sluice operation on Carnsew Pool
- Figure 3.37 Scheme 1 conditions spring tide ebb currents (HW+4.5 Hours), Copperhouse sluice open (summer condition), double sluice operation on Carnsew Pool
- Figure 3.38 Scheme 1 conditions spring tide peak flood currents with impounding in Carnsew and Copperhouse Pools to HW + 3 hours, single sluice operation on Carnsew Pool
- Figure 3.39 Scheme 1 conditions spring tide peak ebb currents with impounding in Carnsew and Copperhouse Pools to HW + 3 hours, single sluice operation on Carnsew Pool
- Figure 3.40 Scheme 1 conditions spring tide peak flood currents with impounding in Carnsew and Copperhouse Pools to HW + 3 hours, double sluice operation on Carnsew Pool
- Figure 3.41 Scheme 1 conditions spring tide peak ebb currents with impounding in Carnsew and Copperhouse Pools to HW + 3 hours, double sluice operation on Carnsew Pool
- Figure 3.42 Scheme 1 conditions net sand flux patterns, Copperhouse sluice open (summer condition), single sluice operation on Carnsew Pool
- Figure 3.43 Scheme 1 conditions net sand flux patterns, Copperhouse sluice open (summer condition), double sluice operation on Carnsew Pool
- Figure 3.44 Scheme 1 conditions net sand flux patterns with impounding in Carnsew and Copperhouse Pools to HW + 3 hours, single sluice operation on Carnsew Pool
- Figure 3.45 Scheme 1 conditions net sand flux patterns with impounding in Carnsew and Copperhouse Pools to HW + 3 hours, double sluice operation on Carnsew Pool
- Figure 3.46 Scheme 1 conditions patterns of erosion and deposition, Copperhouse sluice open (summer condition), single sluice operation on Carnsew Pool
- Figure 3.47 Scheme 1 conditions patterns of erosion and deposition, Copperhouse sluice open (summer condition), double sluice operation on Carnsew Pool
- Figure 3.48 Scheme 1 conditions patterns of erosion and deposition with impounding in Carnsew and Copperhouse Pools to HW + 3 hours, single sluice operation on Carnsew Pool

- Figure 3.49 Scheme 1 conditions patterns of erosion and deposition with impounding in Carnsew and Copperhouse Pools to HW + 3 hours, double sluice operation on Carnsew Pool
- Figure 3.50 Scheme 1 conditions patterns of erosion and deposition in marina area, Copperhouse sluice open (summer condition), double sluice operation on Carnsew Pool
- Figure 3.51 Scheme 1 conditions patterns of erosion and deposition in marina area with impounding in Carnsew and Copperhouse Pools to HW + 3 hours, double sluice operation on Carnsew Pool
- Figure 3.52 Comparison between baseline and Scheme 1 of sand flux at 3 locations in harbour
- Figure 3.53 Model bathymetry, Scheme 2
- Figure 3.54 Scheme 2 conditions spring tide peak flood currents (HW+9.5 Hours), Copperhouse sluice open (summer condition), single sluice operation on Carnsew Pool
- Figure 3.55 Scheme 2 conditions spring tide ebb currents (HW+4.5 Hours), Copperhouse sluice open (summer condition), single sluice operation on Carnsew Pool
- Figure 3.56 Scheme 2 conditions spring tide peak flood currents (HW+9.5 Hours), Copperhouse sluice open (summer condition), double sluice operation on Carnsew Pool
- Figure 3.57 Scheme 2 conditions spring tide ebb currents (HW+4.5 Hours), Copperhouse sluice open (summer condition), double sluice operation on Carnsew Pool
- Figure 3.58 Scheme 2 conditions spring tide peak flood currents with impounding in Carnsew and Copperhouse Pools to HW + 3 hours, single sluice operation on Carnsew Pool
- Figure 3.59 Scheme 2 conditions spring tide peak ebb currents with impounding in Carnsew and Copperhouse Pools to HW + 3 hours, single sluice operation on Carnsew Pool
- Figure 3.60 Scheme 2 conditions spring tide peak flood currents with impounding in Carnsew and Copperhouse Pools to HW + 3 hours, double sluice operation on Carnsew Pool
- Figure 3.61 Scheme 2 conditions spring tide peak ebb currents with impounding in Carnsew and Copperhouse Pools to HW + 3 hours, double sluice operation on Carnsew Pool
- Figure 3.62 Scheme 2 conditions net sand flux patterns, Copperhouse sluice open (summer condition), single sluice operation on Carnsew Pool
- Figure 3.63 Scheme 2 conditions net sand flux patterns, Copperhouse sluice open (summer condition), double sluice operation on Carnsew Pool
- Figure 3.64 Scheme 2 conditions net sand flux patterns with impounding in Carnsew and Copperhouse Pools to HW + 3 hours, single sluice operation on Carnsew Pool
- Figure 3.65 Scheme 2 conditions net sand flux patterns with impounding in Carnsew and Copperhouse Pools to HW + 3 hours, double sluice operation on Carnsew Pool
- Figure 3.66 Scheme 2 conditions patterns of erosion and deposition, Copperhouse sluice open (summer condition), single sluice operation on Carnsew Pool
- Figure 3.67 Scheme 2 conditions patterns of erosion and deposition, Copperhouse sluice open (summer condition), double sluice operation on Carnsew Pool
- Figure 3.68 Scheme 2 conditions patterns of erosion and deposition with impounding in Carnsew and Copperhouse Pools to HW + 3 hours, single sluice operation on Carnsew Pool
- Figure 3.69 Scheme 2 conditions patterns of erosion and deposition with impounding in Carnsew and Copperhouse Pools to HW + 3 hours, double sluice operation on Carnsew Pool

- Figure 3.70 Scheme 2 conditions patterns of erosion and deposition in marina area, Copperhouse sluice open (summer condition), double sluice operation on Carnsew Pool
- Figure 3.71 Scheme 2 conditions patterns of erosion and deposition in marina area with impounding in Carnsew and Copperhouse Pools to HW + 3 hours, double sluice operation on Carnsew Pool
- Figure 3.72 Model bathymetry, Scheme 2 with sand trap
- Figure 3.73 Scheme 2 with sand trap conditions spring tide peak flood currents (HW+9.5 Hours), Copperhouse sluice open (summer condition), double sluice operation on Carnsew Pool
- Figure 3.74 Scheme 2 with sand trap conditions spring tide ebb currents (HW+4.5 Hours), Copperhouse sluice open (summer condition), double sluice operation on Carnsew Pool
- Figure 3.75 Scheme 2 with sand trap conditions net sand flux patterns, Copperhouse sluice open (summer condition), double sluice operation on Carnsew Pool
- Figure 3.76 Scheme 2 with sand trap conditions patterns of erosion and deposition, Copperhouse sluice open (summer condition), double sluice operation on Carnsew Pool
- Figure 3.77 Scheme 2 with sand trap conditions patterns of erosion and deposition in marina area, Copperhouse sluice open (summer condition), double sluice operation on Carnsew Pool
- Figure 3.78 Model bathymetry, Scheme 3
- Figure 3.79 Scheme 3 conditions spring tide peak flood currents (HW+9.5 Hours), Copperhouse sluice open (summer condition), double sluice operation on Carnsew Pool
- Figure 3.80 Scheme 3 conditions spring tide ebb currents (HW+4.5 Hours), Copperhouse sluice open (summer condition), double sluice operation on Carnsew Pool
- Figure 3.81 Scheme 3 conditions spring tide peak flood currents with impounding in Carnsew and Copperhouse Pools to HW + 3 hours, double sluice operation on Carnsew Pool
- Figure 3.82 Scheme 3 conditions spring tide peak ebb currents with impounding in Carnsew and Copperhouse Pools to HW + 3 hours, double sluice operation on Carnsew Pool
- Figure 3.83 Model bathymetry, Scheme 3 with Penpol weir
- Figure 3.84 Scheme 3 with Penpol weir conditions spring tide peak flood currents (HW+9.5 Hours), Copperhouse sluice open (summer condition), double sluice operation on Carnsew Pool
- Figure 3.85 Scheme 3 with Penpol weir conditions spring tide peak ebb currents (HW+4.5 Hours), Copperhouse sluice open (summer condition), double sluice operation on Carnsew Pool
- Figure 3.86 Scheme 3 with Penpol weir conditions neap tide peak flood currents (HW+9.5 Hours), Copperhouse sluice open (summer condition), double sluice operation on Carnsew Pool
- Figure 3.87 Scheme 3 with Penpol weir conditions neap tide peak ebb currents (HW+4.5 Hours), Copperhouse sluice open (summer condition), double sluice operation on Carnsew Pool
- Figure 3.88 Scheme 3 with Penpol weir conditions spring tide peak flood currents (HW+9.5 Hours), with impounding in Carnsew and Copperhouse Pools to HW + 3 hours, double sluice operation on Carnsew Pool
- Figure 3.89 Scheme 3 with Penpol weir conditions spring tide peak ebb currents (HW+4.5 Hours), with impounding in Carnsew and Copperhouse Pools to HW + 3 hours, double sluice operation on Carnsew Pool

- Figure 3.90 Scheme 3 with Penpol weir conditions neap tide peak flood currents (HW+9.5 Hours), with impounding in Carnsew and Copperhouse Pools to HW + 3 hours, double sluice operation on Carnsew Pool
- Figure 3.91 Scheme 3 with Penpol weir conditions neap tide peak ebb currents (HW+4.5 Hours), with impounding in Carnsew and Copperhouse Pools to HW + 3 hours, double sluice operation on Carnsew Pool
- Figure 3.92 Scheme 3 with Penpol weir conditions spring tide peak flood currents (HW+9.5 Hours), with impounding in Carnsew and Copperhouse Pools to HW + 3 hours, double sluice fill, single sluice empty on Carnsew Pool
- Figure 3.93 Scheme 3 with Penpol weir conditions spring tide peak ebb currents (HW+4.5 Hours), with impounding in Carnsew and Copperhouse Pools to HW + 3 hours, double sluice fill, single sluice empty on Carnsew Pool
- Figure 3.94 Comparison of modelled spring tide water levels with and without impounding, Scheme 3
- Figure 3.95 Comparison of modelled neap tide water levels with and without impounding, Scheme 3
- Figure 3.96 Scheme 3 conditions net sand flux patterns, Copperhouse sluice open (summer condition), double sluice operation on Carnsew Pool
- Figure 3.97 Scheme 3 conditions net sand flux patterns with impounding in Carnsew and Copperhouse Pools to HW + 3 hours, double sluice operation on Carnsew Pool
- Figure 3.98 Scheme 3 with Penpol weir conditions, spring tide net sand flux patterns, Copperhouse sluice open (summer condition), double sluice operation on Carnsew Pool
- Figure 3.99 Scheme 3 with Penpol weir conditions, neap tide net sand flux patterns, Copperhouse sluice open (summer condition), double sluice operation on Carnsew Pool
- Figure 3.100 Scheme 3 with Penpol weir conditions, spring tide net sand flux patterns with impounding in Carnsew and Copperhouse Pools to HW + 3 hours, double sluice operation on Carnsew Pool
- Figure 3.101 Scheme 3 with Penpol weir conditions, neap tide net sand flux patterns with impounding in Carnsew and Copperhouse Pools to HW + 3 hours, double sluice operation on Carnsew Pool
- Figure 3.102 Scheme 3 with Penpol weir conditions, spring tide net sand flux patterns with impounding in Carnsew and Copperhouse Pools to HW + 3 hours, double sluice fill, single sluice empty on Carnsew Pool
- Figure 3.103 Scheme 3 conditions patterns of erosion and deposition, Copperhouse sluice open (summer condition), double sluice operation on Carnsew Pool
- Figure 3.104 Scheme 3 conditions patterns of erosion and deposition with impounding in Carnsew and Copperhouse Pools to HW + 3 hours, double sluice operation on Carnsew Pool
- Figure 3.105 Scheme 3 with Penpol weir conditions, spring tide patterns of erosion and deposition, Copperhouse sluice open (summer condition), double sluice operation on Carnsew Pool
- Figure 3.106 Scheme 3 with Penpol weir conditions, neap tide patterns of erosion and deposition, Copperhouse sluice open (summer condition), double sluice operation on Carnsew Pool
- Figure 3.107 Scheme 3 with Penpol weir conditions, spring tide patterns of erosion and deposition with impounding in Carnsew and Copperhouse Pools to HW +3 hours, double sluice operation on Carnsew Pool
- Figure 3.108 Scheme 3 with Penpol weir conditions, neap tide patterns of erosion and deposition patterns with impounding in Carnsew and Copperhouse Pools to HW +3 hours, double sluice operation on Carnsew Pool

- Figure 3.109 Scheme 3 with Penpol weir conditions, spring tide patterns of erosion and deposition with impounding in Carnsew and Copperhouse Pools to HW +3 hours, double sluice fill, single sluice empty on Carnsew Pool
- Figure 3.110 Comparison between baseline and Scheme 3 of sand flux at 3 locations in harbour
- Figure 4.1a Sediment plume concentrations during the dredging operations, HW – HW+10hrs
- Figure 4.1b Sediment plume concentrations during the dredging operations, HW+12hrs – HW+22hrs
- Figure 4.1c Sediment plume concentrations during the dredging operations, HW+24hrs – HW+34hrs
- Figure 4.2a Spring tide background suspended sediment concentrations, HW – HW+6hrs
- Figure 4.2b Spring tide background suspended sediment concentrations, HW+8hrs – HW+12hrs
- Figure 4.3 Peak suspended sediment concentrations occurring at any stage during the three-tide dispersion simulation
- Figure 4.4 Deposition patterns after three-tide simulation

Appendix

- Appendix 1 Numerical model details

1. Introduction

1.1 PROPOSED DEVELOPMENTS IN HAYLE HARBOUR

ING Real Estate Developments, a real estate company, wishes to develop the harbour area in Hayle, Cornwall, UK (Figure 1.1). Under the proposed scheme the main North Quay area will be developed to include a marina and adjacent to this, an improved fishing harbour with solid main breakwater to provide shelter from waves (see Figure 1.2, for a conceptual layout of the scheme, final details to be confirmed). The scheme will involve dredging a large part of Cockle Bank in the middle of the harbour area, and a small area adjacent to South Quay in order to re-establish this quayside. The two historical control structures on the Carnsew Pool are planned to be re-instated, so that sluicing through these gates, as well as the single gate on Copperhouse Pool will be possible. A gate on Penpol Creek is also proposed which will be used to impound water levels at mid-tide level in this Creek on occasions.

1.2 SCOPE OF HR WALLINGFORD STUDY

It was agreed that the work to consider the hydraulic aspects of the project would be undertaken in phases. In Phase 1, which was completed in March 2005, a review of the available data and previous study reports was undertaken and the potential issues regarding sediment and water quality arising from the scheme were considered.

The Phase 2 studies, described in this report, were aimed at applying numerical hydrodynamic and sediment transport models to assess the performance and impact of the scheme on the existing environment.

The Phase 2 studies were aimed at providing the following information:

- A detailed assessment of the present conditions at the site, in respect of hydrodynamic, sedimentological and water and sediment quality
- A quantitative assessment of the impact of the development under normal operating conditions
- A quantitative assessment of the impacts of the development during the construction phase.

1.3 STRUCTURE OF THIS REPORT

The remainder of this report is structured as follows. Chapter 2 summarises the data used in this study. In Chapter 3 the hydrodynamic studies are described, including the flow and sedimentation modelling. Chapter 4 describes the sediment dispersion modelling undertaken, and Chapter 5 summarises the water quality assessment for Penpol Quay. Chapter 6 gives a brief appraisal of the potential impacts of power generation on Penpol Quay. Conclusions drawn from this project are included in Chapter 7.

2. *Data Summary*

Relevant field data available for these studies was described in the Phase 1 study report (HR Wallingford, 2005) but is summarised again in this section for completeness. Additional data collected since the Phase 1 study is also included.

2.1 BATHYMETRY

Sea Sediments undertook comprehensive survey measurement in the Hayle area in April and May 1983 (Sea Sediments 1983). This included bathymetric measurements along approximately fifty transects within the estuary and the beach area. In addition a series of transects extending 1.5 to 2.5km seawards from the mouth of the estuary were surveyed on 16 June 1983. The locations of these transects are shown in Figure 2.1 and the data is available as a chart attachment with the Sea Sediments reference.

Some additional sounding from a local survey of the Cockle Bank area made by Sir Alexander Gibb and Partners in 1989 were used for the HR Wallingford 1989 study.

In support of their plans for Hayle ING Real Estate Developments commissioned two LiDAR surveys in July and November 2004. Data from a previous LiDAR survey in March 2003 was also made available to Buro Happold. The LiDAR surveys included full coverage of the area that was modelled for the Phase 2 study but the data is limited to the areas that were dry at the time of the surveys. In order to fill gaps in the data within the confines of the harbour additional measurements were undertaken in the form of cross-sections between Fisherman's Quay and the North Quay and the data was supplied to HR Wallingford by Buro Happold.

2.2 TIDAL LEVELS

According to the UK Hydrographic Office Tide Tables the mean spring tidal range at the nearby port of St Ives is 5.8m with a neap tide range of 2.5m.

The height of	MHWS is	+6.6m CD	+3.2m OD
	MHWN	+4.9m CD	+1.5m OD
	MLWN	+2.4m CD	-1.0m OD
	MLWS	+0.8m CD	-2.6m OD

Local Chart Datum at St Ives is 3.4m below OD.

As part of the 1989 HR Wallingford survey water level observations were made at six sites within Hayle harbour (Figure 2.2). The sites were manned for a 12.5 hour period on 10 January and levels were recorded every 10 minutes. At position A (Chapel Anjou) similar observations were also made on 11 and 12 January. This data is presented in graphical form in HR Wallingford 1989.

For the present study, additional water level measurements were made under spring tide conditions over the period 6-8 July 2005.

2.3 TIDAL FLOWS

Sea Surveys measured current velocities at four sites near the estuary mouth during the period 10 May to 27 June 1983 (Figure 2.3). Velocities were recorded at 4 second intervals for 6 minutes out of every 10. The data is presented in graphical form in the

Sea Surveys report. However, as discussed in the Phase 1 report (HR Wallingford, 2005) since water levels were not measured at the same time, this data set is of less value for model calibration.

In January 1989 HR Wallingford undertook a field survey to provide calibration data for a physical model study and to establish a relationship between tidal current strength and transport rates for Hayle sands.

Current velocity was observed at half hourly intervals over a 12.5 hour period at three sites (Figure 2.2). Near bed measurements were made with a bed frame and higher levels using a roving current meter. Depth-averaged current velocities were derived and are presented in graphical form in HR Wallingford 1989 (and reproduced in the calibration stage of this report).

2.4 FRESHWATER INPUTS

The main Hayle River flows through the Lelant on the west side of the estuary, separated from the Harbour by the Fisherman's Quay. Two further small streams flow into the Hayle Harbour system. The Angarrack flows into Copperhouse Pool and has a two year return discharge of $8\text{m}^3/\text{s}$ and 100 year discharge of $23\text{m}^3/\text{s}$, and the Mellanear Stream flows into the Penpol Quay area with equivalent figures of $2\text{m}^3/\text{s}$ and $6.5\text{m}^3/\text{s}$.

2.5 WAVES

Wave conditions within the harbour are limited to those which are locally generated by the wind blowing across the relatively limited fetch, and any swell which is able to penetrate in from St Ives Bay. In comparison to the tidal energy, wave energy in the harbour area is relatively low. Clearly, on the open coast outside the harbour waves play a significant role in transporting coastal sediment, but since all proposed developments are within the harbour area the data gathering on wave conditions was minimal.

Although some measurements were made by HR Wallingford and the Ministry of Defence off Perranporth from the mid 1970s to the early 1980s it is considered that the most reliable offshore data for the proposed study could be obtained from the UK Meteorological Office if required for design purposes. For the purposes of the Phase 2 hydraulic studies described herein, however, wave climate information was not necessary.

2.6 BED SEDIMENTS

Intertidal sediment samples were collected at 175 points during the 1983 Sea Sediments survey. The locations of these samples are shown in Figure 2.3. An analysis of the samples led to the conclusion that the estuary and beaches at Hayle are predominantly composed of sand. Muddy deposits were found around the periphery and the head of Lelant Water, at the western end of Carnsew and in the Penpol Dock and Copperhouse Pool. There was also a small amount of mud in the offshore sediments which was considered to represent the "fine tail" of the fine sand population found in the area. Overall it was considered that the sediment dynamics within the estuary are dominated by sand transport with muds and gravels playing only a minor role in determining the form of the estuary.

The Phase 1 study concluded that the bed sediment data available from the 1983 study was sufficient for the proposed assessment and no additional sampling was necessary. As expected, this extensive data set shows variability in the sediment class size distribution over the area surveyed, with a typical median grain diameter in the harbour area of 0.35mm.

2.7 SAND FLUX MEASUREMENTS

The 1989 HR Wallingford field exercise included measurements of sand transport and suspended solids concentrations at the same locations as the flow measurements (Figure 2.2). These measurements were made at half-hourly intervals over a full tidal period (12.5 hours) at three sites using bed frames and roving units to cover the full water depth.

The subsequent analysis of the sand transport rate against tidal current strength indicated that there was a clear correlation between depth mean velocity and transport. This relationship was subsequently applied in the Phase 2 sediment transport modelling studies.

3. *Hydrodynamic modelling studies*

3.1 MODELLING APPROACH

The hydrodynamic processes operating within the Hayle Harbour system are dominated by tidal action. Freshwater flow effects, and wind and wave effects play a relatively minor role. However, the processes of wave action in driving longshore sediment transport in St Ives Bay are important and are covered in Section 3.3.

To establish the detailed effects on the hydrodynamic characteristics of the proposed development in Hayle Harbour, and to allow for the effects of variations to be assessed it was proposed that the Phase 2 study utilises a numerical flow model to replicate the tidal conditions over an area covering St Ives Bay and Hayle Harbour.

Tidal currents were simulated using the finite element flow model, TELEMAC, which uses a completely unstructured mesh and has the advantage of a variable grid which allows very fine resolution in specified areas. Output from TELEMAC was then used as input to the HR Wallingford sand transport model SANDFLOW, and sediment dispersion model, SEDPLUME-RW. Full details of these models is provided in Appendix 1.

The modelling approach comprised establishing the flow models for the historical scenario for calibration and thereafter applying the flow and sediment transport models using the present day conditions. This latter set of results was used as the baseline against which the effects and impacts of the proposed development could be compared.

3.2 FLOW MODEL SETUP AND CALIBRATION

3.2.1 *Model Setup*

The purpose of calibration of the flow model was to fix the free parameters associated with the bed friction and the eddy viscosity (diffusivity for momentum), and to confirm that the model is capable of reproducing the main tidal processes in terms of the tidal water levels and currents.

At this site, the most comprehensive bathymetric data set was that measured in 1983 as part of the Sea Sediments study, supplemented with the additional cross-sections measured in 2005 as described in Section 2.1, and data from Admiralty Chart 1168 for offshore areas. Whilst not synoptic, the field data collected in 1989 in the form of tidal currents and water levels was considered sufficient to use to calibrate and validate the flow model. Given the timescale between these two data sets, the natural variability in the seabed levels (especially at the entrance to the harbour) and the inherent measurement errors it was not anticipated that the model should reproduce the tidal conditions exactly, but that this exercise should provide confidence that the model was capable of adequately reproducing the tidal exchange. Comparison between measured and modelled water levels is relatively straightforward although it should be borne in mind that low tide levels may be influenced by the specific seabed levels; hence the model may not reproduce the tide curves in the event of drying at the measurements station. When comparing measured and modelled tidal currents there may also be discrepancies induced by any differences in seabed level.

3.2.2 *Sluice gates and culverts*

A key consideration in the calibration procedure for this study involved the simulation of the exchange of water in the two storage basins, Copperhouse and Carnsew Pool. Throttling of the flux of water into these pools means that the tidal levels do not reach the level attained outside in the main harbour. These flows into and out of Copperhouse Pool and Carnsew Reservoir were modelled using TELEMAR's culvert formulation. This is designed to simulate the transfer of water through a pipe, with a flow rate which depends on the water elevation at either end and a number of parameters which define properties of the pipe, such as cross-sectional area and associated head loss terms. The water level measurements made in each of these pools in 1989 were used to calibrate the culvert parameters.

Several different configurations were used. At Carnsew Reservoir there are two entrances; a set of existing culverts towards the northeast corner and derelict, infilled sluice gates at the southeast. At present the sluice gates are not in operation, but some simulations were undertaken with these gates reinstated. At Copperhouse, the sluice gates have two modes: summer operation, where they are opened fully, and winter operation, where they are lowered to leave a gap of 0.6m depth. Both of these modes were simulated, by varying the cross-sectional area of the modelled culvert, although the effect on the levels and currents in the study area were not particularly sensitive to this factor.

Figure 3.1 shows the model domain and bathymetry whereby the entire south St Ives Bay was covered, resulting in a single open boundary extending from St Ives to Godrevy Point. Levels are referred to Ordnance Datum Newlyn (ODN) and positions to British National Grid. The open boundary was specified with tidal water levels which were derived from tidal harmonics from Astronomical Tide Tables for St Ives. This figure highlights the relatively shallow depths in the Hayle Harbour entrance and the narrow entrance to this natural harbour.

Figure 3.2 shows the size of the model mesh used in the simulations, which ranged from 500m at the open boundary to less than 5m in the area around the entrances to the two pools.

3.2.3 Model calibration

Tidal levels at the open boundary were derived using the Admiralty TIDECALC software to reproduce the tide curve for the period of field measurements in 1989 from 10-13 January. The field data consists of tidal levels recorded at 6 locations (A-F) during daylight hours on 10th January 1989, and a longer record (spanning 3 days, from 10th to 12th January) at Chapel Anjou Point, labelled location A. Current speed readings were obtained at 3 locations (1-3) over the same three days (i.e. one location each day). Locations of these positions are shown in Figure 2.2.

Figure 3.3 shows the comparison of modelled and measured tide at Location A (Chapel Anjou Point) at the Harbour entrance. This figure shows excellent reproduction of the high water levels and the shape of the tide curves in general. Note that due to slight differences between the true bed level and that in the model, low water levels may not be exactly reproduced.

Figures 3.4 and 3.5 show measured and modelled tidal levels for locations within the Harbour, Figure 3.4 showing levels in the Hayle River (Lelant Water) where the high water values are comparable with those at Chapel Anjou Point. Figure 3.5 shows the levels measured in Copperhouse and Carnsew pool and at the entrance to Penpol Creek, highlighting the reduced high water levels in the two pools. These figures show good representation of the tidal levels by the TELEMAC model, and in particular good calibration of the culvert routines to represent the discharge into and out of the two pools.

Figure 3.6 shows comparison of the modelled and measured tidal currents, with very good agreement between these two data sets, giving further evidence of the model's capability in simulating the tidal processes. Whereas the agreement between model and observations is not as close as in the water level comparison these figures indicate that the tidal exchange is reproduced and that the tidal currents are typically represented. It is postulated above that these discrepancies may be in part related to the possible differences in bathymetry from 1989 (the time of the current measurements) and 1983 (the time of the bathymetric survey). The validation procedure described in Section 3.2.4 below allowed this sensitivity to be examined and confirmed: by incorporating an alternative bathymetry (in this case a more recent bathymetry measured in 2005) it is shown that the tidal currents can be significantly altered.

3.2.4 Model validation

Having calibrated (and fixed) the various model parameters validation was carried out by simulating another period of measurement in 6-8 July 2005 when water levels were measured at four locations within the Harbour. At the same time, bathymetric transects were collected in order to supplement the LiDAR data collected during this period. The TELEMAC flow model was modified to incorporate the LiDAR and transect data, as shown in Figure 3.7, and tidal conditions during the period of field measurements were calculated.

The water level time histories, shown in Figures 3.8 to 3.9, again show very good agreement between model and measurements over most of the tidal cycle (excepting perhaps the drying out levels). Peak tidal levels are well represented.

Having incorporated an alternative recent bathymetry into the model domain, it was apposite to investigate the sensitivity to the predicted tidal currents as a consequence of this change in bathymetry alone. Accordingly, the calibration period tides (January

1989) were re-simulated using the 2005 bathymetry and the results were processed to give time histories at the same calibration stations. Figure 3.10 clearly highlights the sensitivity of the tidal currents to the seabed levels, confirming the earlier possible explanation for the apparent discrepancies in the calibration against the measured currents.

Following the calibration and validation exercise it was concluded that the tidal flow model was capable of accurately simulating the tidal processes in the study area. In particular, tidal exchange of the entire Harbour basin is well reproduced and the previously collected field data allowed the potentially complex exchange in Copperhouse and Carnsew Pools to be accurately represented. The model therefore constituted a reliable tool for assessing the effects of the proposed schemes on the tidal conditions.

3.3 BASELINE SIMULATIONS

3.3.1 *Flow modelling*

Having calibrated the flow model, baseline simulations of the existing conditions were simulated to provide a series of fields for comparison against those including the scheme. For comparative purposes simulations were also carried out in which the second sluice on Carnsew Pool was re-instated (without any other developments) and in addition, tests were carried out to show the effects of impounding in the Pools under the present scenario.

The baseline model bathymetry used in these tests was the same as that generated for the validation procedure, comprising the recently collected LiDAR data together with new bathymetric transects in the inner harbour, supplemented with information from Admiralty Chart 1168 for the St Ives Bay area.

Tidal currents were simulated for both spring and neap tide conditions. Spring tides were based on the 10th January 1989 tides as used in the calibration tests since this range was comparable to a mean spring tide. Neap tides were based on 30th January, being representative of mean neap conditions. In each case, the preceding tide was included, to allow the model to ‘spin up’ from static conditions.

Flow vectors at the time of peak current in the main harbour are shown in Figures 3.11 and 3.12 (spring) and Figures 3.13 and 3.14 (neap). These show strong spring tide currents between the Fisherman’s Quay and North Quay which accord with anecdotal information on the tidal streams in this area provided by the Harbour Master (pers. comm.). As expected, neap tide currents are significantly lower than under springs.

Further baseline simulations were performed for spring and neap tides with the sluice gates on Carnsew Pool reinstated (so that Carnsew fills and empties through two sets of openings). The corresponding currents at peak flood and ebb tide are shown in Figures 3.15, 3.16, 3.17 and 3.18.

For the baseline scenario (without the marina development included) impounding simulations were carried out in which the tidal level was held at high water for a period before releasing. Initial runs were carried out with release occurring at the time close to low water in the main Harbour (order HW+6hours). Following a site visit and meeting with local authorities, however, it was established that the previous sluicing operations took place at approximately HW+3hours and accordingly impounding simulations were carried out for this scenario. Figure 3.19 shows the peak ebb flow vectors for the case

with impounding and release from Copperhouse and the existing culvert at Carnsew. Figure 3.20 shows the corresponding peak ebb flow vectors for the case with impounding and release from Copperhouse and both sets of sluices on Carnsew Pool.

The impounding and sluicing operations clearly alters the tidal levels in the two Pools and adjacent waters. Figures 3.21 and 3.22 show spring and neap tide levels in Copperhouse, Carnsew and in the main harbour (at the entrance to Penpol Creek) for the various simulations performed comprising normal tidal exchange in the Pools and with impounding. This information was tabulated and passed to Buro Happold for calculation of the associated impact on inundation and exposure of intertidal areas.

3.3.2 *Sediment transport modelling*

Sediment transport modelling was carried out using the HR Wallingford model, SANDFLOW, which is appropriate to simulate the predominantly non-cohesive sediment in the main harbour as identified in the earlier study (Section 2.6) and confirmed by site visit. All sand transport simulations were carried out using a representative median grain diameter of 0.35mm, in accord with the seabed sediment data summarised in Section 2.6.

SANDFLOW takes as input the tidal information generated by TELEMAC, and computes the entrainment, transport and settling of sand by the tidal currents on the same model mesh. Output from SANDFLOW comprises through-tide sand fluxes and the corresponding patterns of erosion and deposition. Further details of SANDFLOW are provided in Appendix 1.

Unusually, at this site, comprehensive sand flux measurements were made in the earlier 1989 study (see Section 2.7) and in this study the data was processed to yield a relationship between the tidal current and sand flux magnitude. This relationship is reproduced in Figure 3.23 and this graph highlights a functional form of sand transport where the sand flux follows a power law relationship with the tidal current, given by the following formula:

$$Q = 0.0694U^{3.74} \quad (1)$$

in which $Q(\text{kg/m/s})$ is the sand transport rate and $U(\text{m/s})$ is the depth-averaged velocity.

This formula was incorporated in the SANDFLOW code so that this site-specific relationship could be applied in this study. On this basis the sand transport predictions are considered to be representative of the actual transport occurring within the Harbour area, although it should also be borne in mind that there will remain a degree of uncertainty in any sand transport predictions as a consequence of other factors (including availability of sediment, mixtures of sediment, density effects). Notwithstanding this latter comment, the sediment transport model provided an effective tool to assess the effects of the proposed scheme on the present sediment regime.

Figures 3.24 and 3.25 show the net tidal sand transport vectors due to spring and neap tides respectively, for the present day scenario. Whereas tidal current magnitudes can reach approximately 2m/s, due to the non-linear relationship of sediment flux with current (as highlighted by Equation 1 above) the range of sediment flux in the marine environment can be many orders of magnitude. Accordingly, the sand transport vectors

are presented on a colour scale as well as vector length scale in order that the entire field can be visualised.

As expected, the sediment transport rate during spring tides is significantly higher than that during neap tides. These figures highlight that under tidal action, sand is brought into the Harbour area, and the currents are sufficiently strong to mobilise sand over much of the Harbour.

On either side of the Fisherman's Weir, the apparent import of sand into the Lelant is consistent with the observed build up of sand in this area, and the import of sand toward the Harbour is also consistent with sand deposits in the vicinity of Cockle Bank.

Integrating the sand flux at the harbour mouth, however, indicates that under tidal action, there is net export of sand which is not consistent with the overall pattern of general accretion within the harbour (and the historical requirement for the impounding and sluicing). This discrepancy is explained by the contribution to the sand transport at the harbour entrance by wave action, as described in the following section.

3.3.3 *Wave-induced sediment transport*

In order to confirm the contribution of waves to the sediment budget at the entrance to the Hayle Estuary, simulations were carried out to reproduce wave-driven currents in combination with tidal effects, for example waves of height 1m and 2m propagating southwards through St Ives Bay from the northern model boundary.

Note that it was not intended to attempt to reproduce the entire littoral drift due to all waves, since this drift will vary from year on year giving variable patterns of beach erosion and accretion in the south of St Ives Bay as evidenced by historical photographs showing large beach level variations (Hayle Harbour Master, pers comm). Furthermore, the proposed scheme comprising a dredged marina, was not expected to alter the sediment budget at the Harbour entrance. Hence the simulations performed were aimed at confirming that wave action plays a significant role in the import of sediment into the harbour.

Figures 3.26 to 3.29 show the wave generated currents at times of spring tide peak flood and ebb for 1m (6s) and 2m (8s) waves respectively. These figures clearly show the effect of wave breaking, and consequent current generation at the coast. Figures 3.30 and 3.31 show the corresponding net tidal sand flux patterns for each wave condition, and these highlight the strong flux of sediment into the Harbour in the shallower water.

Integrating the sediment flux at the Harbour entrance indicates that wave action is responsible for significant import of sand around the sides of the Harbour entrance, and this is consistent with the large sand bank observed on the north side of the inner harbour.

3.3.4 *The effects of sluicing on the sediment transport*

The effects of flow impounding and sluicing from HW+3hrs on the sediment transport in the harbour was analysed by importing the flow conditions into the SANDFLOW model. The resulting spring tide net sediment transport patterns are shown in Figure 3.32 This result clearly shows that in the inner harbour area the sediment flux vectors are reversed suggesting that the sluicing would be effective in flushing sediment out of the harbour. It is not possible to determine the timescale for flushing of the sediment to

the former historical depths, especially since it is likely that the effectiveness of the sluicing from Copperhouse Pool is likely to have reduced due to reduced storage volume. It is apparent, however, that the sluicing simulated has an effect which extends out as far as the offshore bar outside the Harbour, and this result is in accord with anecdotal evidence of the effectiveness of the previous (historical) sluicing.

3.3.5 *Summary of sediment transport regime*

From the information gathered from the site visit, the available data, and the baseline simulations described above, the following summary points are made:

- Tidal processes are capable of sweeping sediment into the harbour area, and as far inside as the inner harbour and also into the Lelant. The modelling predictions are in accord with observed sedimentation patterns;
- The tidal processes alone give rise to net potential export of sediment and this is consistent with the morphology in the form of an offshore bar;
- Historically, sluicing was carried out to sweep the harbour clear of sediment. Since sluicing stopped the harbour has accreted, suggesting net import of sediment. Wave effects play a role in the import of sediment into the harbour, as confirmed from the simulations including wave effects and littoral drift;
- Even with the likely reduced storage volume of Copperhouse Pool (due to the accretion which has occurred since the former sluicing operations) the simulations confirmed that sluicing would still be effective in flushing sediment seawards;
- Waves and tides are responsible for the general morphology in the south of St Ives Bay. Whereas the tidal processes are quasi-steady and deterministic, wave energy will vary from season to season and year to year: as a consequence the morphology will also vary and this is consistent with the observed evidence for relatively large scale beach changes at the harbour entrance;
- Historical evidence indicates that Copperhouse Pool has accreted substantially over the past decades. Conversely, Carnsew Pool has not experienced the same degree of accretion: the north-eastern end of Carnsew still showing a deepened area which was dredged to create a cooling water pool for the power station which ceased operation years previously. This information suggests that Copperhouse pool has accreted due to sediment import from the Angarrack stream (there being no stream discharging into Carnsew Pool). That the accreted areas in Copperhouse Pool include areas of vegetation suggests finer, cohesive sediment which is also more likely to be derived from the Angarrack Stream rather than from the marine source.

3.4 SIMULATIONS INCLUDING THE SCHEME

3.4.1 *Scheme Layout 1*

Flow modelling

The baseline numerical model geometry was modified to include the proposed scheme, as shown in Figure 3.33 comprising:

- Removal of most of Cockle Bank (leaving the most easterly end where the historic turning post is located) to create a dredged area at the site of the proposed marina with new solid breakwater immediately seawards
- Reinstatement of the quay immediately outside the presently derelict sluice on South Quay.

Flow simulations were repeated for spring tide conditions with the summer (open) sluice operation at the Copperhouse flood gate. Four conditions were simulated:

- Normal culver operation (without impounding) with second sluice gates at Carnsew closed
- Normal culver operation (without impounding) with second sluice gates at Carnsew open
- Impounding and flushing with second sluice gates at Carnsew closed
- Impounding and flushing with second sluice gates at Carnsew open.

Peak flow vectors for each of these cases are shown in Figures 3.34 to 3.41.

Sediment transport modelling

Sand transport simulations were carried out for the four conditions described above, and the corresponding patterns of sediment flux are presented in Figures 3.42 to 3.45. In comparison to the corresponding baseline figures these show that the solid breakwater has a tendency to increase the import of sediment into the inner harbour.

Figures 3.46 to 3.49 show the corresponding patterns of erosion and deposition, and Figures 3.50 and 3.51 show the detail of sediment infill in the marina area for the case with and without sluicing. This analysis indicated that with the present bathymetry and source of sediment in the inner harbour, sediment is swept into the dredged marina area, and that furthermore, due to the increased cross-sectional area of the inner harbour (with the removal of Cockle Bank) the impounding and sluicing is not effective in removing this sediment.

[Note that the model assumes abundant supply of sand in all wet areas of the domain, and therefore predicts very high erosion and consequent deposition at the sluices/culverts whereas in fact these areas are either composed of hard (concrete) revetment or have naturally coarser material which is less erodible.]

Hence whereas conclusions from the baseline modelling indicate that impounding and sluicing may flush sediment out of the inner harbour, thereby removing it as a source for subsequent infill in the dredged marina. Conversely, without relatively regular impounding and sluicing sediment brought in to the inner harbour under wave and tidal action will be swept into the dredged area, and subsequent impounding and sluicing is unlikely to be effective in removing this accretion from the marina.

Integrating the volume of sediment in the marina for the spring tides and assuming a reduced volume of infill under neap tide conditions, the annual sedimentation in the marina was estimated to be of the order of 10,000-20,000m³.

Figure 3.52 shows the effects of the scheme on the sediment flux at three locations in the study area: at the entrance to the harbour, at the entrance to The Lelant, and close to the proposed marina. This analysis shows that at the Harbour entrance the scheme reduces the ebb flux, and marginally increases the flood flux, suggesting a small additional import of sand into the harbour (in the absence of sluicing). As already identified, the proposed new breakwater has a significant effect on the sediment flux, particularly during the flooding phase of the tide. The sediment flux at the entrance to the Lelant is generally unchanged.

3.4.2 Scheme Layout 2

The results of the first scheme layout indicated that the marina area may infill with sand sourced primarily from outside the Harbour and that this sediment would not be able to be flushed by impounding and sluicing. Whilst it would be possible to dredge within the marina, it was considered by the team of architects and engineers that a designated sand trap immediately seawards of the marina would provide an effective area for sedimentation, thereby reducing the infill in the marina itself. In addition, it was considered by the architects that a second breakwater structure to the west of the marina may on its own promote settling out of sediment before reaching the marina.

Scheme 2 therefore comprised a second breakwater, with and without a large conceptual sand trap. The scheme without the sand trap is shown in Figure 3.53.

Flow modelling

The same four operational regimes outlined in Section 3.4.1 above were simulated with this layout, and the results are shown in Figures 3.54 to 3.62.

Sediment transport modelling

Sand transport simulations were carried out for the four conditions described above, and the corresponding patterns of sediment flux are presented in Figures 3.62 to 3.65. In comparison to Scheme 1 it can be seen that the additional breakwater has a significant influence on the sediment transport patterns.

Figures 3.66 to 3.69 show the corresponding patterns of erosion and deposition, and Figures 3.70 and 3.71 show the detail of sediment infill in the marina area for the case with and without sluicing. These figures highlight, however, that without a sand trap the infill in the marina is comparable to that obtained with Scheme 1.

Simulations were subsequently repeated with a large sand trap between the breakwaters as shown in Figure 3.72. Corresponding plots of peak flood and ebb speed, sediment transport rate and patterns of erosion and deposition are shown in Figure 3.73 to 3.76. Figure 3.77 shows that the infill in the marina is effectively reduced.

This analysis indicated that compared to Scheme 1, the sand trap is effective in reducing the infill in the marina area. Furthermore, it was concluded that the conceptual sand trap was longer than required. Given the presence of a buried power cable running across the inner harbour it was concluded that a smaller sand trap would still be effective. In addition, information provided by the architects confirmed that the second breakwater was no longer planned. Hence Scheme 3 was proposed comprising a layout similar to Scheme 1 but with a smaller sand trap.

3.4.3 Scheme Layout 3

Flow modelling

The third version of the scheme returned to the general layout of Scheme 1 (i.e. without the additional breakwater) but added a refined sand trap, of smaller size than that used in Scheme 2. This is shown in Figure 3.78. The model with this geometry was run for two conditions only, with the second sluice gates at Carnsew open. Flow results are shown in Figures 3.79 to 3.82.

A variation on the third version introduced a scheme for impounding water in Penpol Creek, which was modelled as a weir at +1.3mOD, which is the level of mid-tide for the

spring tide. This was simulated by raising the bed level across the entrance to the harbour. In accordance with the design drawing provided by Buro Happold (Drawing BHW D 1601 00.dwg) the width was reduced by approximately two thirds, again by raising the bathymetry. The updated bathymetry is shown in Figure 3.83.

Simulations were repeated for spring and neap tides and with impounding in Carnsew and Copperhouse Pools. The full set of tests comprised:

- Normal culvert operation (without impounding) with second sluice gates at Carnsew open
- Impounding and flushing with second sluice gates at Carnsew open
- Impounding and flushing, with second sluice gate on Carnsew allowing water in, but flushing out through only one culvert, spring tide only. This test was carried out to investigate the effect of sluicing on the intertidal levels within Carnsew Pool.

Figures 3.84 to 3.93 show the peak flood and ebb currents for the various tests performed.

Figures 3.94 and 3.95 show spring and neap tide levels in Copperhouse, Carnsew and in the main harbour (at the entrance to Penpol Creek) for the various simulations performed comprising normal tidal exchange in the Pools and with impounding. This information was passed to Buro Happold for calculation of the associated impact on inundation and exposure of intertidal areas.

Sediment transport modelling

Sand transport simulations were carried out for the various conditions described in the section above, and the corresponding patterns of spring and neap net tidal sediment flux are presented in Figures 3.96 to 3.102. Figures 3.103 to 3.109 show the pattern of erosion and deposition for the various tests. These show that the smaller sand trap is effective in trapping sediment and that there is correspondingly lower rate of infill in the marina area. It is concluded that the sand trap could provide a means of reducing the maintenance dredging of the marina, by inducing infill in the trap which would be easier to maintain. The volume of sand entering the sand trap is estimated to be of the order of 5,000-10,000m³ per year, and from the simulations carried out it is anticipated that this sediment will comprise relatively clean sand from marine sources (brought in through the harbour entrance).

As already identified in the earlier tests, sluicing would be effective in flushing sand out of the estuary, if this procedure was carried out regularly and frequently. This process could also potentially render the sand trap unnecessary. Similarly, without the sand trap the marina area would tend to infill as in the Scheme 1 simulations, but this may also be considered manageable. The results also indicate, however, that the impounding and sluicing operations would not be effective in removing sand from the marina area.

Figure 3.110 shows the effects of the scheme (without sluicing) on the sediment flux at three locations in the study area: at the entrance to the harbour, at the entrance to The Lelant, and close to the proposed marina. This analysis shows that at the Harbour entrance the scheme increases the ebb flux, and marginally increases the flood flux, suggesting no significant overall change in the tidal sand flux into the harbour (in the absence of sluicing). As already identified, the proposed new breakwater has a significant effect on the sediment flux, particularly during the flooding phase of the tide. As with Scheme 1, at the entrance to The Lelant at location shown there is a small

reduction in the flood flux, whilst the ebb flux is largely unchanged. Also shown on this figure is a line across which the total flux was integrated throughout the tidal cycle. This analysis confirmed that there is a small net reduction in the import of sand into The Lelant.

3.5 HYDRODYNAMIC MODELLING CONCLUSIONS

General conclusions arising from the hydrodynamic modelling studies are as follows.

1. Dredging the marina is likely to lead to a degree of sedimentation in this area. The volumes associated are not especially high (10,000-20,000m³/year), and dredging from within the marina could be managed (as occurs in other marinas). Alternatively, the modelling has shown that a sand trap immediately to the west of the marina would be effective in reducing the marina sedimentation, and provide an easier area for maintenance of dredging.
2. As occurred historically, impounding and sluicing would be effective in driving the marine-derived sand out of the estuary, out beyond the bar. By this means, the sluicing could counteract the strong import of sand at the Harbour entrance which is due to both tides and waves.
3. Given the increase in the cross-sectional area in the marina caused by the removal of Cockle Bank, sluicing would not, however, be effective in removing the marina sedimentation.
4. Impacts of the scheme are localised. There is evidence to suggest a small reduction in the sand import into The Lelant, and indeed, sluicing would tend to drive sediment out of the estuary so that the import of sand into the Lelant would tend to be further reduced.
5. Sluicing will clearly alter the tidal characteristics of the two Pools (Carnsew and Copperhouse), and information on the tidal levels was passed to Buro Happold for further processing.

4. *Dispersion of sediment arising from dredging during the construction phase*

Studies were undertaken to assess the dispersion of fine-grained sediment arising from the removal of Cockle Bank, which comprises a matrix of materials ranging from rock to fines. The principal aim of this assessment was to investigate the sediment transport pathways away from the site and identify areas that could be potentially affected by the fine sediment released. The quantities of fine sediment released into the water column will depend on the amount available in the Bank and the proportion of this amount which is lost during dredging or removal, which will also depend on the plant used and the particulars of the operations. Whilst it was anticipated that the concentrations of sediment released are likely to be small in comparison to the natural background concentrations, the analysis also tracked the sediment as it dispersed in order that areas of potential deposition of this sediment could also be identified.

Given the proximity of Cockle Bank to the proposed marina (which is due to be dredged), this assessment also provides relevant information on the potential dispersion of sediment released during the construction of the marina.

The dispersion of the plumes of sediment arising from the proposed dredging of Cockle Bank was simulated using the HR SEDPLUME-RW model (see Appendix 1). The

model uses the hydrodynamic output from the TELEMAC-2D flow model of the area and the assumption of a logarithmic velocity profile through the water column to track the 3-dimensional movement of sediment particles. Dispersal in the direction of flow is provided by the shear action of differential speeds through the water column while turbulent dispersion is modelled using a random walk technique. The deposition and resuspension of particles are modelled by establishing critical shear stresses for erosion and deposition. Erosion of deposited material occurs when the bed shear stress exceeds the critical shear stress for erosion while deposition of suspended material occurs when the bed shear stress falls below the critical shear stress for deposition.

Note that the dispersion modelling undertaken does not represent background concentrations but simulates the increase of suspended sediment concentrations above background conditions caused by the works.

At the time of undertaking this assessment the method of removal of Cockle Bank was not defined, and hence typical, representative parameters relating to the release of the fine sediment were applied.

The model was set up to represent a dredger working at Cockle Bank releasing material for ½ hour every hour during the 1st tide of the simulation. Material was released through out the water column at the dredging site and the simulation continued for another 2 tides after the dredging finished, allowing settled sediment to be re-eroded and transported.

The following typical sediment parameters were used for the modelling:

- Critical shear stress for deposition (of settled sediment) = 0.1 N/m²
- Critical shear stress for erosion (of settled sediment) = 0.2 N/m²
- Erosion constant (of settled sediment) = 0.001 m⁻¹s
- Dry density of released material = 500 kg/ m³

For the purposes of this study the rate of release of sediment into the water column (from the dredging operations) was set to a nominal 1.0kg/s. The actual release rate will depend on the availability of the fine sediment in the load, and the plant used and operational methods. In any event the results provided herein are directly scalable, so that, for example a release rate of 0.1kg/s would give rise to concentrations and deposition values a factor 10 smaller.

The model was run using:

- Release rate = 1.0 kg/s
- Settling velocity = 0.001 m/s
- No deposition in St Ives Bay (assuming wave action keeps the sediment in suspension)

Output from the SEDPLUME model was processed to provide through-tide concentration fields every two hours starting from the initial release at HW, and the ultimate pattern of deposition at the end of this three-tide simulation. In addition, the maximum concentration reached at any point during the simulation is also presented.

Figure 4.1 shows the concentration plume at two-hourly intervals over the simulation period, which clearly show the release of sediment over the first tide (12 hours) and its subsequent dispersal, with re-erosion and transport when the tidal currents are strong enough to mobilise it.

By way of comparison, Figure 4.2 shows output from the earlier SANDFLOW studies highlighting the typical background concentrations during spring tides that occur in the estuary under present day (spring tide) conditions. This information clearly highlights that over the areas affected by the dredging plume, the peak natural background concentrations are typically much larger.

Figure 4.3 shows the peak concentrations occurring throughout the dredging and dispersal simulation and highlights the benefit of “capturing” the peak at any given stage. Comparison of this figure with the images in Figure 4.2 confirms that other than close to the release point, the concentrations generated by the dredging are generally lower than background levels. It is re-iterated that the actual concentrations occurring as a consequence of the dredging will be strongly dependent on the availability of fine sediment, and on the plant and operations used. Hence the model output presented herein should be considered as indicative only and as stated above, the concentration fields are generally scalable with the release rate.

Figure 4.4 shows where the material released from the dredging point at Cockle Bank deposited at the end of the three-tide simulation. This indicates that there is the potential for the sediment released to be dispersed over a relatively wide area extending from the Carnsew and Copperhouse Pools to outside the estuary, with the potential for a small proportion of the material possibly settling out into these Pools and also into the Lelant area. Again, as stated above the actual quantities of material settling out will depend on the release rate from the source. If required, the amount of material being dispersed could be reduced by specialist plant as well as by restricting the dredging to specific periods within the tidal cycle.

5. *Desk assessment of water quality issues in Penpol Creek*

5.1 PHASE 1 ASSESSMENT

Available data

The main sources of information used in the Phase 1 assessment were from studies carried out in 1988 and 1998 related to previous plans to re-develop the harbour. These studies were mainly focussed on metal concentrations in the water column and in the sediments in Copperhouse Pool (Smith, October 1988 and November 1988; WSP Environmental, 1998; Aquatic Environmental Consultants, 1998).

Additional background information on the Hayle Estuary was obtained from a Nature Conservancy Council Report from 1989 (Field Studies Council Research Centre), and additional more recent summary water quality data were obtained from the Environment Agency website (www.environment-agency.gov.uk).

Freshwater inputs

Hayle Harbour and estuary are fed by two main rivers – River Hayle and Angarrack Stream. The River Hayle enters the estuary outside the harbour, while Angarrack Stream enters the harbour via Copperhouse Pool. The River Hayle has a mean river flow of about 1 m³/s and the Angarrack has an estimated mean flow of 0.1m³/s. The Angarrack flows into Copperhouse Pool and has a two year return discharge of 8m³/s and 100 year discharge of 23m³/s. Copperhouse Pool is also fed by the Mill Leat, an old millstream that is assumed to have a very low flow.

The Environment Agency website provides summary water quality data for the River Hayle and Angarrack Stream up to 2002. Both streams are Grade A for chemical quality – which essentially means that they are free of any significant sewage effluent. The River Hayle did not however meet its water quality target in 2002 for total zinc, with the 95 percentile value being too high. Angarrack Stream met all its water quality targets even though its mean zinc concentrations are similar to those in the Hayle. Both streams have low concentrations of phosphorus and moderately high concentrations of nitrate.

Studies carried out in 1988 and 1998 have highlighted the high levels of arsenic in Angarrack Stream and particularly in Mill Leat. These have led to very high values in the sediment in Copperhouse Pool – reputedly one of the highest concentrations ever recorded in an estuary in the UK. (Smith, October 1988; Smith, November 1988; WSP Environmental; Aquatic Environmental Consultants 1988.)

Consequently, the freshwater entering the harbour and estuary can be considered to be of reasonably good quality with the exception of the zinc and arsenic concentrations. It is unlikely that the presence of a half tide barrier will lead to any problems related to dissolved oxygen and eutrophication largely because the harbour is likely to continue to have a reasonably rapid flushing time.

Sewage inputs

As far as can be ascertained there are no inputs of treated sewage to the estuary or the harbour. Sewage for the area is treated at the Hayle (Gwithian) sewage treatment works and discharged via a long sea outfall into St Ives Bay to the north-east of Hayle. Buro Happold have reported that there may be some combined sewer overflows (CSOs) that

discharge to the harbour in wet weather. It is unlikely the volumes arising from these CSOs are significant. However it is good marina management to divert any outfalls that discharge directly into the marina, but care would have to be taken regarding the location of any such diverted outfalls to avoid the possibility of the discharge returning to the impoundment.

Metals

As mentioned above, most water quality concerns in past studies have been raised in regard to metals. Sediments in Copperhouse Pool were found in 1988 to have very high copper, zinc and arsenic concentrations. High levels are also reported in the overlying water column. Data collected on the Cockle Bank in 1998 show concentrations much lower than in Copperhouse Pool (WSP Environmental 1988; Aquatic Environmental Consultants 1988).

Dr Smith's 1988 report suggests that the copper, zinc and arsenic concentrations in the water column in Copperhouse Pool although high were not likely to be a problem for human health (Smith, November 1988). There was some doubt over the accuracy of the measurements of copper and zinc in the water column, and it was Dr Smith's opinion that the values were likely to be higher than the environmental quality standards (EQS). The levels of copper and zinc in sediments were considered to be very high, although the limited fauna are well adapted for living in such conditions. However, Dr Smith had concerns about the exceptionally high levels of arsenic in the sediments and the implications for human health.

Thus, the main issue in Copperhouse Pool is that any changes to the hydrodynamic or chemical regime in the estuary would lead to the release of metals particularly arsenic from the sediments.

Sampling in the main part of Hayle Harbour was carried out by WSP Environmental in 1998, which included metal concentrations in the sediment and the water column. In all cases, arsenic, zinc and copper concentrations in Cockle Bank were significantly lower than those observed in Copperhouse Pool in the earlier survey.

5.2 PHASE 2 ASSESSMENT

The Phase 1 study (HR Wallingford, 2005) considered the general water quality issues in the whole Hayle Harbour area, with particular regard to the freshwater inputs and contamination from metals. The discussion presented there remains valid, in general terms, for the developments discussed herein.

Here, attention is focused on two aspects of water quality:

- resuspension and transport of contaminated sediment
- effect of impoundment in Penpol.

Baseline conditions

At present, the Penpol area is open to the estuary, and experiences good flushing on all tides. The area is fed directly by Mellanear Stream, a small freshwater stream. No data is available for this creek, but its properties have been estimated by comparison with the Angarrack Stream, which flows into Copperhouse Pool. Angarrack Stream shows low concentrations of all tested substances except nitrates and phosphates, which according to the Environment Agency are classified as 'High'. Its mean flow rate is estimated to be in the order of $0.1 \text{ m}^3/\text{s}$.

Taking the assumption that Mellanear Stream has similar concentrations, and an even lower flow rate than Angarrack Stream, the overall levels of nutrients in the Penpol harbour area are expected to be rather low.

Under present conditions, Penpol is readily flushed by the tide, and there are no known problems with water quality.

Effect of proposed impoundment in Penpol

It is proposed to introduce a half-tide impoundment at Penpol. The flow model has been run with this in place; details of the model are discussed in Section 3.4.3. The results indicate that with the half-tide weir, the Penpol area will be very poorly flushed during neap tides, but will flush almost completely during two or three spring tides.

This suggests that Penpol will effectively behave as a closed system during the neap part of the tidal cycle, when the tidal range is small, and then flush completely as springs are approached. The residence time between flushings will be approximately one week. This period is probably too short for any significant algal blooming to occur in the impounded harbour, even allowing for the possibility that small amounts of nutrients will be supplied by Melanear Stream.

It is therefore considered that the water quality is likely to be acceptable in the Penpol Harbour area.

6. *Power generation on Penpol*

As part of the impoundment in Penpol, it has been proposed to incorporate a tidal power generation facility. In basic form, this would consist of one or more turbines generating power on the ebb tide only, with the Penpol basin being filled on the flood tide through the standard sluices over the half-tide weir. During the ebb tide, these sluices would be closed, so that the flow was directed through the turbine channel.

According to Garrett and Cummins (2004), the optimum regime for power generation reduces the tidal range inside the impoundment to 74% of that outside (i.e. from 3.75m to 2.8m in this case). Following their assumptions indicates that the power available in the Penpol system is approximately 43kW on average, over a spring tide. This calculation has assumed that the full tidal range can be utilised, i.e. the basin is filled to the undisturbed high water level, and allowed to drain completely through the turbines, to a level close to the existing low water. This model of proposed operation may not be consistent with the construction or desired operation of the half-tide weir.

Over the course of a year, this would amount to 126,000 kWh, allowing a reduction factor of 3 to account for the variation in tidal range over the year. This value for 'available power' is an absolute maximum value; it does not include any efficiency losses, which would necessarily be a feature of the precise turbine design and layout.

Any restrictions to the operating regime would also reduce the amount of power which could be obtained in practice. As an initial guide, the available power reduces with the square of the permitted tidal range. Turbine efficiencies are likely to decrease even more rapidly with a reduction in the usable head.

Information from the DTI (<http://www.dti.gov.uk/files/file27540.xls>) indicates that the available power value quoted above (126,000 kWh) is roughly equivalent to the annual electrical energy needs of fifty people (assuming two per household) in the South West of England.

7. *Summary and conclusions*

Calibrated flow and sand transport models were established for this project, using site-specific measurements. Specific attention was required to reproduce the water exchange between the main estuary and the two former sluicing ponds (Carnsew and Copperhouse). Thereafter, spring and neap tide simulations were performed to establish a recent baseline regime against which the effects of the proposed development could be assessed.

The baseline scenarios confirmed that the sediment transport processes within the harbour are dominated by tidal effects. Waves and tides are responsible for the general morphology in the south of St Ives Bay. Whereas the tidal processes are quasi-steady and deterministic, wave energy will vary from season to season and year to year: as a consequence the morphology will also vary and this is consistent with the observed evidence for relatively large scale beach changes at the harbour entrance.

Historically, sluicing was carried out to sweep the harbour clear of sediment. Since sluicing stopped the harbour has accreted, suggesting net import of sediment. Even with the likely reduced storage volume of Copperhouse Pool (due to accretion) the simulations confirmed that sluicing would be effective in flushing sediment seawards.

Historical evidence indicates that Copperhouse Pool has accreted substantially over the past decades. Conversely, Carnsew Pool has not experienced the same degree of accretion: the northern end of Carnsew still showing a deepened area which was dredged to create a cooling water pool for the power station which ceased operation years previously. This information suggests that Copperhouse pool has accreted due to sediment import from the Angarrack stream (there being no stream discharging into Carnsew Pool). That the accreted areas in Copperhouse Pool include areas of vegetation suggests finer, cohesive sediment which is also more likely to be derived from the Angarrack Stream rather than from marine sources.

Simulations including the proposed development were based on an initial design comprising:

- Removal of most of Cockle Bank (leaving the most easterly end where the historic turning post is located) to create a dredged area at the site of the proposed marina with new solid breakwater immediately seawards;
- Reinstatement of the quay immediately outside the presently derelict sluice on South Quay.

For the final layout a half-tide weir on Penpol Creek was also included, in order to impound this area at approximately mean water level.

Flow simulations were performed for spring and neap tide conditions, and including the effects of sluicing. These tests indicated that the marina may experience some infill of marine-derived sand, and subsequent layouts involved the design of structured and a sand trap in order to minimise the amount of infill in the marina. Ultimately, a solution

was obtained comprising a small sand trap immediately seaward of the marina. The amount of sedimentation in this sand trap and also in the marina will depend on whether or not impounding and sluicing is re-instated. Without sluicing the amount of infill is estimated to be of the order of 10,000-20,000m³/year. Regular sluicing from both Pools would tend to drive sediment back out of the estuary as occurred in the past, and in this case the degree of sedimentation in the sand trap (or marina) would reduce.

Impounding and sluicing will alter the tidal regimes of the Pools, and water level information was extracted from the flow model and passed to Buro Happold for input into an analysis of the impact on the exposure/inundation of inter-tidal areas.

Under normal operating conditions (ie without sluicing), the modelling also indicated that the scheme would tend to have little overall effect on the sand flux at the entrance to the Harbour. Whilst the predictions suggest a small increase in the flood flux into the Lelant this would be short-lived since the budget at the Harbour entrance is largely unchanged.

Construction impacts were assessed by considering the dispersion of fine material released from the removal of Cockle Bank and associated dredging of the proposed marina area. The quantities of fine material released into the water column are likely to be relatively small (in comparison to the volume of fine sediment naturally entrained into the water column by the tide and wave action), and will depend on the type of dredging plant used. Dispersion pathways were investigated, and these indicated that there is the potential for the sediment released to be dispersed over a relatively wide area extending from the Pools to outside the estuary, with a proportion of the material possibly settling out into the Pools and also into the Lelant area. The amount of material being dispersed into these areas could be reduced by specialist plant as well as by restricting the dredging to specific periods within the tidal cycle.

Water quality in the area focused on the potential effect of impounding water in Penpol Creek with a half-tide weir. Under present conditions, Penpol is readily flushed by the tide, and there are no known problems with water quality. The flow modelling results indicate that with the half-tide weir, the Penpol area will be very poorly flushed during neap tides, but will flush almost completely during two or three spring tides. This suggests that Penpol will effectively behave as a closed system during the neap part of the tidal cycle, when the tidal range is small, and then flush completely as springs are approached. The residence time between flushings will be approximately one week. This period is probably too short for any significant algal blooming to occur in the impounded Creek, even allowing for the possibility that small amounts of nutrients will be supplied by Penpol Creek. It is therefore considered that the water quality is likely to be acceptable in the Penpol area.

8. *References and Bibliography*

Aldersgate Developments Ltd 1988. Hayle Harbour Development. Engineering Appraisal. Sir Alexander Gibb & Partners, December.

Aquatic Environmental Consultants 1998. Impact of proposed engineering works on the intertidal invertebrates of Copperhouse Pool, Hayle.

Babtie Group 2002. Hayle Harbour. Hydrodynamic Modelling Report. Final Report R02.

Buro Happold 2005a. Hayle Harbour Redevelopment. Progress Report. Cockle Bank Re-use Assessment. Job 007838.

Buro Happold 2005b. Sediment Exchange monitoring Job 007838 February.

Smith P, October 1988. Report on macroinvertebrates and sediment chemistry of Copperhouse Pool, Hayle.

Smith P, November 1988. Report on Arsenic, Copper and Zinc in Copperhouse Pool and other sites in Hayle, Cornwall.

Field Studies Council Research Centre, August 1989. Surveys of Harbours, Rias and Estuaries in Southern Britain. Hayle Estuary. Volume 1. A report to the Nature Conservancy Council from the, Fort Popton, Pembroke, Dyfed, C Gill.

Garrett, C and Cummins, P 2004, *J. Waterway, Port, Coastal, and Ocean Engineering*, **130**, 3

Gill C 1989. Surveys of Harbours, Rias and Estuaries in Southern Britain. Hayle Estuary. Volume 1. A report to the Nature Conservancy Council from the Field Studies. Fort Popton, Pembroke, Dyfed.

Hayle Harbour Development 1998. Sediment and water quality analysis. WSP Environmental, February.

HR Wallingford, June 1976. The Port of Hayle. Aspects to be considered in relation to future requirements.

HR Wallingford, October 1988. Hayle Harbour. Preliminary hydraulic appraisal of proposed development works on entrance channel siltation. EX1814.

HR Wallingford, April 1989. Hayle Harbour. Hydraulic and siltation studies. Report EX1911.

HR Wallingford, April 2005. Hayle Harbour Development. Hydraulic Studies Phase 1. Report EX5120.

Sea Sediments 1983. An investigation of sediment dynamics in the Hayle Estuary, Cornwall, September.

WSP Environmental, February 1998. Hayle Harbour Development. Sediment and water quality analysis.

Figures

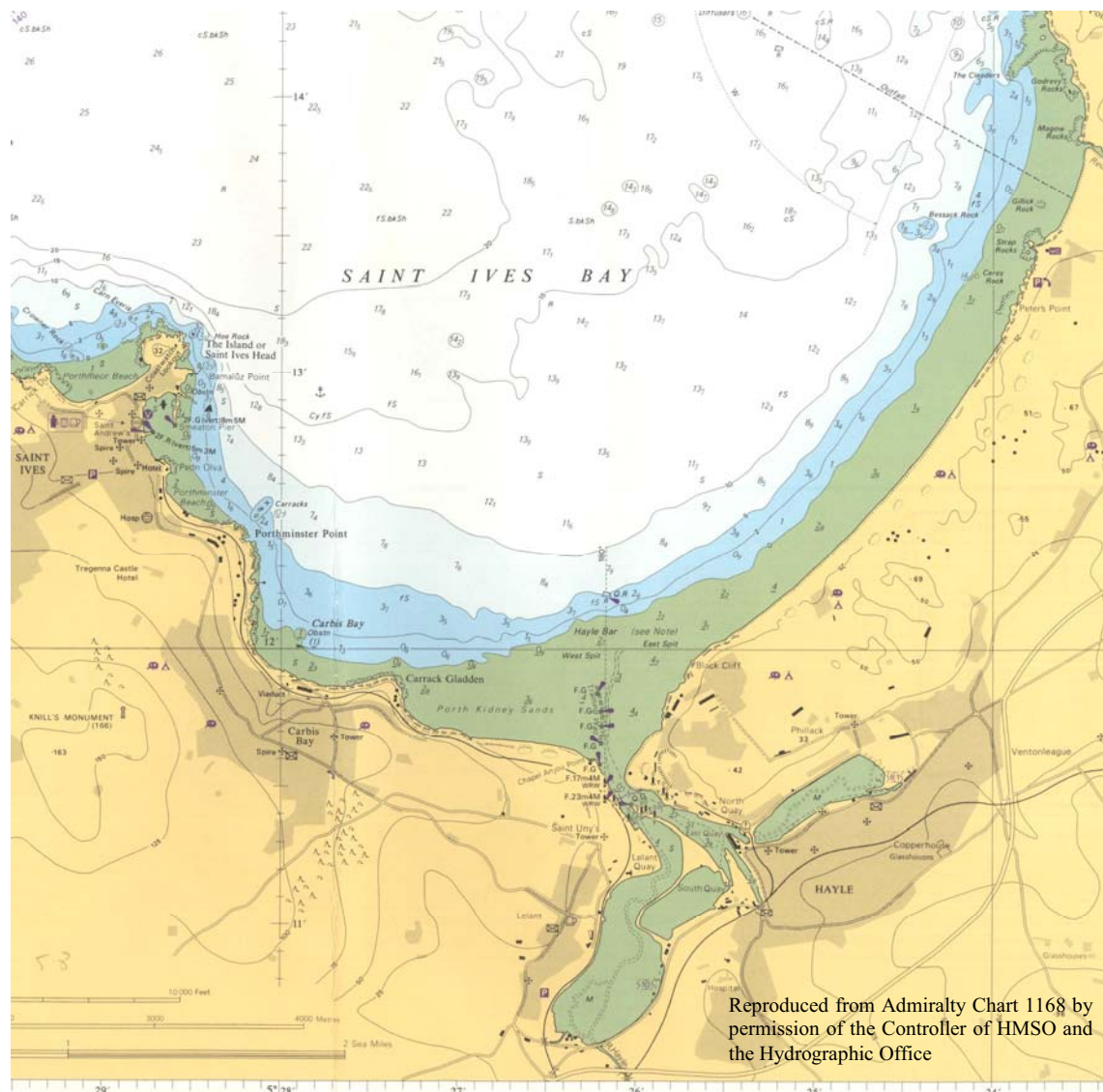


Figure 1.1 Location map

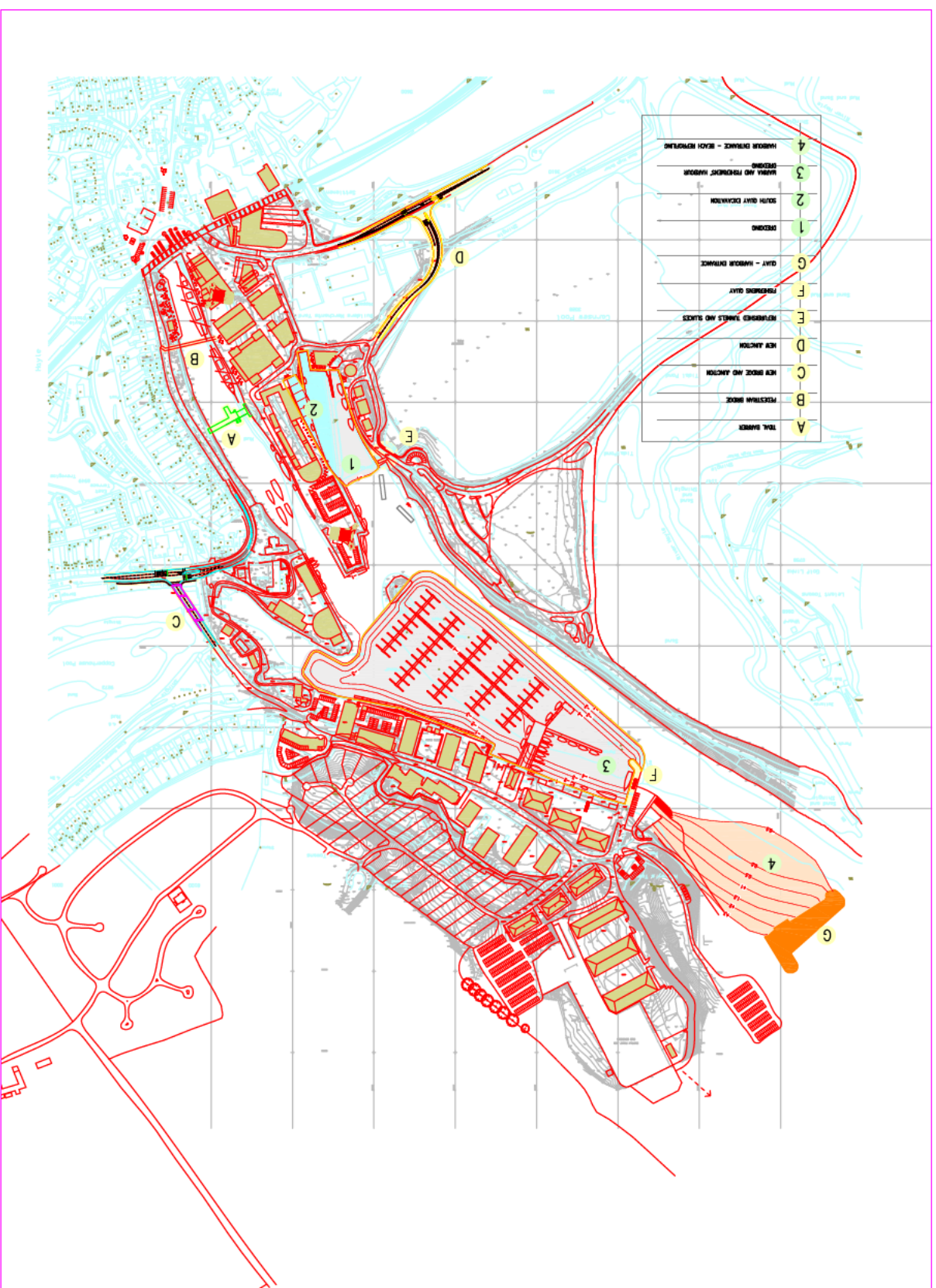


Figure 1.2 Proposed outline development at Hayle

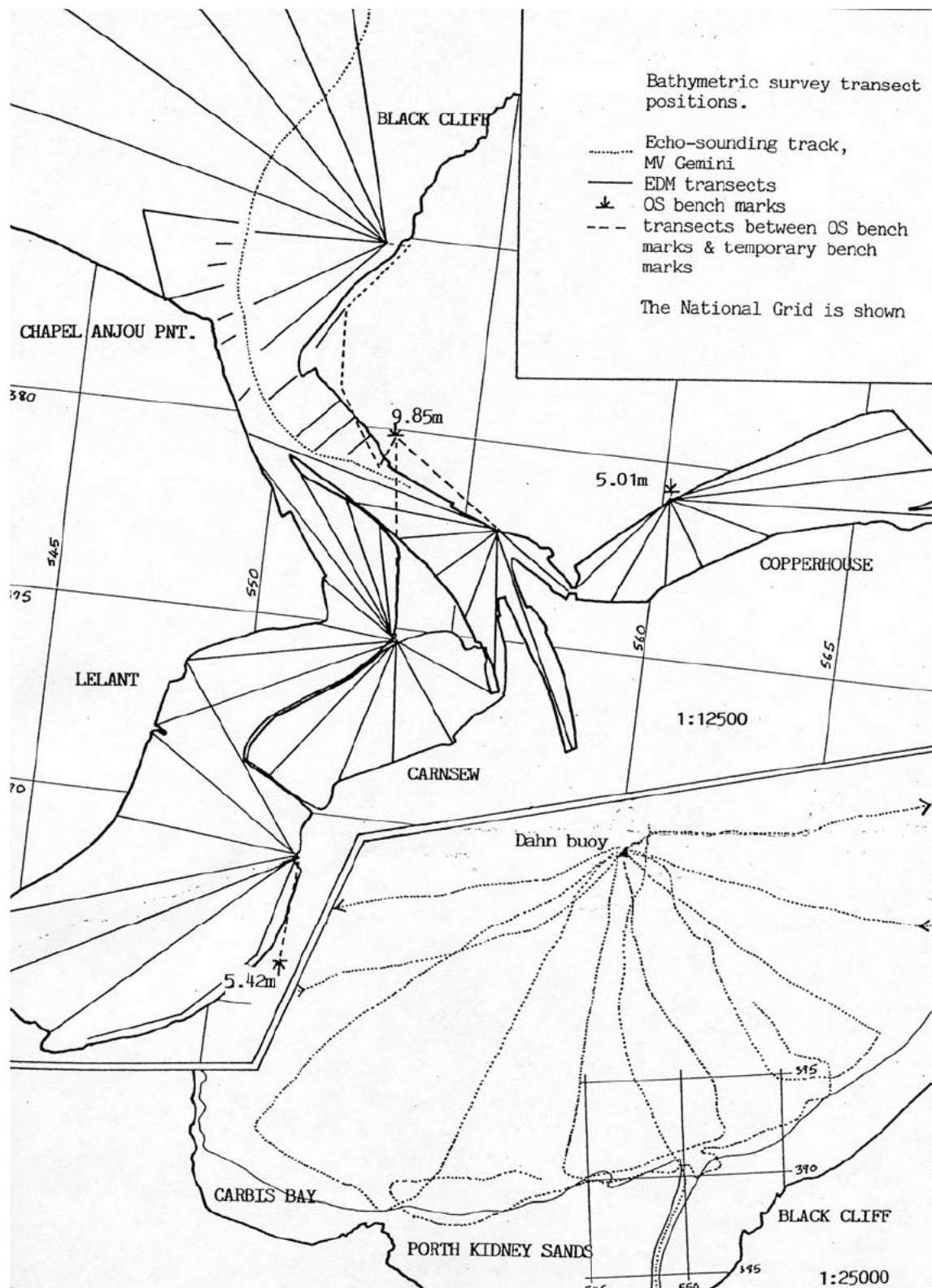
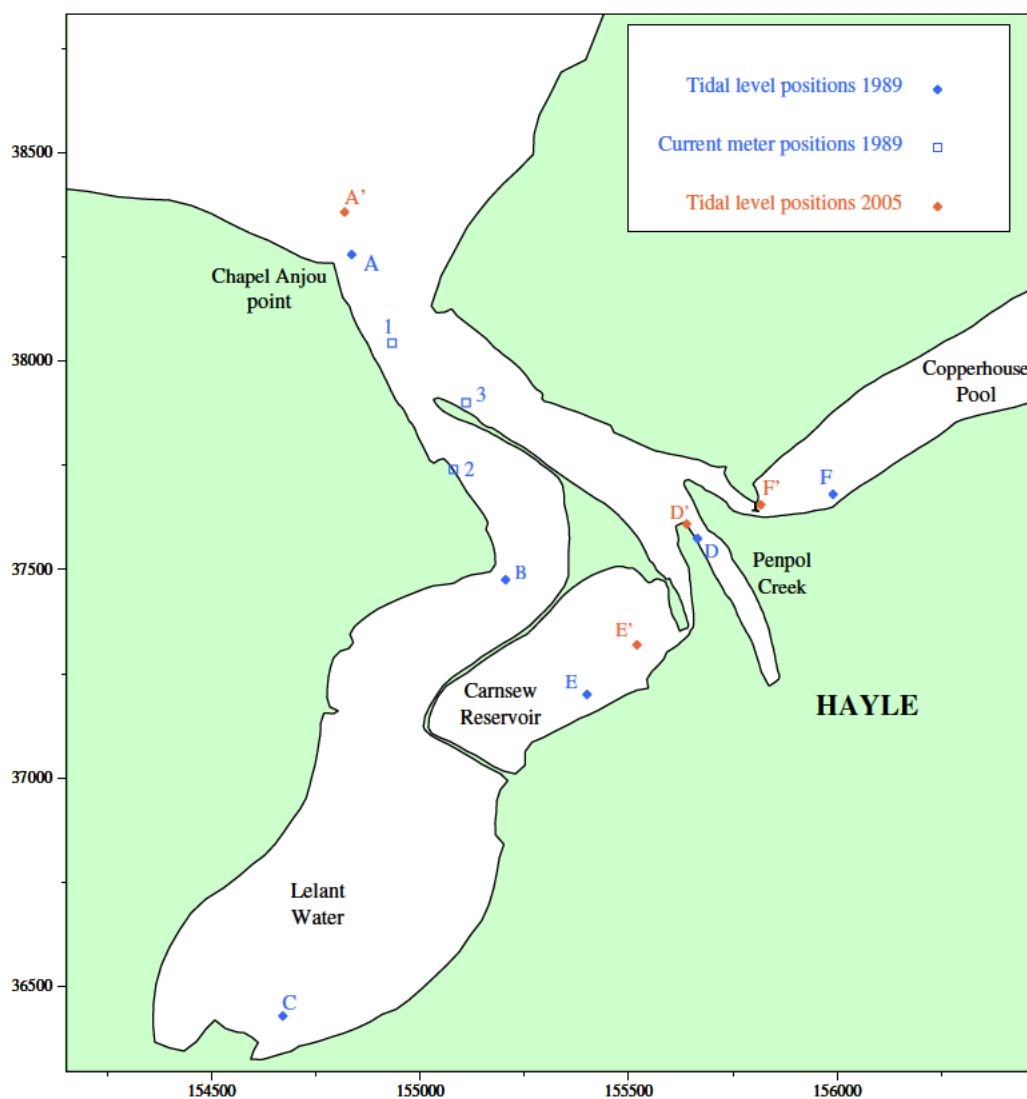
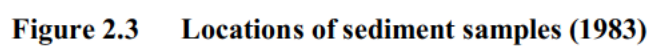


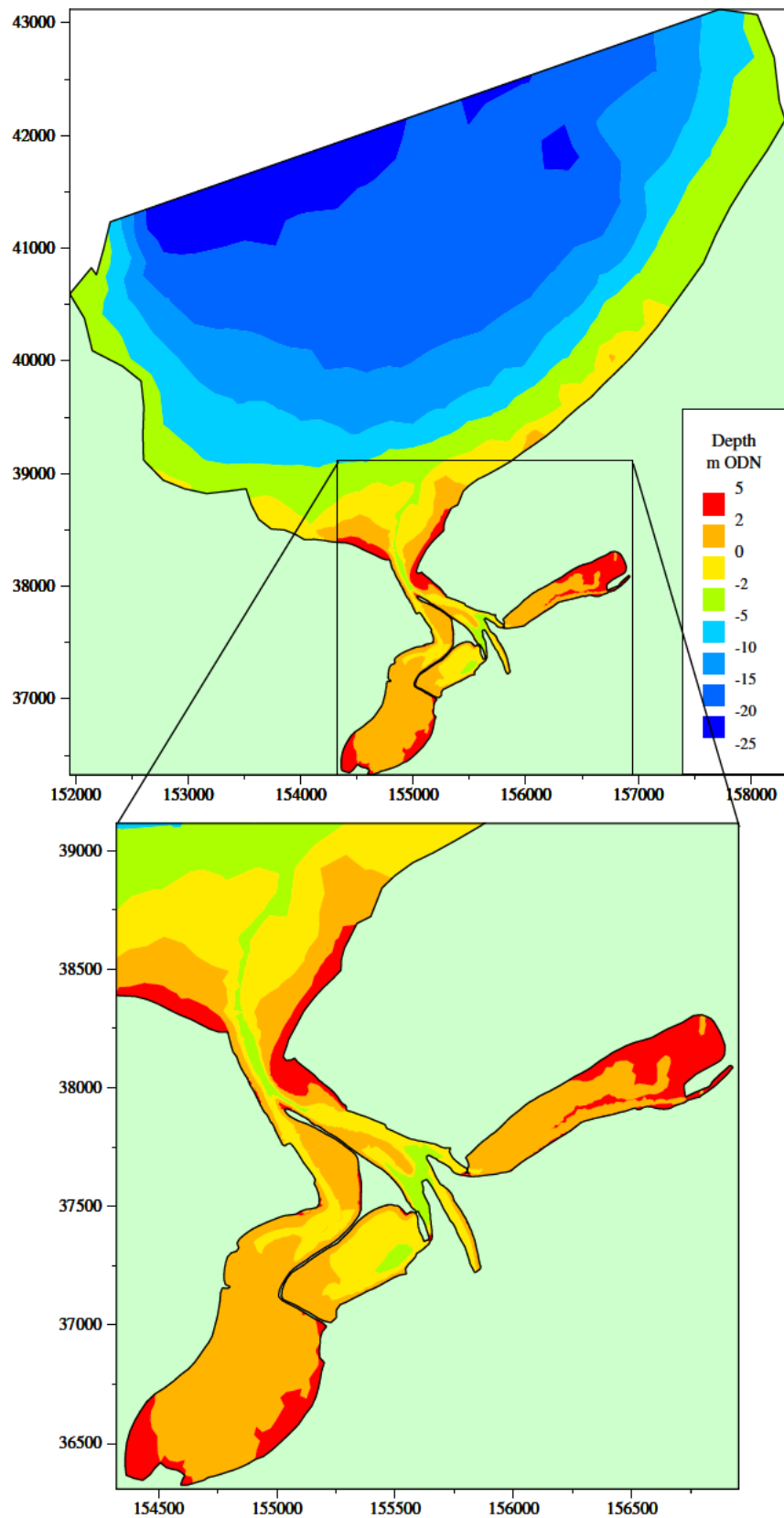
Figure 2.1 Bathymetric survey transect positions (1983)



/HR_projects/ddr3839/model/SedimentTransport/report/Rubensp/flow_10c.RUB/fig2.2.i

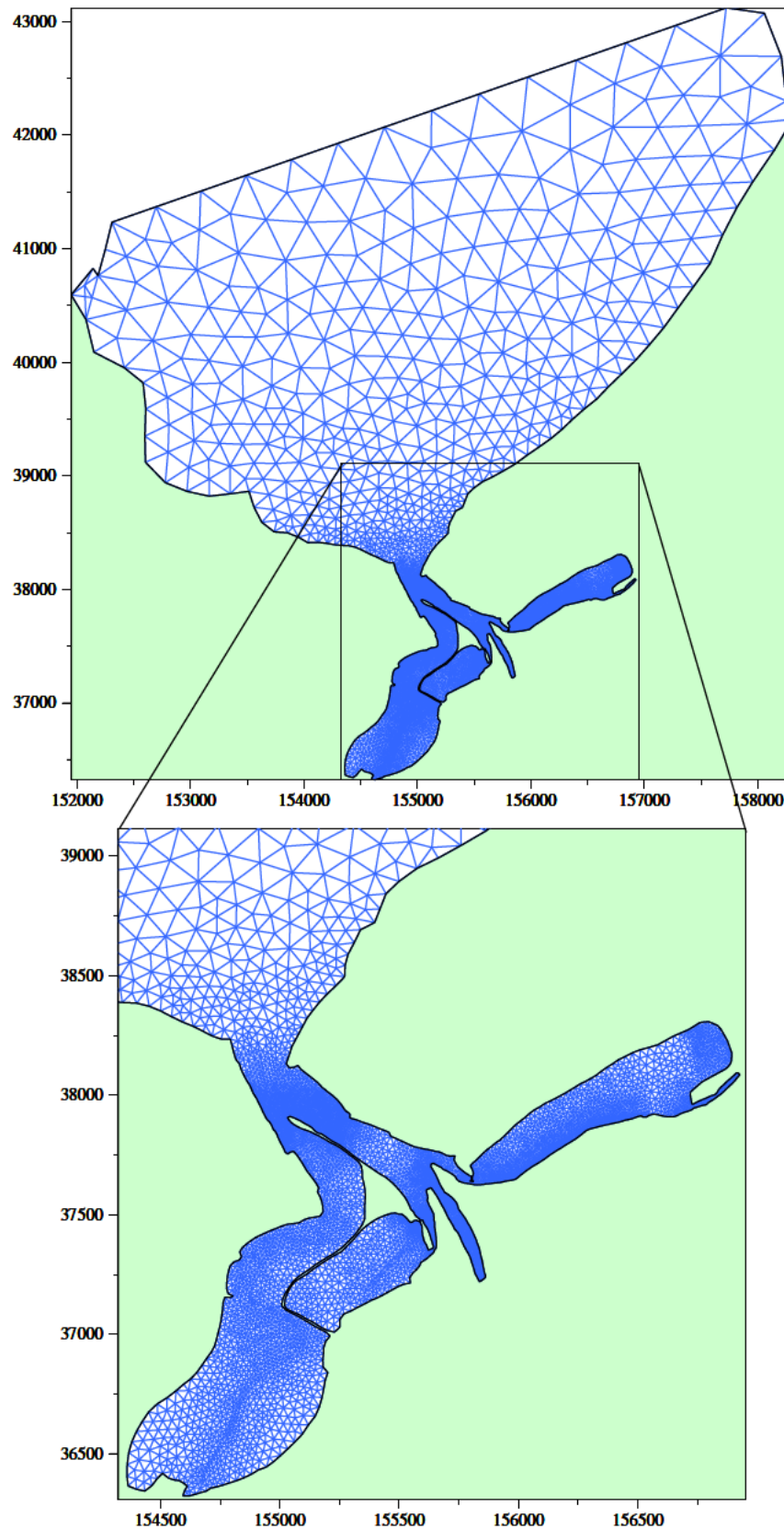
Figure 2.2 Locations of tidal level metering stations (1989 and 2005) and current meter stations (1989)





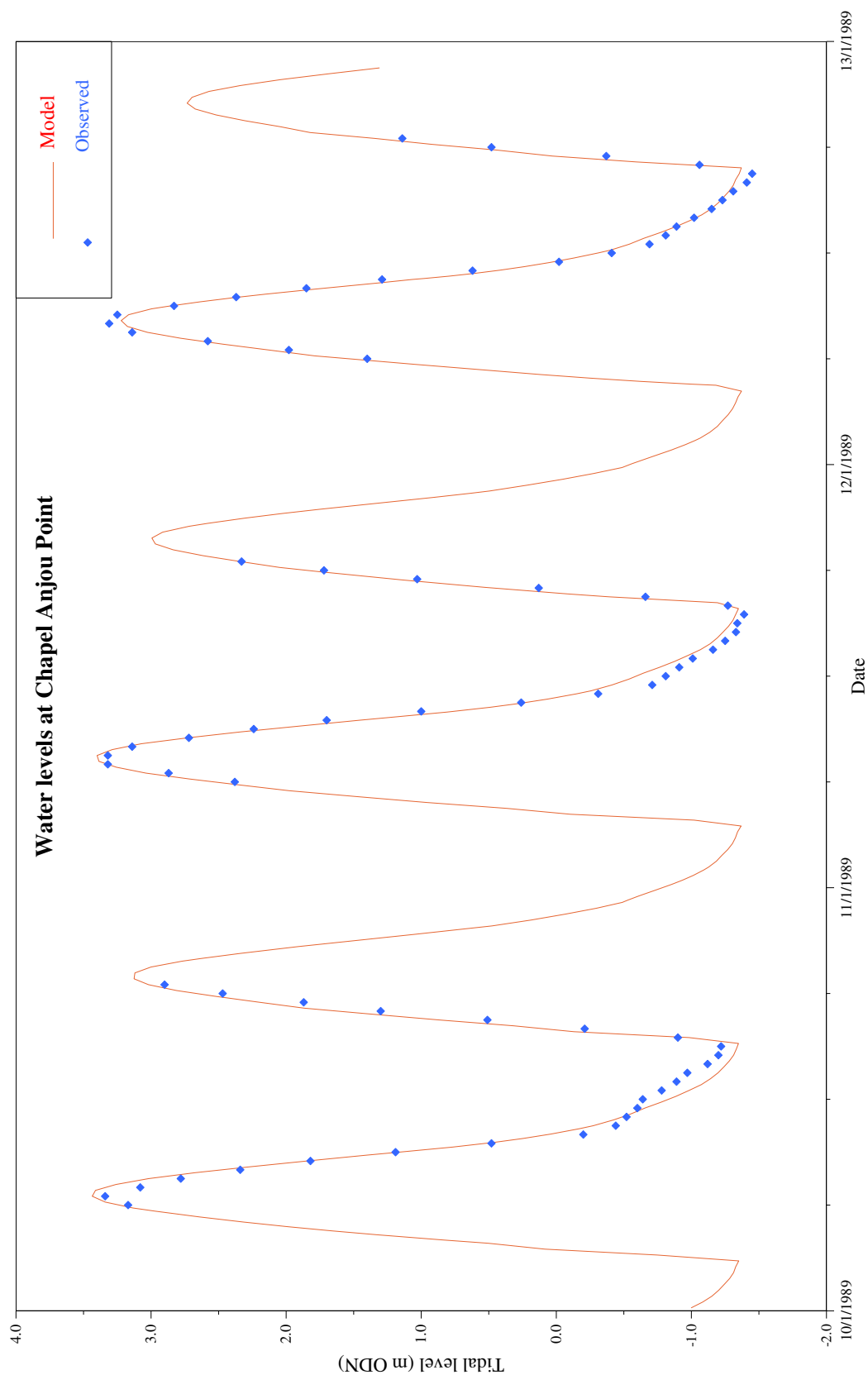
/HR_projects/ddr3839/model/SedimentTransport/report/Rubensp/flow_10c.RUB/fig3.1.i

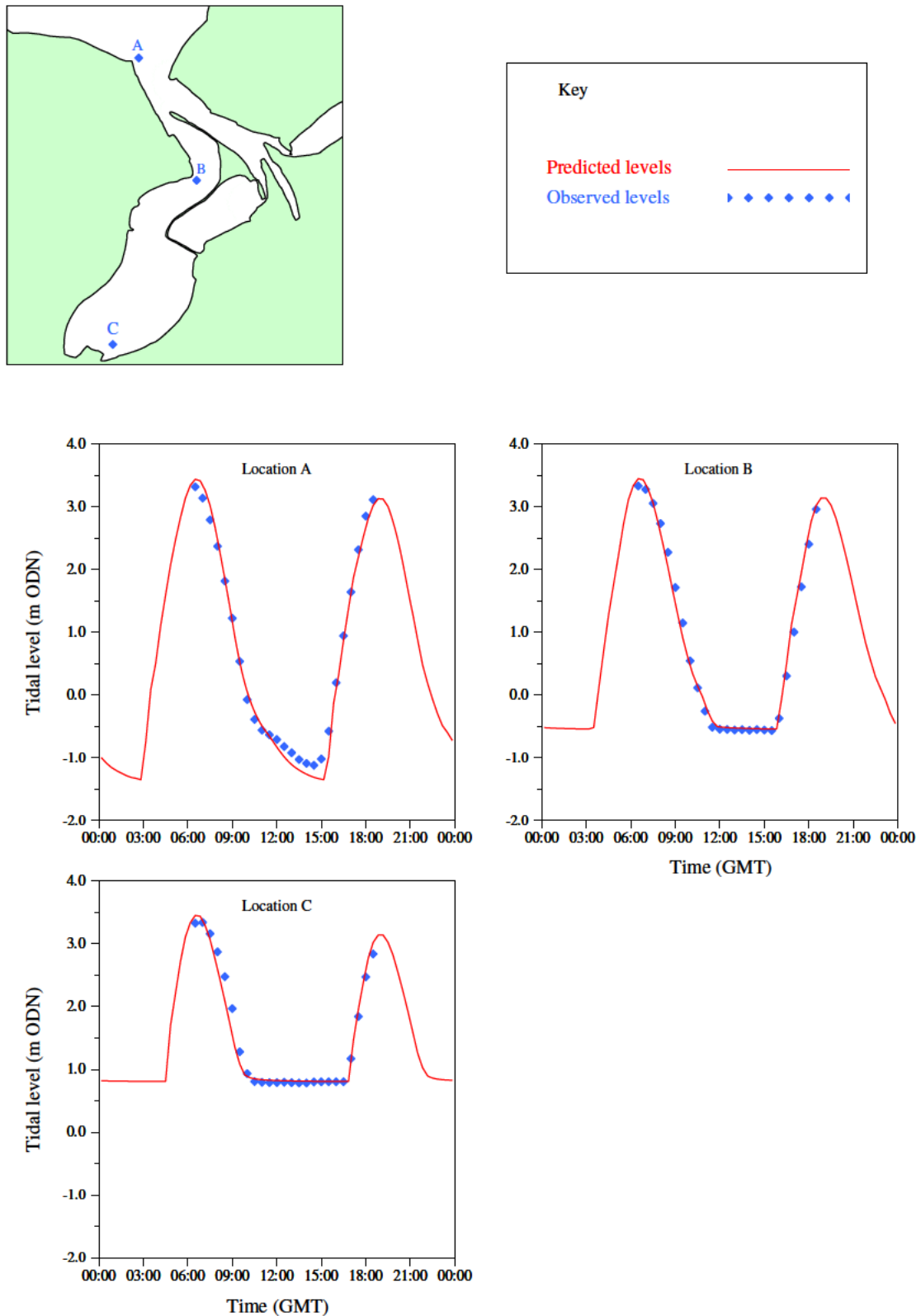
Figure 3.1 Model bathymetry (1983 data)



/HR_projects/ddr3839/model/SedimentTransport/report/Rubensp/flow_10c.RUB/fig3.2 i

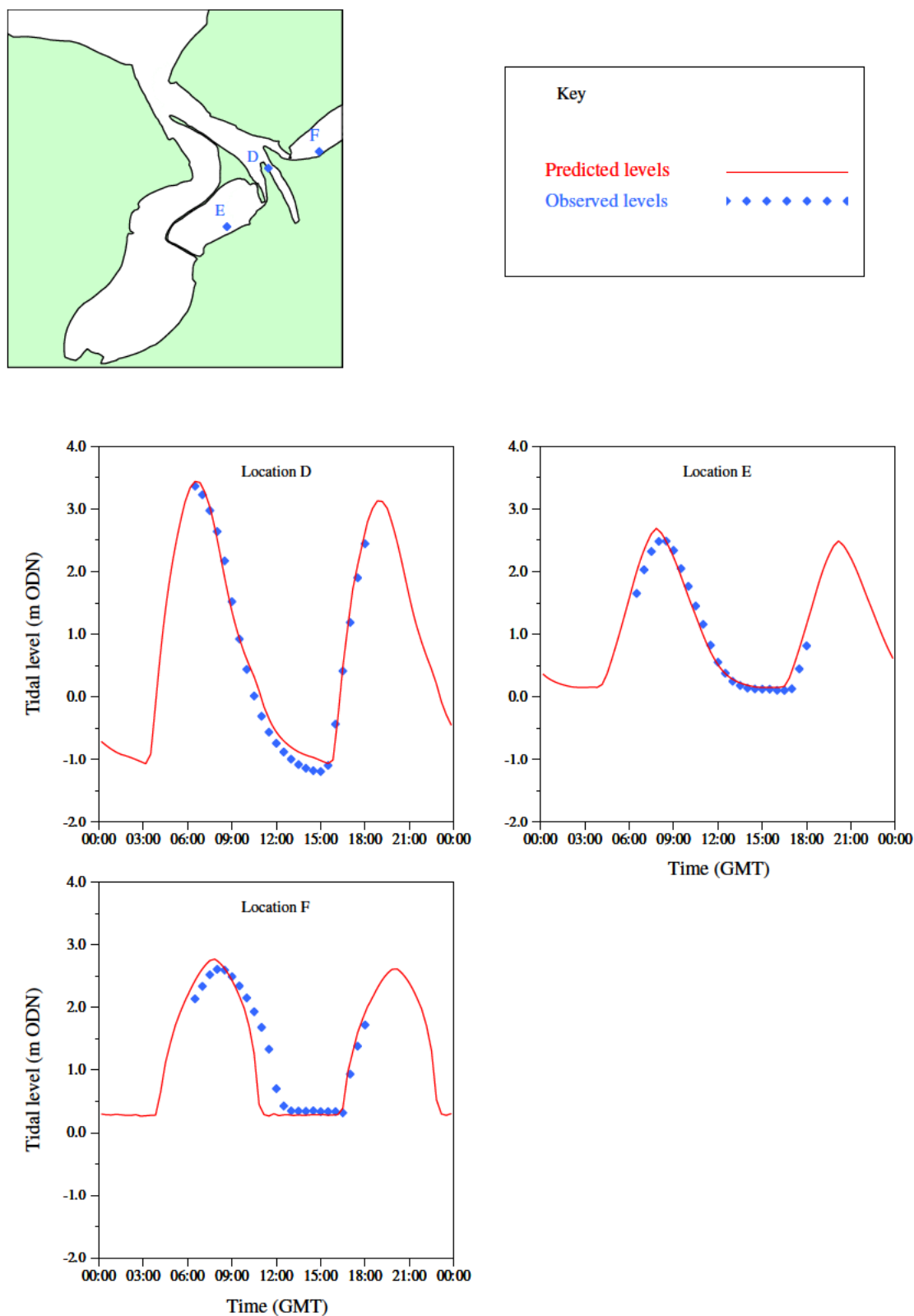
Figure 3.2 Model mesh





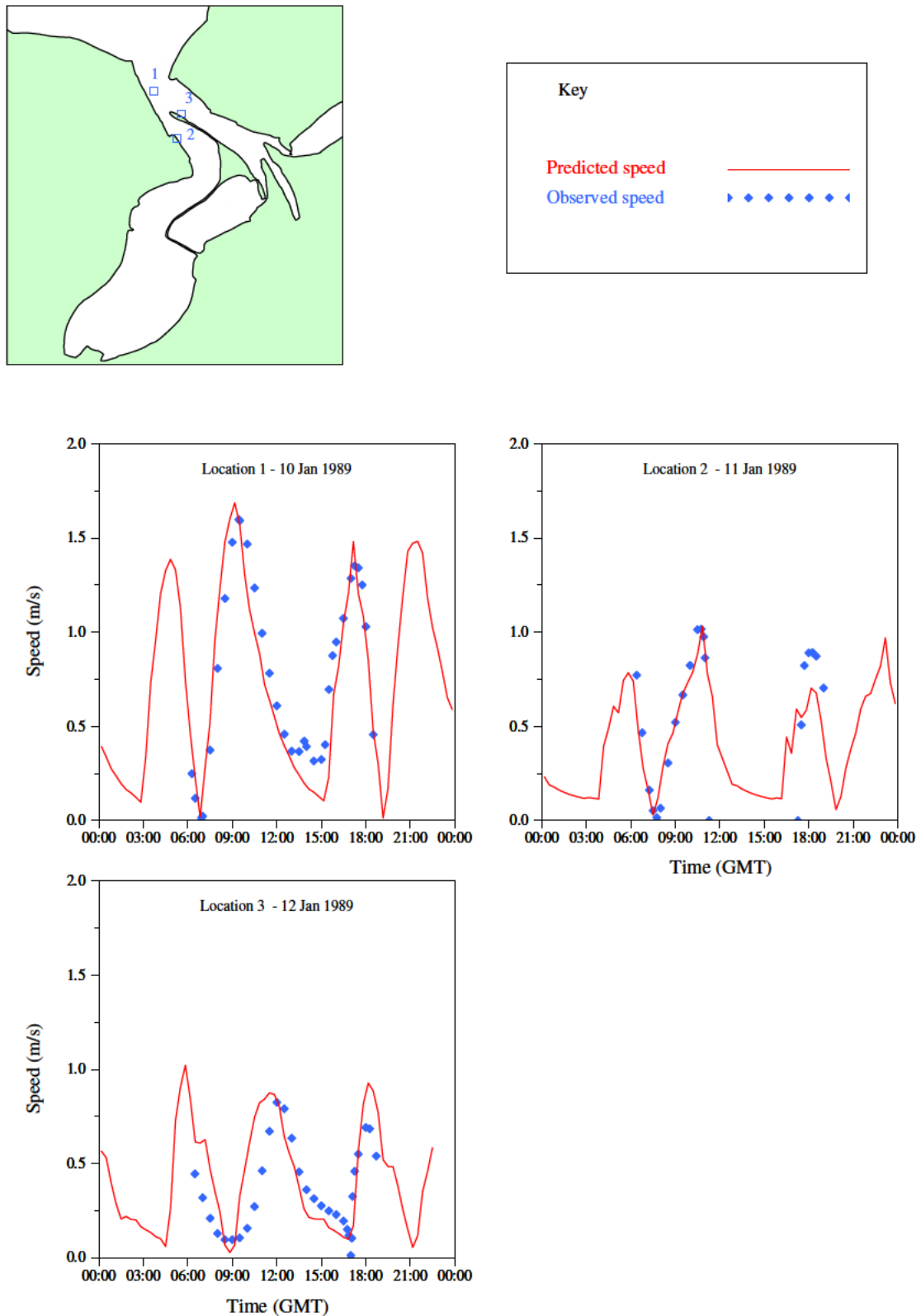
/HR_projects/ddr3839/model/SedimentTransport/report/Rubensp/flow_10c.RUB/fig3.4.i

Figure 3.4 Comparison of modelled and observed water level at Locations A,B,C 10 January 1989



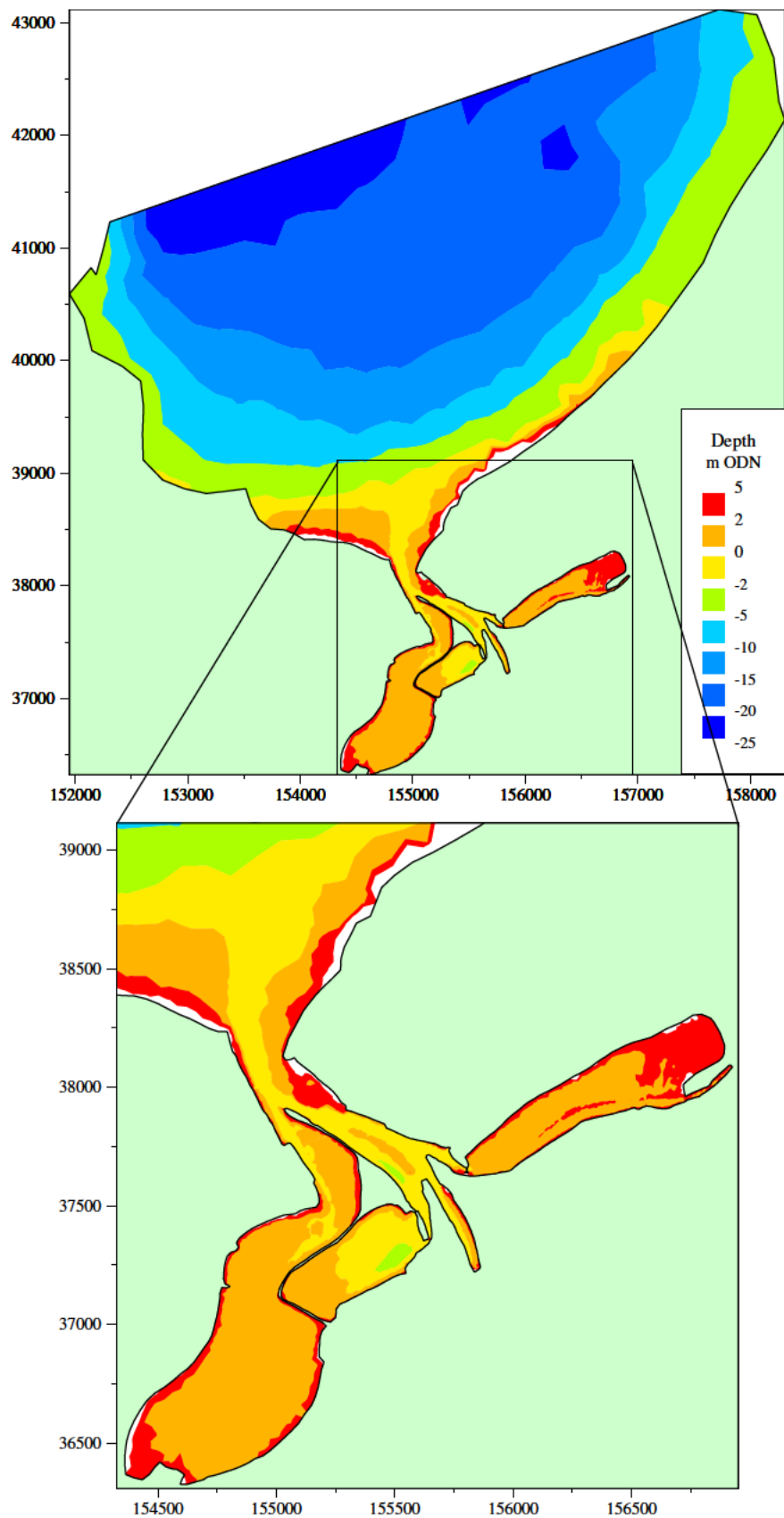
/HR_projects/ddr3839/model/SedimentTransport/report/Rubensp/flow_10c.RUB/fig3.5.i

Figure 3.5 Comparison of modelled and observed water level at Locations D,E,F 10 January 1989



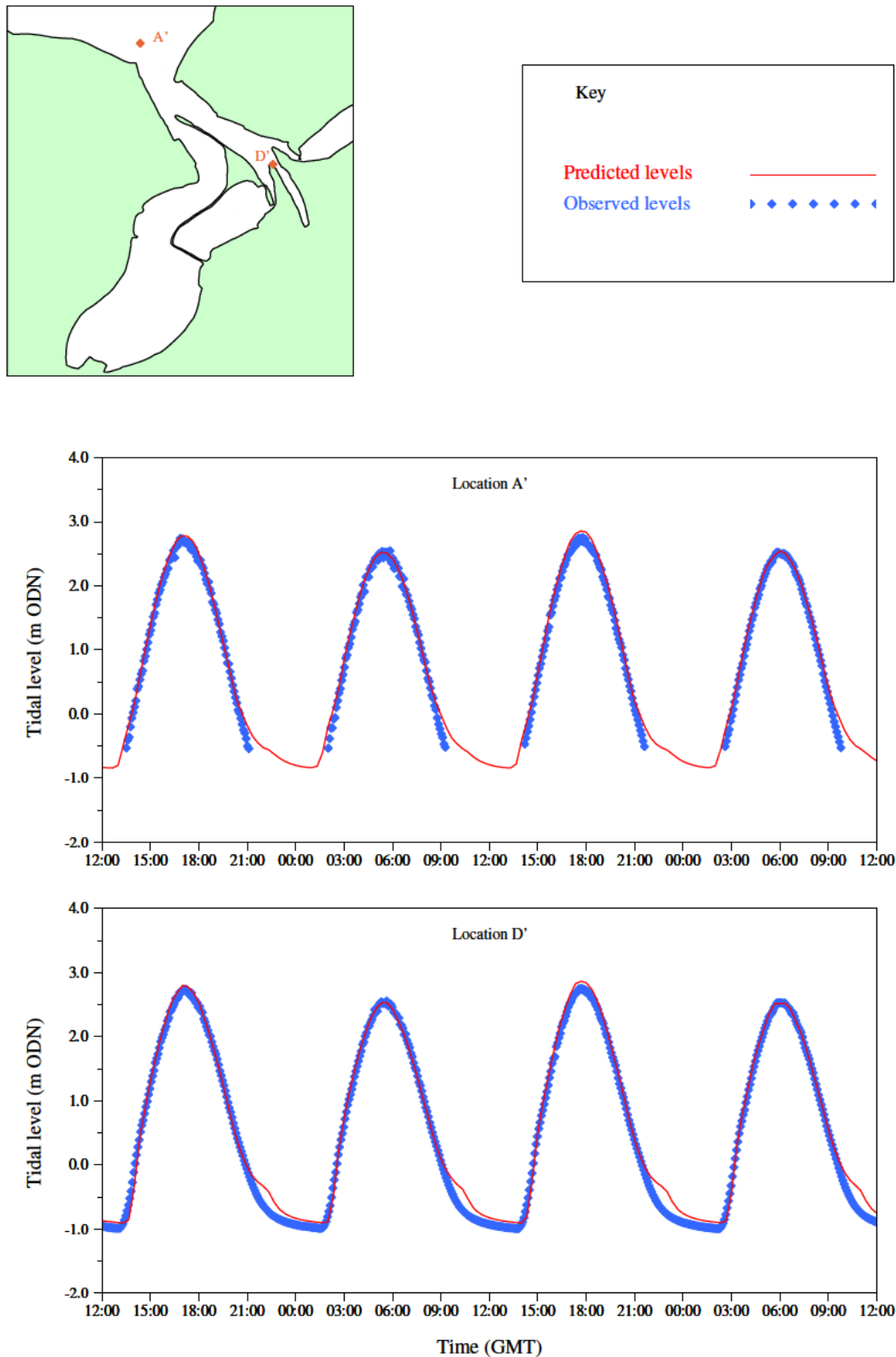
/HR_projects/ddr3839/model/SedimentTransport/report/Rubensp/flow_10c.RUB/fig3.6.i

Figure 3.6 Comparison of modelled and observed tidal currents at Locations 1,2,3 10-12 January 1989



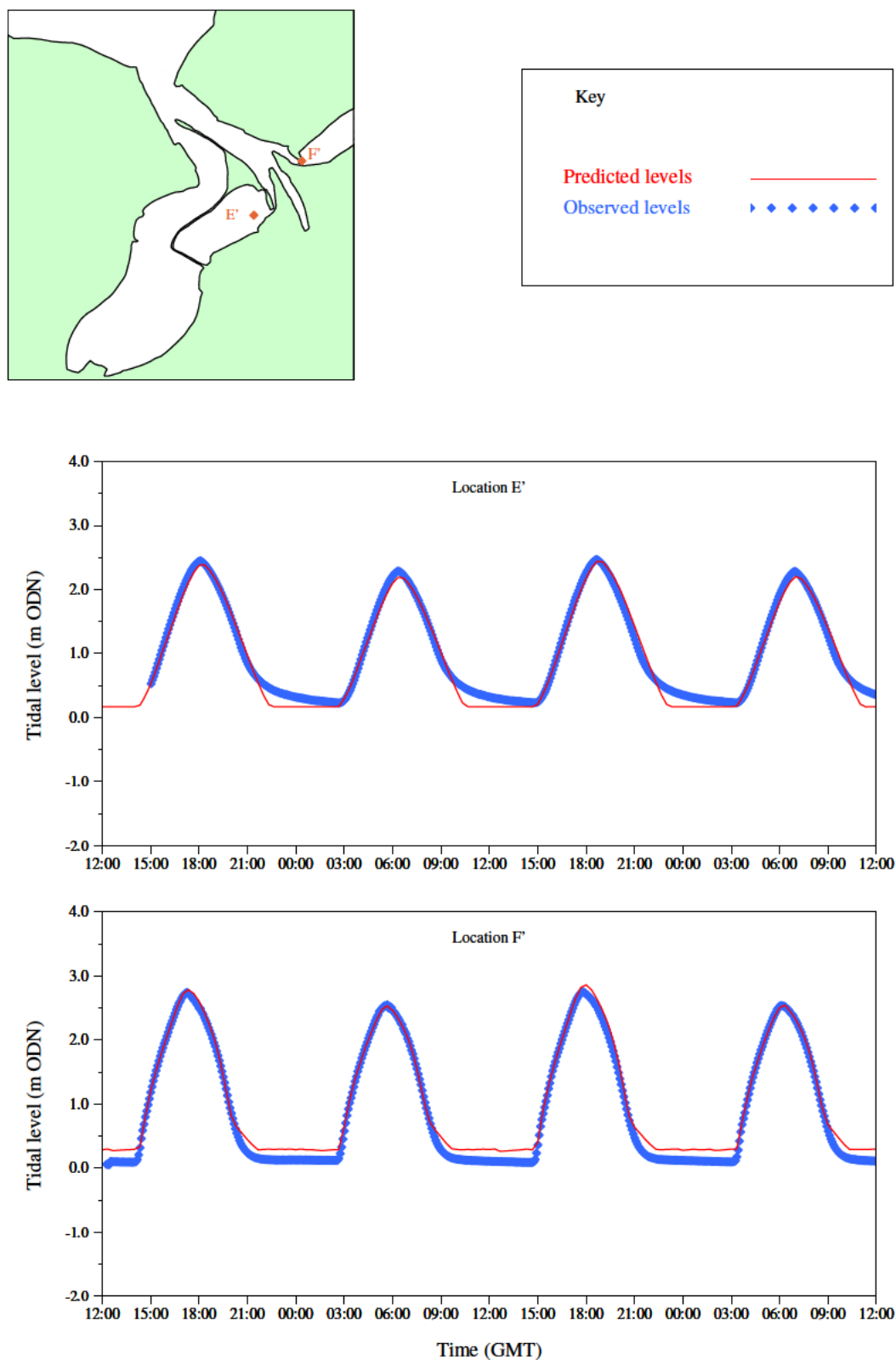
/HR_projects/ddr3839/model/SedimentTransport/report/Rubensp/flow_valid02.RUB/fig3.7.i

Figure 3.7 Model baseline bathymetry (2005 data)



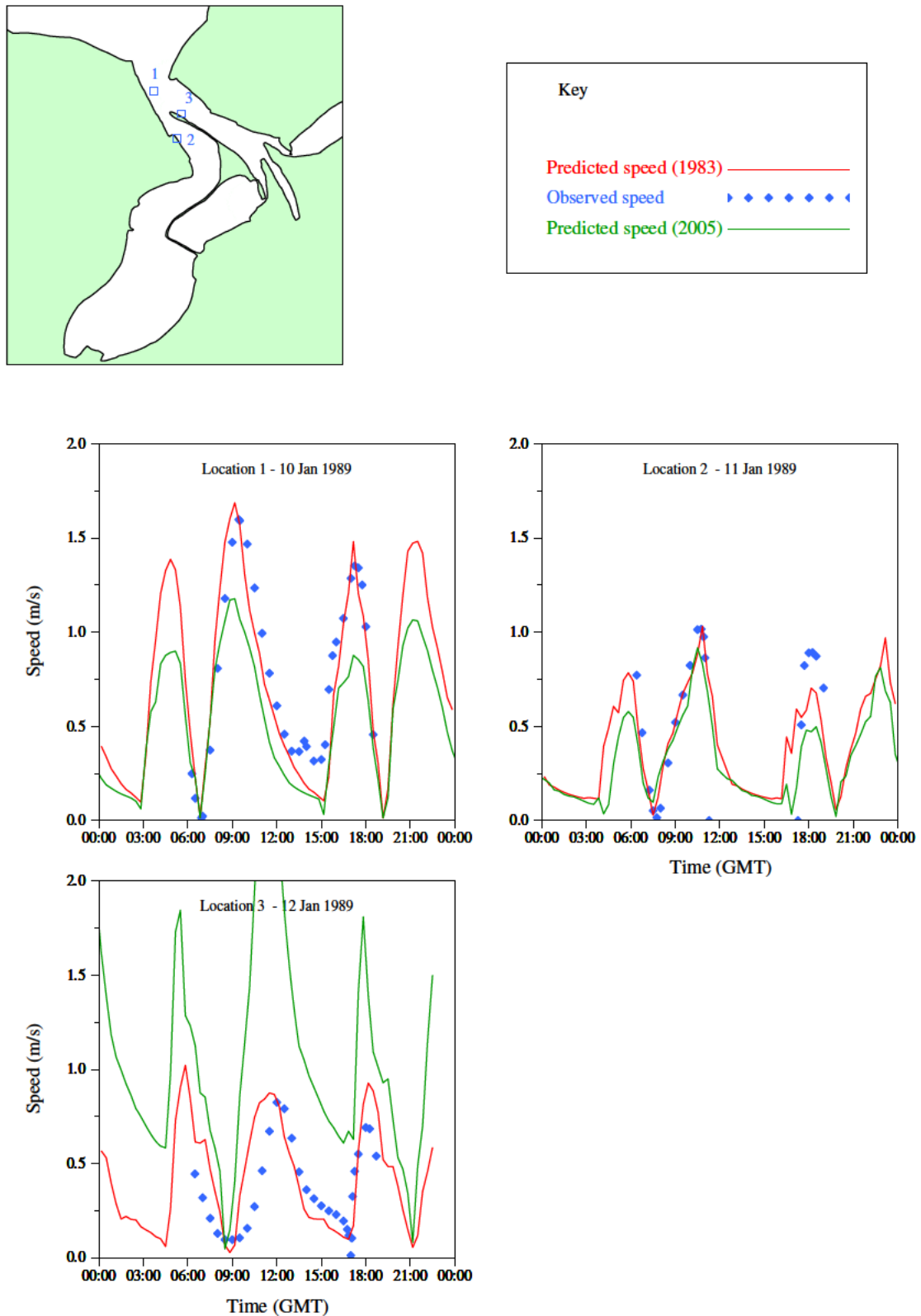
/HR_projects/ddr3839/model/SedimentTransport/report/Rubensp/flow_valid02.RUB/fig3.8.i

Figure 3.8 Comparison of modelled and observed water level at Locations A' and D' 6-8 July 2005



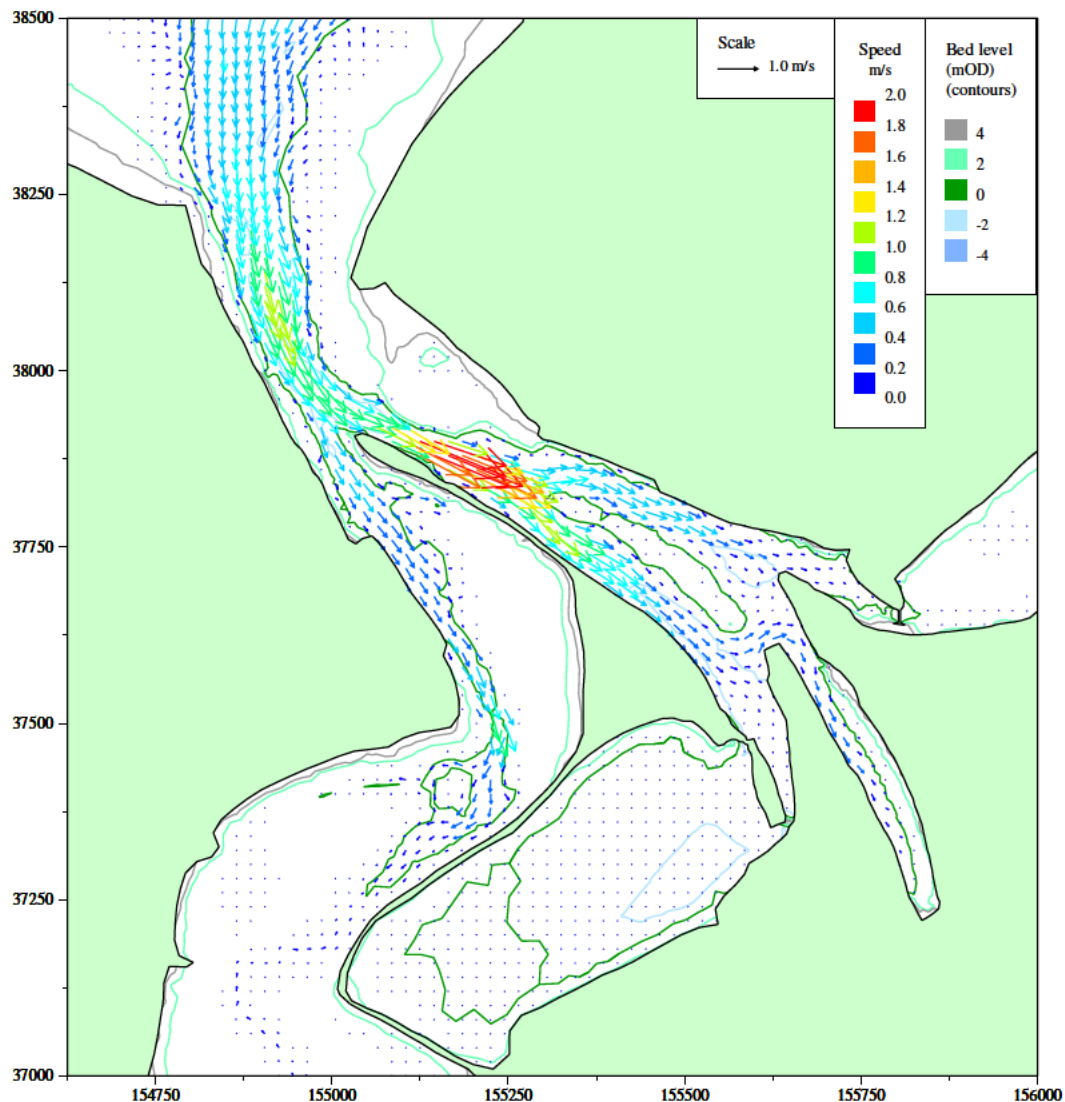
/HR_projects/ddr3839/model/SedimentTransport/report/Rubensp/flow_valid02.RUB/fig3.9.i

Figure 3.9 Comparison of modelled and observed water level at Locations E' and F' 6-8 July 2005



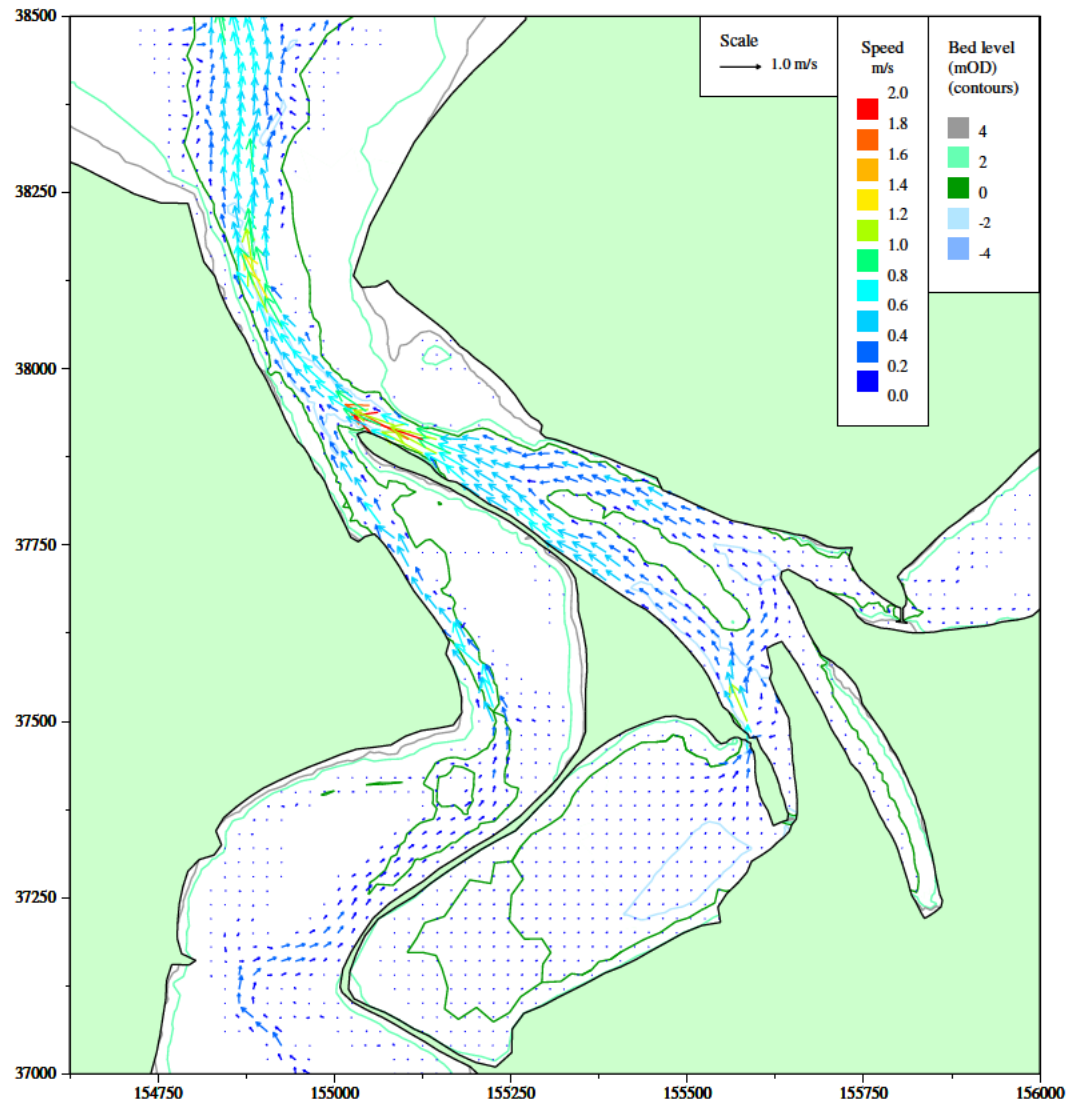
/HR_projects/ddr3839/model/SedimentTransport/report/Rubensp/flow_exist02c.RUB/fig3.10.i

Figure 3.10 Highlighting variability in modelled tidal currents for identical tide conditions (10 Jan 1989) using 1983 and 2005 bathymetry



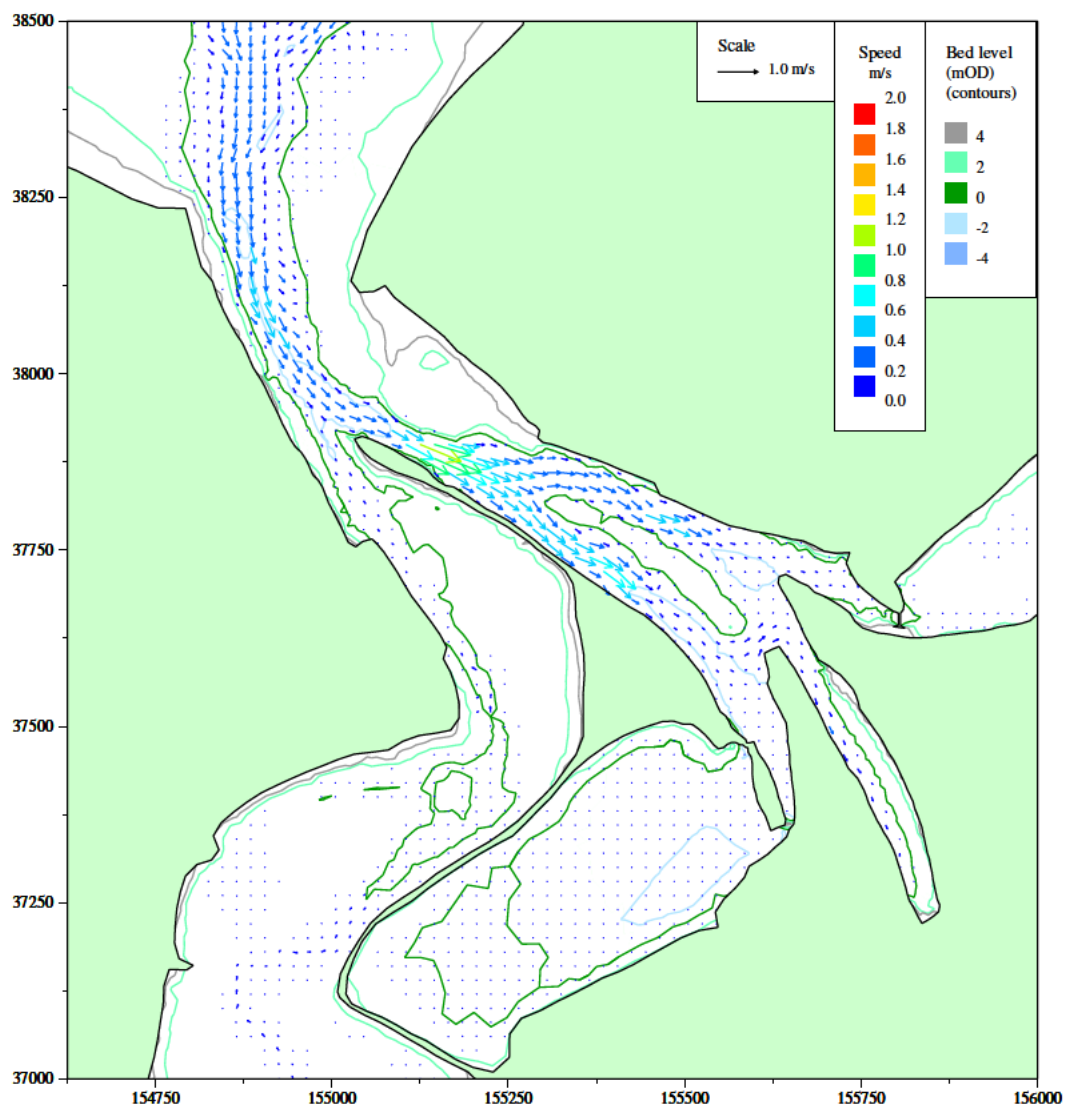
/HR_projects/ddr3839/model/SedimentTransport/report/Rubensp/flow_sp_sum05a.RUB/fig3.11.i

Figure 3.11 Baseline conditions spring tide flood currents (HW+9.5 Hours), Copperhouse sluice open (summer condition), single sluice operation on Carnsew Pool



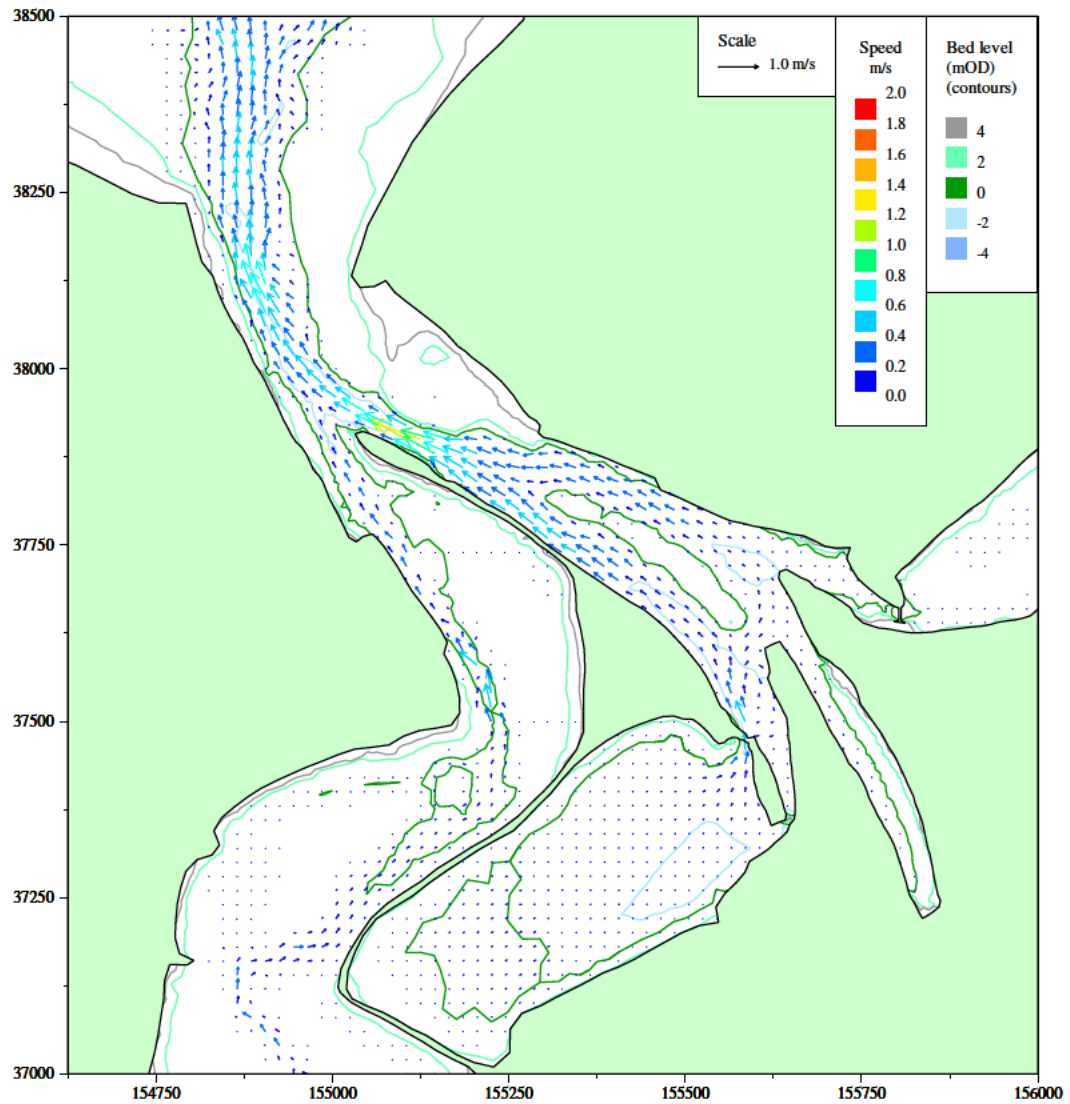
/HR_projects/ddr3839/model/SedimentTransport/report/Rubensp/flow_sp_sum05a.RUB/fig3.12.i

Figure 3.12 Baseline conditions spring tide ebb currents (HW+4.5 Hours), Copperhouse sluice open (summer condition), single sluice operation on Carnsew Pool



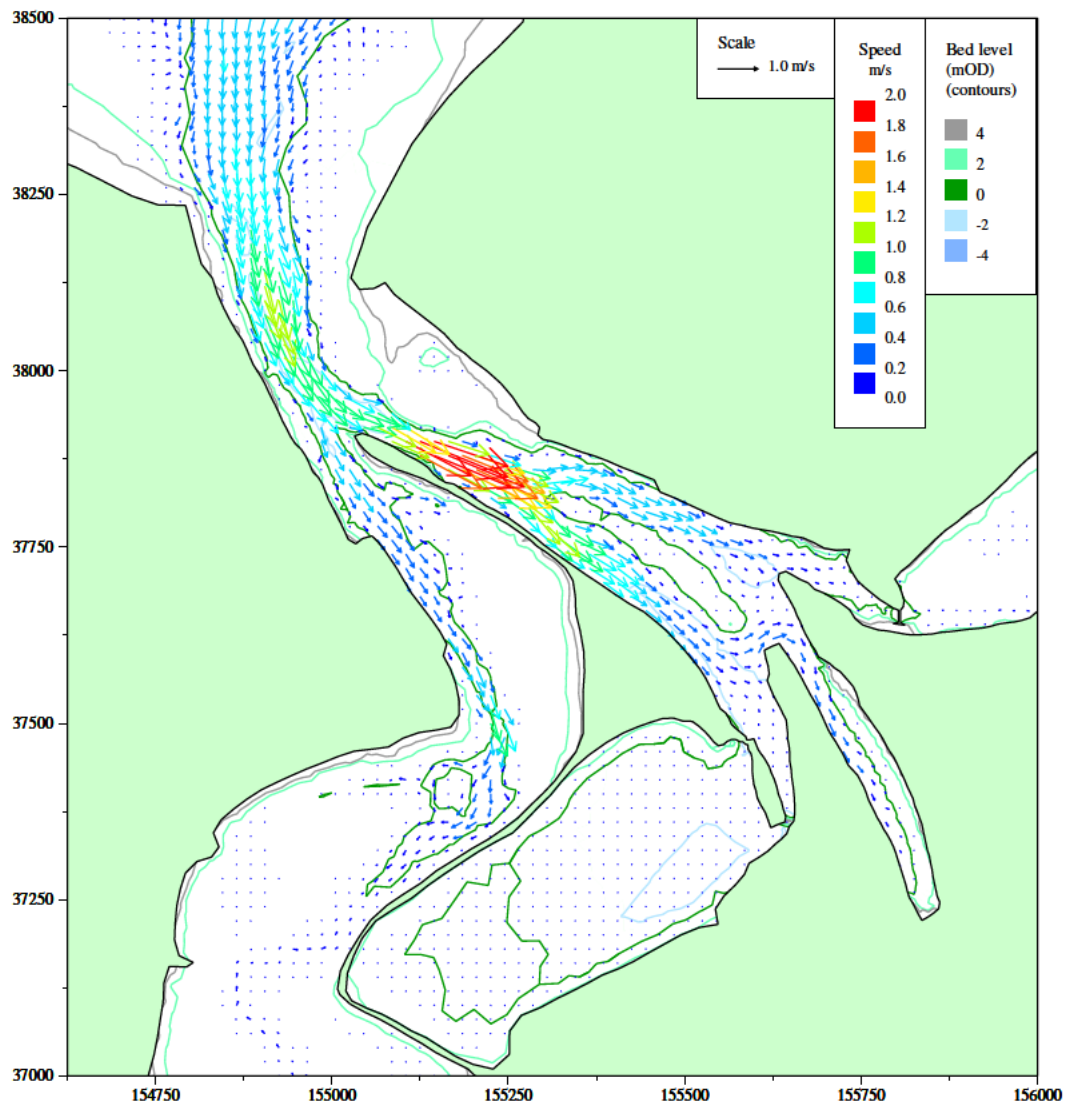
/HR_projects/ddr3839/model/SedimentTransport/report/Rubensp/flow_neap05.RUB/fig3.13.i

Figure 3.13 Baseline conditions neap tide flood currents (HW+9.0 Hours), Copperhouse sluice open (summer condition), single sluice operation on Carnsew Pool



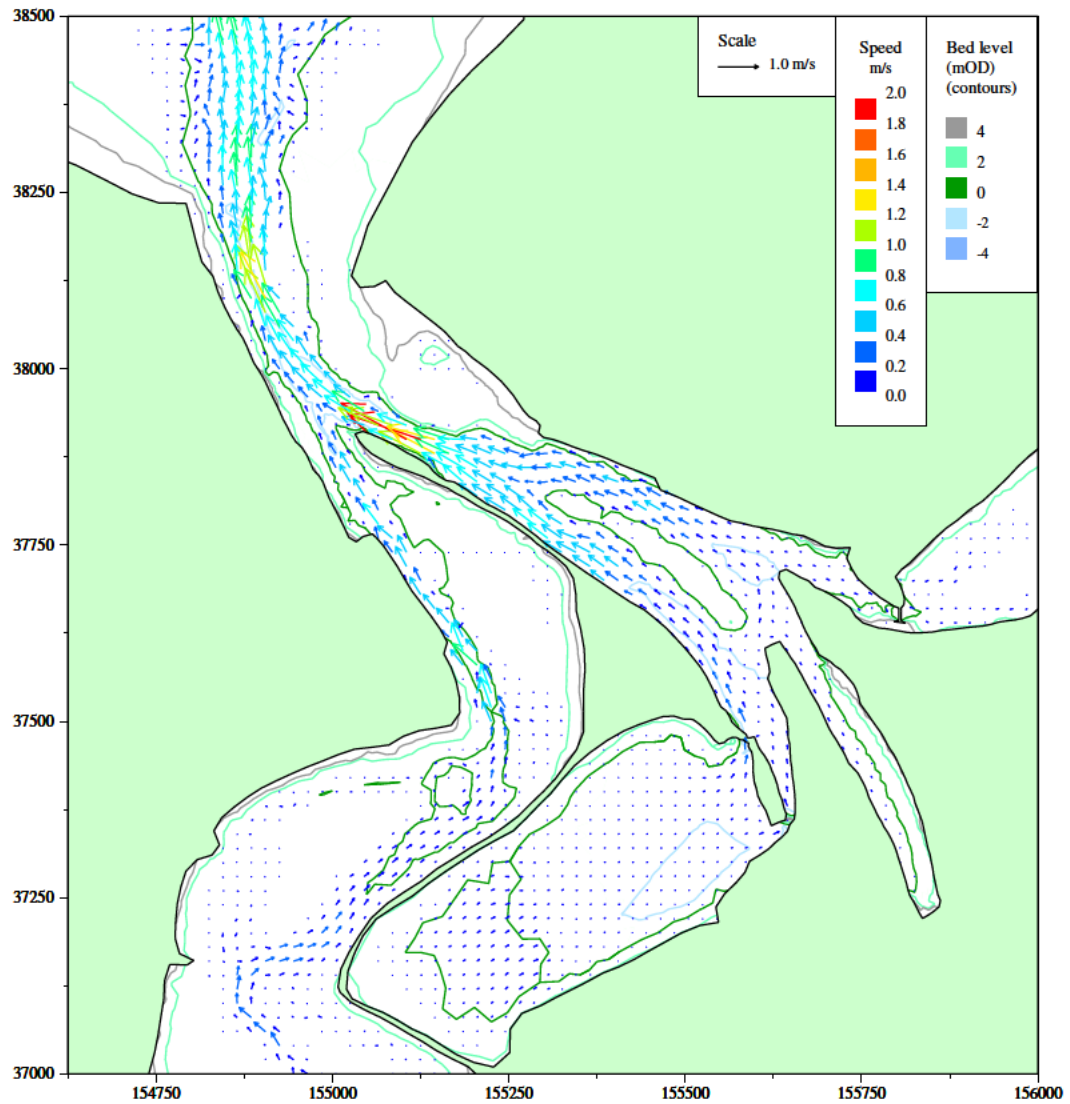
/HR_projects/ddr3839/model/SedimentTransport/report/Rubensp/flow_neap05.RUB/fig3.14.i

Figure 3.14 Baseline conditions neap tide ebb currents (HW+4.5 Hours), Copperhouse sluice open (summer condition), single sluice operation on Carnsew Pool



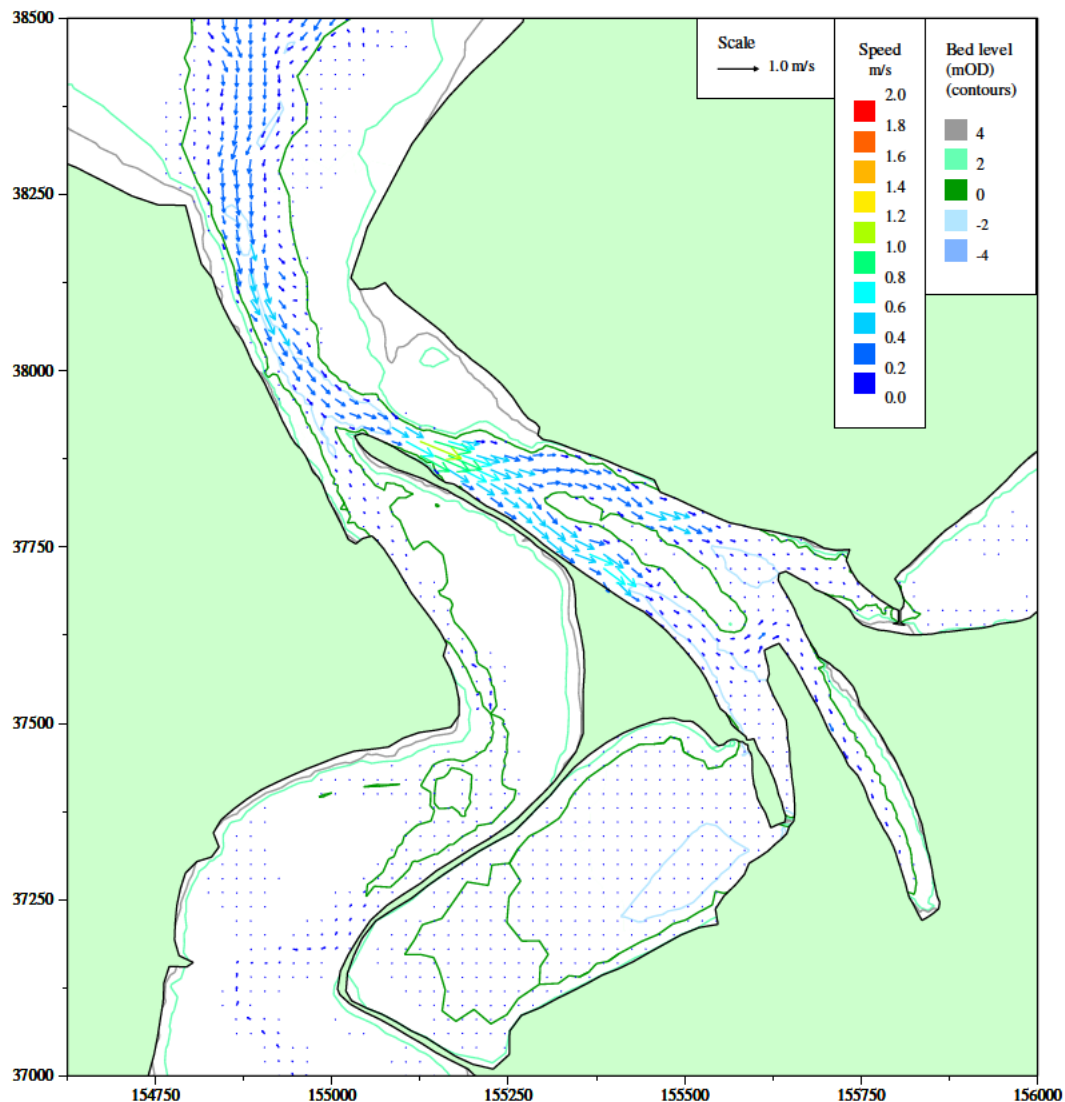
/HR_projects/ddr3839/model/SedimentTransport/report/Rubensp/flow_sp_sum05b.RUB/fig3.15.i

Figure 3.15 Baseline conditions spring tide flood currents (HW+9.5 Hours), Copperhouse sluice open (summer condition), double sluice operation on Carnsew Pool



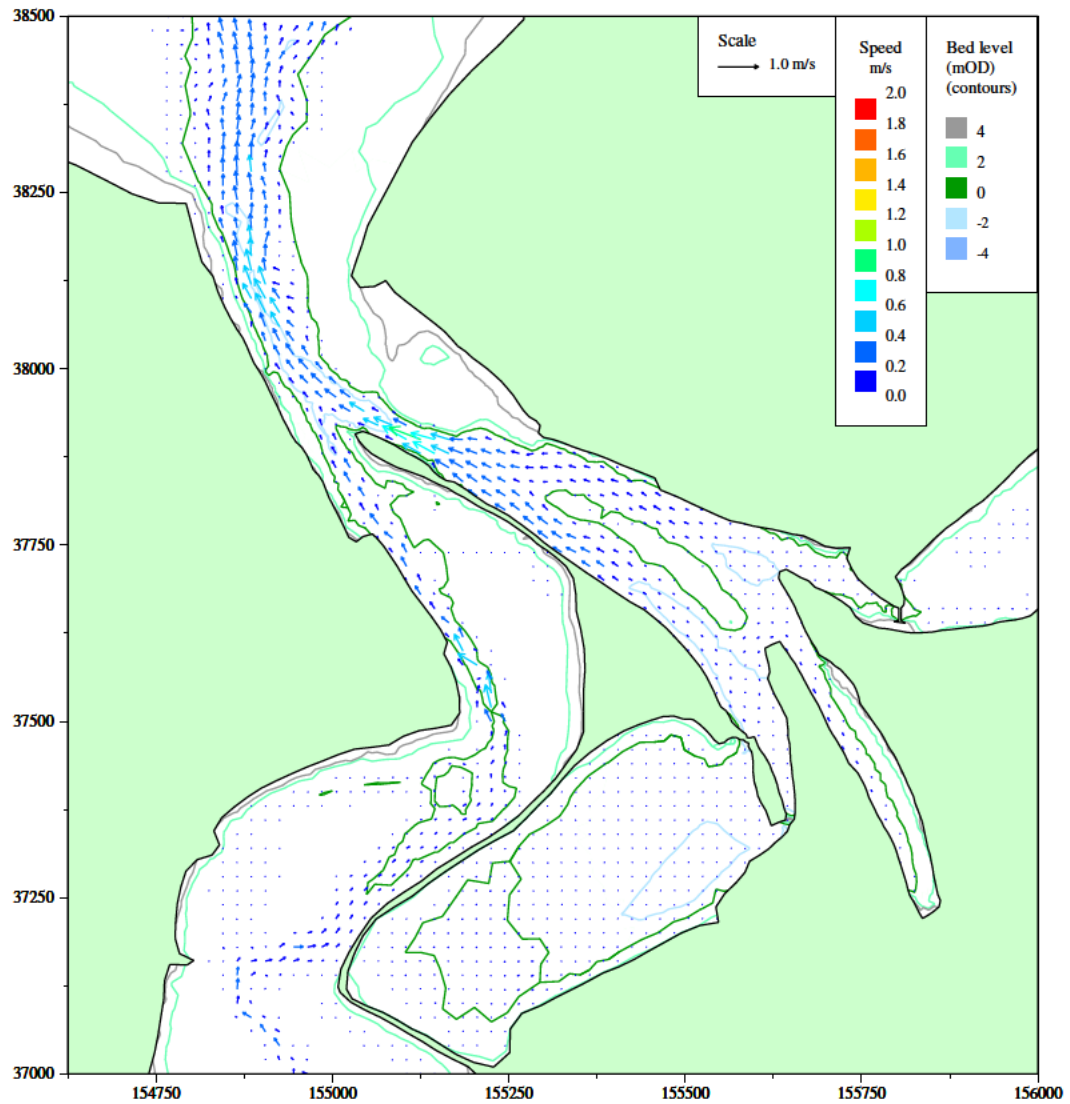
/HR_projects/ddr3839/model/SedimentTransport/report/Rubensp/flow_sum05b.RUB/fig3.16.i

Figure 3.16 Baseline conditions spring tide ebb currents (HW+4.5 Hours), Copperhouse sluice open (summer condition), double sluice operation on Carnsew Pool



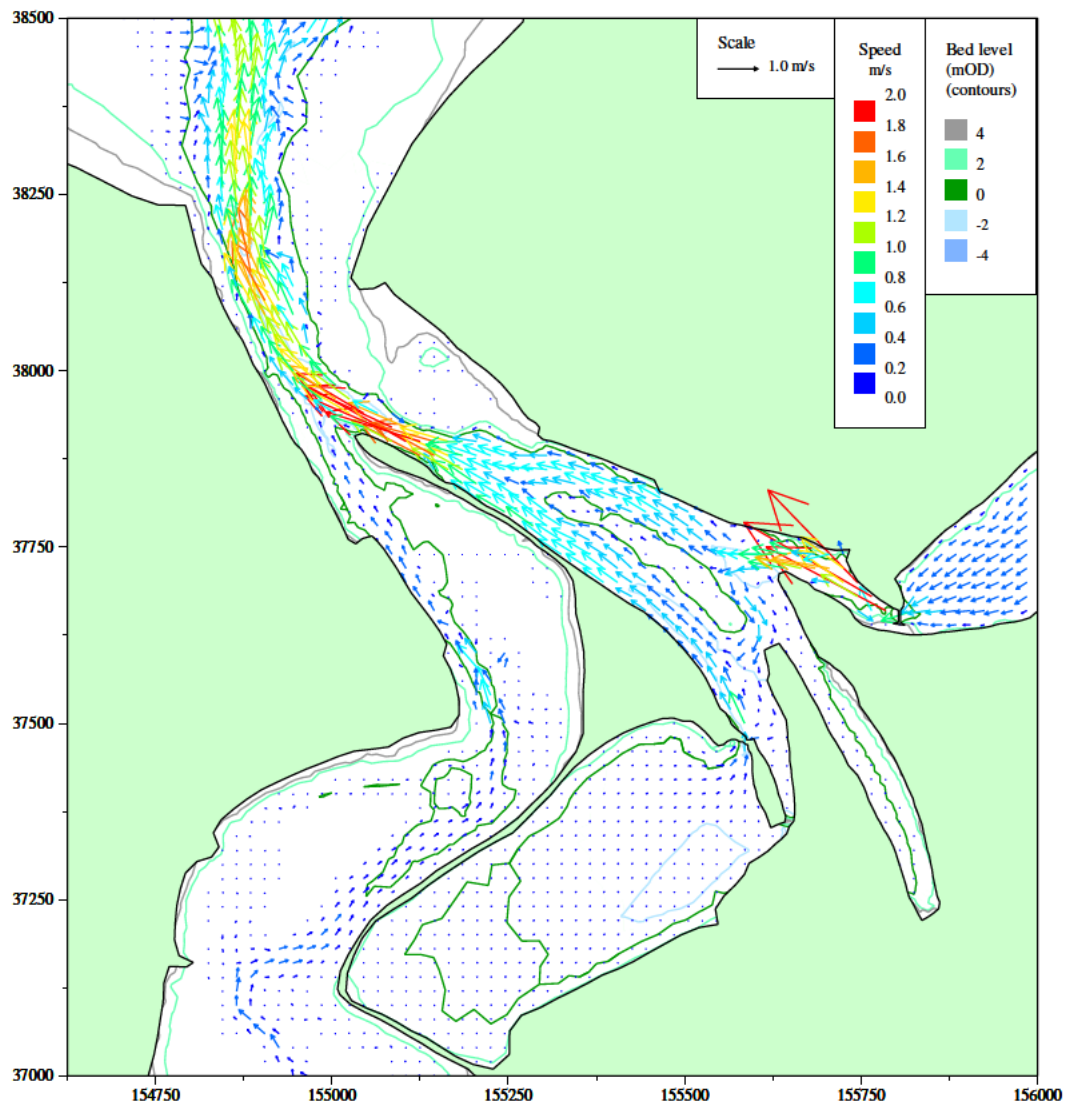
/HR_projects/ddr3839/model/SedimentTransport/report/Rubensp/flow_neap05b.RUB/fig3.17.i

Figure 3.17 Baseline conditions neap tide flood currents (HW+9.0 Hours), Copperhouse sluice open (summer condition), double sluice operation on Carnsew Pool



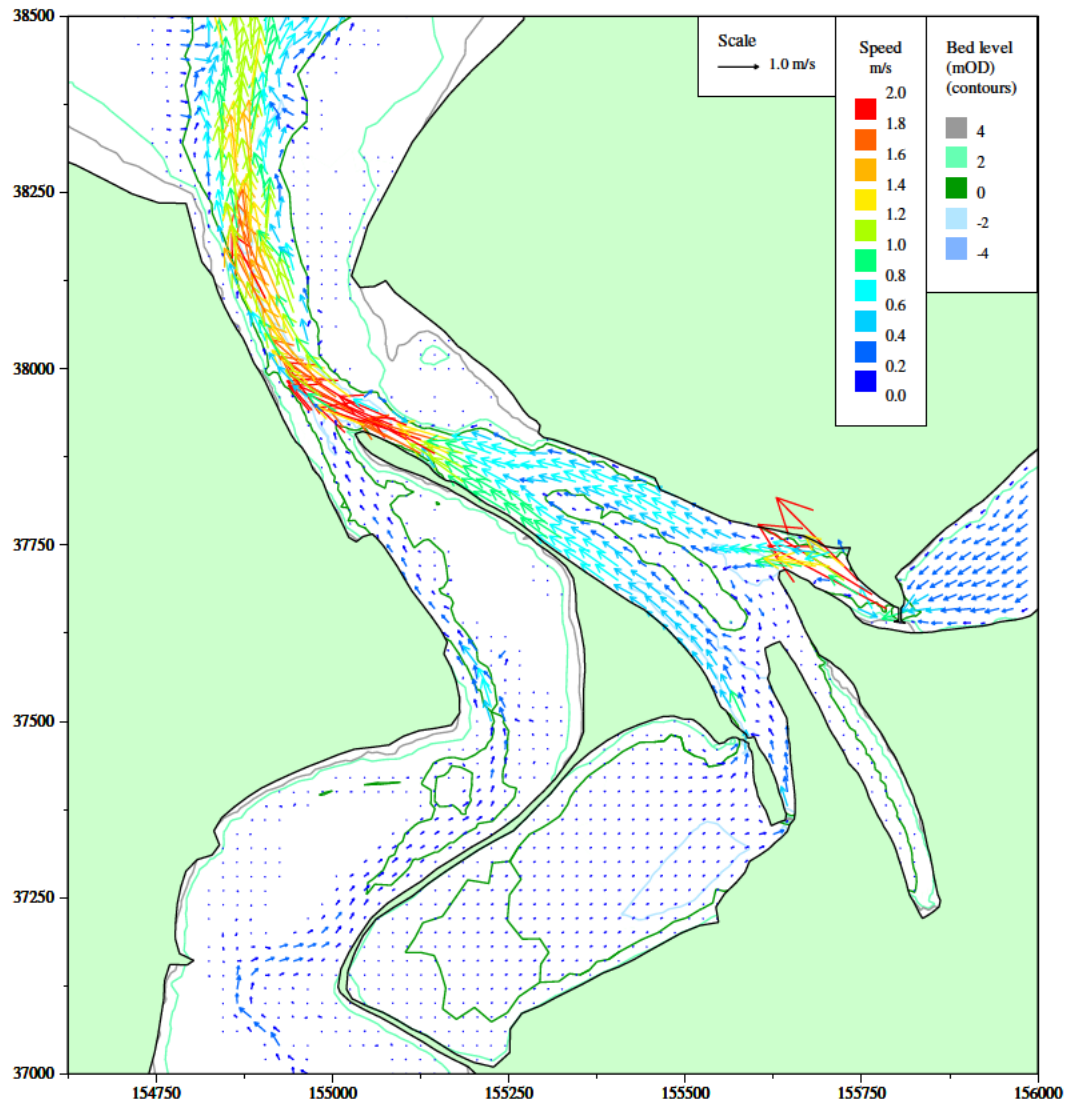
/HR_projects/ddr3839/model/SedimentTransport/report/Rubensp/flow_neap05b.RUB/fig3.18.i

Figure 3.18 Baseline conditions neap tide ebb currents (HW+4.5 Hours), Copperhouse sluice open (summer condition), double sluice operation on Carnsew Pool



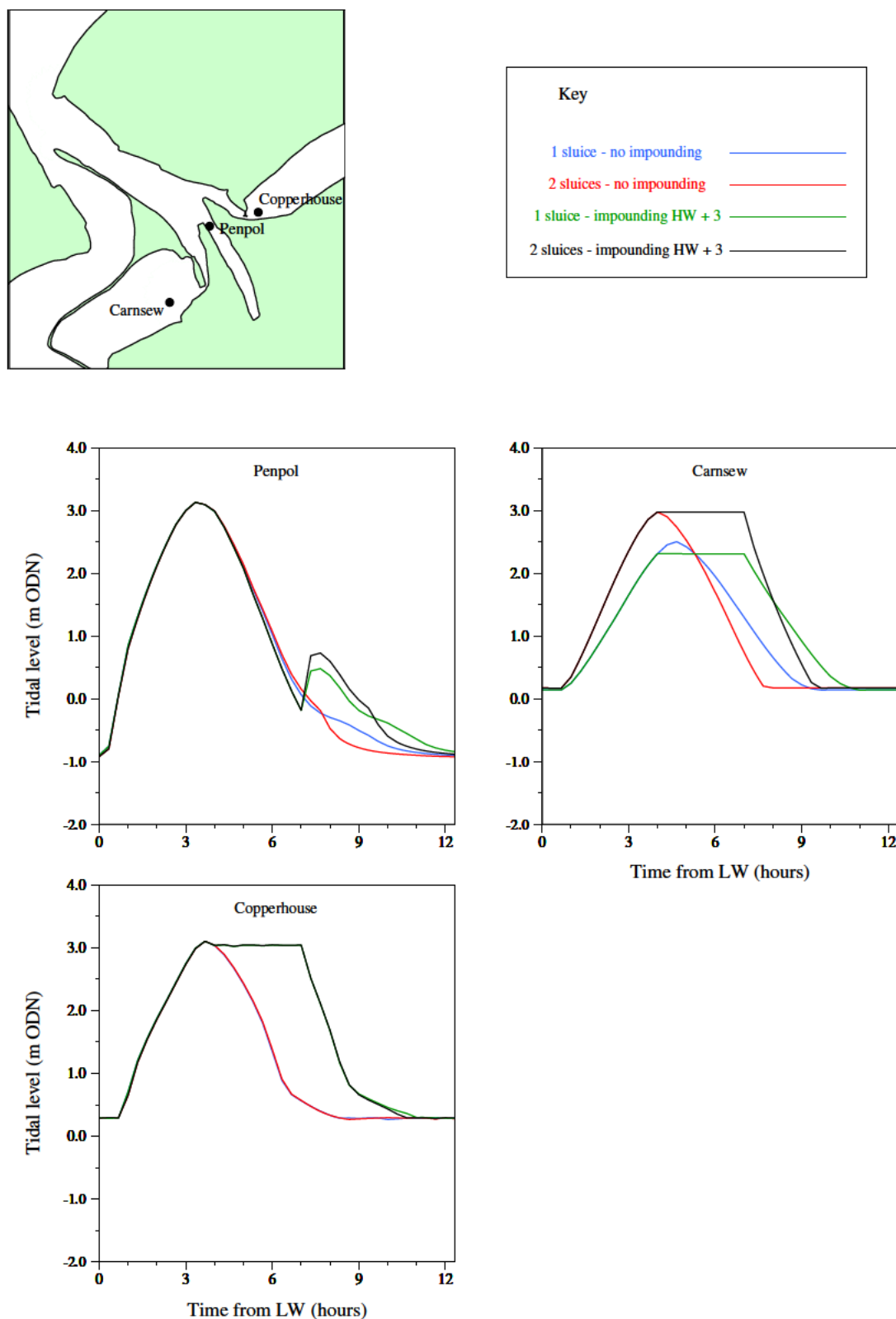
/HR_projects/ddr3839/model/SedimentTransport/report/Rubensp/flow_impound05a.RUB/fig3.19.i

Figure 3.19 Baseline conditions spring tide peak ebb currents with impounding in Carnsew and Copperhouse Pools to HW + 3 hours, single sluice operation on Carnsew Pool



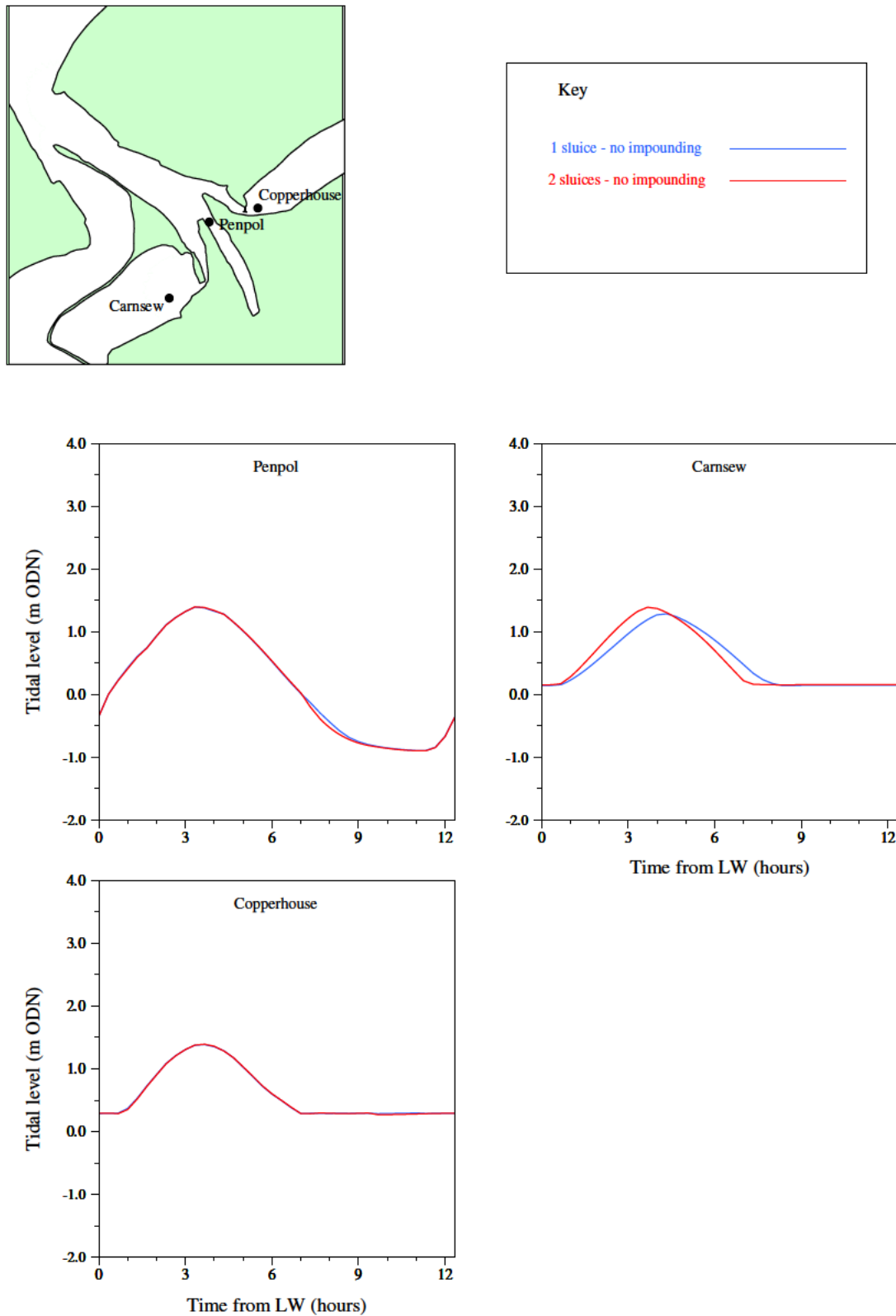
/HR_projects/ddr3839/model/SedimentTransport/report/Rubensp/flow_impound05b.RUB/fig3.20.i

Figure 3.20 Baseline conditions spring tide peak ebb currents with impounding in Carnsew and Copperhouse Pools to HW + 3 hours, double sluice operation on Carnsew Pool



/HR_projects/ddr3839/model/SedimentTransport/report/Rubensp/flow_sp_sum05a.RUB/fig3.21.i

Figure 3.21 Comparison of modelled spring tide water levels



/HR_projects/ddr3839/model/SedimentTransport/report/Rubensp/flow_neap05.RUB/fig3.22.i

Figure 3.22 Comparison of modelled neap tide water levels

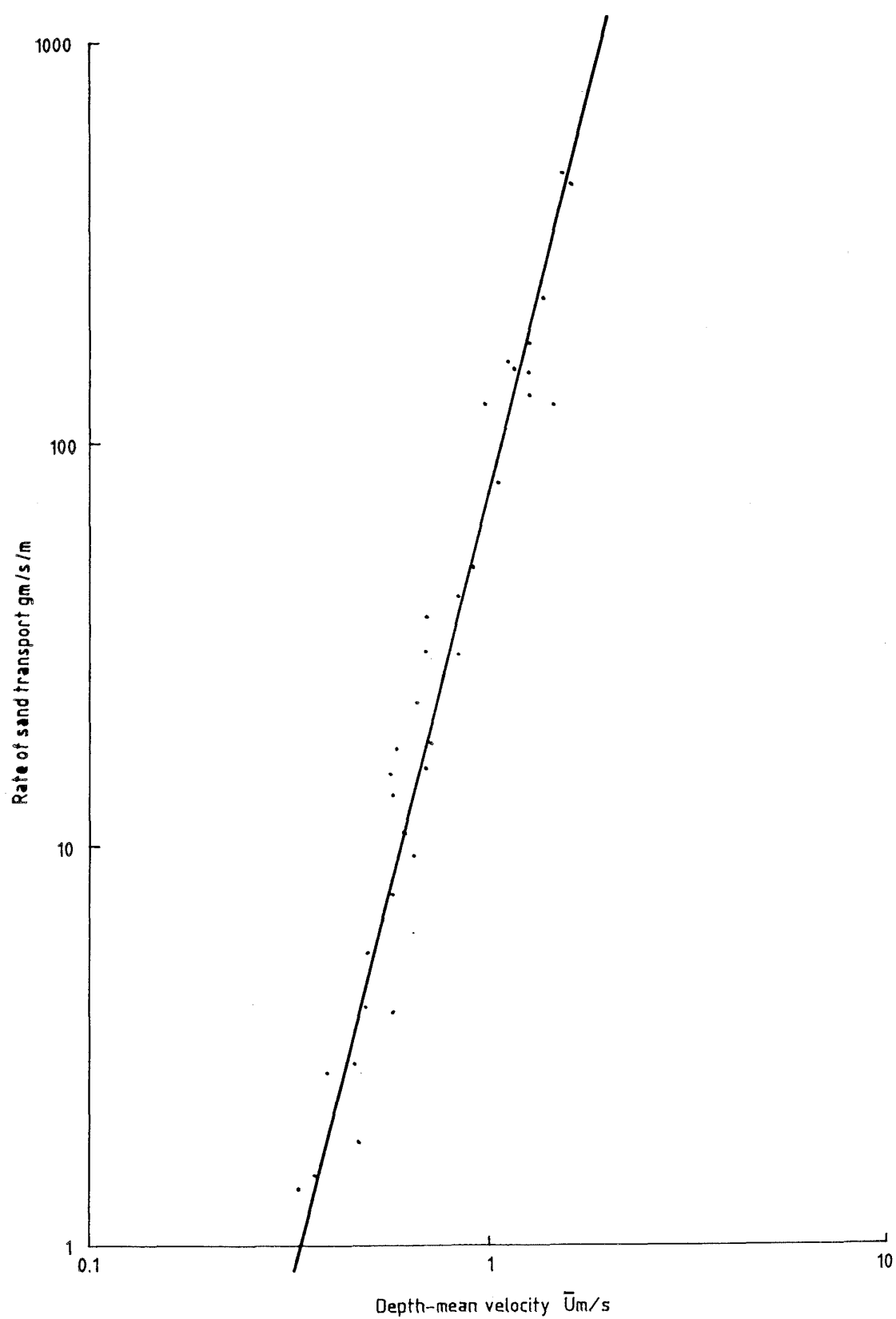
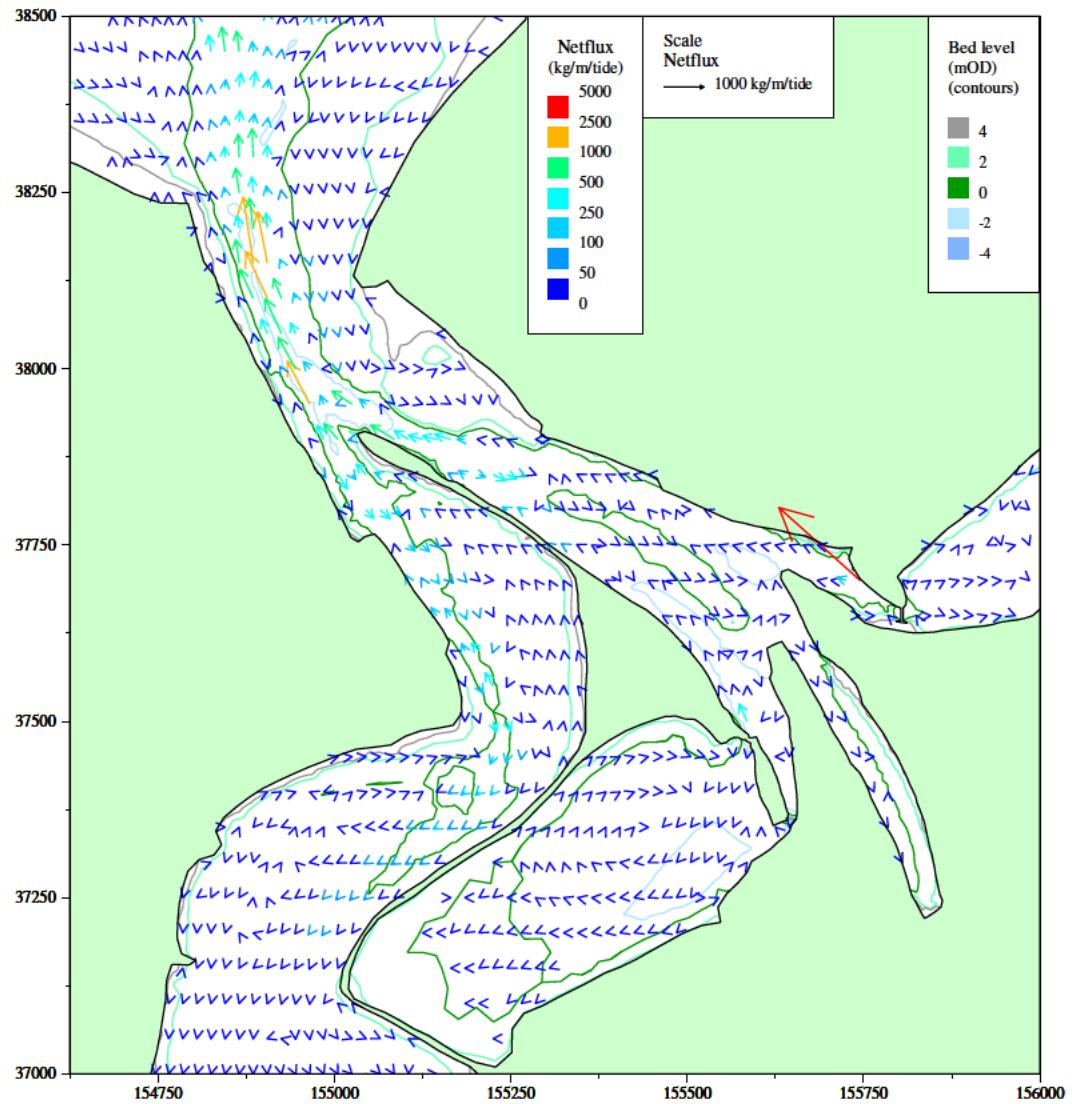
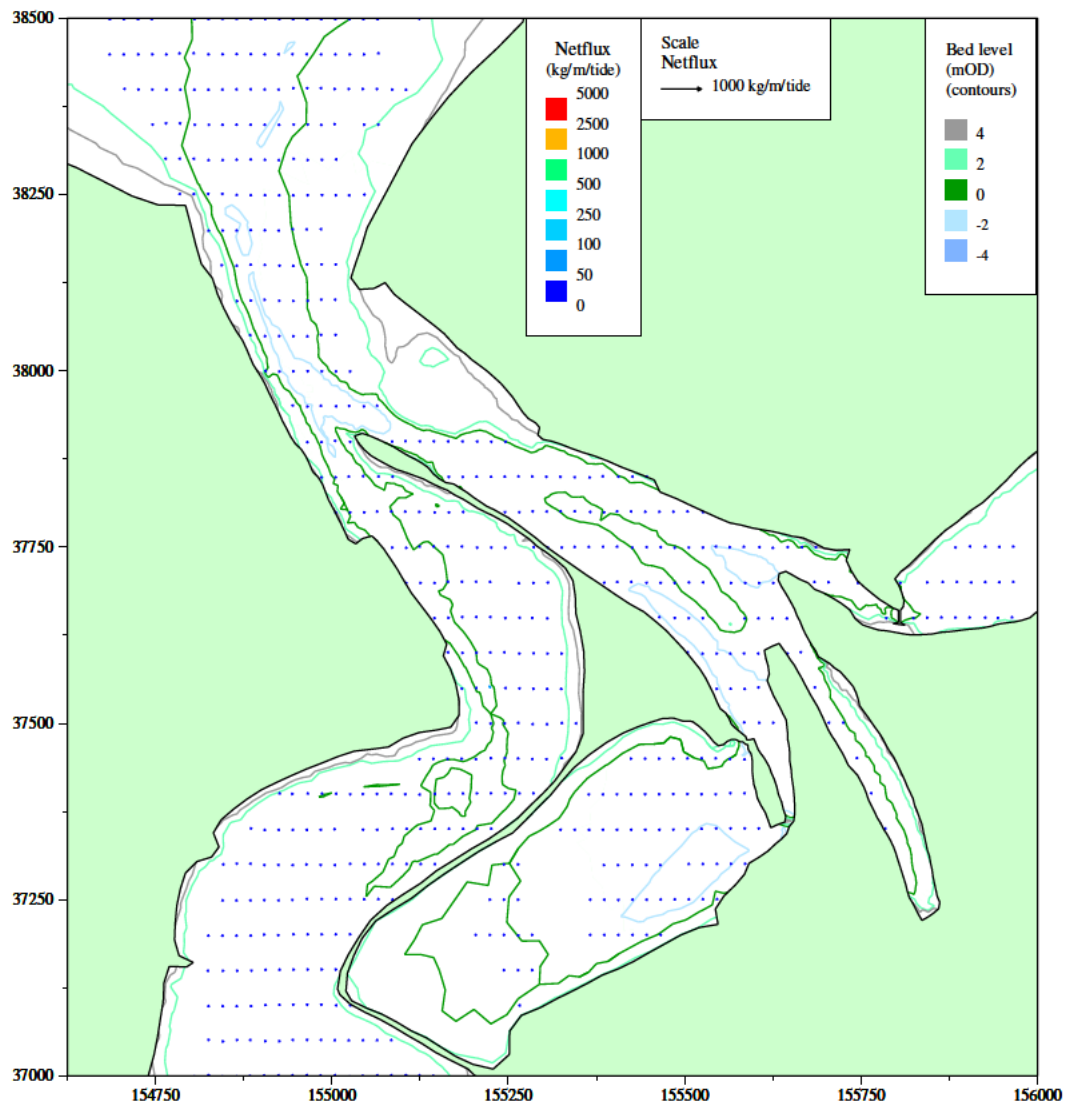


Figure 3.23 Sand transport algorithm



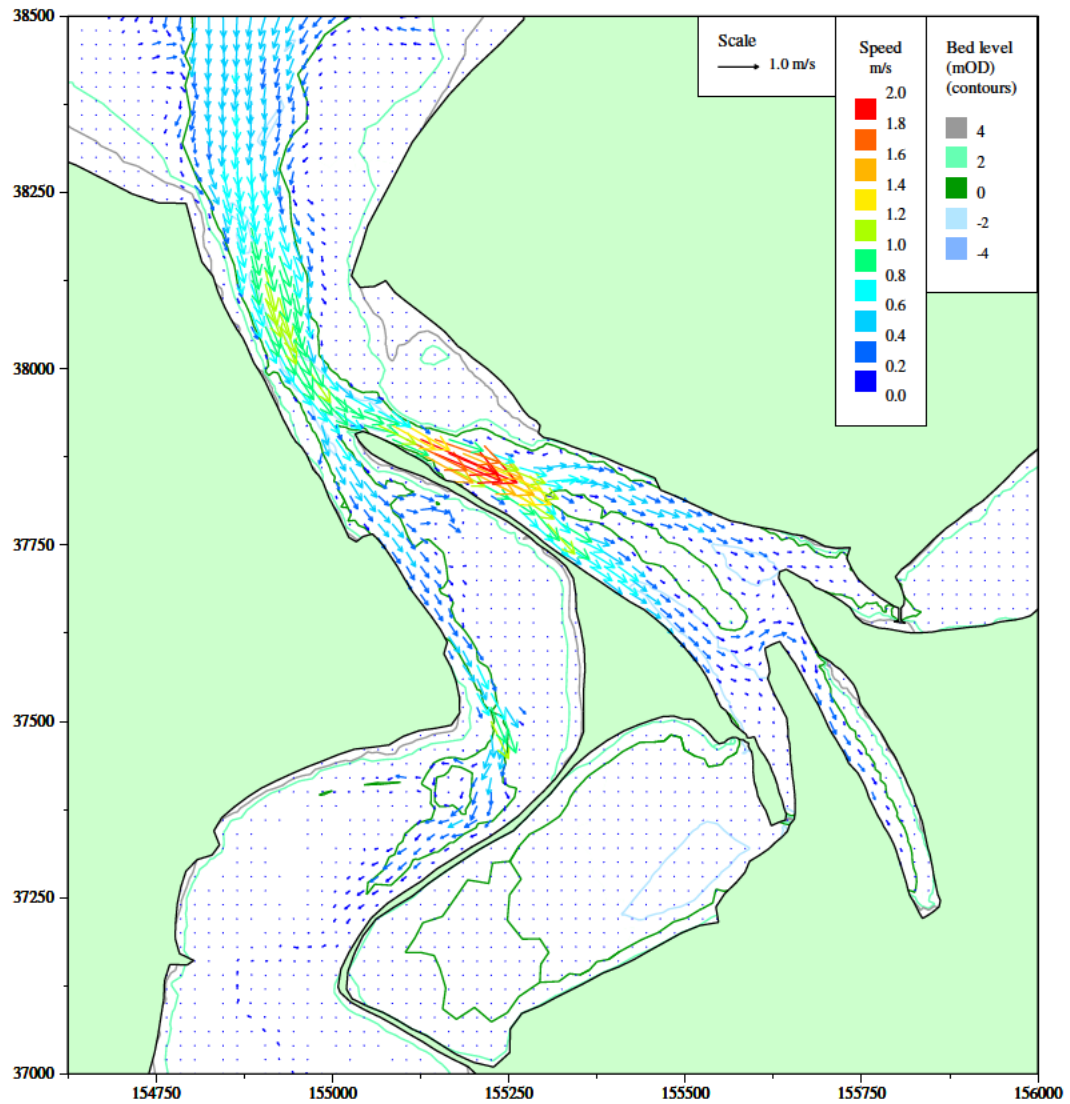
/HR_projects/ddr3839/model/SedimentTransport/report/Rubensp/sand_spr_nowaves.RUB/fig3.24.i

Figure 3.24 Baseline conditions spring tide net sand flux patterns



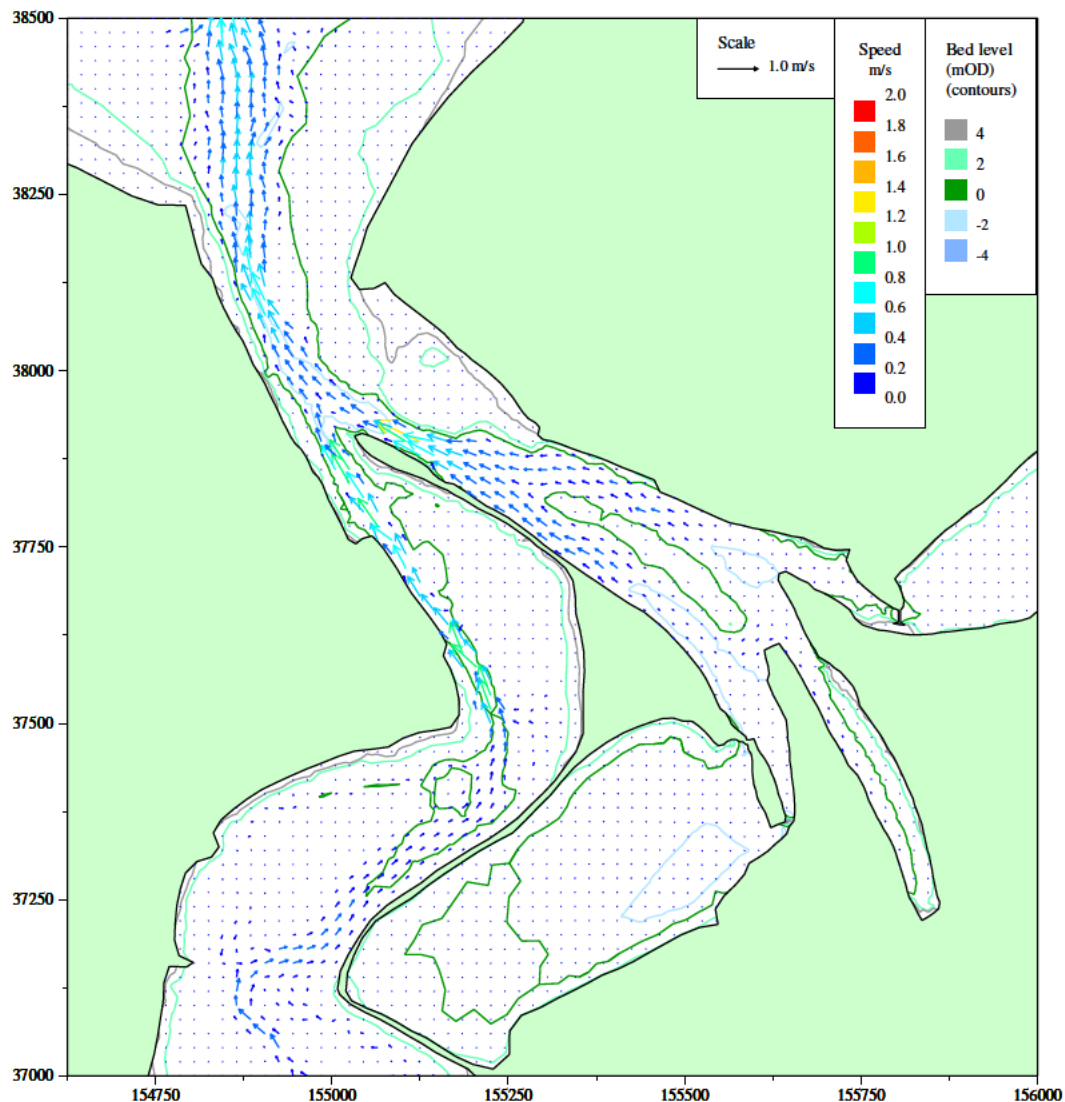
/HR_projects/ddr3839/model/SedimentTransport/report/Rubensp/sand_neap05.RUB/fig3.25.i

Figure 3.25 Baseline conditions neap tide net sand flux patterns



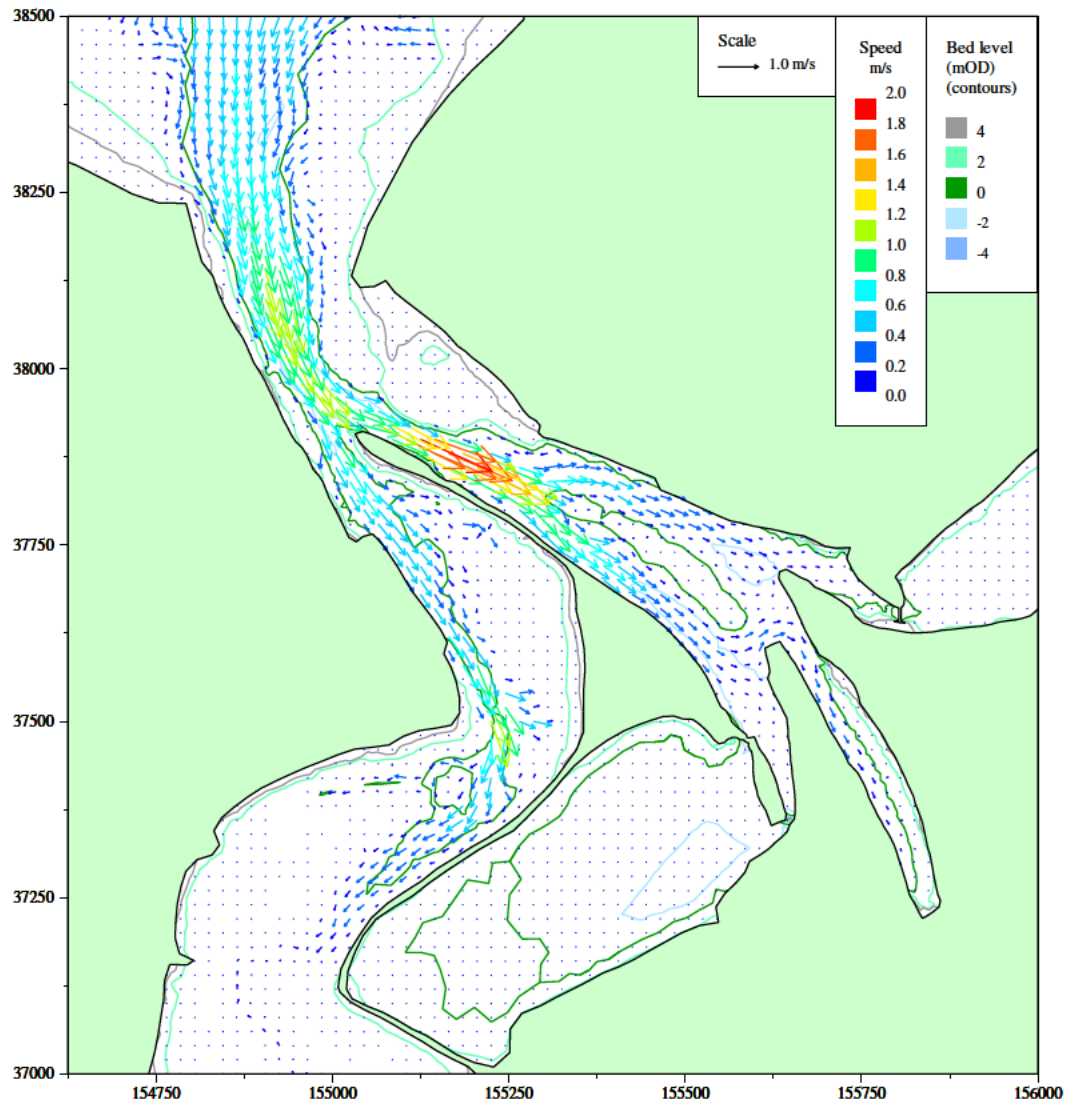
/HR_projects/ddr3839/model/SedimentTransport/report/Rubensp/flow_wave1m.RUB/fig3.26.i

Figure 3.26 Baseline conditions spring tide flood currents (HW+9.5 Hours), generated by 1m waves



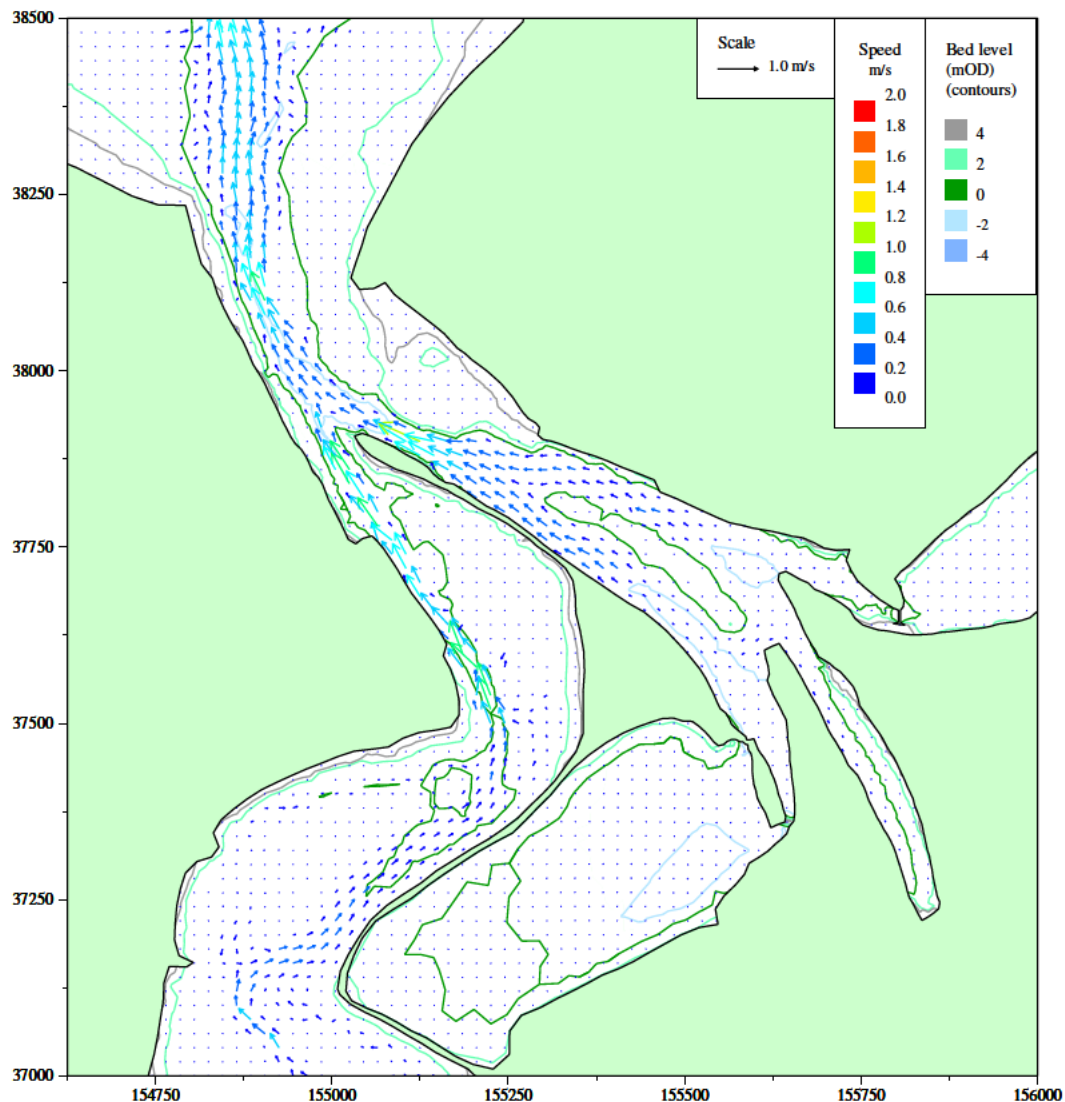
/HR_projects/ddr3839/model/SedimentTransport/report/Rubensp/flow_wave1m.RUB/fig3.27.i

Figure 3.27 Baseline conditions spring tide ebb currents (HW+4.5 Hours), generated by 1m waves



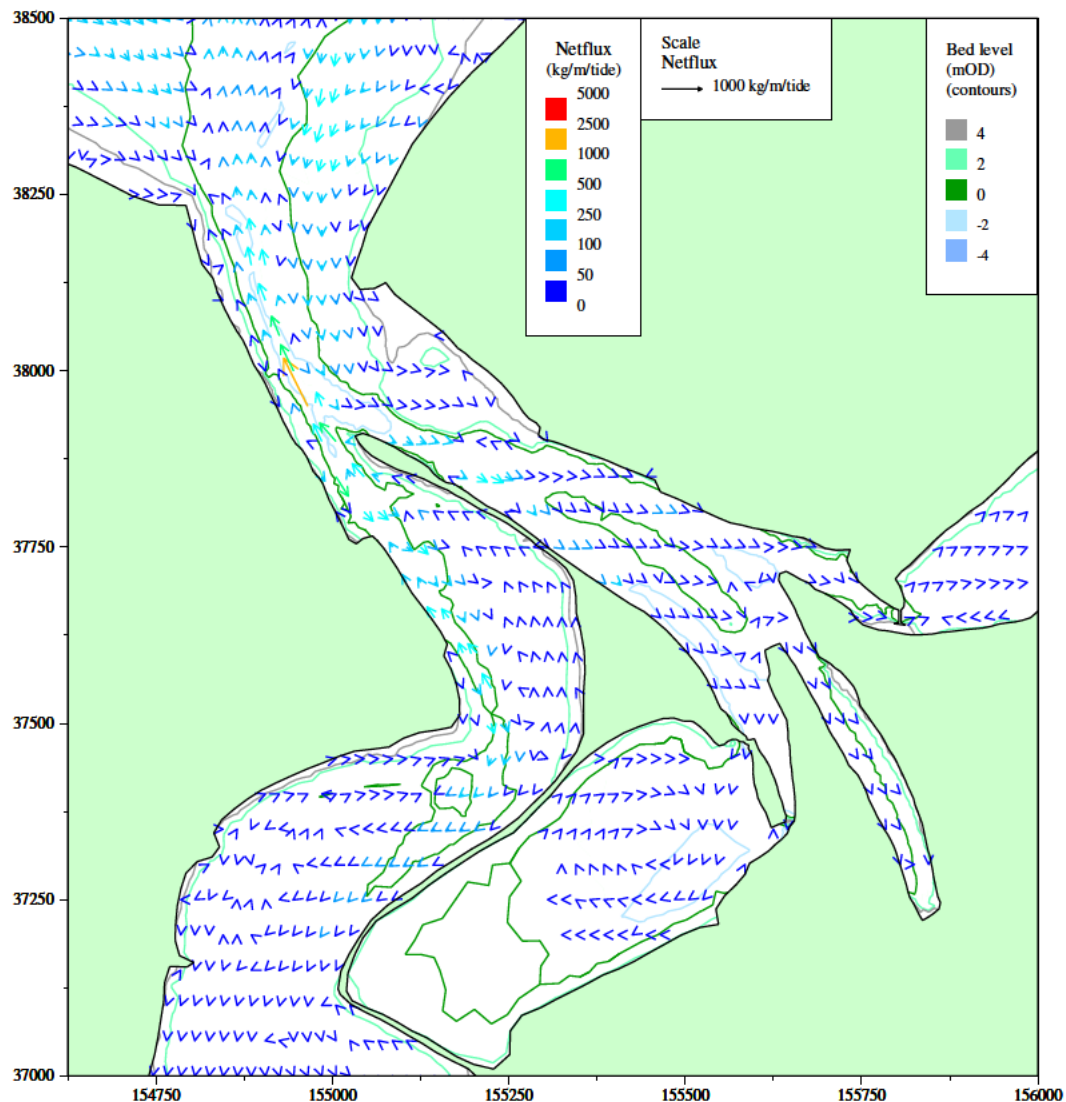
/HR_projects/ddr3839/model/SedimentTransport/report/Rubensp/flow_wave2m.RUB/fig3.28.i

Figure 3.28 Baseline conditions spring tide flood currents (HW+9.5 Hours), generated by 2m waves



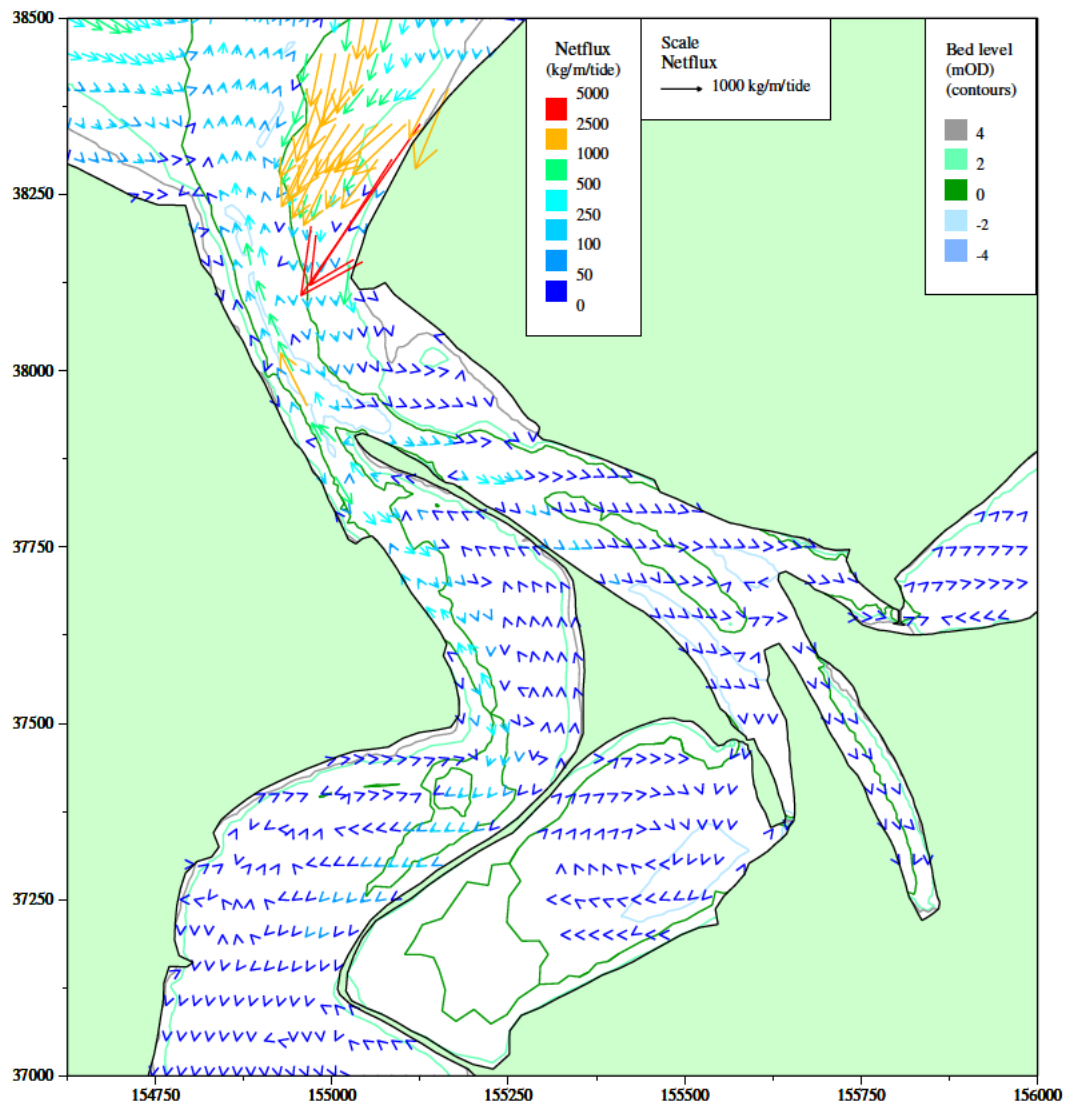
/HR_projects/ddr3839/model/SedimentTransport/report/Rubensp/flow_wave2m.RUB/fig3.29.i

Figure 3.29 Baseline conditions spring tide ebb currents (HW+4.5 Hours), generated by 2m waves



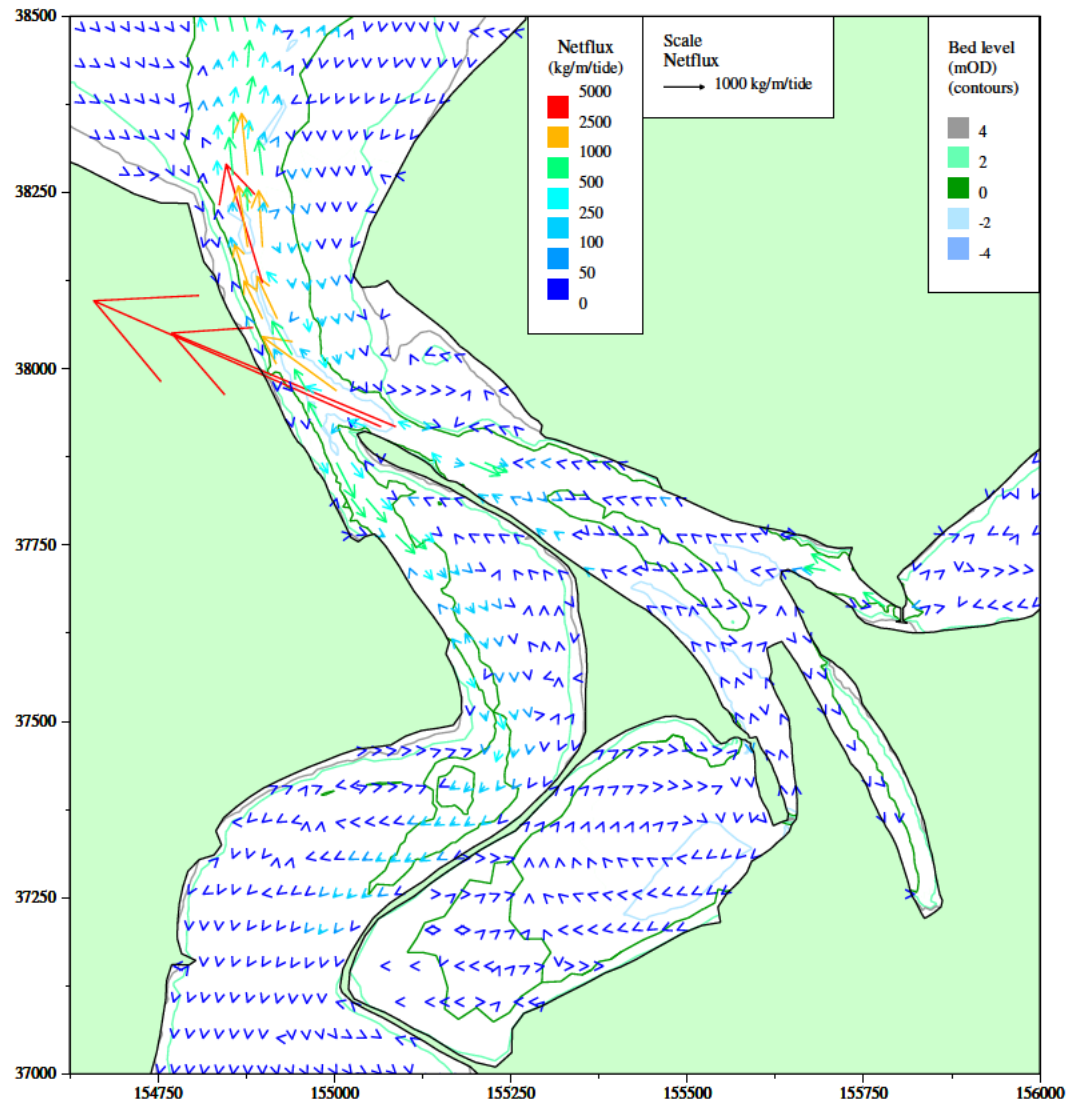
/HR_projects/ddr3839/model/SedimentTransport/report/Rubensp/sand_spr_1m_waves.RUB/fig3.30.i

Figure 3.30 Baseline conditions spring tide with 1m waves, net sand flux patterns



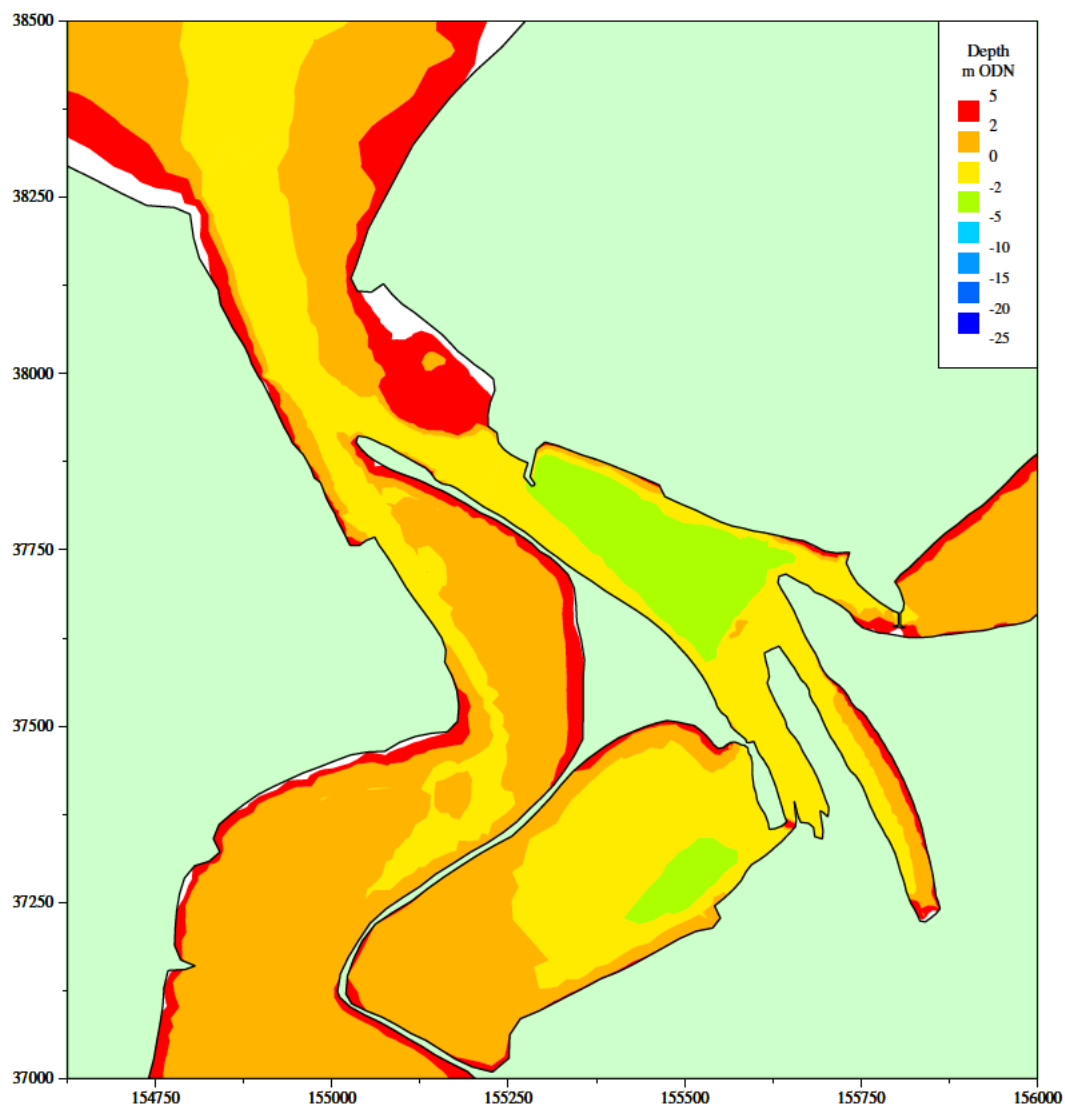
/HR_projects/ddr3839/model/SedimentTransport/report/Rubensp/sand_spr_2m_waves.RUB/fig3.31.i

Figure 3.31 Baseline conditions spring tide with 2m waves, net sand flux patterns



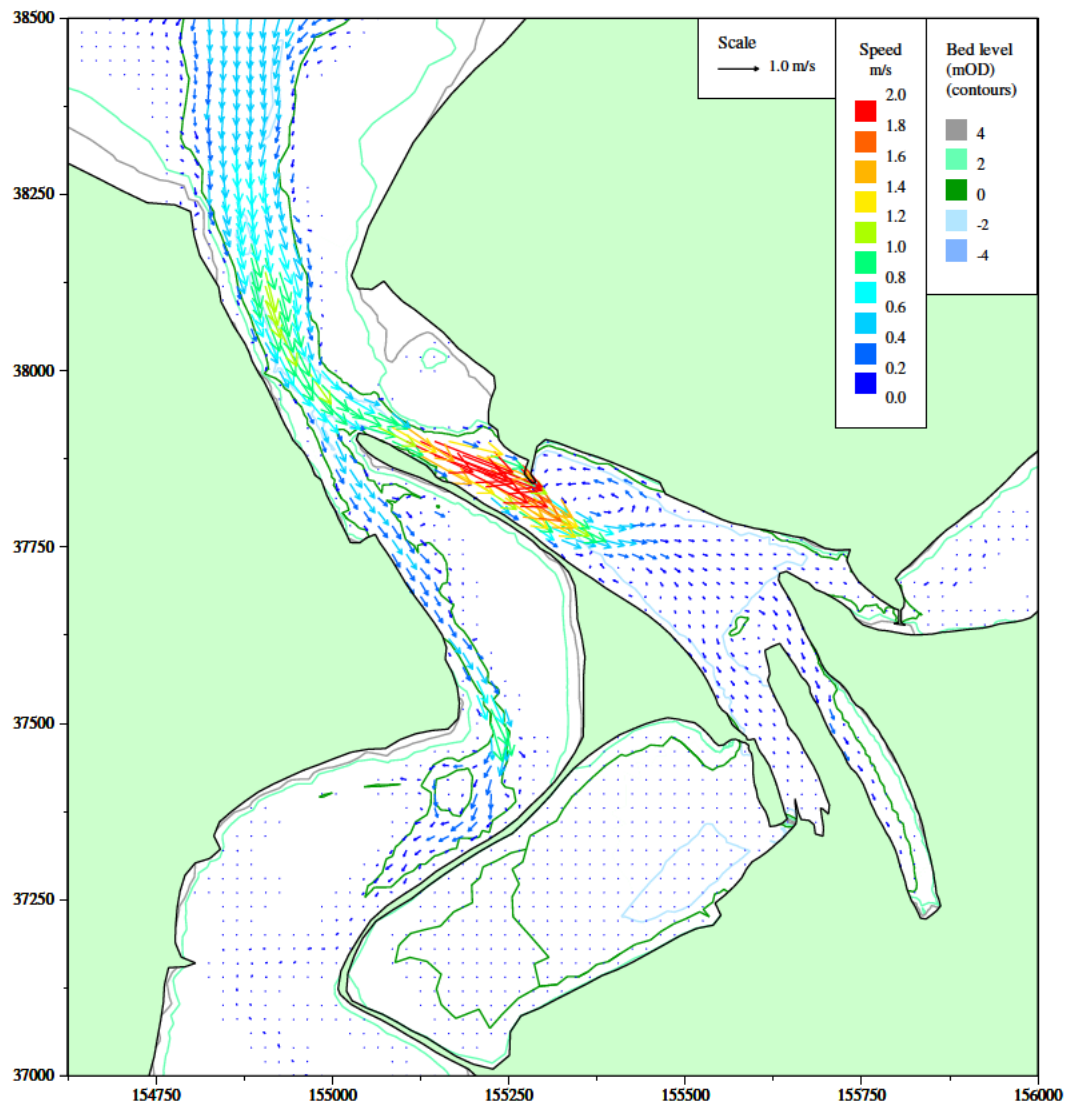
/HR_projects/ddr3839/model/SedimentTransport/report/Rubensp/sand_imp05b.RUB/fig3.32.i

Figure 3.32 Baseline conditions spring tide net sand flux patterns, impounding in Carnsew and Copperhouse Pools to HW + 3 hours, double sluice operation on Carnsew Pool



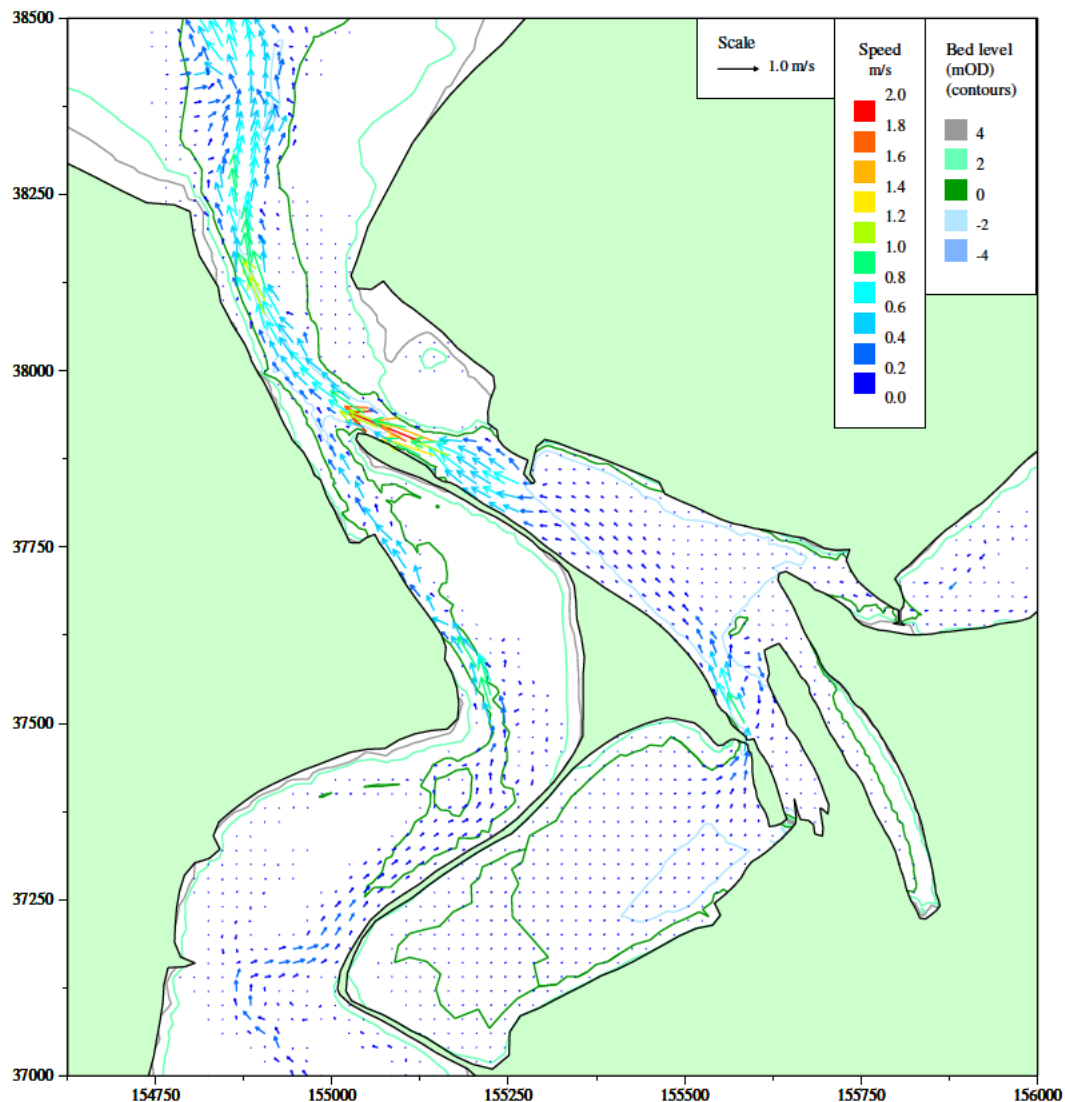
/HR_projects/ddr3839/model/SedimentTransport/report/Rubensp/flow_dev08a.RUB/fig3.33.i

Figure 3.33 Model bathymetry, Scheme 1



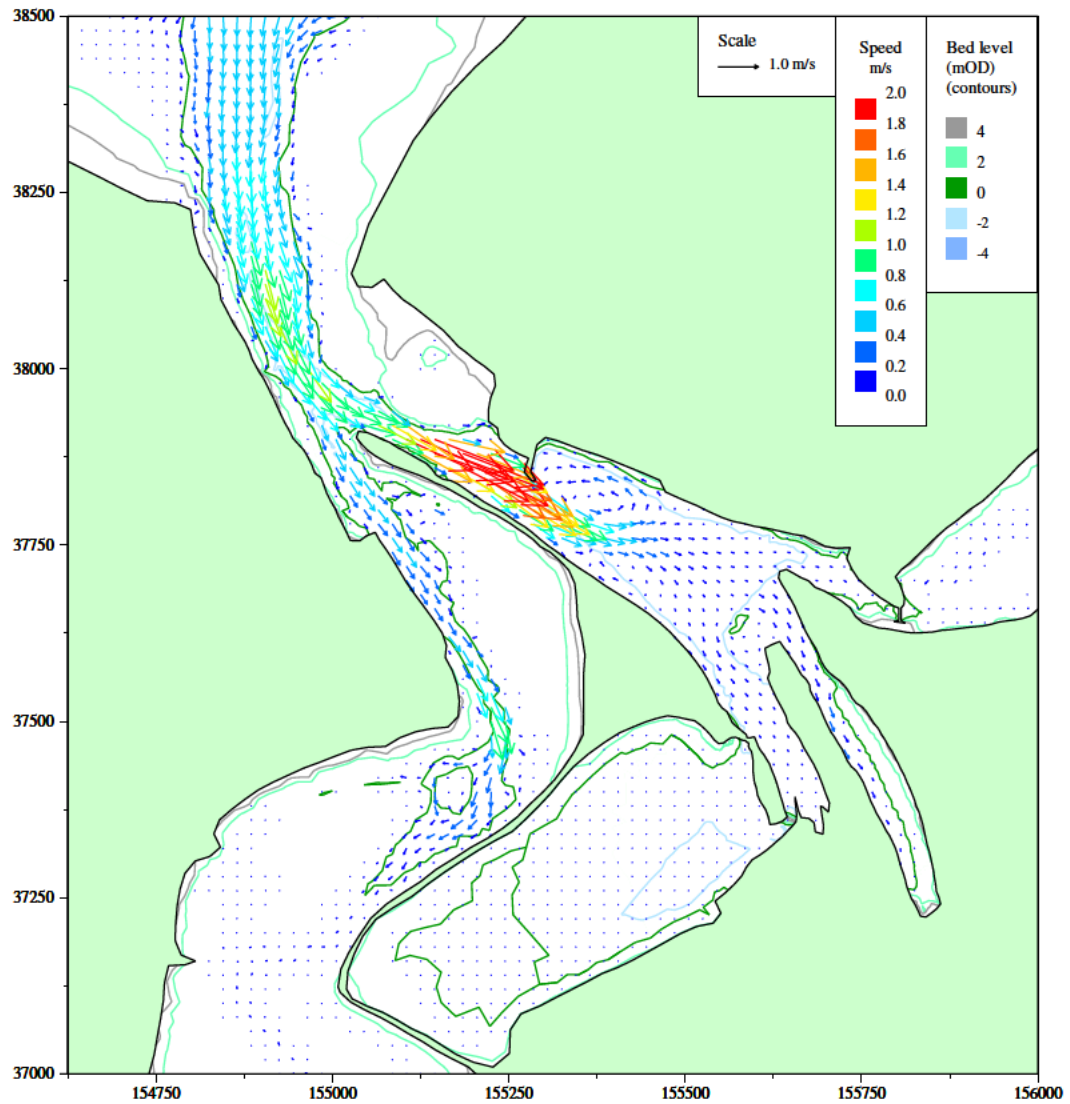
/HR_projects/ddr3839/model/SedimentTransport/report/Rubensp/flow_dev08a.RUB/fig3.34.i

Figure 3.34 Scheme 1 conditions spring tide peak flood currents (HW+9.5 Hours), Copperhouse sluice open (summer condition), single sluice operation on Carnsew Pool



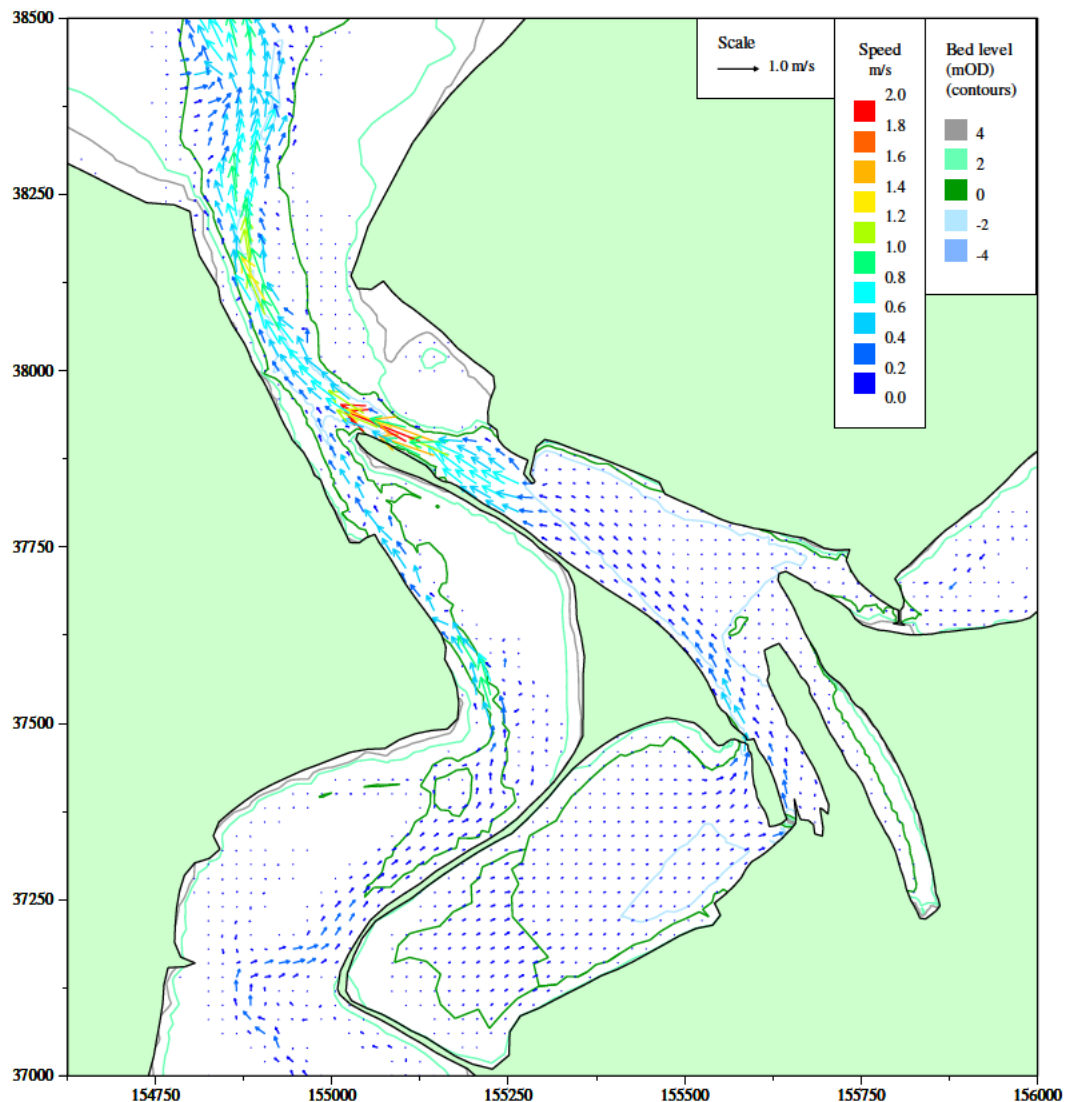
/HR_projects/ddr3839/model/SedimentTransport/report/Rubensp/flow_dev08a.RUB/fig3.35.i

Figure 3.35 Scheme 1 conditions spring tide ebb currents (HW+4.5 Hours), Copperhouse sluice open (summer condition), single sluice operation on Carnsew Pool



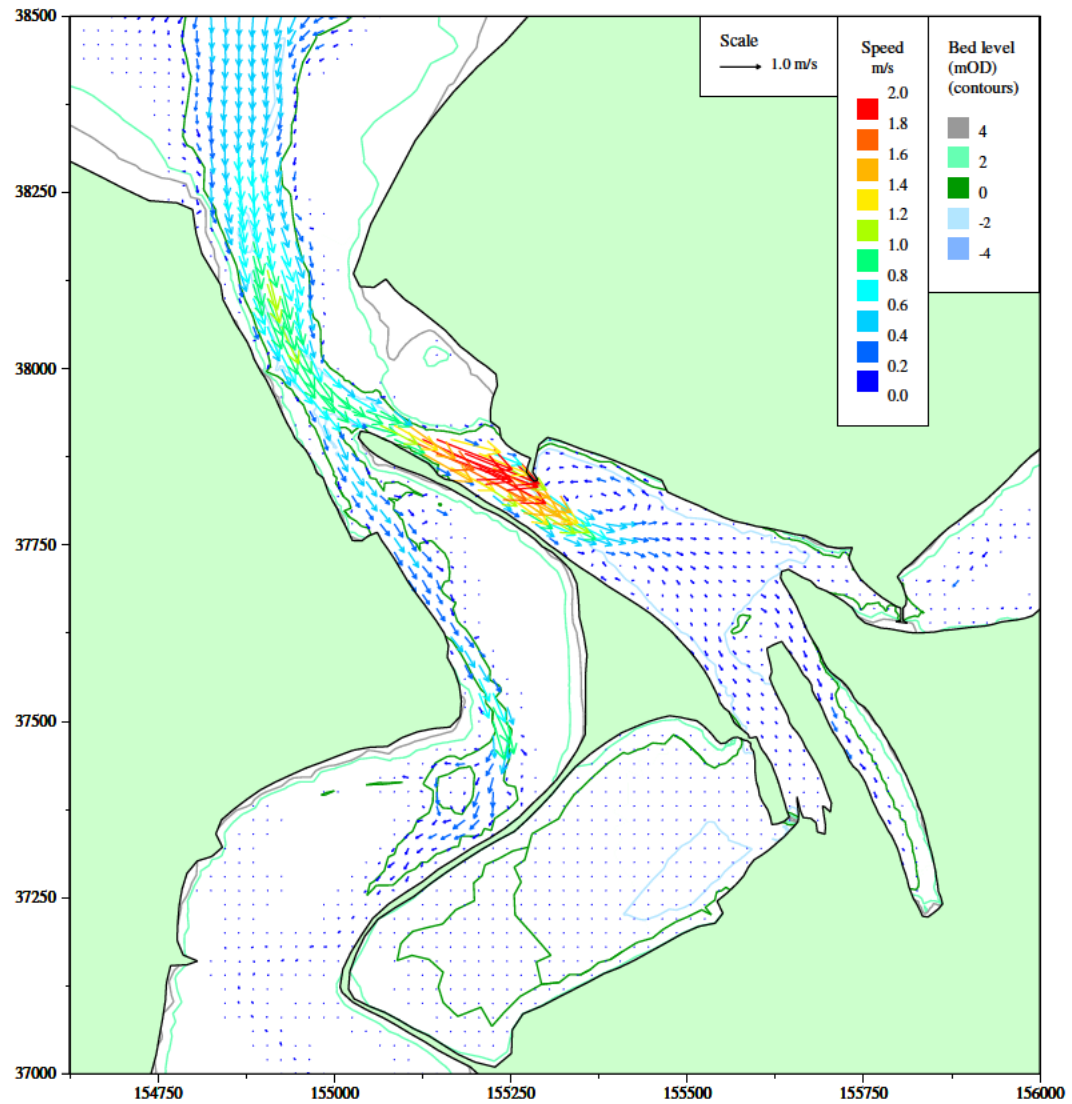
/HR_projects/ddr3839/model/SedimentTransport/report/Rubensp/flow_dev08b.RUB/fig3.36.i

Figure 3.36 Scheme 1 conditions spring tide peak flood currents (HW+9.5 Hours), Copperhouse sluice open (summer condition), double sluice operation on Carnsew Pool



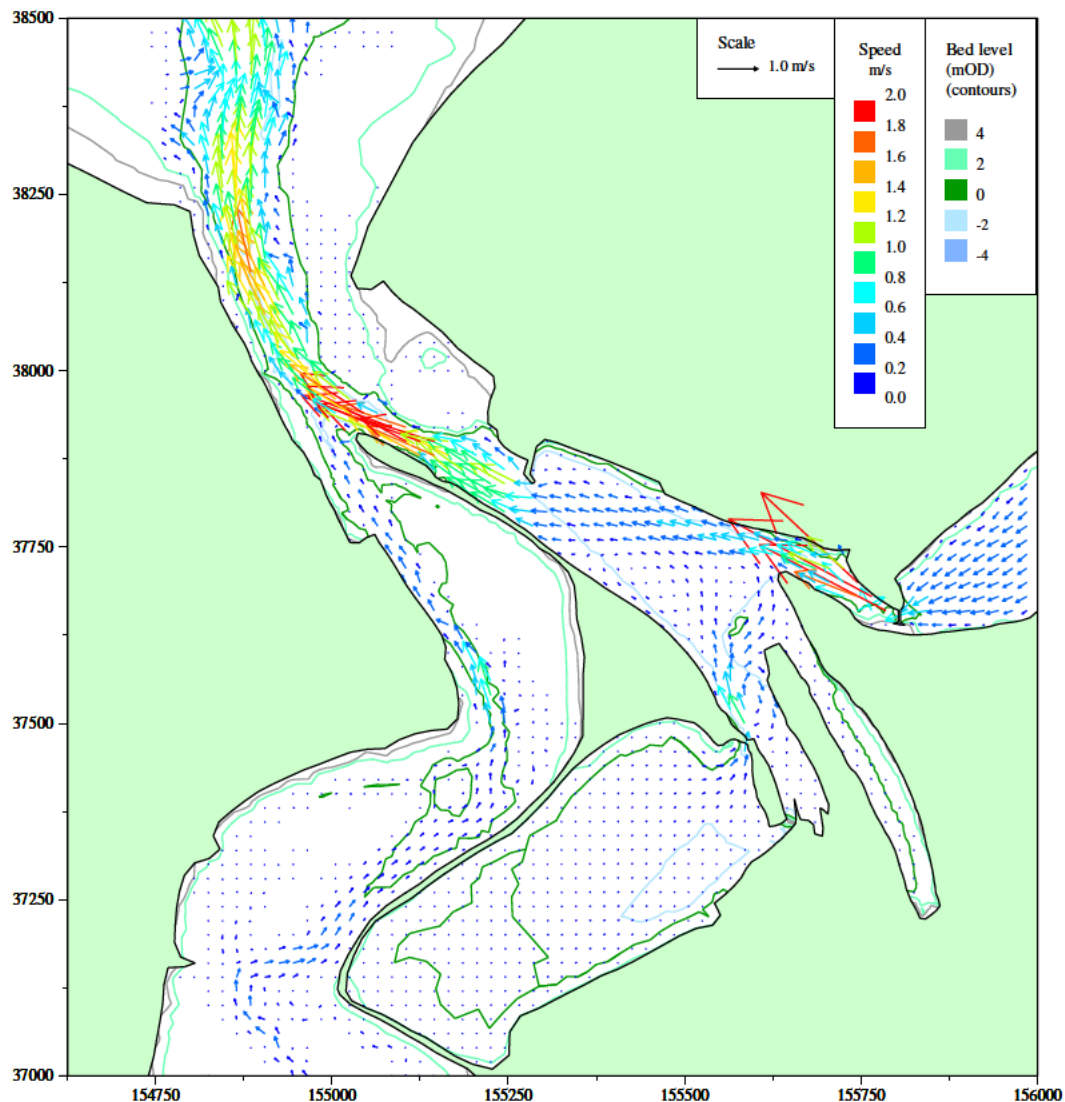
/HR_projects/ddr3839/model/SedimentTransport/report/Rubensp/flow_dev08b.RUB/fig3.37.i

Figure 3.37 Scheme 1 conditions spring tide ebb currents (HW+4.5 Hours), Copperhouse sluice open (summer condition), double sluice operation on Carnsew Pool



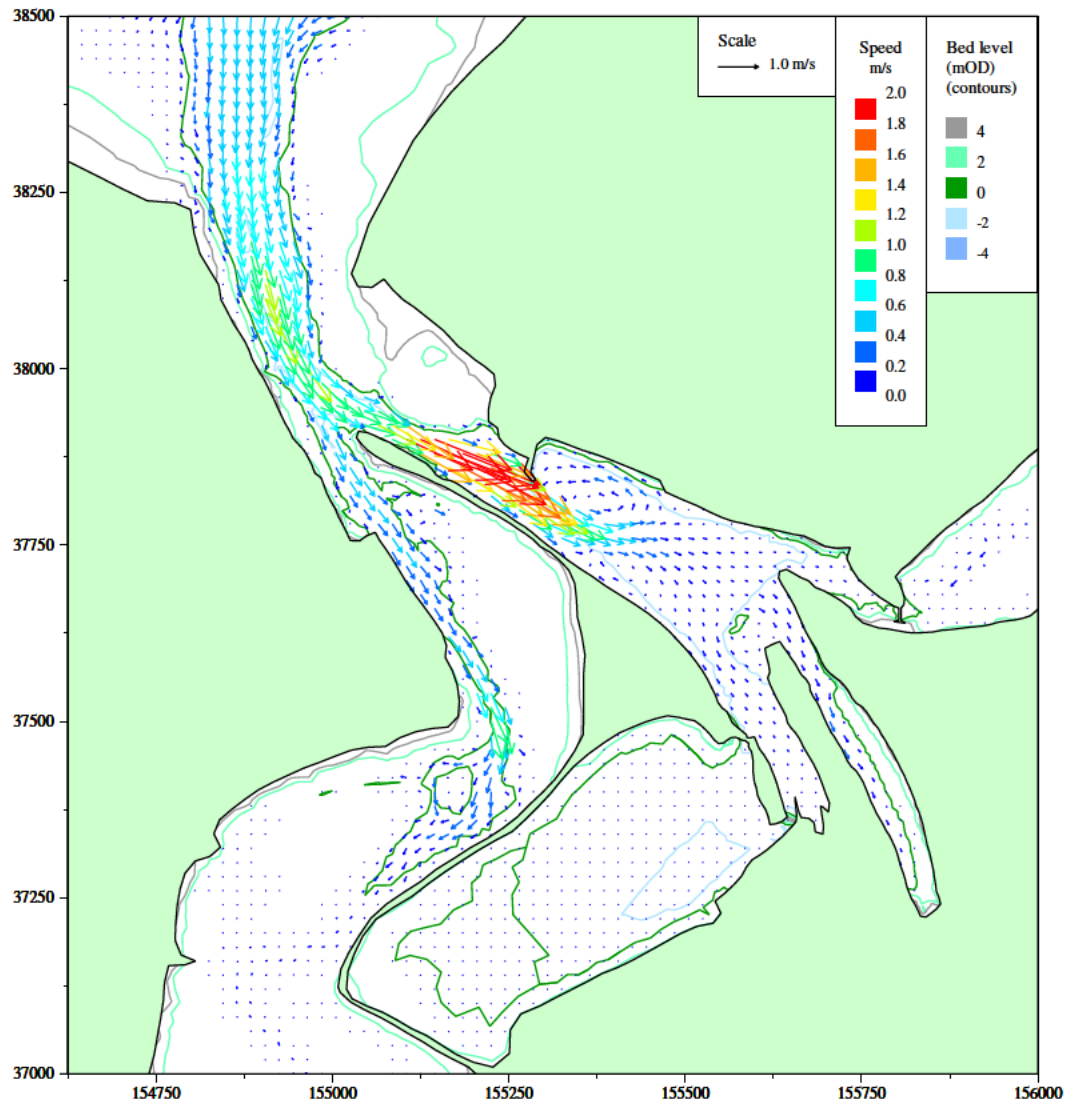
/HR_projects/ddr3839/model/SedimentTransport/report/Rubensp/flow_dev08c.RUB/fig3.38.i

Figure 3.38 Scheme 1 conditions spring tide peak flood currents with impounding in Carnsew and Copperhouse Pools to HW + 3 hours, single sluice operation on Carnsew Pool



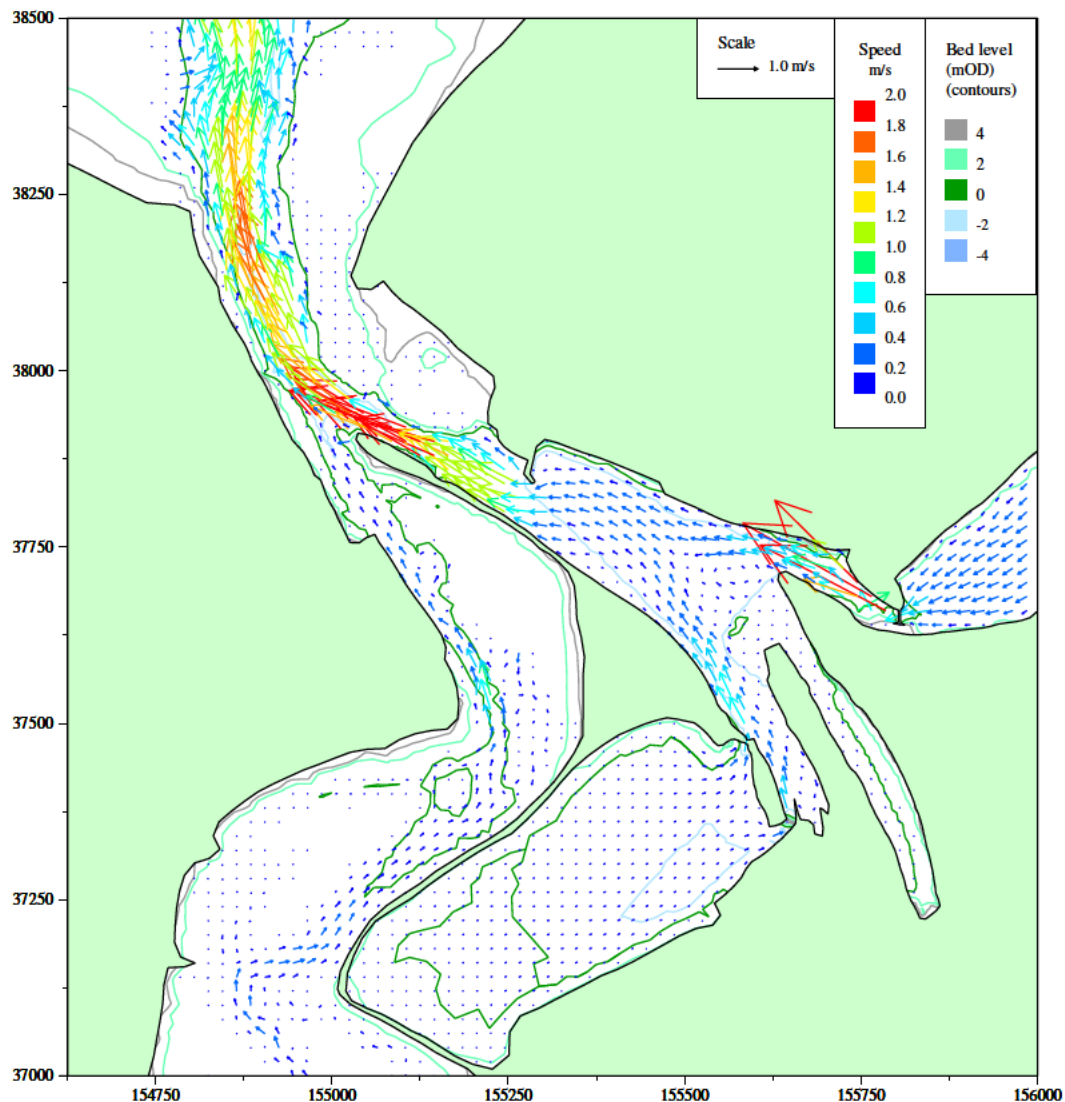
/HR_projects/ddr3839/mode/SedimentTransport/report/Rubensp/flow_dev08c.RUB/fig3.39.i

Figure 3.39 Scheme 1 conditions spring tide peak ebb currents with impounding in Carnsew and Copperhouse Pools to HW + 3 hours, single sluice operation on Carnsew Pool



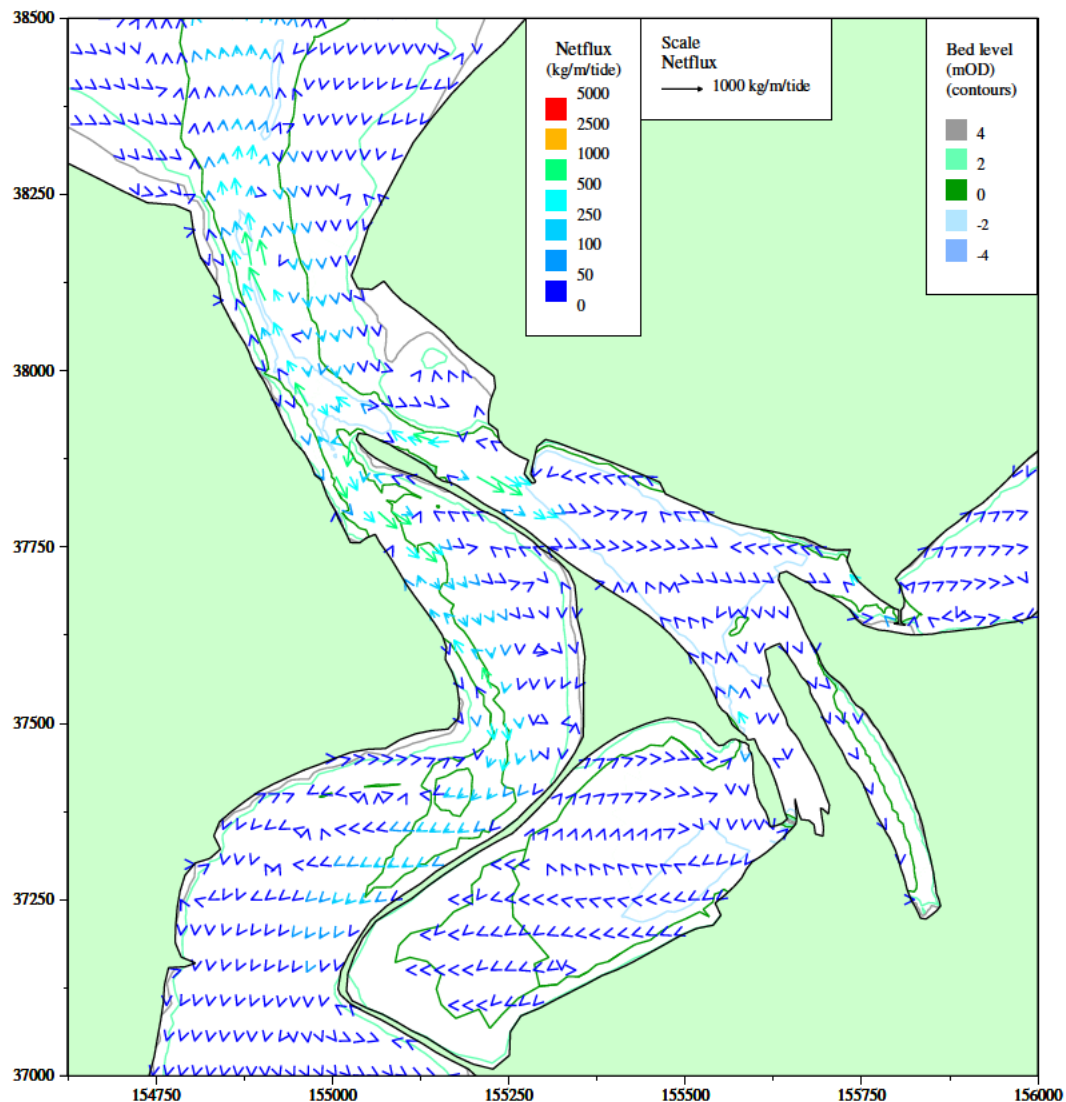
/HR_projects/ddr3839/model/SedimentTransport/report/Rubensp/flow_dev08d.RUB/fig3.40.i

Figure 3.40 Scheme 1 conditions spring tide peak flood currents with impounding in Carnsew and Copperhouse Pools to HW + 3 hours, double sluice operation on Carnsew Pool



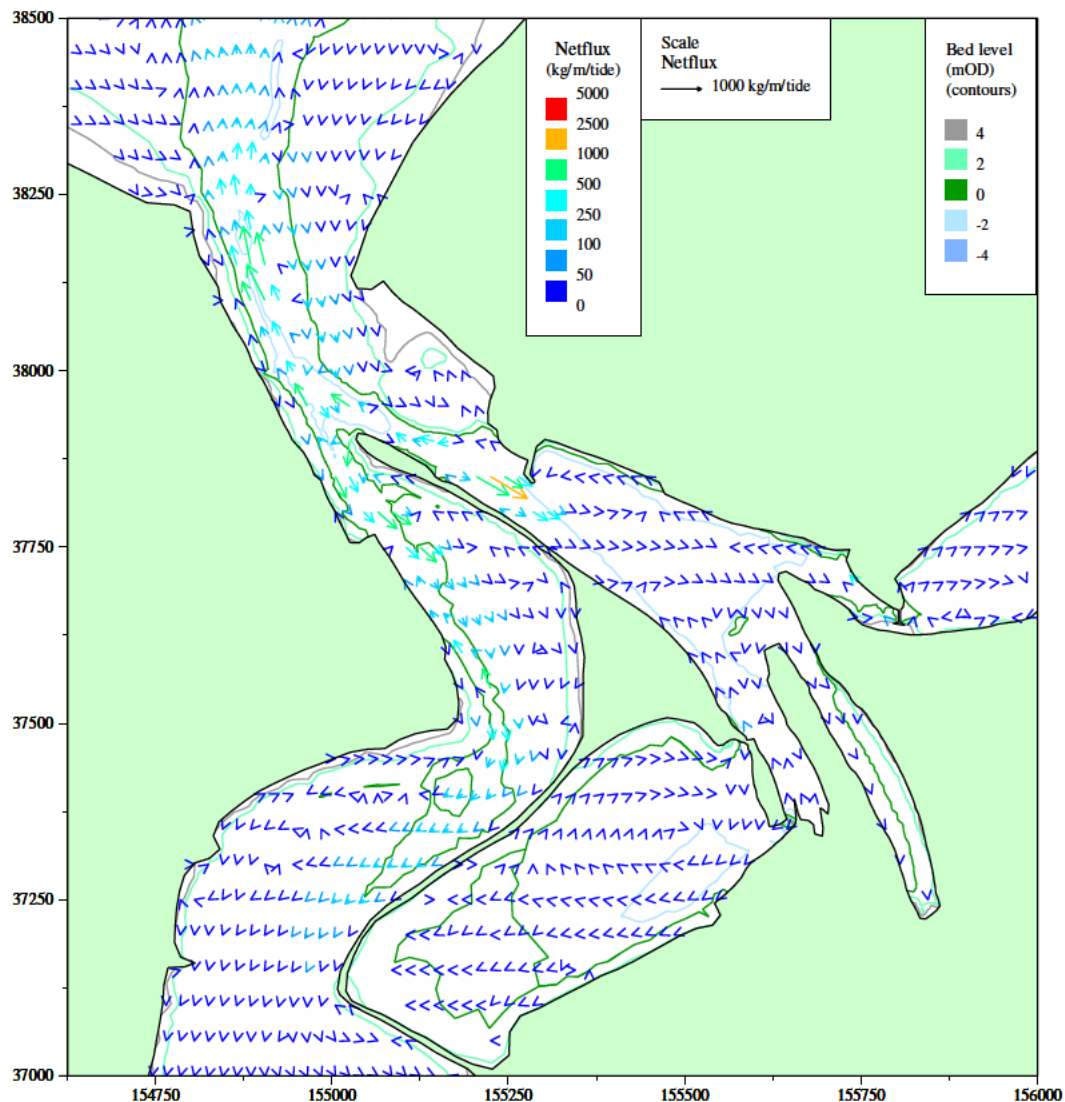
/HR_projects/ddr3839/model/SedimentTransport/report/Rubensp/flow_dev08d.RUB/fig3.41.i

Figure 3.41 Scheme 1 conditions spring tide peak ebb currents with impounding in Carnsew and Copperhouse Pools to HW + 3 hours, double sluice operation on Carnsew Pool



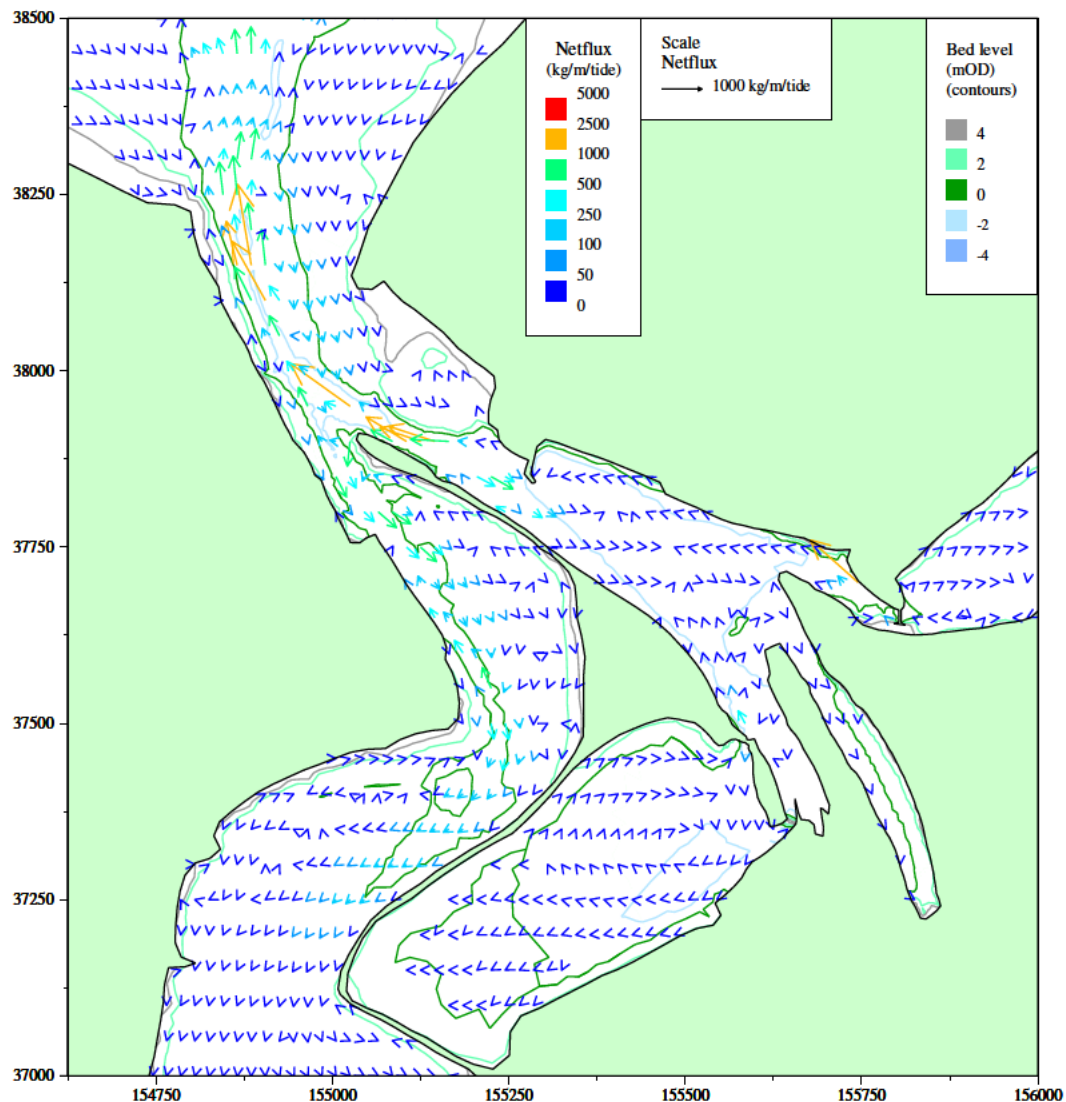
/HR_projects/ddr3839/model/SedimentTransport/report/Rubensp/sand_dev08a.RUB/fig3.42.i

Figure 3.42 Scheme 1 conditions net sand flux patterns, Copperhouse sluice open (summer condition), single sluice operation on Carnsew Pool



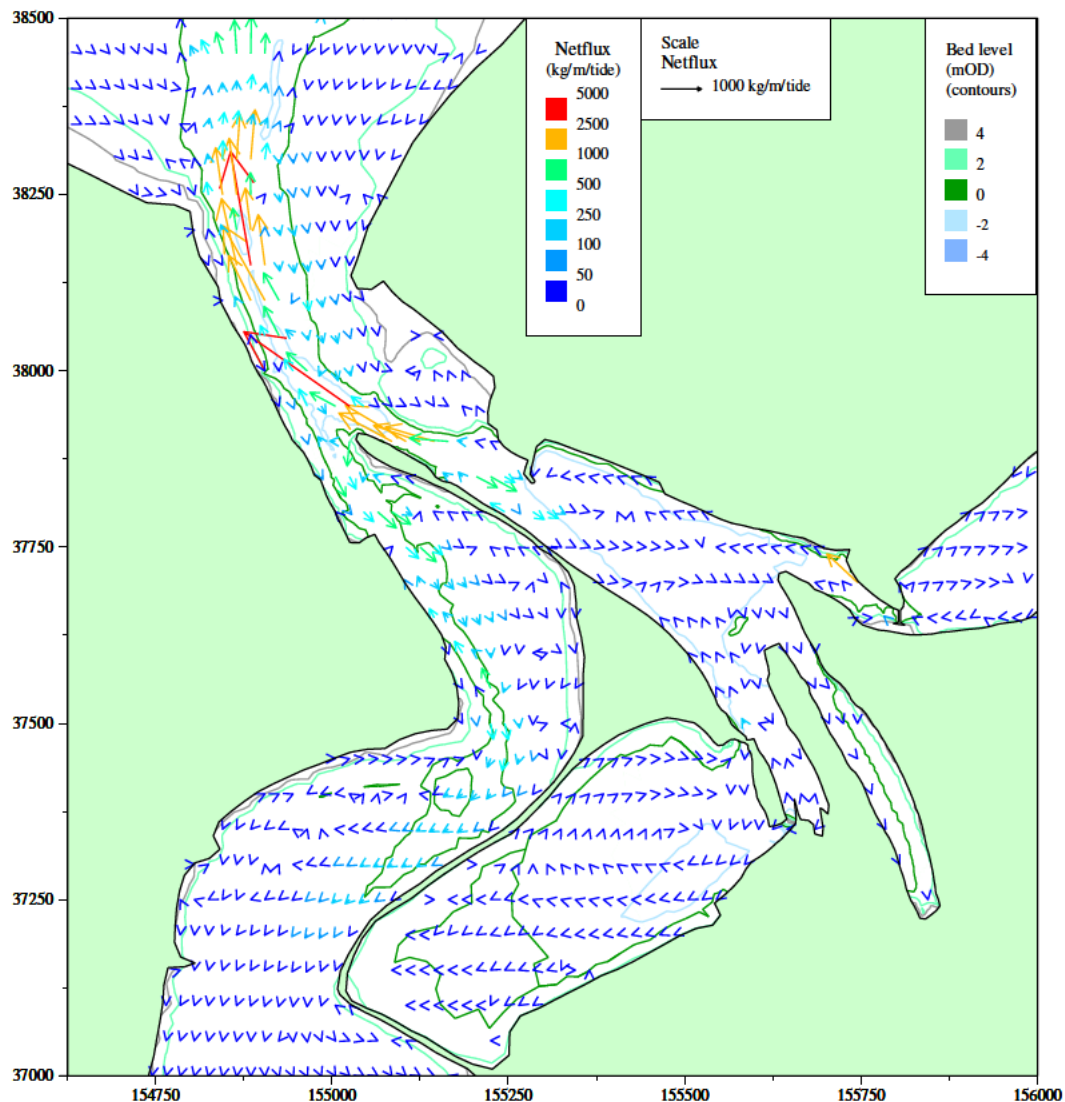
/HR_projects/ddr3839/model/SedimentTransport/report/Rubensp/sand_dev08b.RUB/fig3.43.i

Figure 3.43 Scheme 1 conditions net sand flux patterns, Copperhouse sluice open (summer condition), double sluice operation on Carnsew Pool



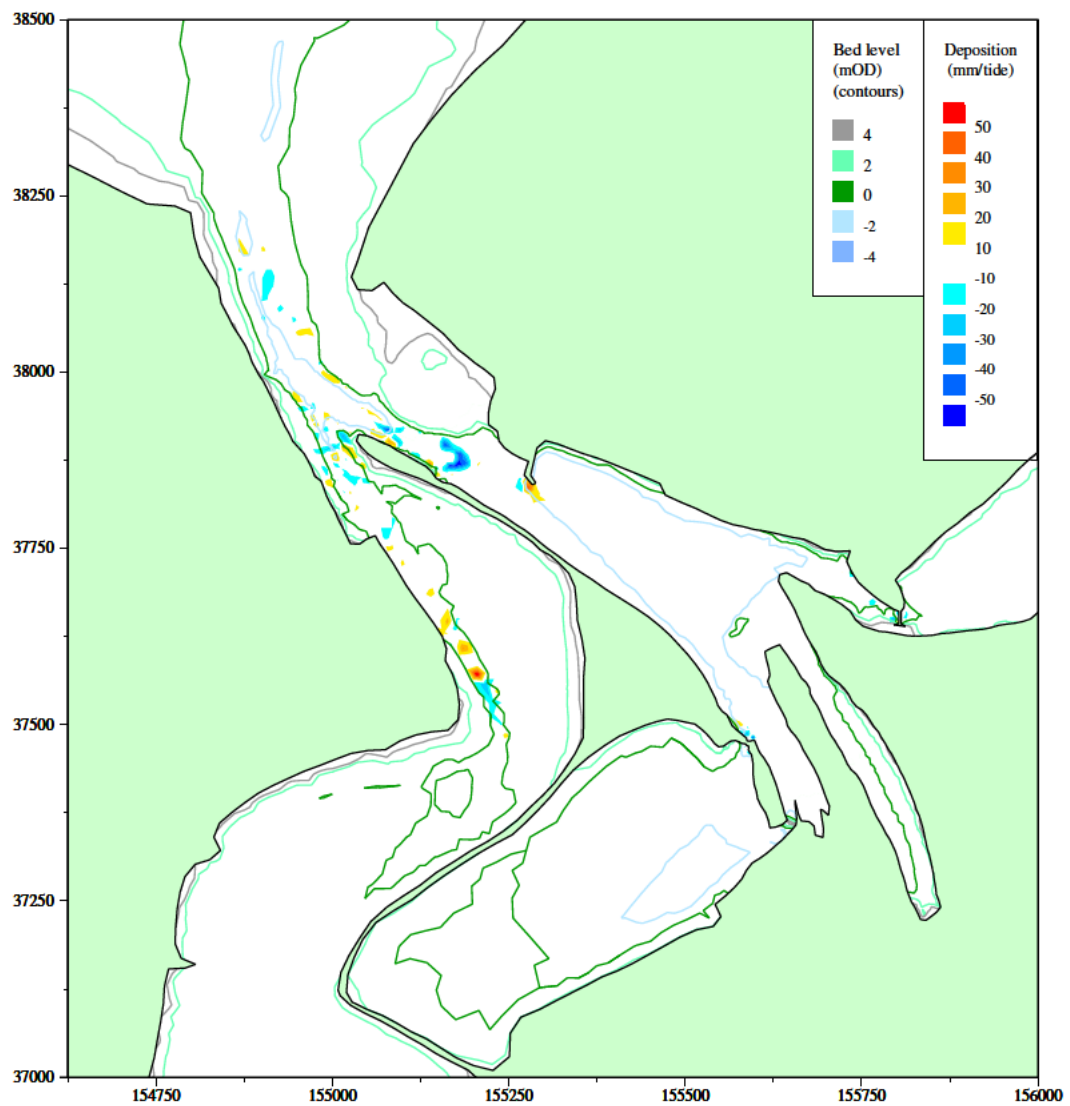
/HR_projects/ddr3839/model/SedimentTransport/report/Rubensp/sand_dev08c.RUB/fig3.44.i

Figure 3.44 Scheme 1 conditions net sand flux patterns with impounding in Carnsew and Copperhouse Pools to HW + 3 hours, single sluice operation on Carnsew Pool



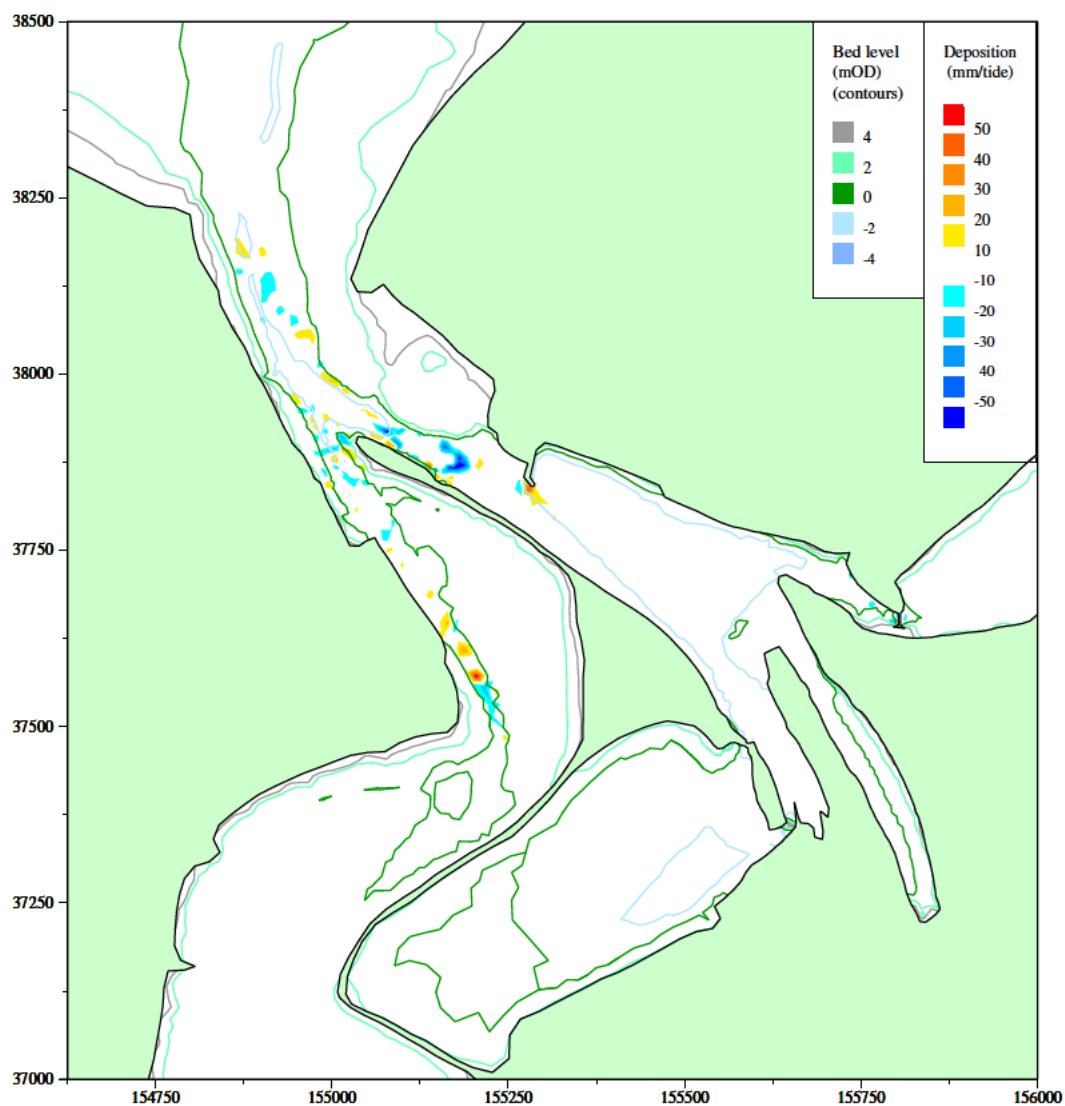
/HR_projects/ddr3839/model/SedimentTransport/report/Rubensp/sand_dev08d.RUB/fig3.45.i

Figure 3.45 Scheme 1 conditions net sand flux patterns with impounding in Carnsew and Copperhouse Pools to HW + 3 hours, double sluice operation on Carnsew Pool



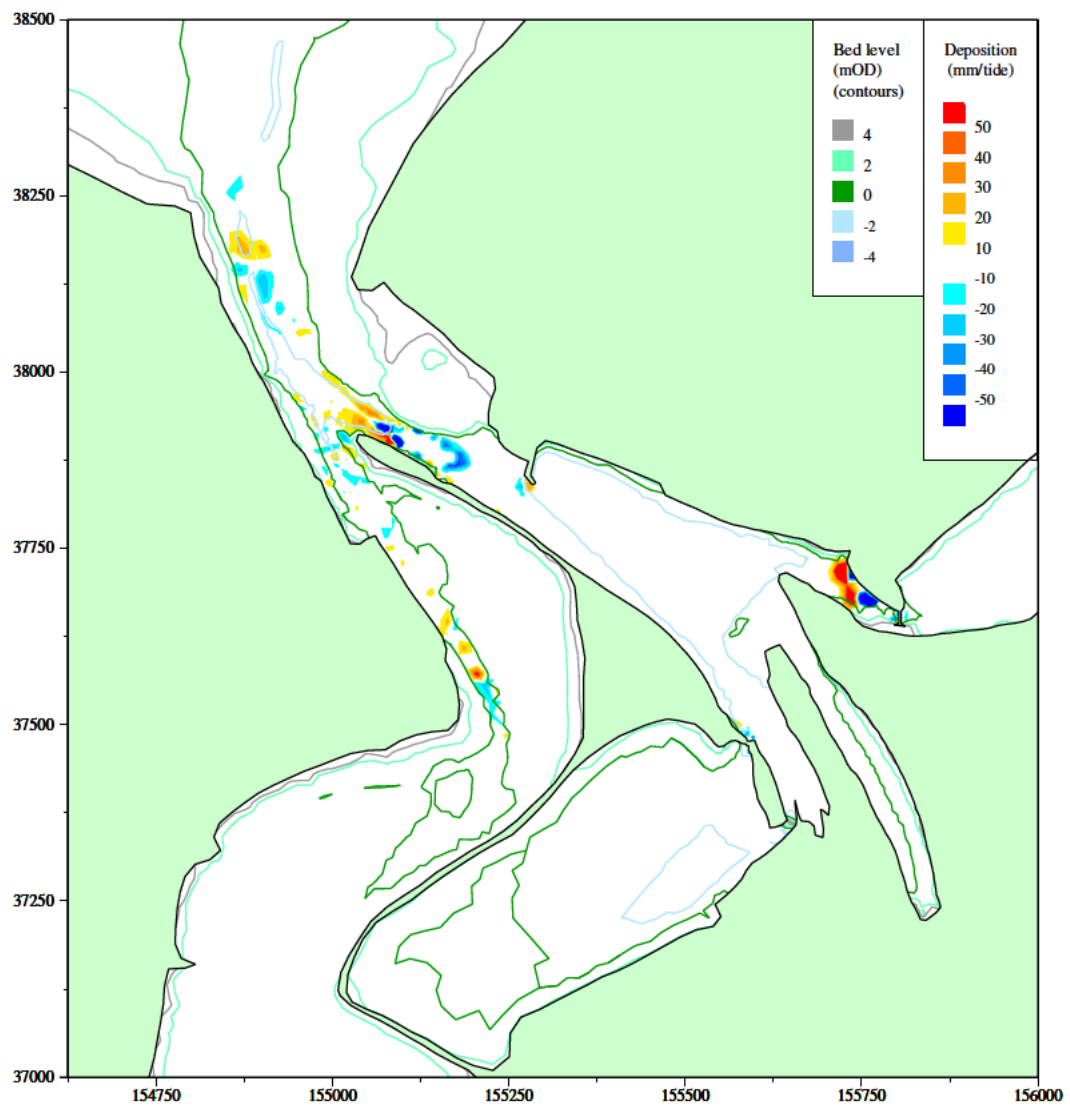
/HR_projects/ddr3839/model/SedimentTransport/report/Rubensp/sand_dev08a.RUB/fig3.46.i

Figure 3.46 Scheme 1 conditions patterns of erosion and deposition, Copperhouse sluice open (summer condition), single sluice operation on Carnsew Pool



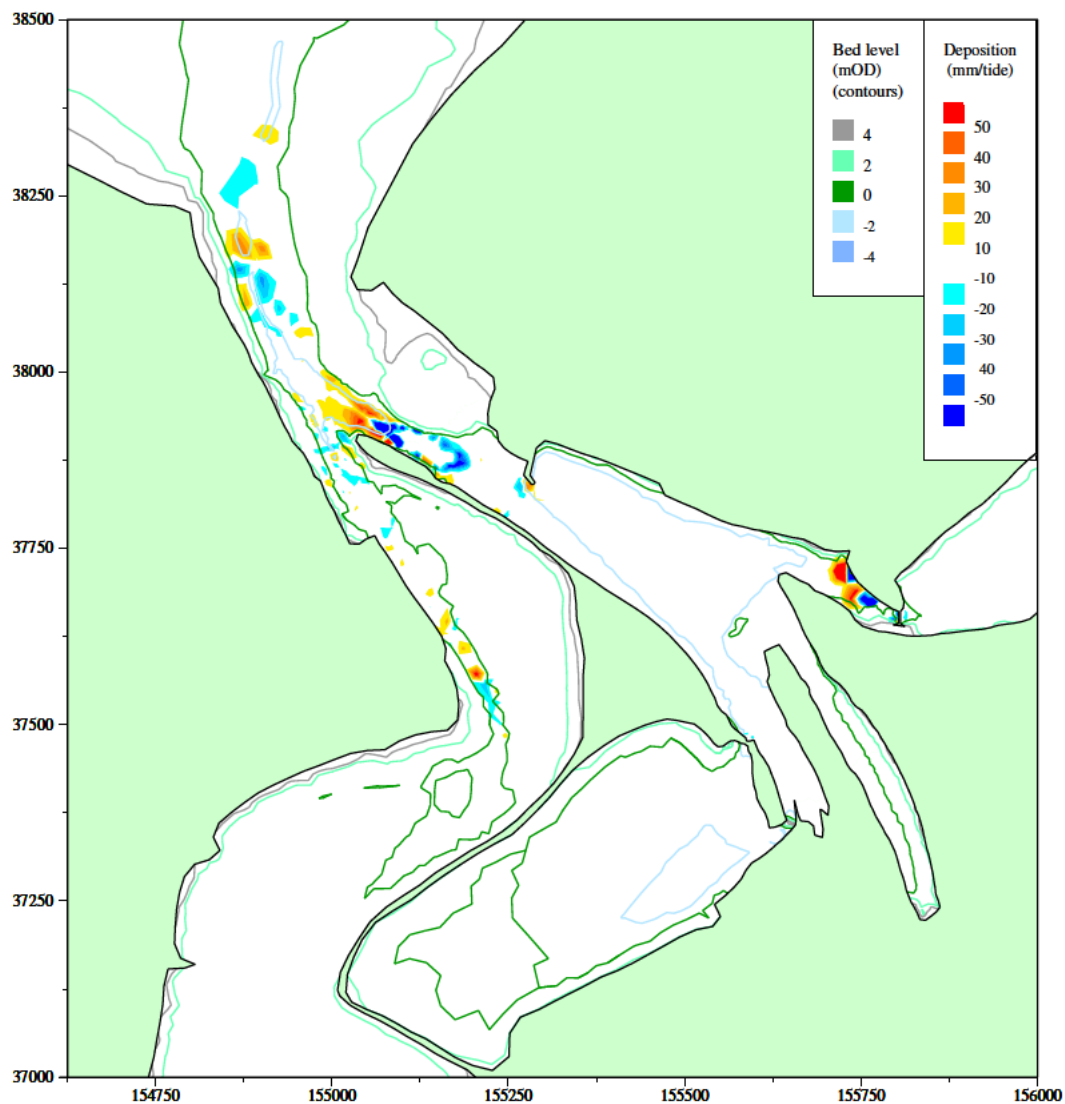
/HR_projects/ddr3839/model/SedimentTransport/report/Rubensp/sand_dev08b.RUB/fig3.47.i

Figure 3.47 Scheme 1 conditions patterns of erosion and deposition, Copperhouse sluice open (summer condition), double sluice operation on Carnsew Pool



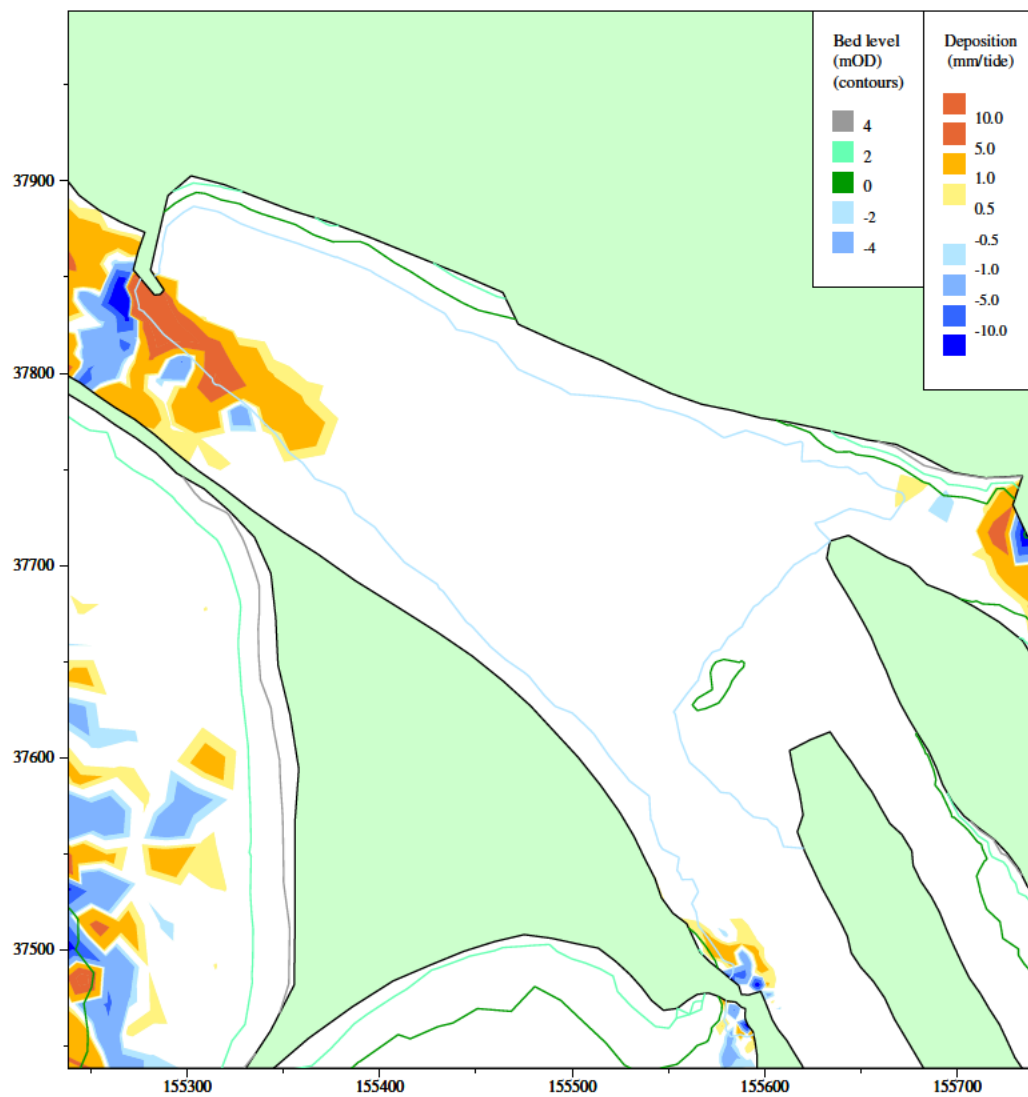
/HR_projects/ddr3839/model/SedimentTransport/report/Rubensp/sand_dev08c.RUB/fig3.48.i

Figure 3.48 Scheme 1 conditions patterns of erosion and deposition with impounding in Carnsew and Copperhouse Pools to HW + 3 hours, single sluice operation on Carnsew Pool



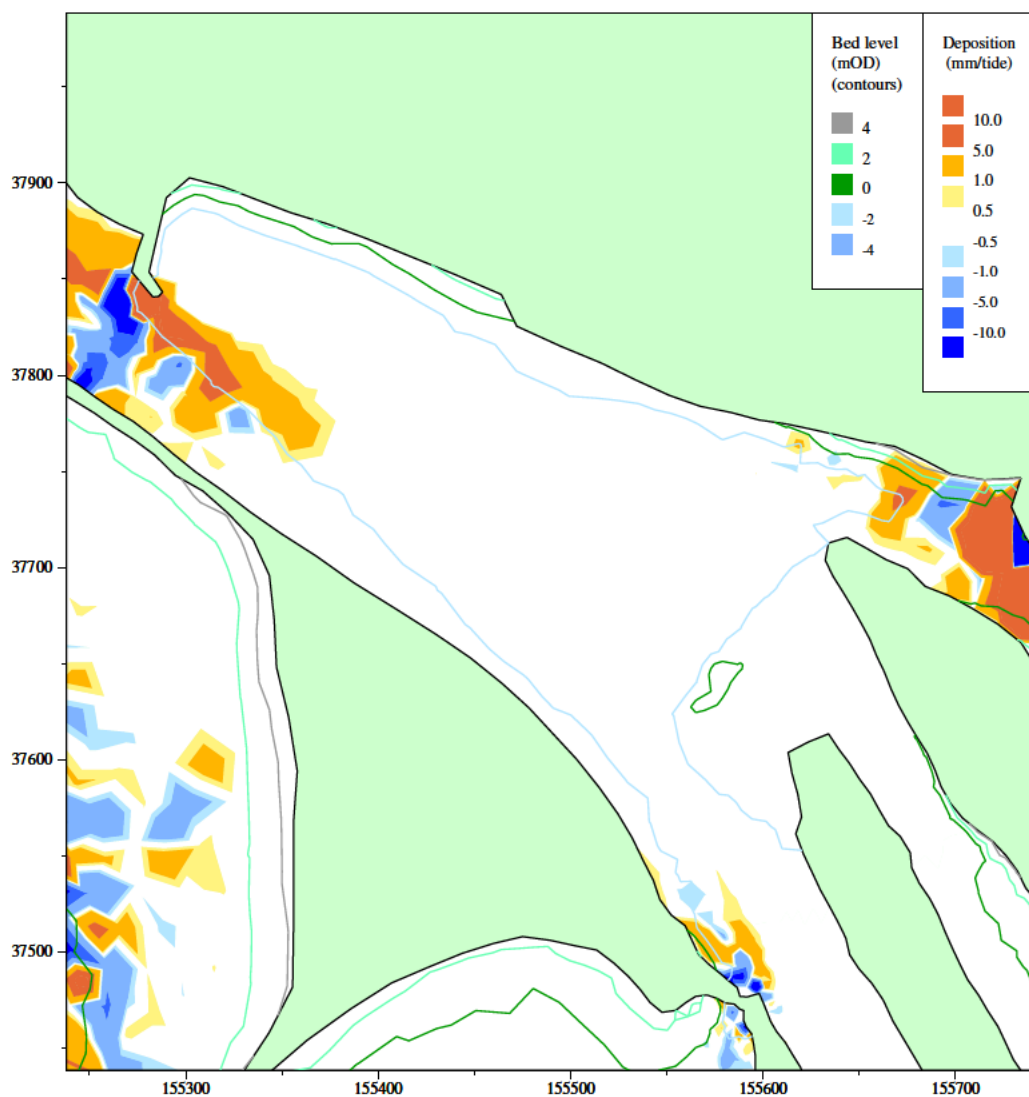
/HR_projects/ddr3839/model/SedimentTransport/report/Rubensp/sand_dev08d.RUB/fig3.49.i

Figure 3.49 Scheme 1 conditions patterns of erosion and deposition with impounding in Carnsew and Copperhouse Pools to HW + 3 hours, double sluice operation on Carnsew Pool



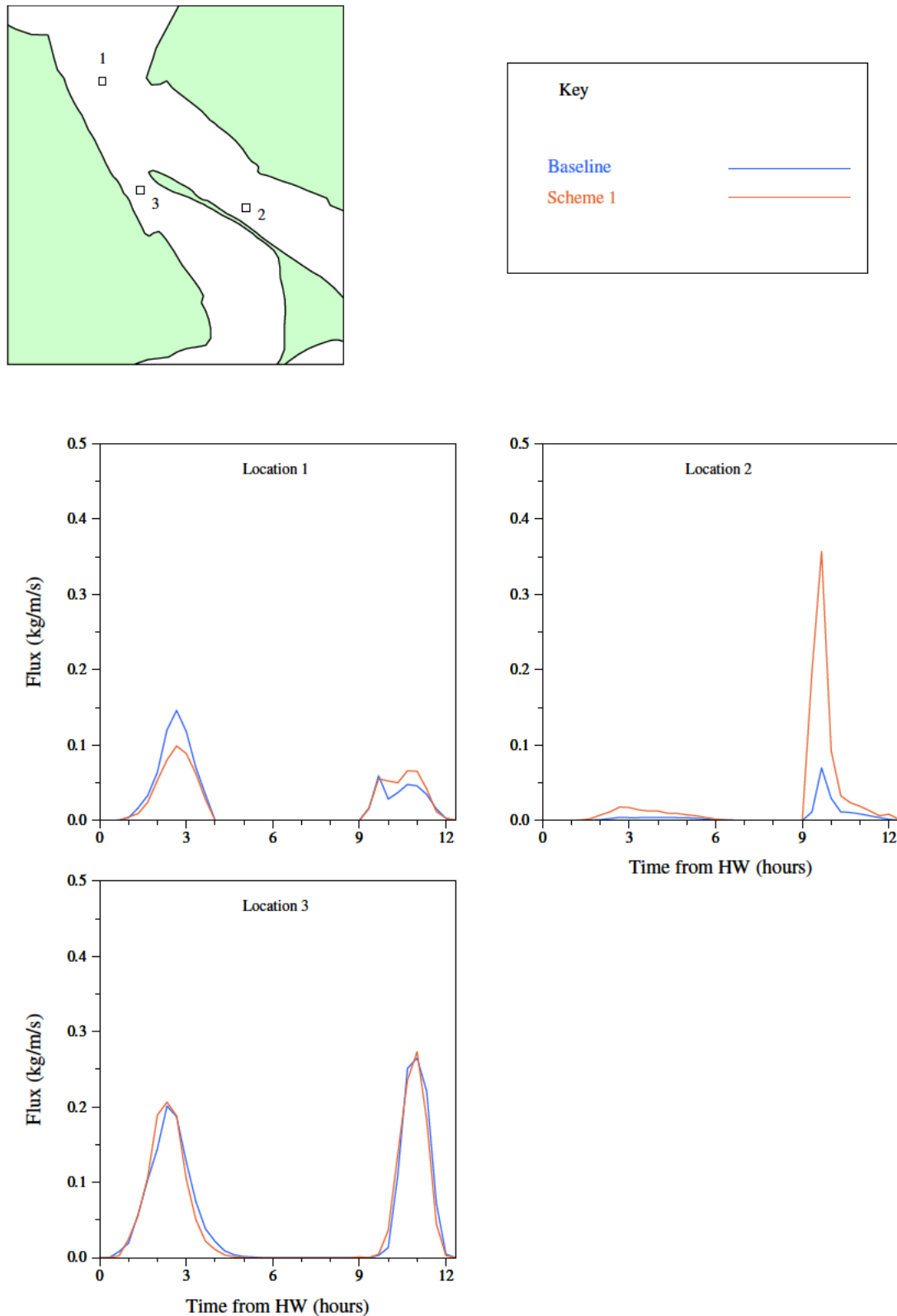
/HR_projects/ddr3839/model/SedimentTransport/report/Rubensp/sand_dev08b.RUB/fig3.50.i

Figure 3.50 Scheme 1 conditions patterns of erosion and deposition in marina area, Copperhouse sluice open (summer condition), double sluice operation on Carnsew Pool



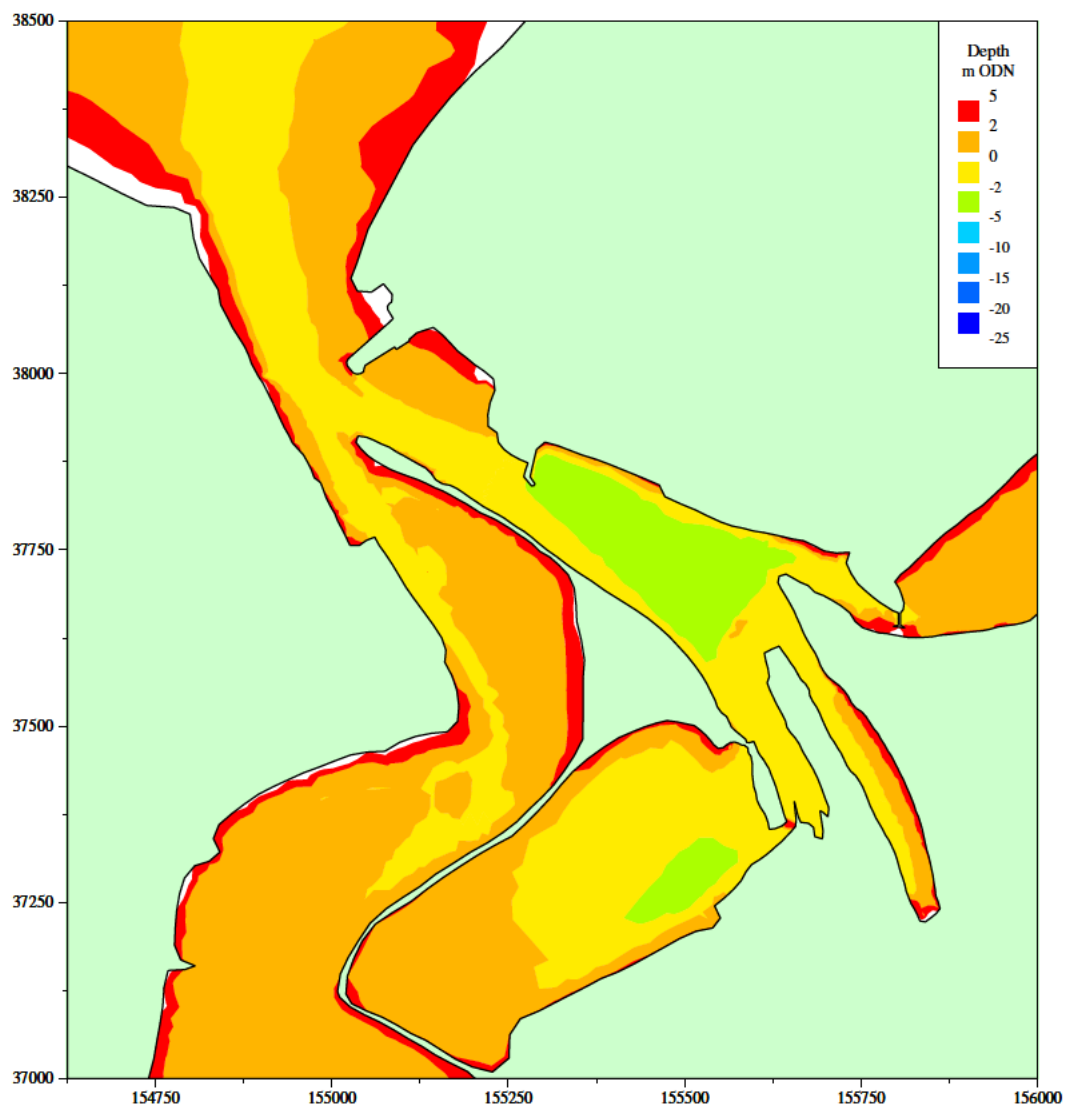
/HR_projects/ddr3839/model/SedimentTransport/report/Rubensp/sand_dev08d.RUB/fig3.51.i

Figure 3.51 Scheme 1 conditions patterns of erosion and deposition in marina area with impounding in Carnsew and Copperhouse Pools to HW + 3 hours, double sluice operation on Carnsew Pool



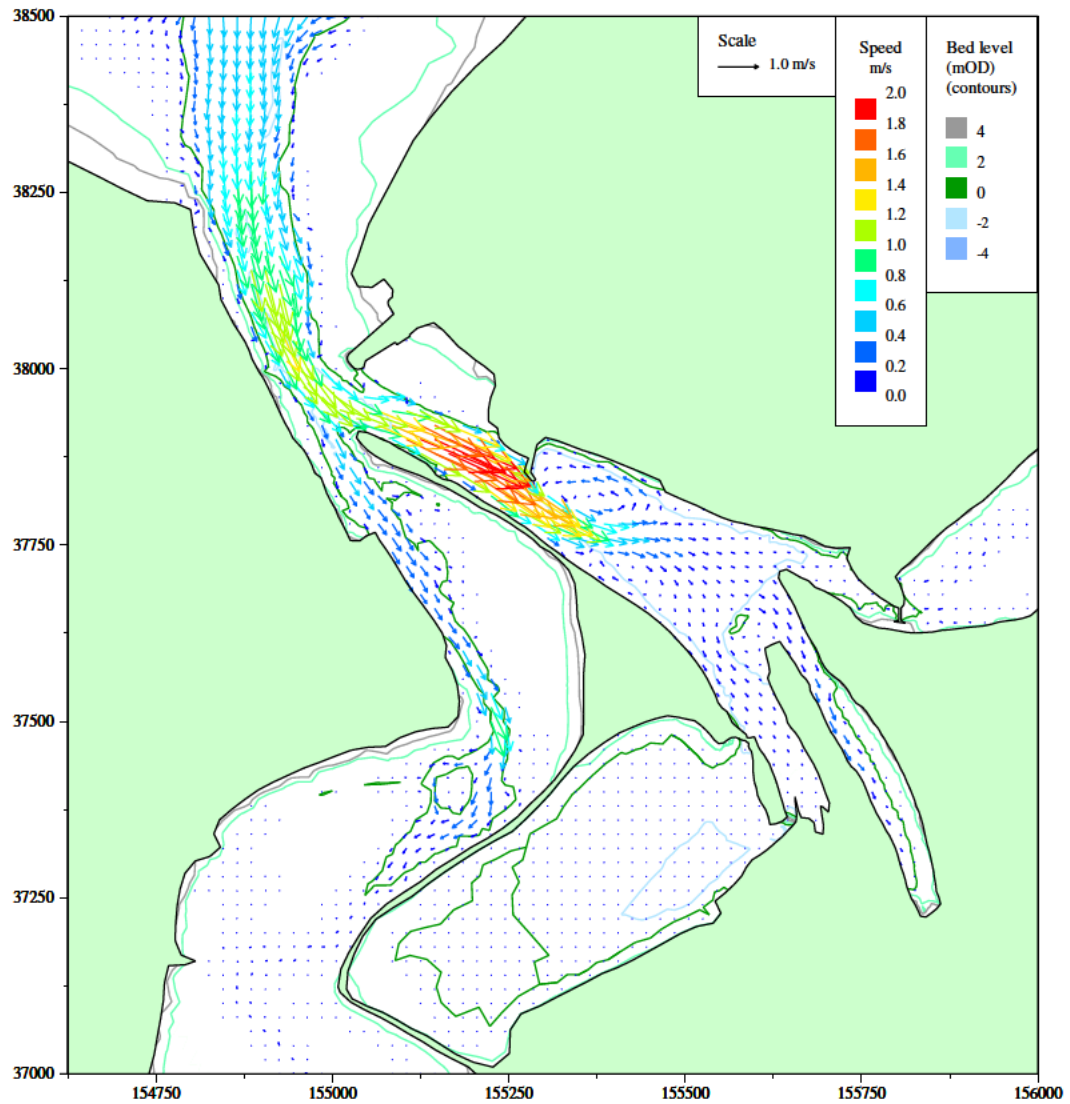
/HR_projects/ddr3839/model/SedimentTransport/report/Rubensp/sand_dev08a.RUB/fig3.52.i

Figure 3.52 Comparison between baseline and Scheme 1 of sand flux at 3 locations in harbour



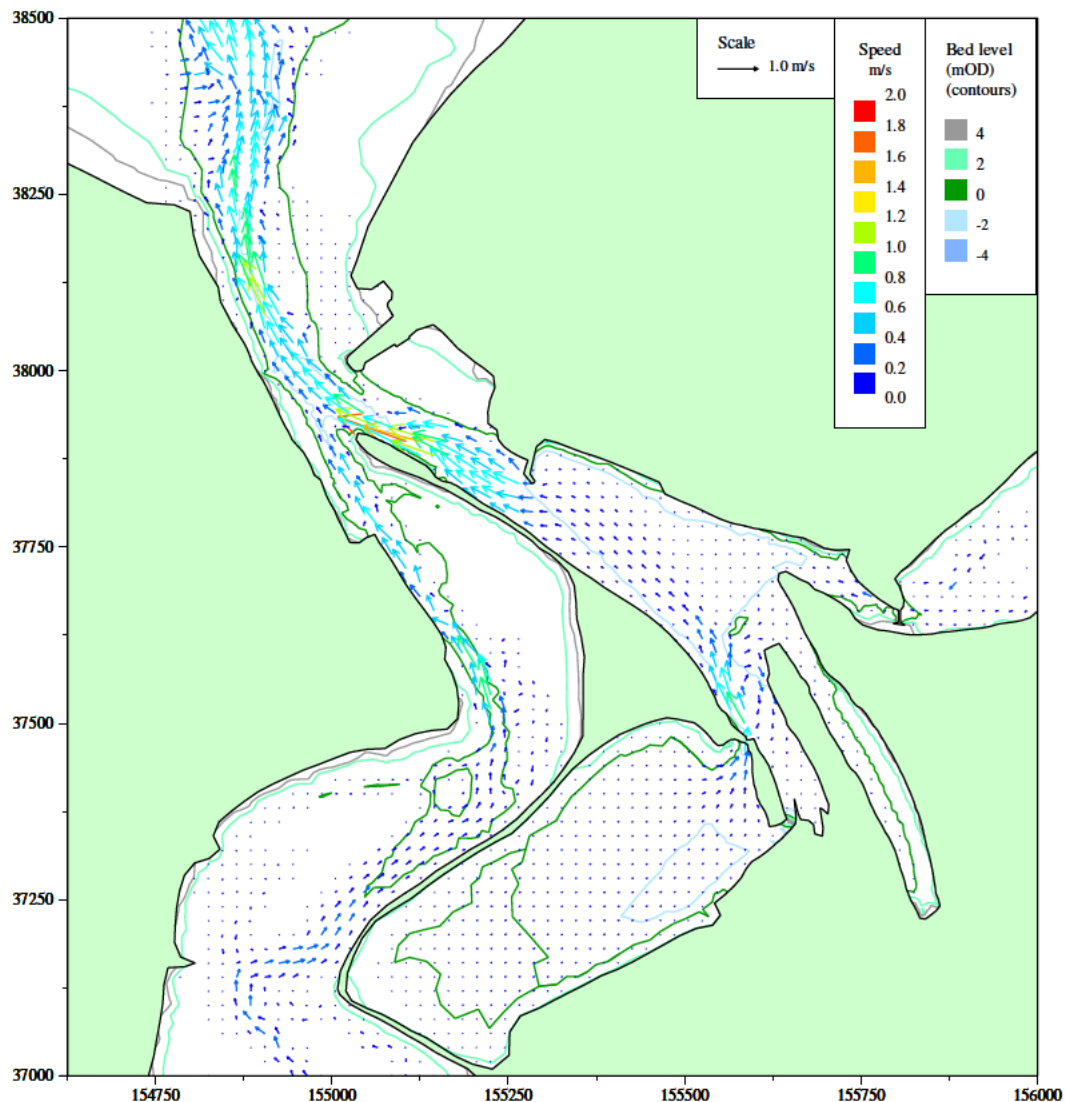
/HR_projects/ddr3839/model/SedimentTransport/report/Rubensp/flow_dev09a.RUB/fig3.53.i

Figure 3.53 Model bathymetry, Scheme 2



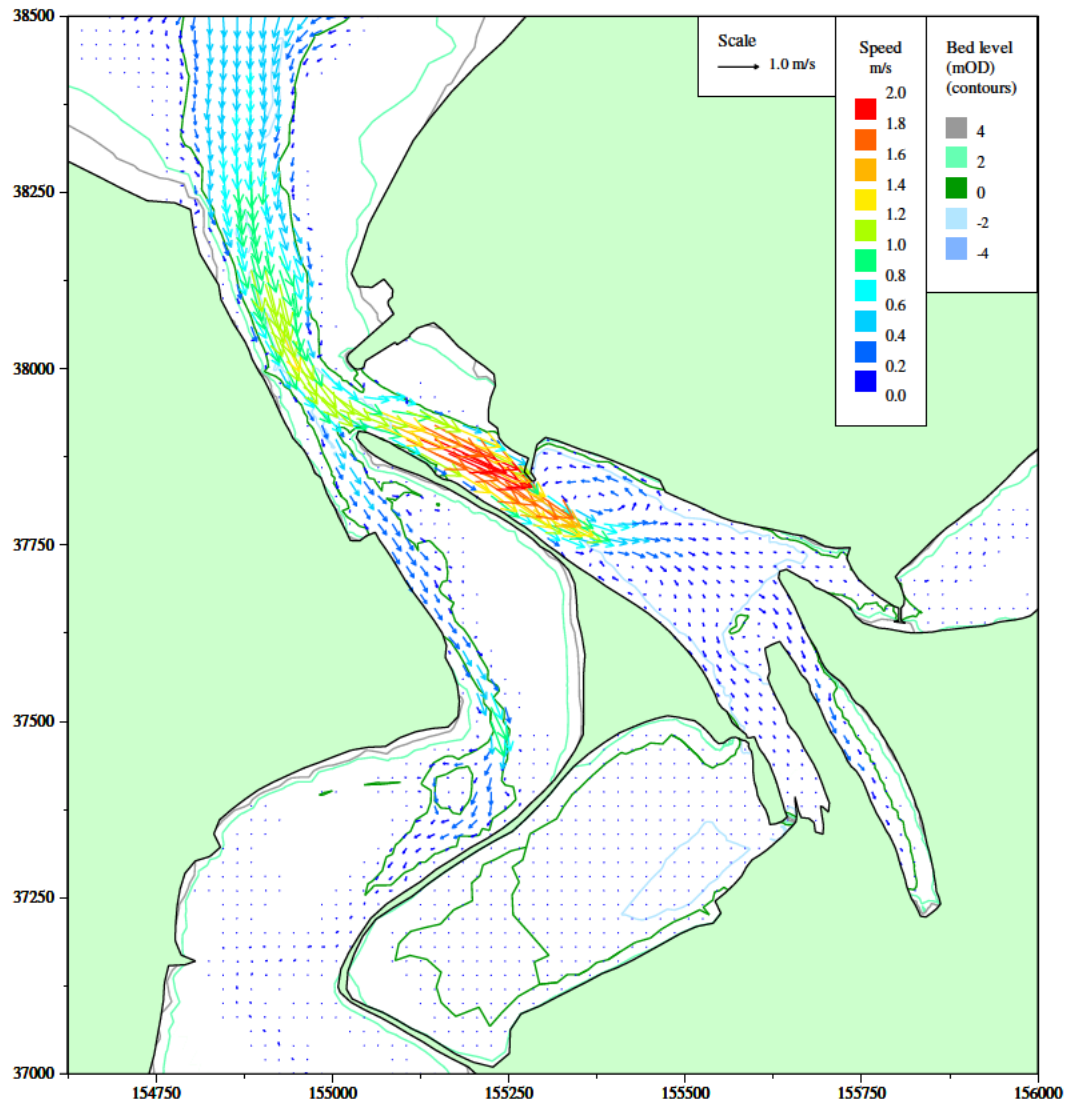
/HR_projects/ddr3839/model/SedimentTransport/report/Rubensp/flow_dev09a.RUB/fig3.54.i

Figure 3.54 Scheme 2 conditions spring tide peak flood currents (HW+9.5 Hours), Copperhouse sluice open (summer condition), single sluice operation on Carnsew Pool



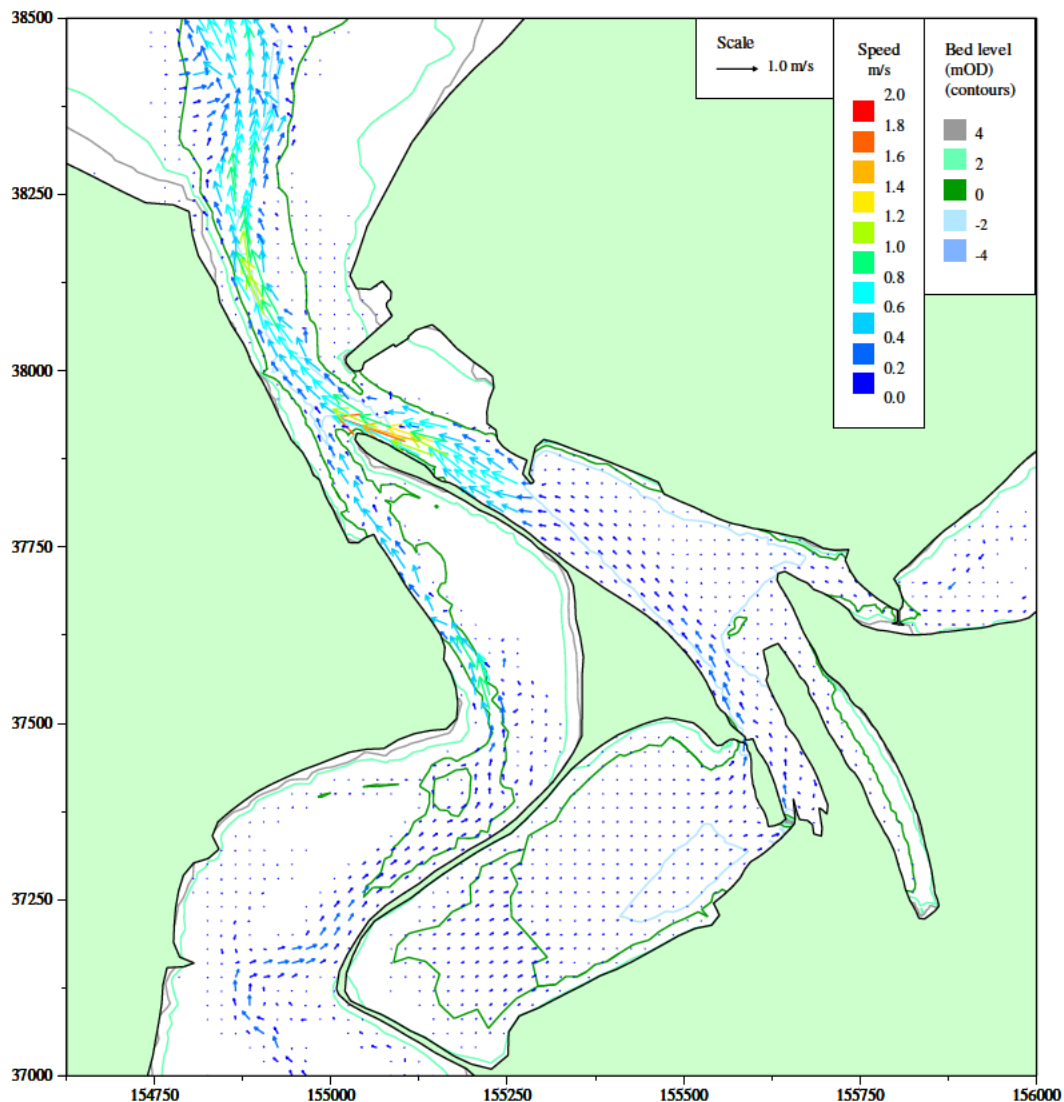
/HR_projects/ddr3839/model/SedimentTransport/report/Rubensp/flow_dev09a.RUB/fig3.55.i

Figure 3.55 Scheme 2 conditions spring tide ebb currents (HW+4.5 Hours), Copperhouse sluice open (summer condition), single sluice operation on Carnsew Pool



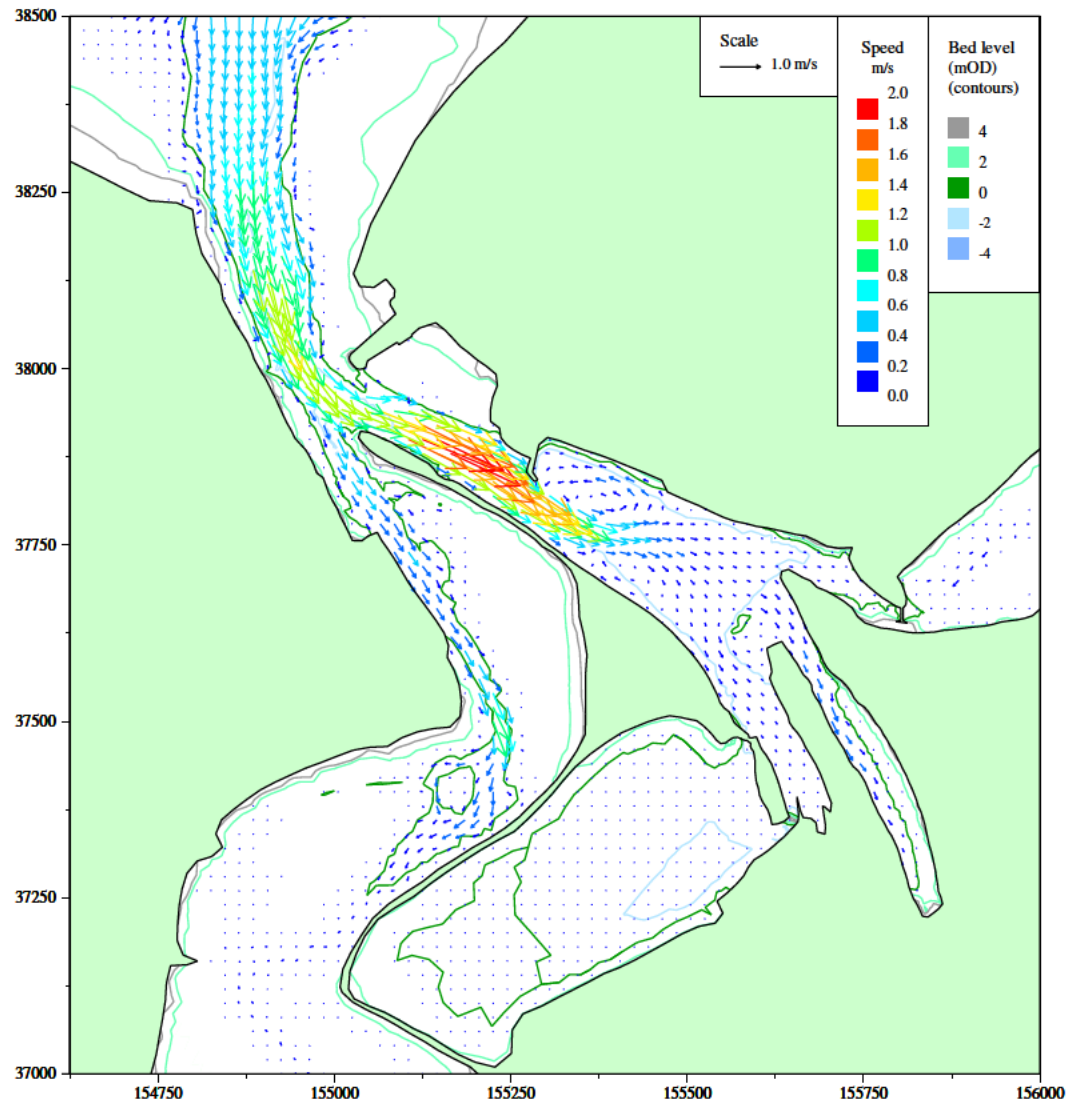
/HR_projects/ddr3839/model/SedimentTransport/report/Rubensp/flow_dev09b.RUB/fig3.56.i

Figure 3.56 Scheme 2 conditions spring tide peak flood currents (HW+9.5 Hours), Copperhouse sluice open (summer condition), double sluice operation on Carnsew Pool



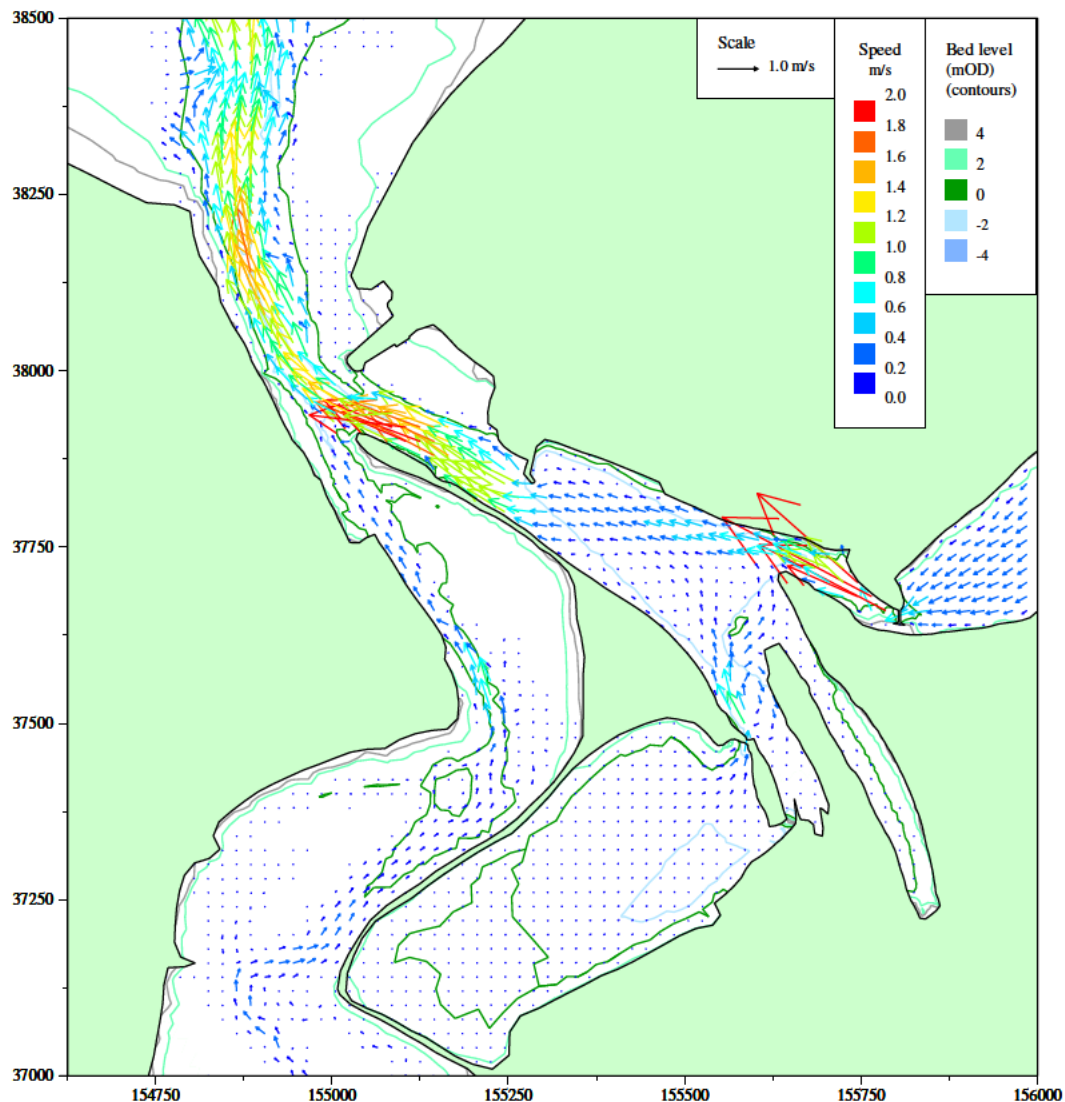
/HR_projects/ddr3839/model/SedimentTransport/report/Rubensp/flow_dev09b.RUB/fig3.57.i

Figure 3.57 Scheme 2 conditions spring tide ebb currents (HW+4.5 Hours), Copperhouse sluice open (summer condition), double sluice operation on Carnsew Pool



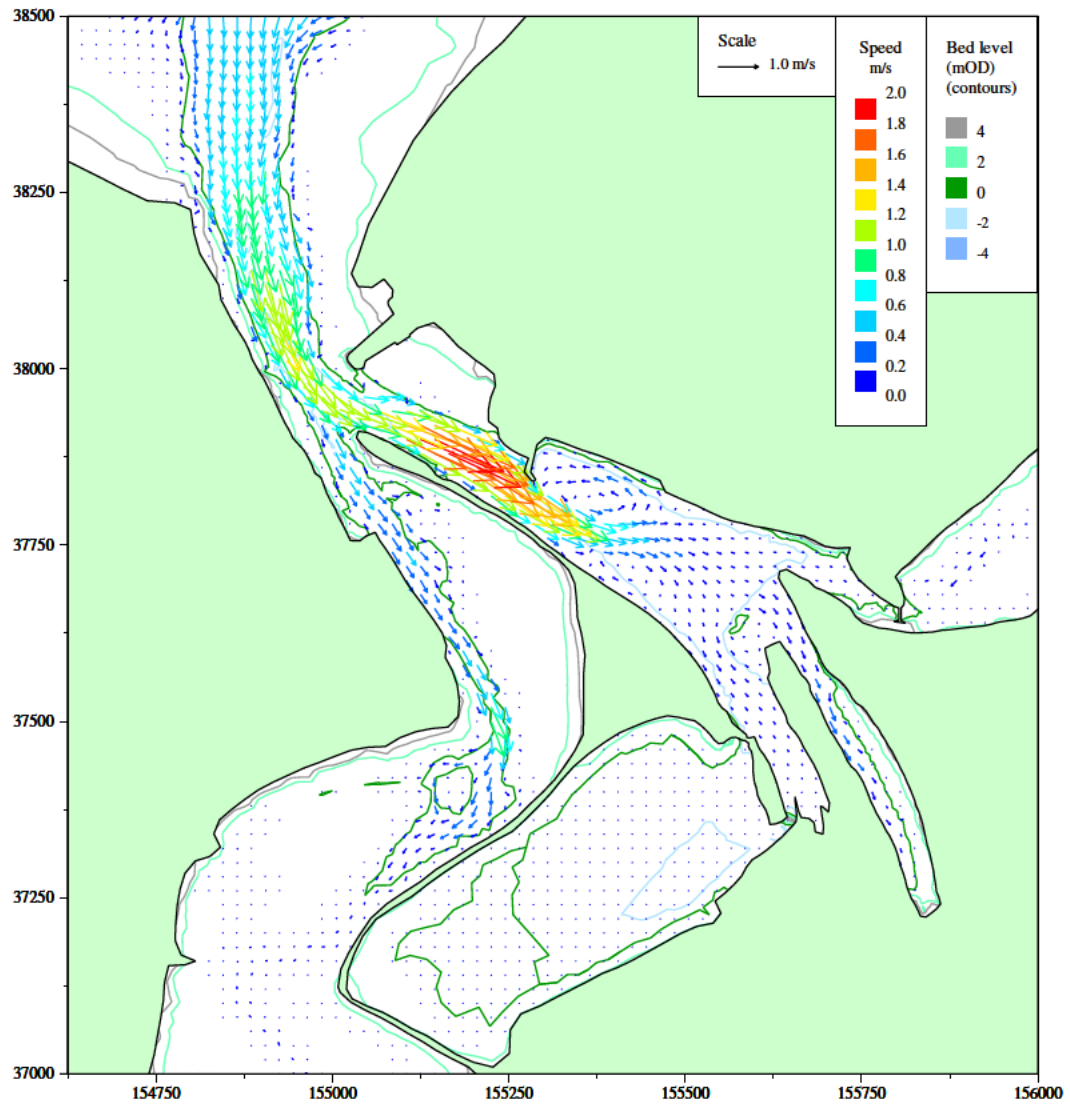
/HR_projects/ddr3839/model/SedimentTransport/report/Rubensp/flow_dev09c.RUB/fig3.58.i

Figure 3.58 Scheme 2 conditions spring tide peak flood currents with impounding in Carnsew and Copperhouse Pools to HW + 3 hours, single sluice operation on Carnsew Pool



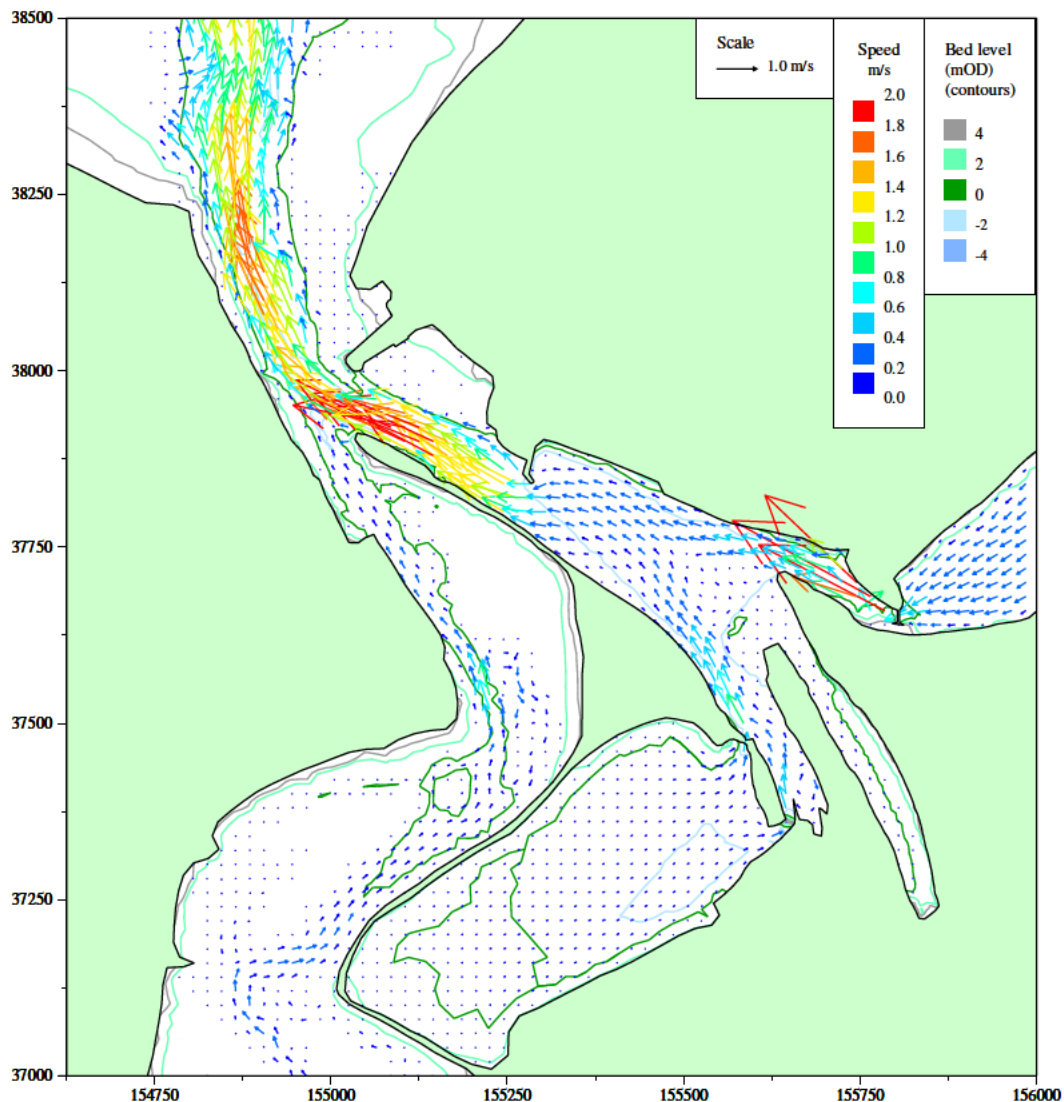
/HR_projects/ddr3839/mode/I/SedimentTransport/report/Rubensp/flow_dev09c.RUB/fig3.59.i

Figure 3.59 Scheme 2 conditions spring tide peak ebb currents with impounding in Carnsew and Copperhouse Pools to HW + 3 hours, single sluice operation on Carnsew Pool



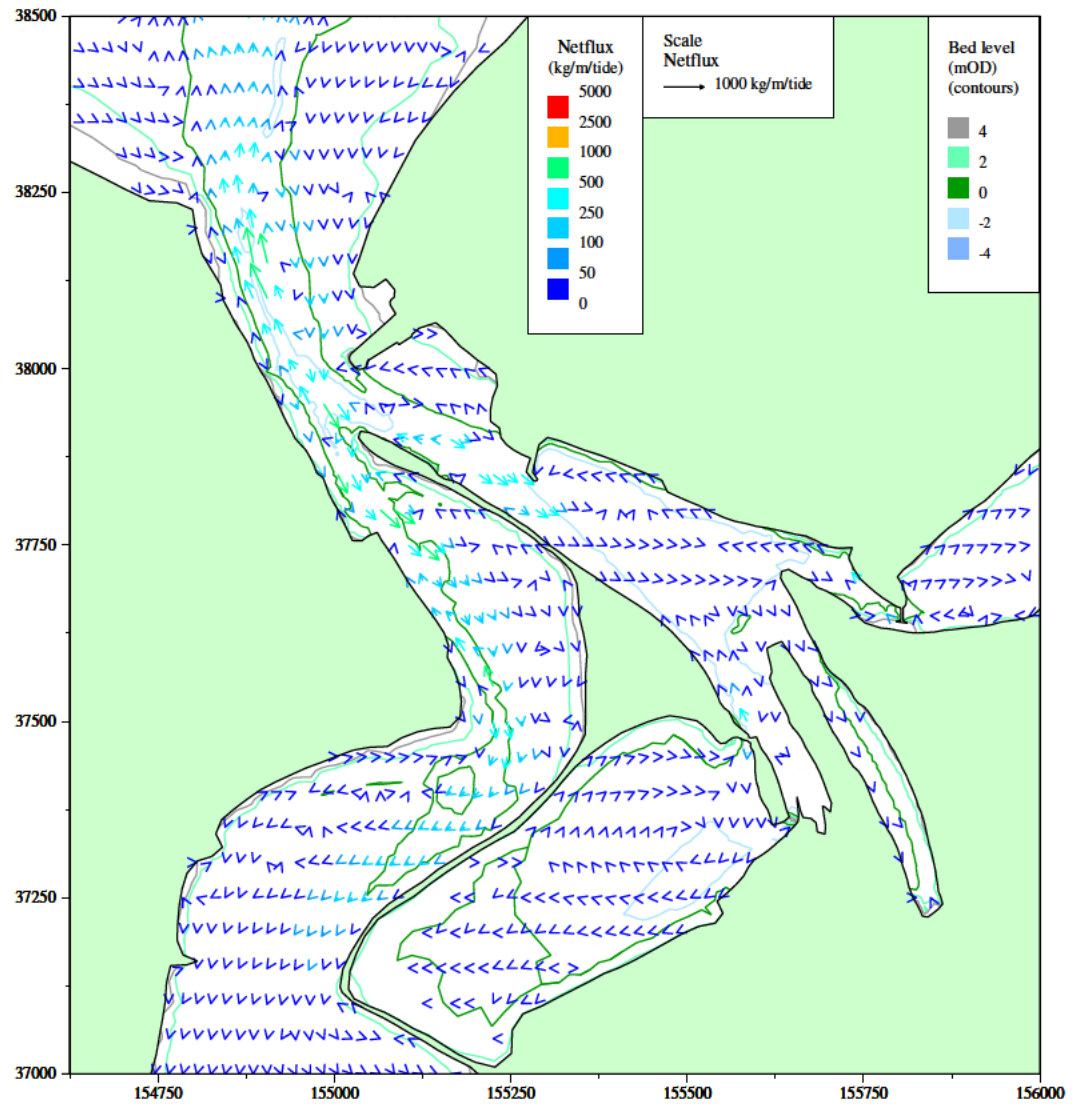
/HR_projects/ddr3839/model/SedimentTransport/report/Rubensp/flow_dev09d.RUB/fig3.60.i

Figure 3.60 Scheme 2 conditions spring tide peak flood currents with impounding in Carnsew and Copperhouse Pools to HW + 3 hours, double sluice operation on Carnsew Pool



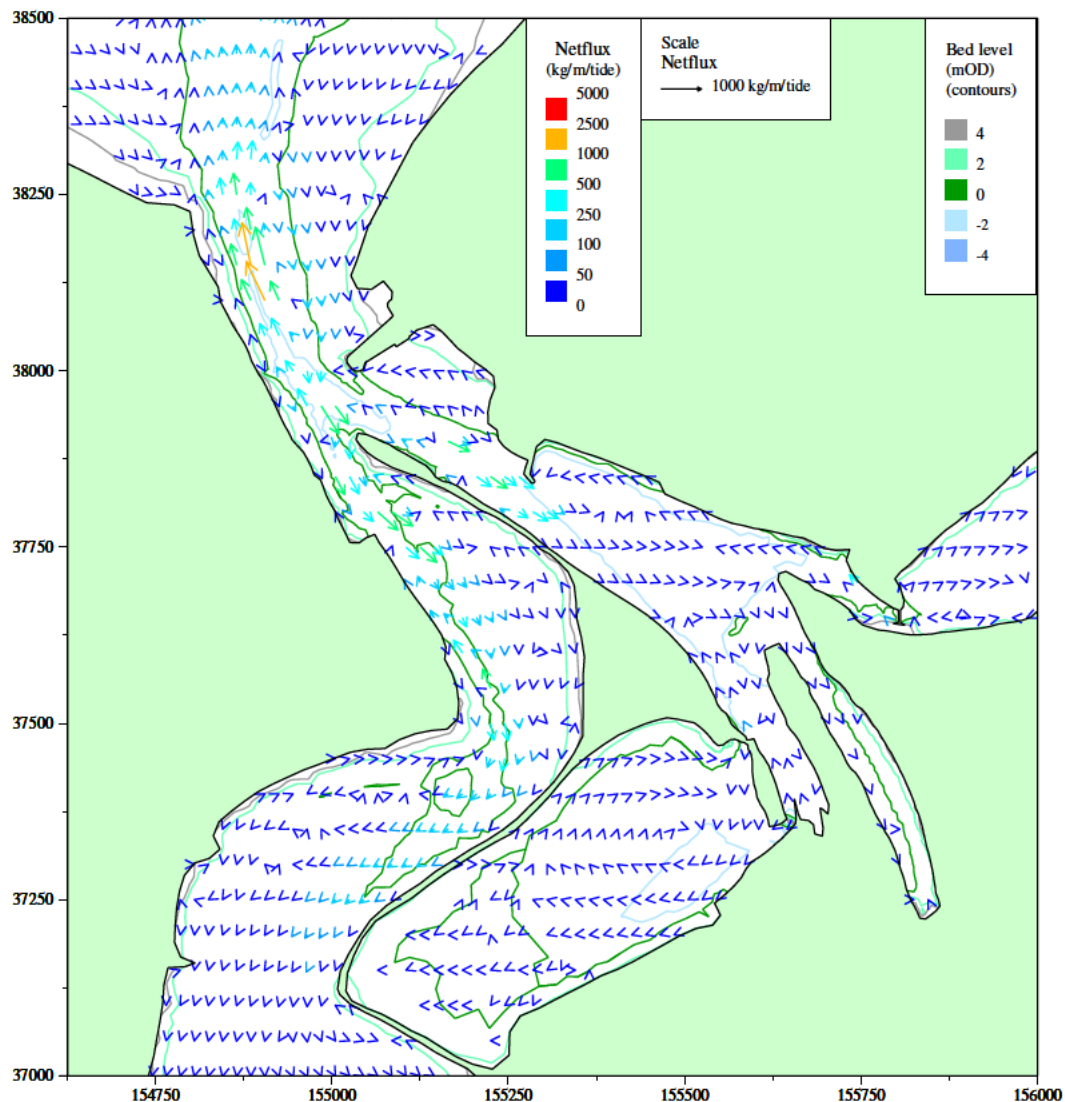
/HR_projects/ddr3839/model/SedimentTransport/report/Rubensp/flow_dev09d.RUB/fig3.61.i

Figure 3.61 Scheme 2 conditions spring tide peak ebb currents with impounding in Carnsew and Copperhouse Pools to HW + 3 hours, double sluice operation on Carnsew Pool



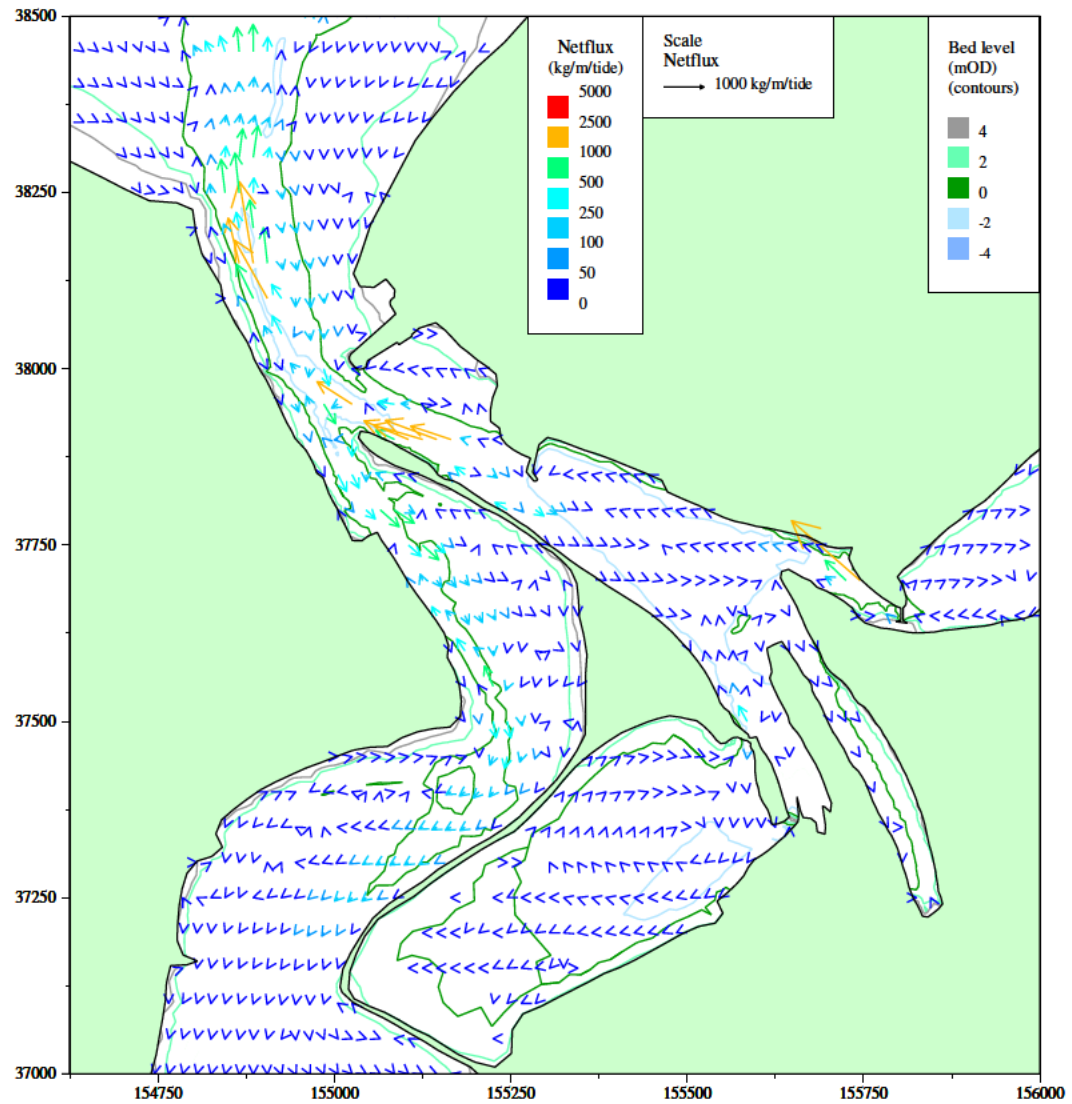
/HR_projects/ddr3839/model/SedimentTransport/report/Rubensp/sand_dev09a.RUB/fig3.62.i

Figure 3.62 Scheme 2 conditions net sand flux patterns, Copperhouse sluice open (summer condition), single sluice operation on Carnsew Pool



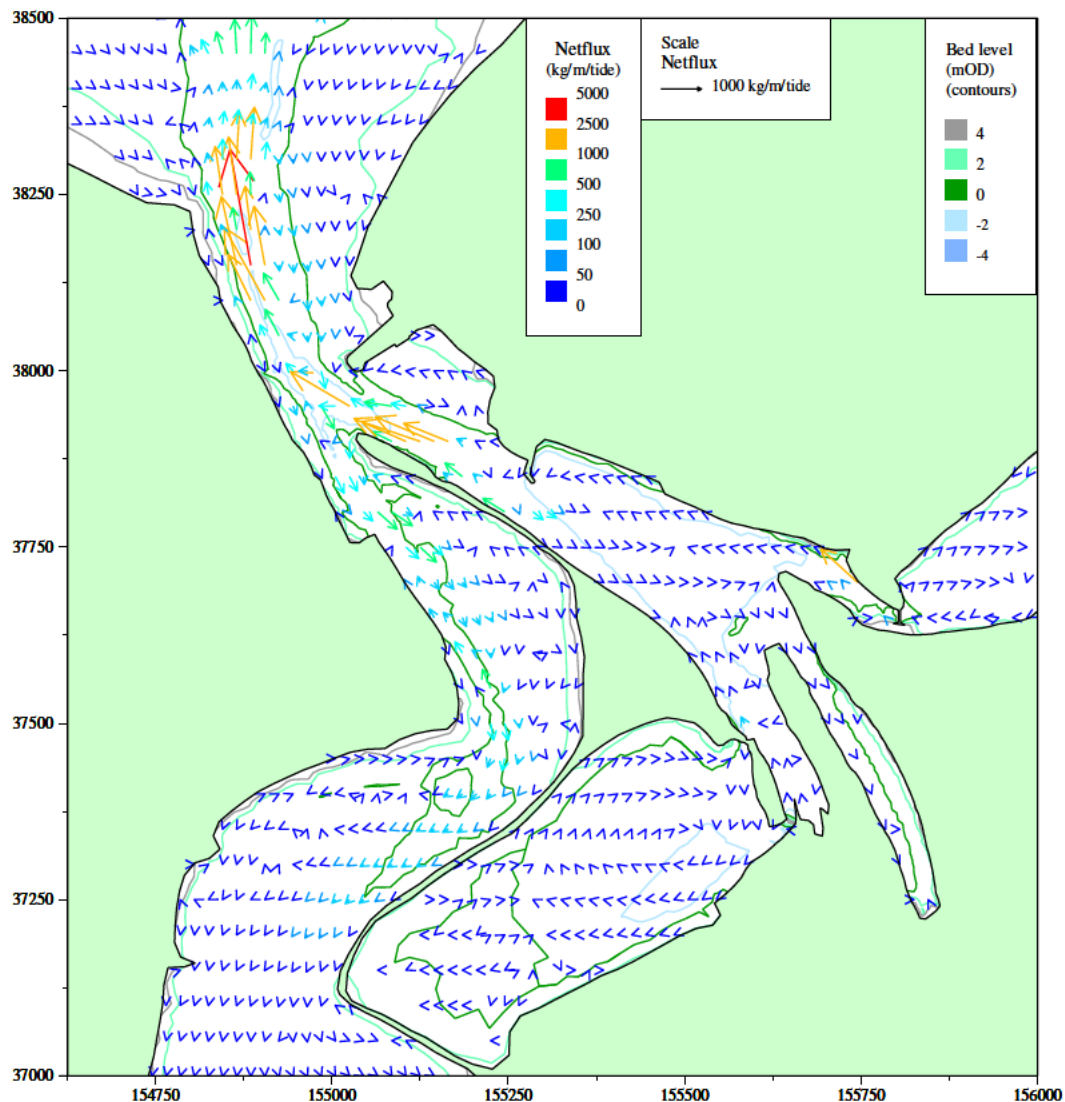
/HR_projects/ddr3839/model/SedimentTransport/report/Rubensp/sand_dev09b.RUB/fig3.63.i

Figure 3.63 Scheme 2 conditions net sand flux patterns, Copperhouse sluice open (summer condition), double sluice operation on Carnsew Pool



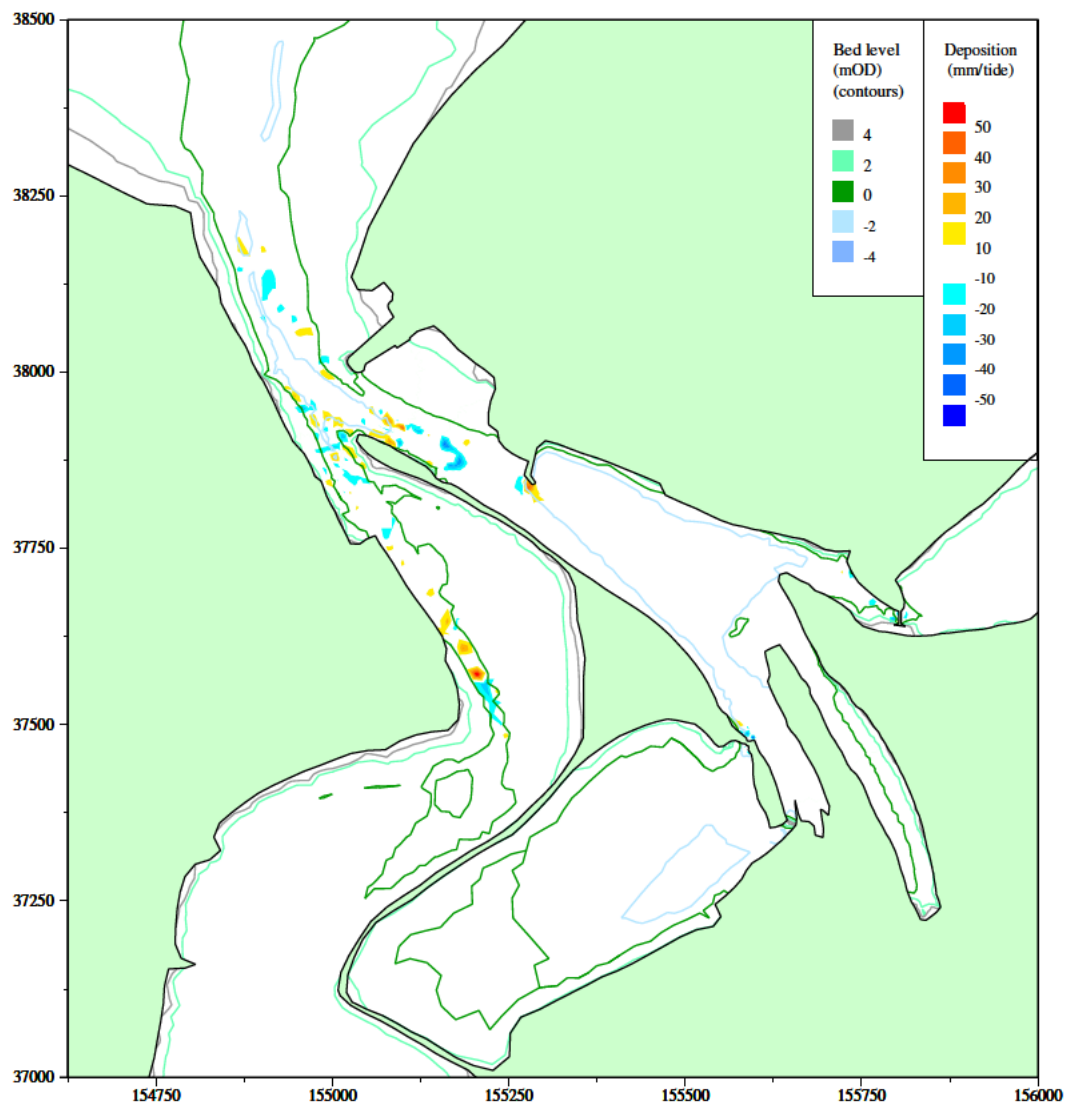
/HR_projects/ddr3839/model/SedimentTransport/report/Rubensp/sand_dev09c.RUB/fig3.64.i

Figure 3.64 Scheme 2 conditions net sand flux patterns with impounding in Carnsew and Copperhouse Pools to HW + 3 hours, single sluice operation on Carnsew Pool



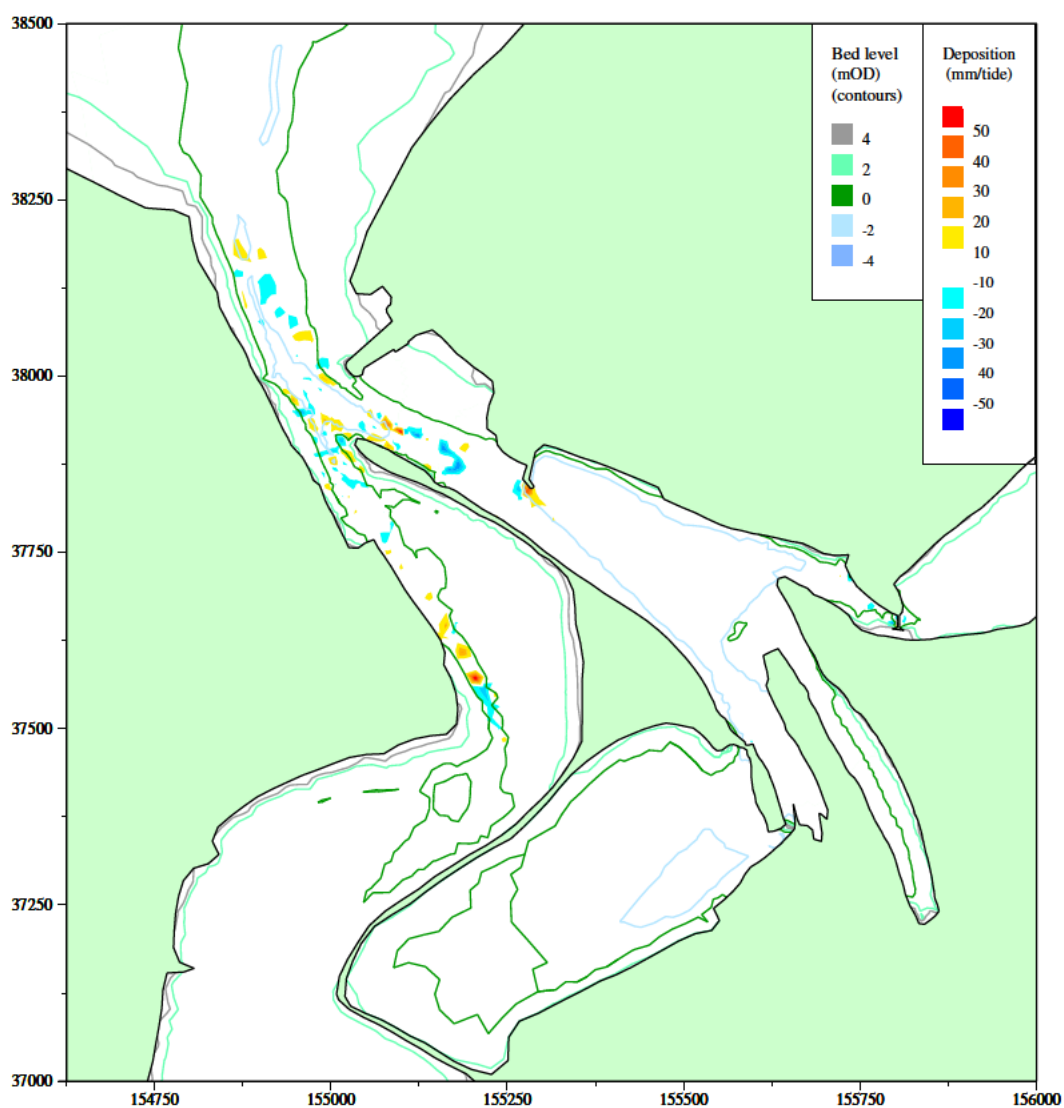
/HR_projects/ddr3839/model/SedimentTransport/report/Rubensp/sand_dev09d.RUB/fig3.65.i

Figure 3.65 Scheme 2 conditions net sand flux patterns with impounding in Carnsew and Copperhouse Pools to HW + 3 hours, double sluice operation on Carnsew Pool



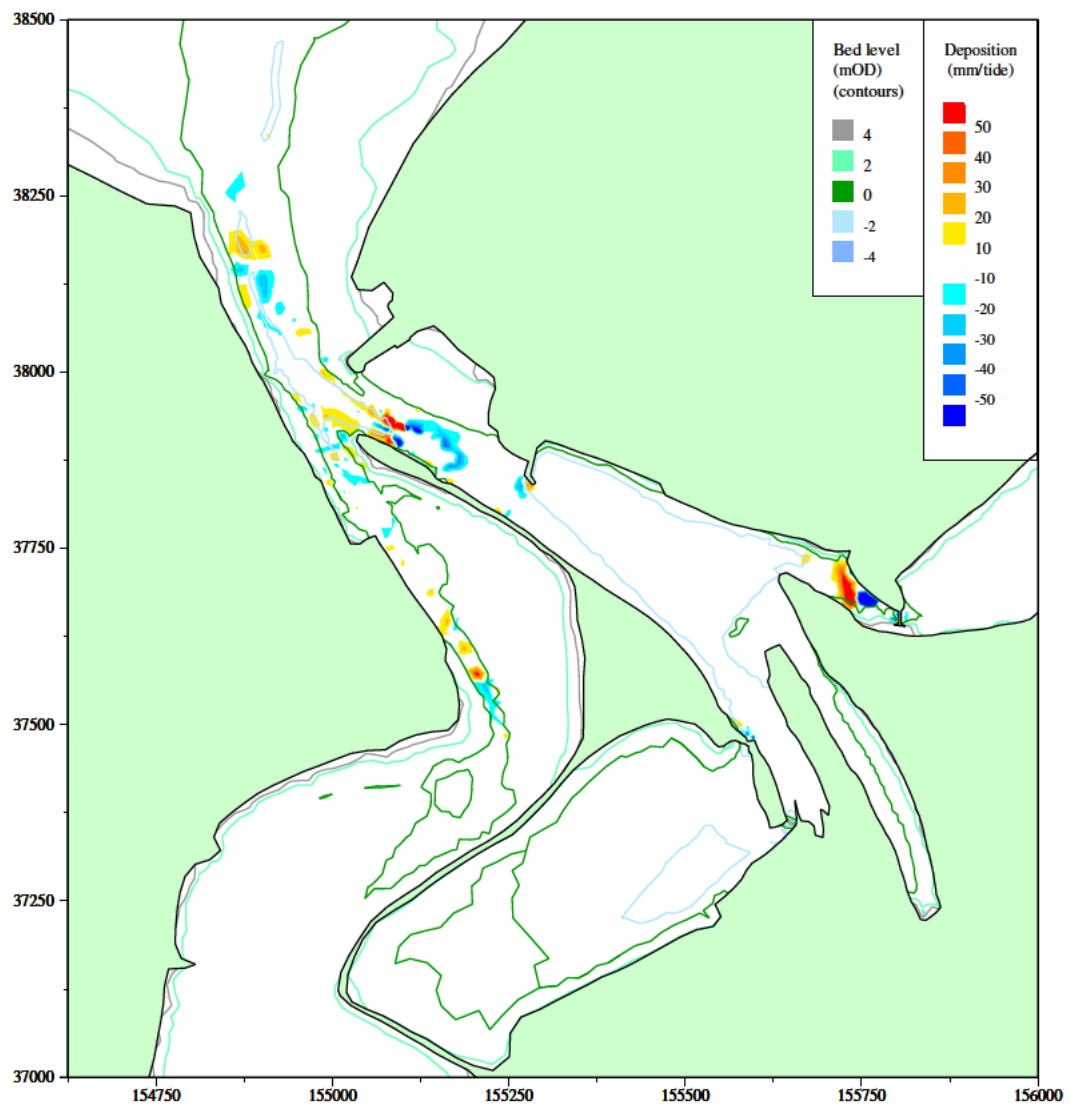
/HR_projects/ddr3839/model/SedimentTransport/report/Rubensp/sand_dev09a.RUB/fig3.66.i

Figure 3.66 Scheme 2 conditions patterns of erosion and deposition, Copperhouse sluice open (summer condition), single sluice operation on Carnsew Pool



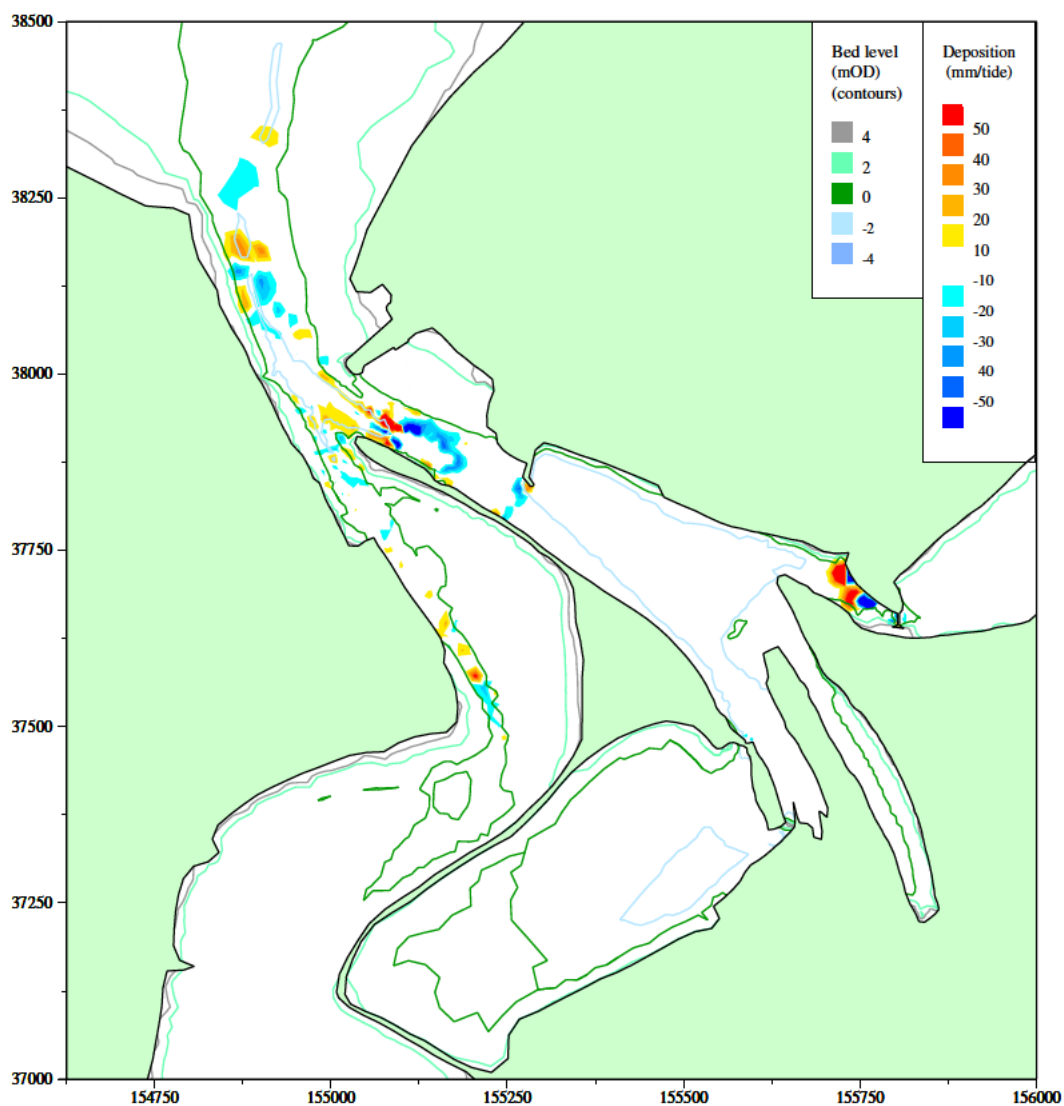
/HR_projects/ddr3839/model/SedimentTransport/report/Rubensp/sand_dev09b.RUB/fig3.67.i

Figure 3.67 Scheme 2 conditions patterns of erosion and deposition, Copperhouse sluice open (summer condition), double sluice operation on Carnsew Pool



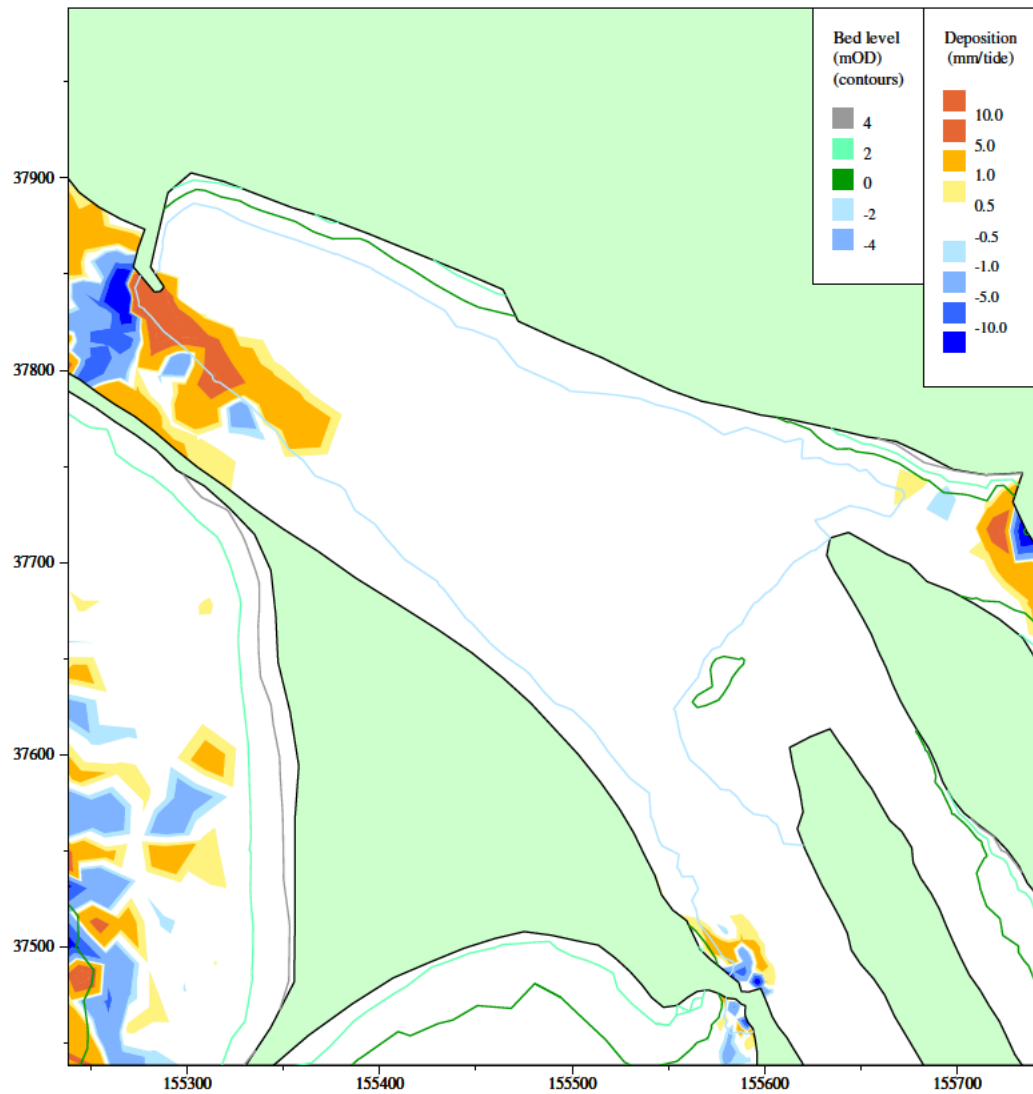
/HR_projects/ddr3839/model/SedimentTransport/report/Rubensp/sand_dev09c.RUB/fig3.68.i

Figure 3.68 Scheme 2 conditions patterns of erosion and deposition with impounding in Carnsew and Copperhouse Pools to HW + 3 hours, single sluice operation on Carnsew Pool



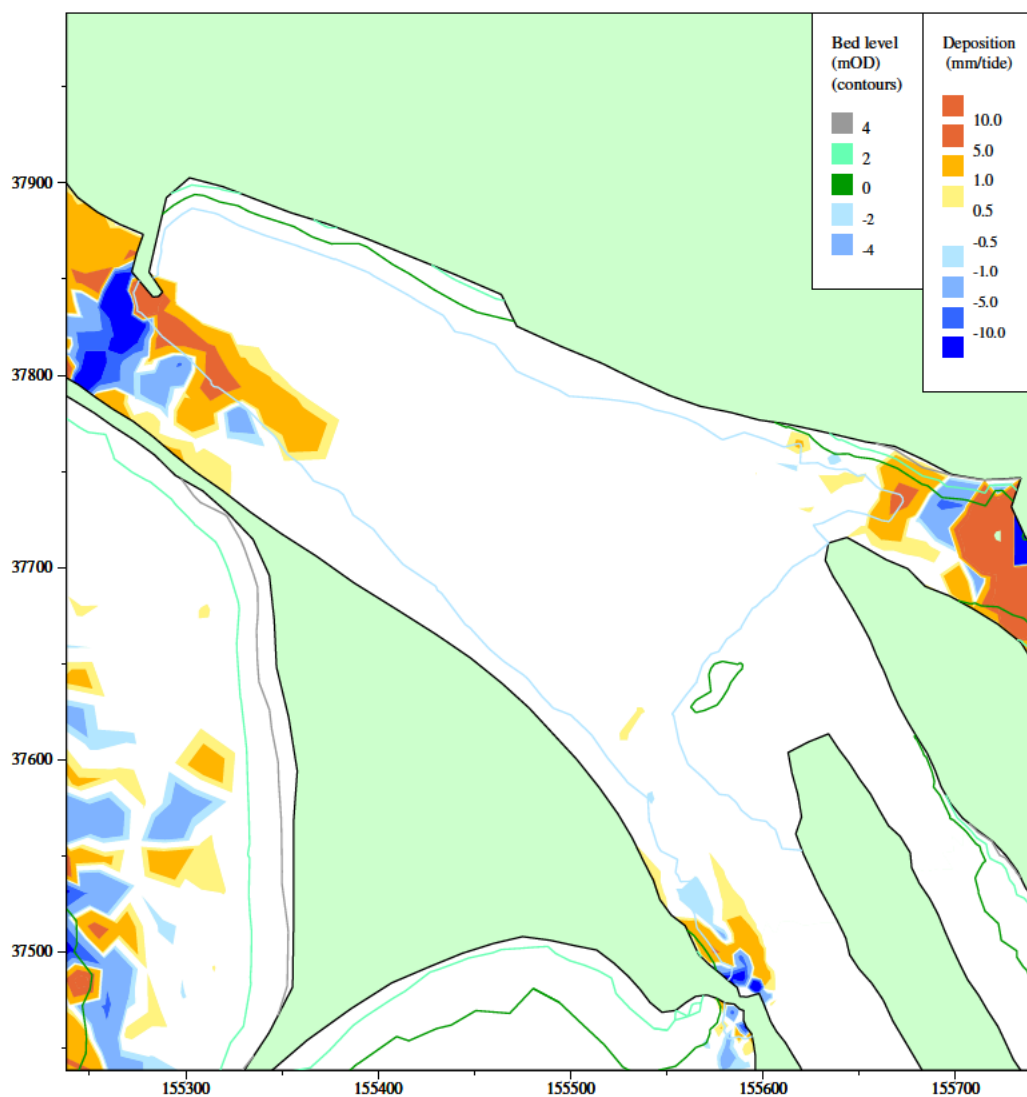
/HR_projects/ddr3839/model/SedimentTransport/report/Rubensp/sand_dev09d.RUB/fig3.69.i

Figure 3.69 Scheme 2 conditions patterns of erosion and deposition with impounding in Carnsew and Copperhouse Pools to HW + 3 hours, double sluice operation on Carnsew Pool



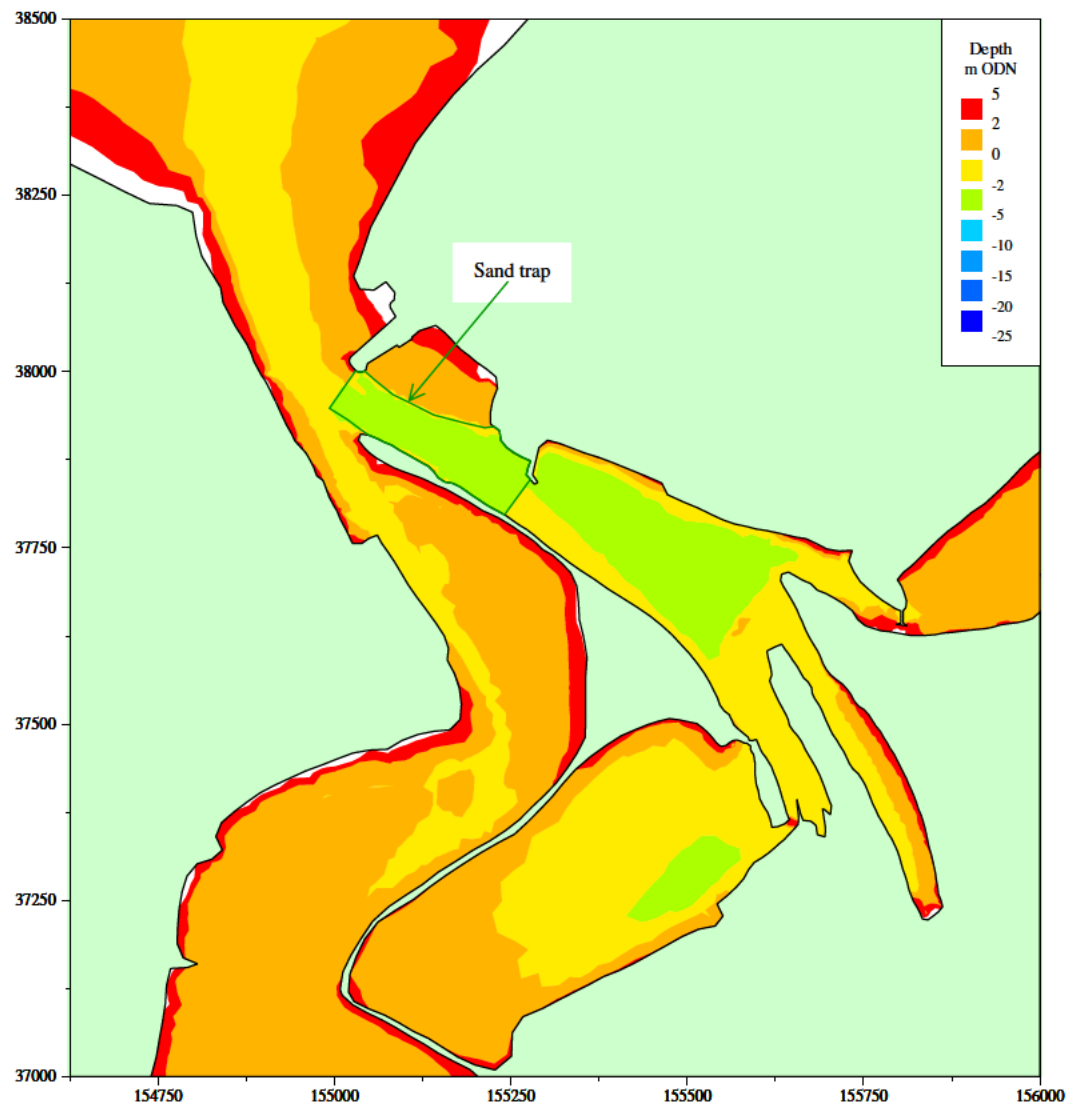
/HR_projects/ddr3839/model/SedimentTransport/report/Rubensp/sand_dev09b.RUB/fig3.70.i

Figure 3.70 Scheme 2 conditions patterns of erosion and deposition in marina area, Copperhouse sluice open (summer condition), double sluice operation on Carnsew Pool



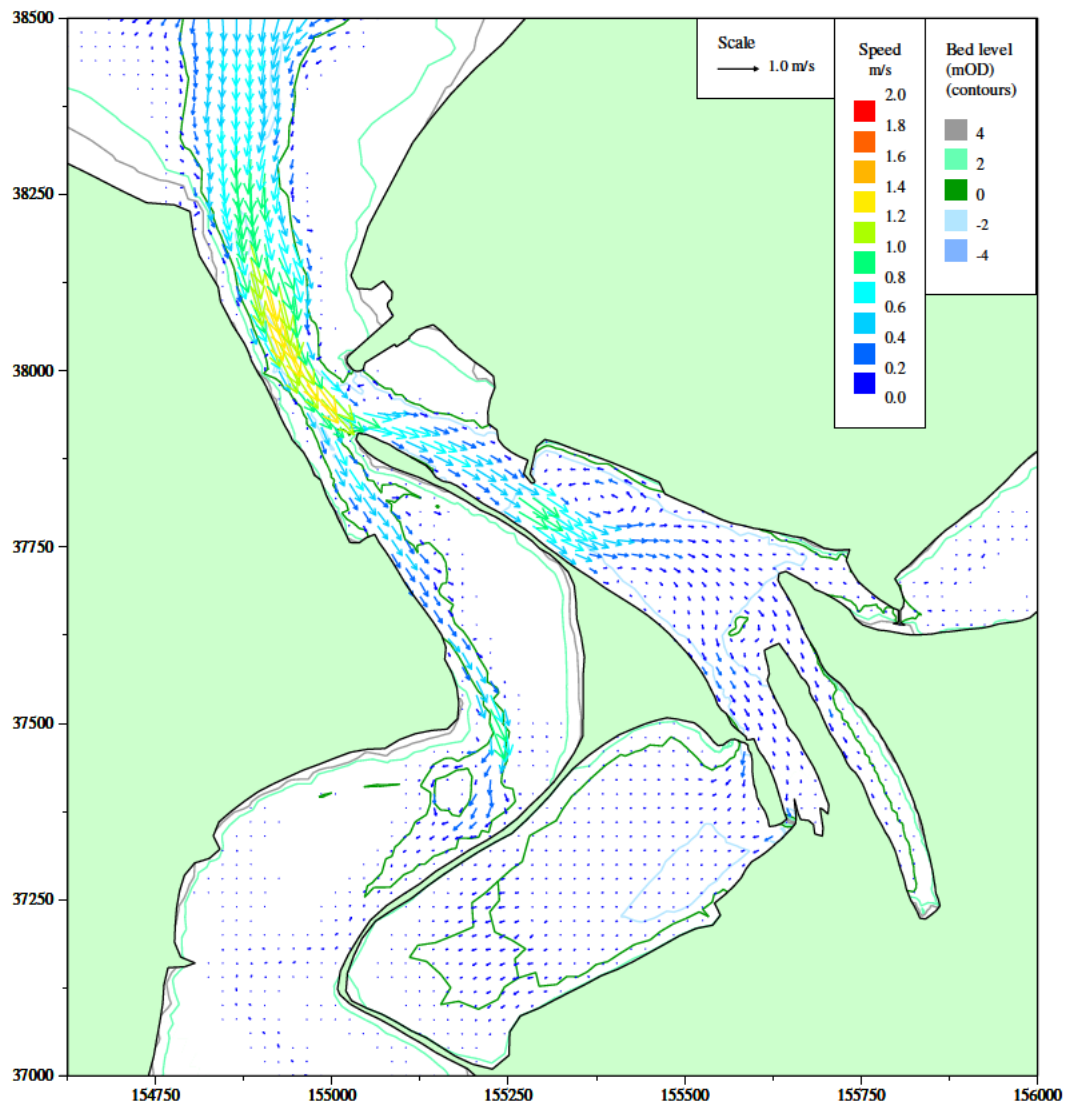
/HR_projects/ddr3839/model/SedimentTransport/report/Rubensp/sand_dev09d.RUB/fig3.71.i

Figure 3.71 Scheme 2 conditions patterns of erosion and deposition in marina area with impounding in Carnsew and Copperhouse Pools to HW + 3 hours, double sluice operation on Carnsew Pool



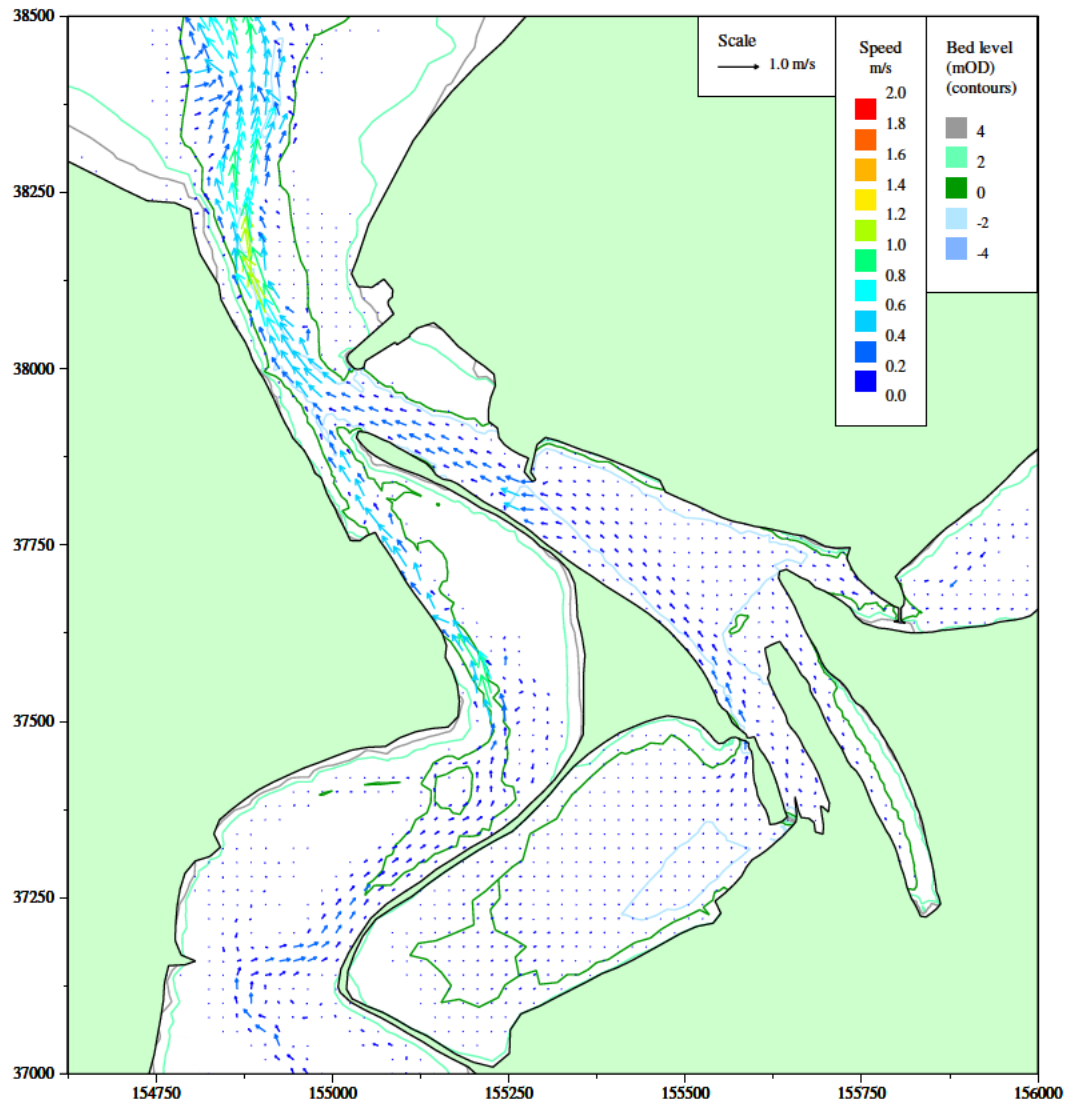
/HR_projects/ddr3839/model/SedimentTransport/report/Rubensp/flow_dev09b_st.RUB/fig3.72.i

Figure 3.72 Model bathymetry, Scheme 2 with sand trap



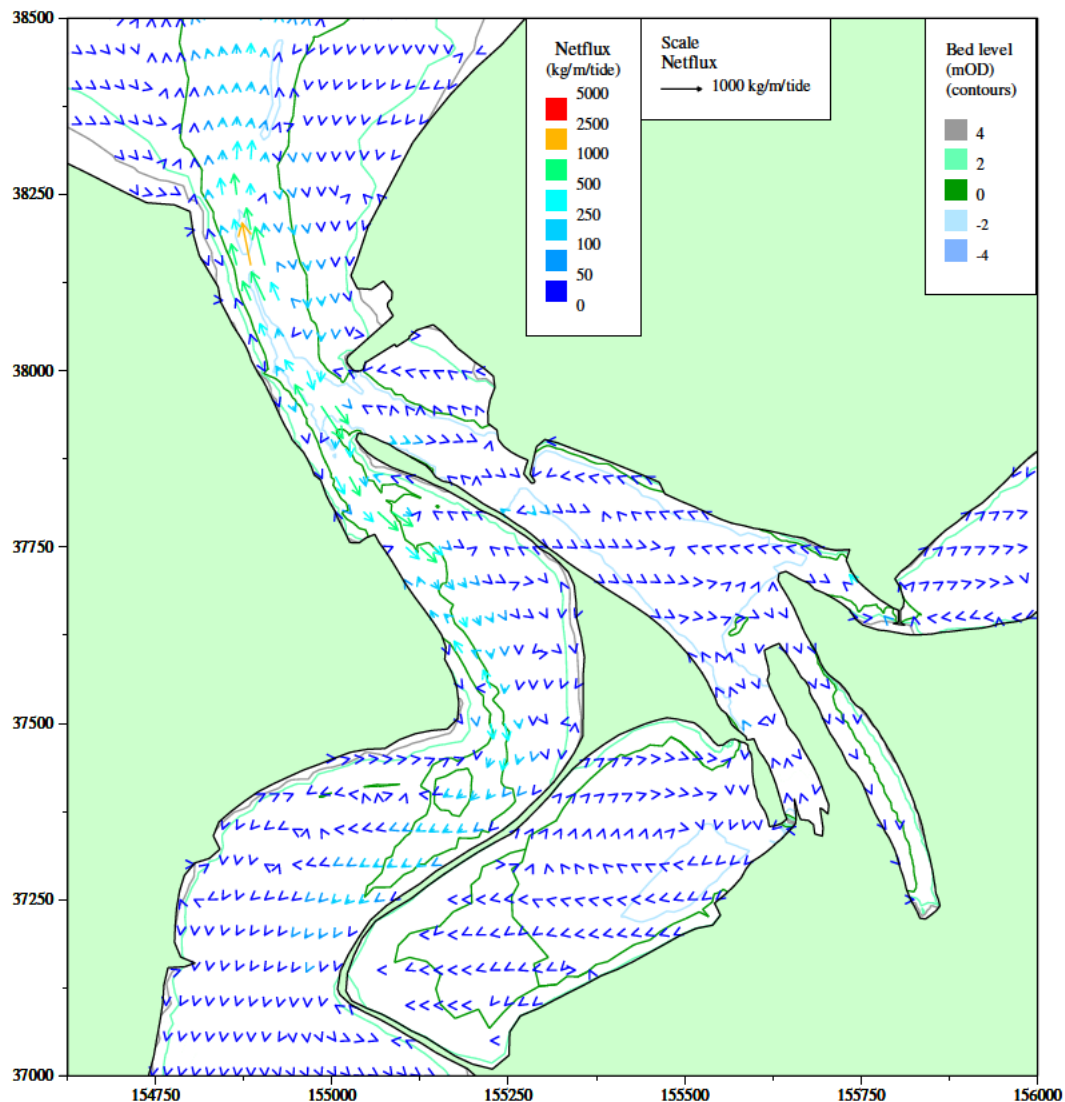
/HR_projects/ddr3839/model/SedimentTransport/report/Rubensp/flow_dev09b_st.RUB/fig3.73.i

Figure 3.73 Scheme 2 with sand trap conditions spring tide peak flood currents (HW+9.5 Hours), Copperhouse sluice open (summer condition), double sluice operation on Carnsew Pool



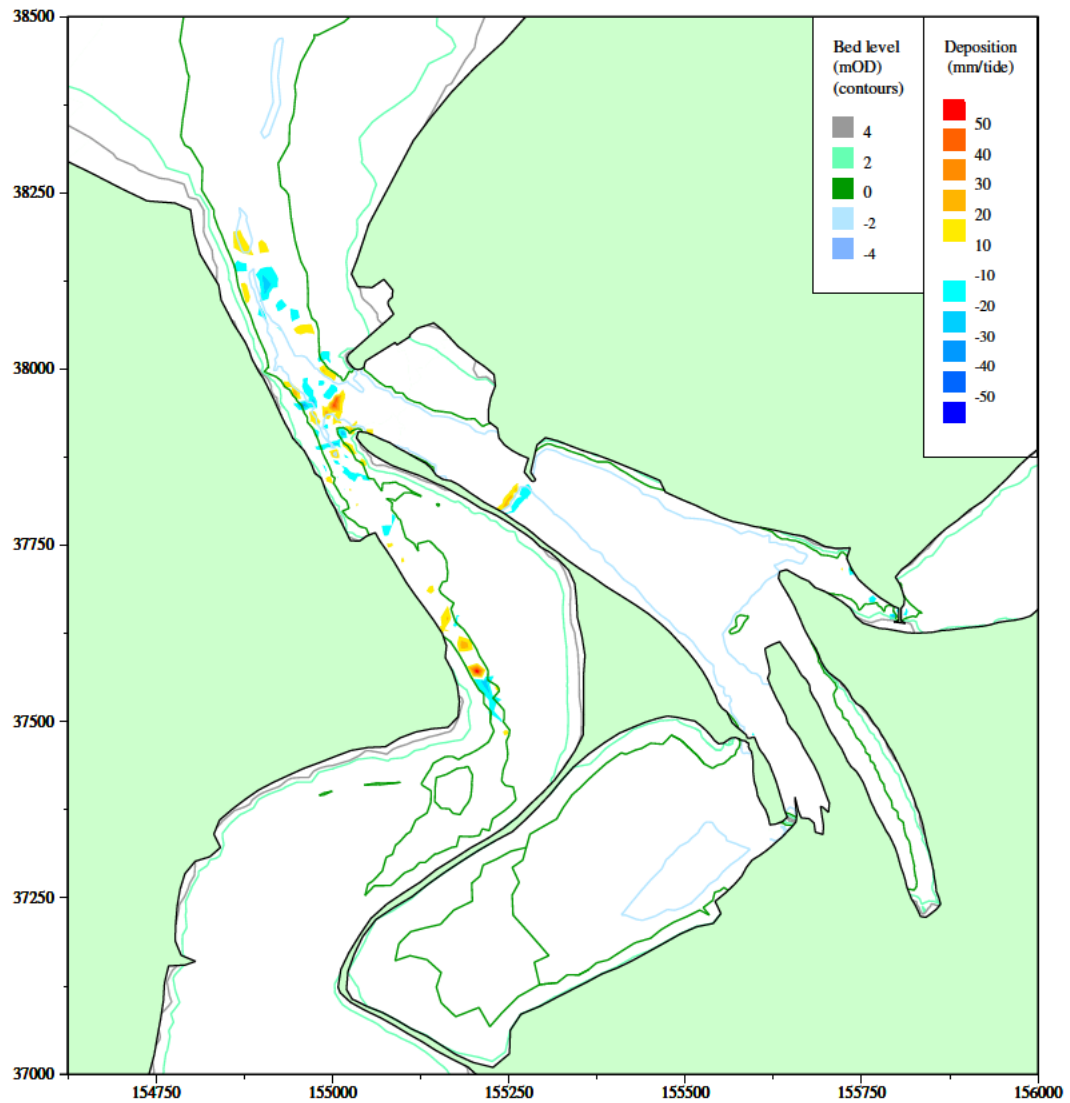
/HR_projects/ddr3839/model/SedimentTransport/report/Rubensp/flow_dev09b_st.RUB/fig3.74.i

Figure 3.74 Scheme 2 with sand trap conditions spring tide ebb currents (HW+4.5 Hours), Copperhouse sluice open (summer condition), double sluice operation on Carnsew Pool



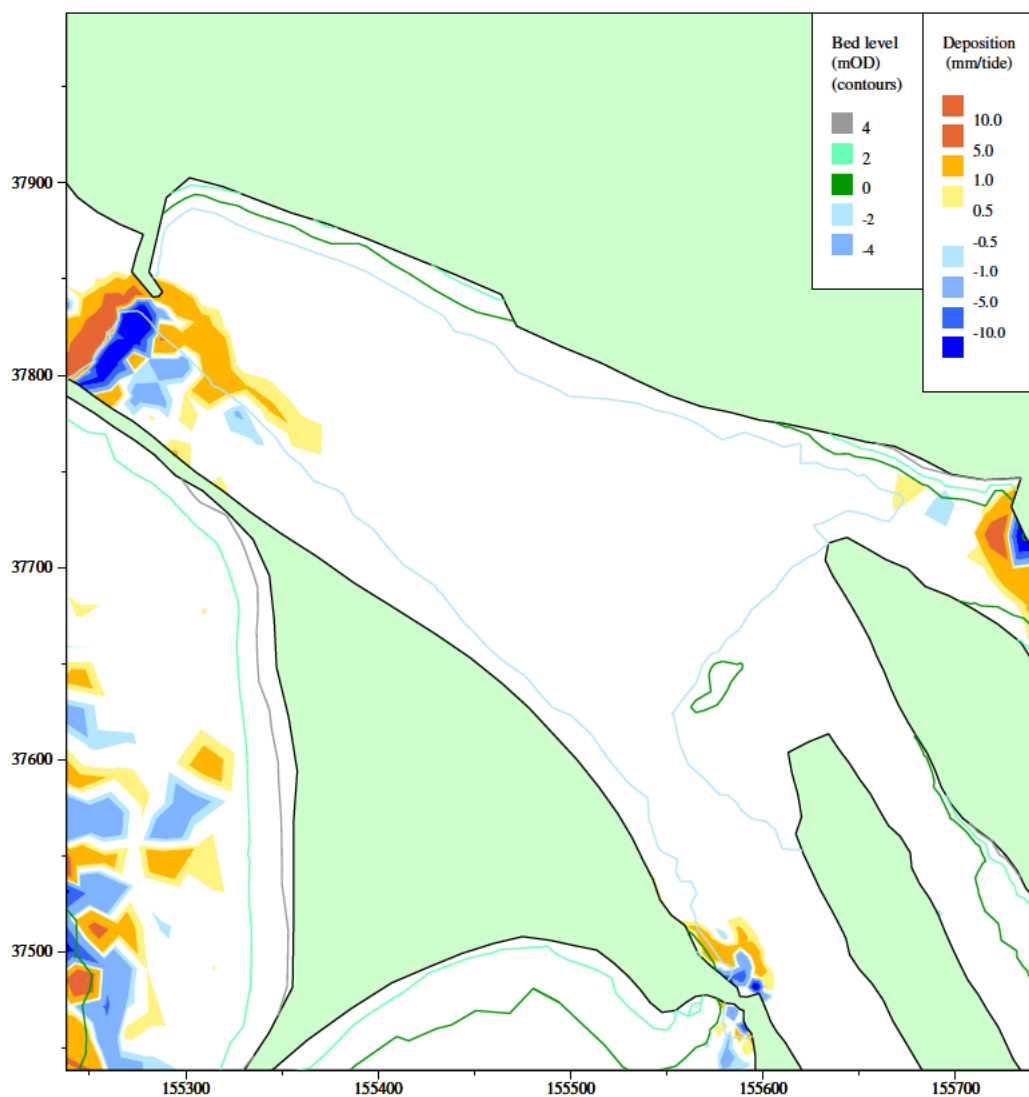
/HR_projects/ddr3839/model/SedimentTransport/report/Rubensp/sand_dev09b_st.RUB/fig3.75.i

Figure 3.75 Scheme 2 with sand trap conditions net sand flux patterns, Copperhouse sluice open (summer condition), double sluice operation on Carnsew Pool



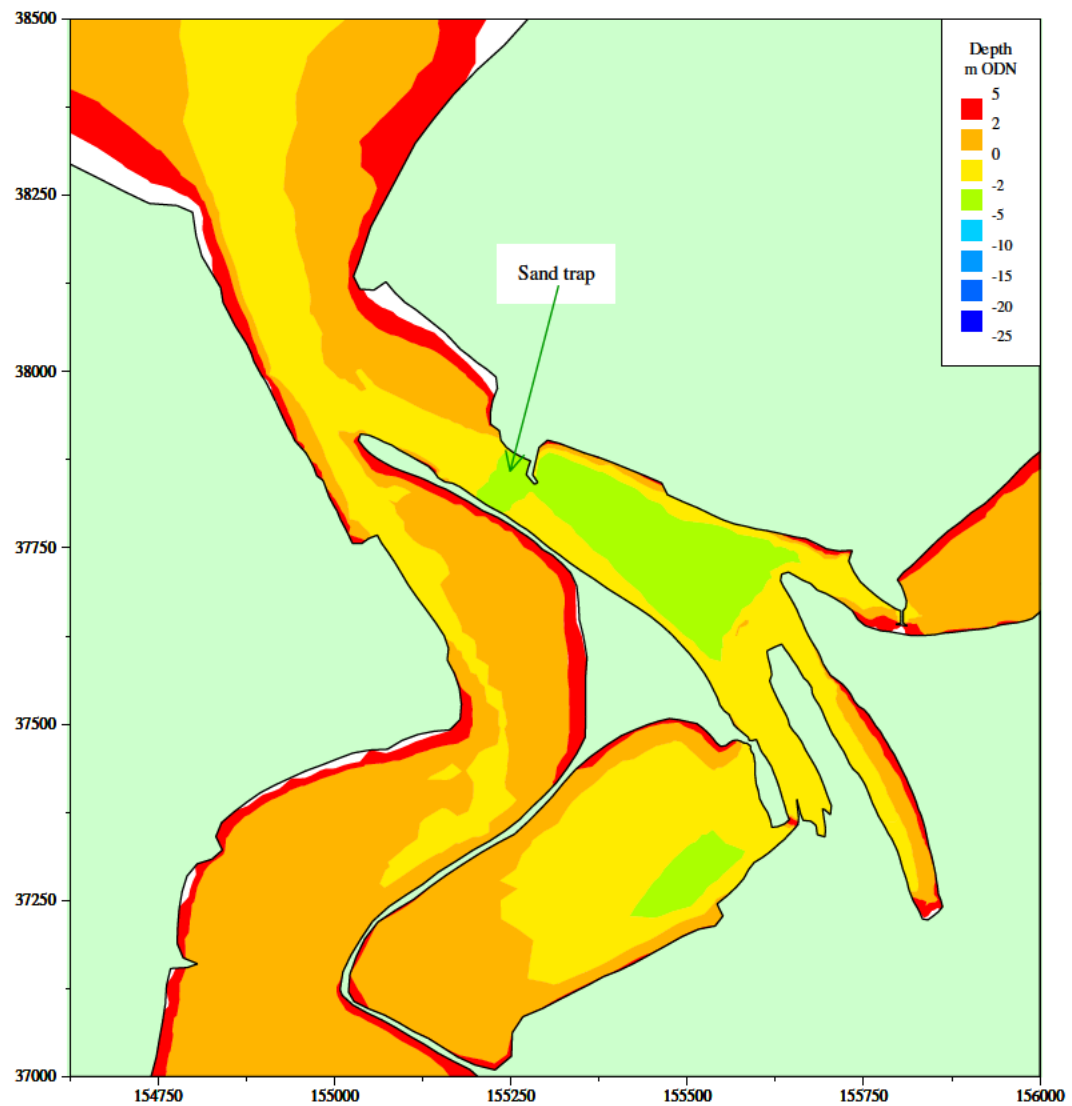
/HR_projects/ddr3839/model/SedimentTransport/report/Rubensp/sand_dev09b_st.RUB/fig3.76.i

Figure 3.76 Scheme 2 with sand trap conditions patterns of erosion and deposition, Copperhouse sluice open (summer condition), double sluice operation on Carnsew Pool



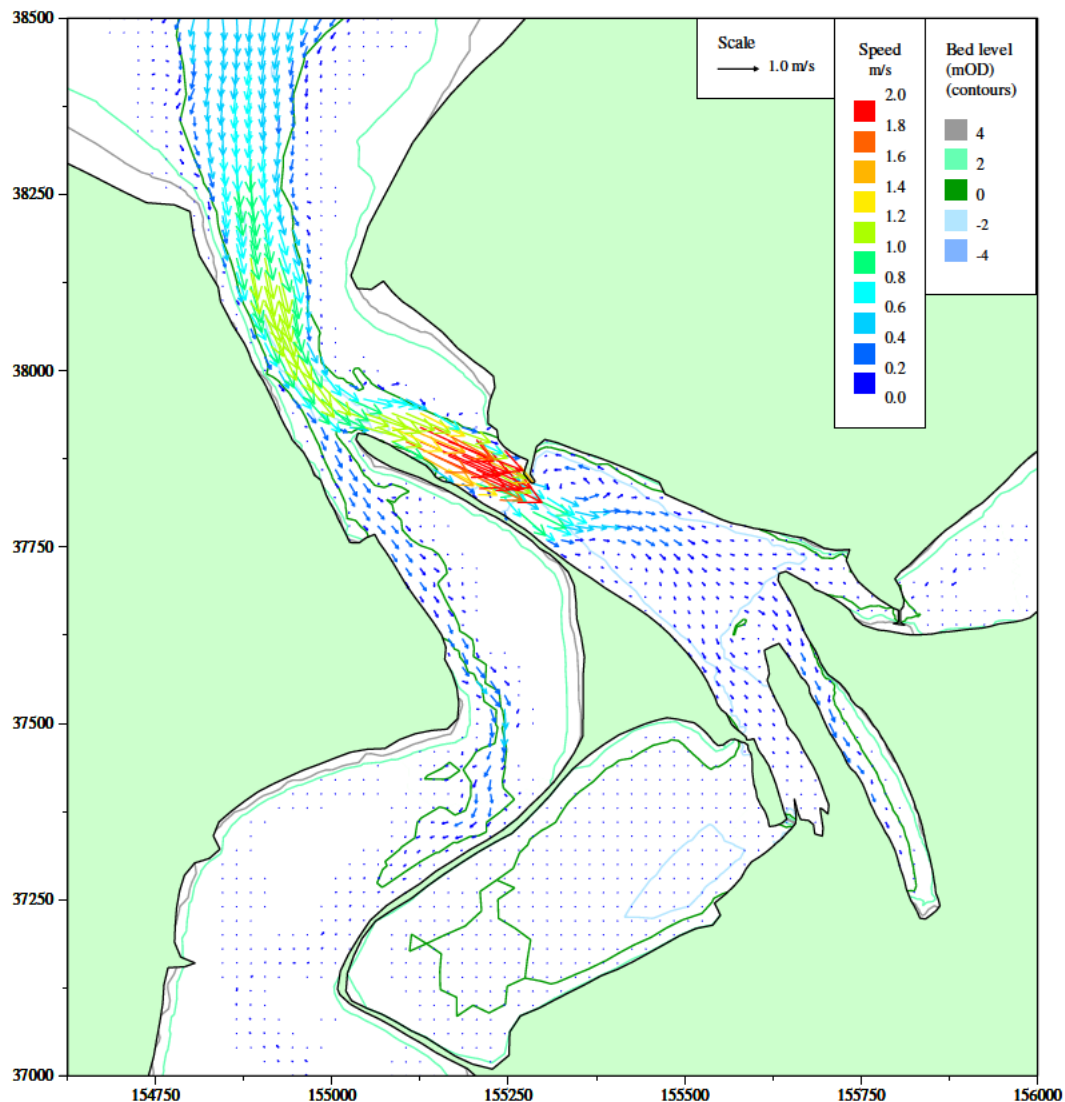
/HR_projects/ddr3839/model/SedimentTransport/report/Rubens/sand_dev09b_st.RUB/fig3.77.i

Figure 3.77 Scheme 2 with sand trap conditions patterns of erosion and deposition in marina area, Copperhouse sluice open (summer condition), double sluice operation on Carnsew Pool



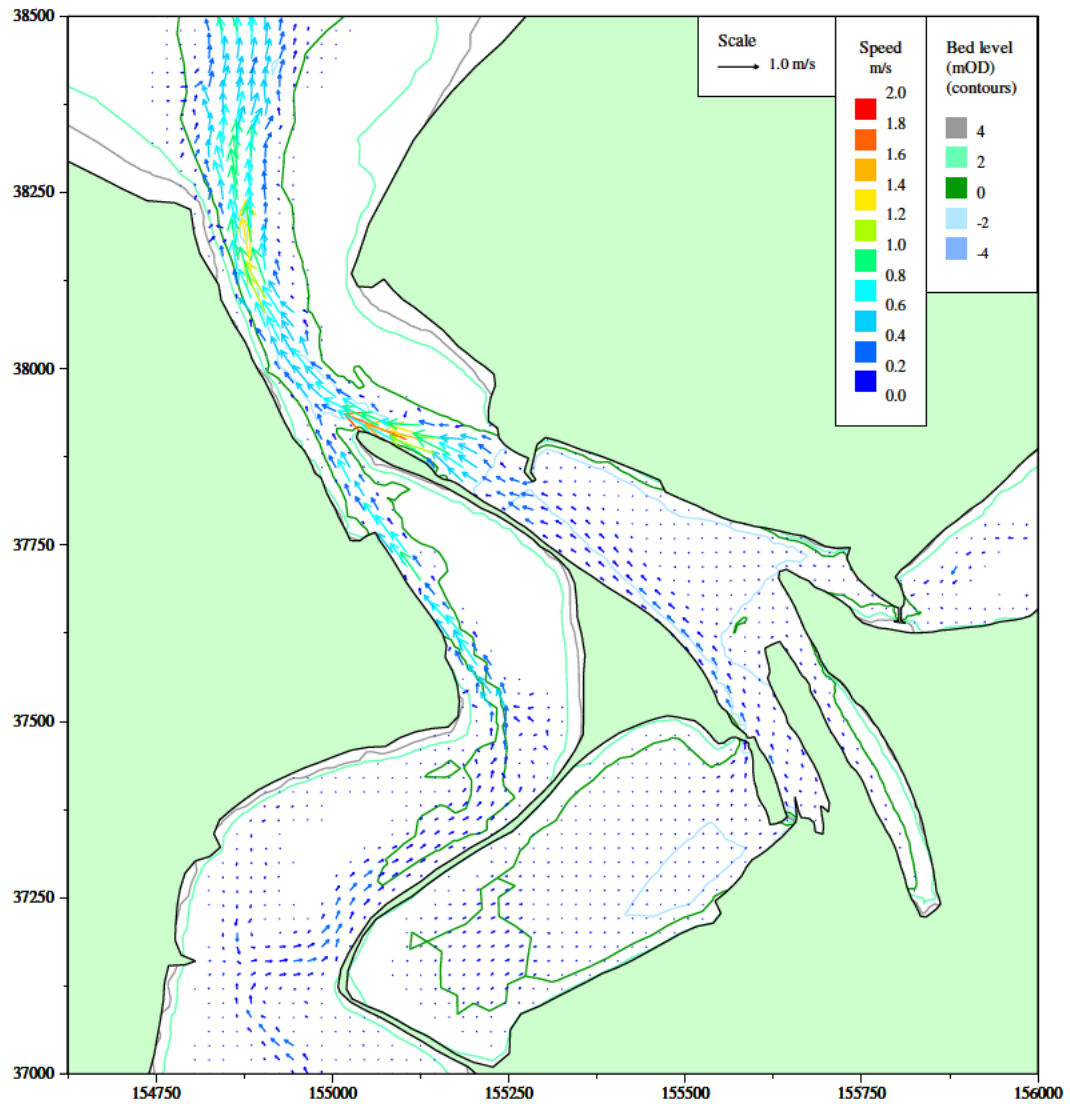
/HR_projects/ddr3839/model/SedimentTransport/report/Rubensp/flow_dev10b.RUB/fig3.78.i

Figure 3.78 Model bathymetry, Scheme 3



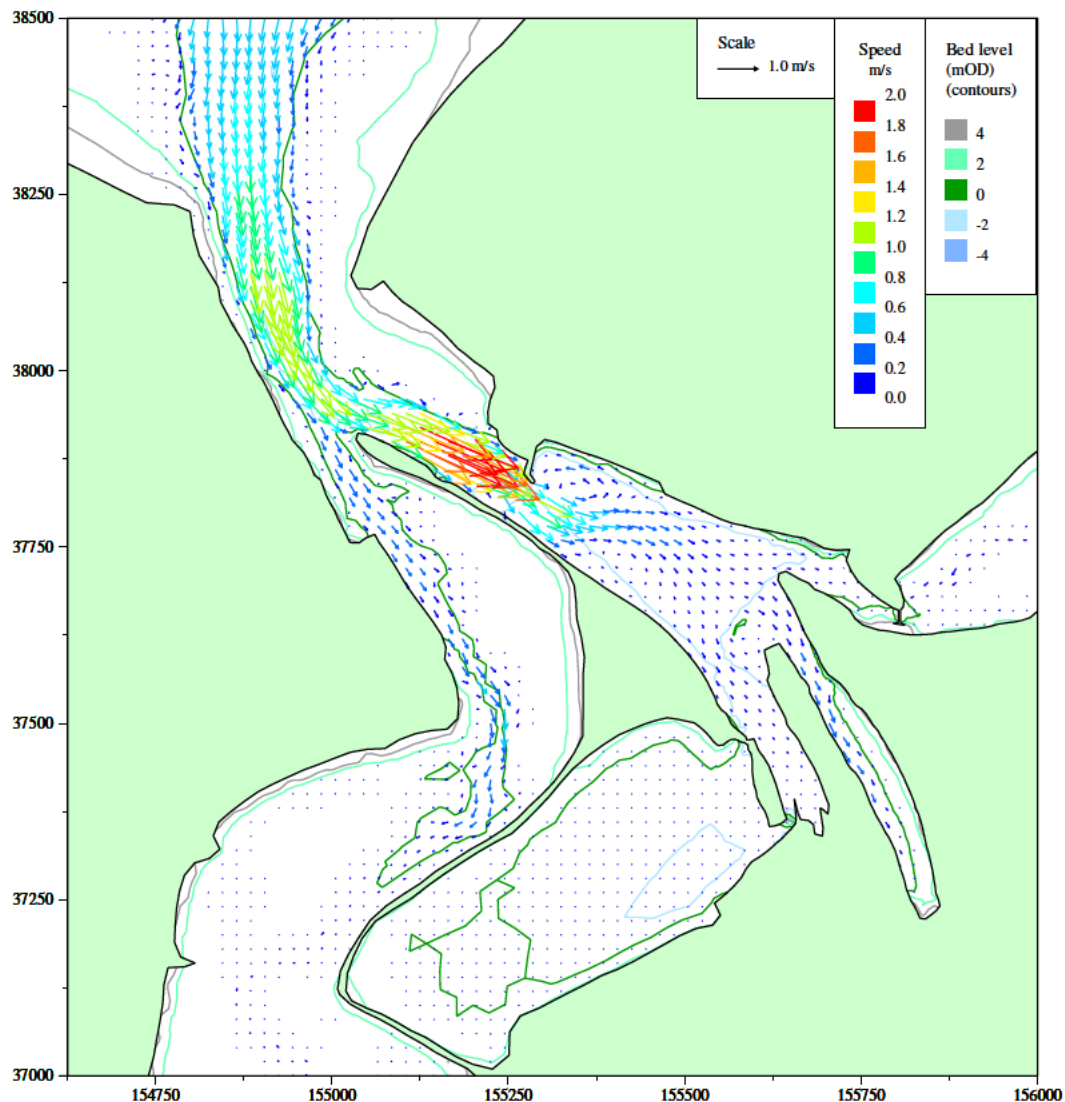
/HR_projects/ddr3839/model/SedimentTransport/report/Rubensp/flow_dev10b.RUB/fig3.79.i

Figure 3.79 Scheme 3 conditions spring tide peak flood currents (HW+9.5 Hours), Copperhouse sluice open (summer condition), double sluice operation on Carnsew Pool



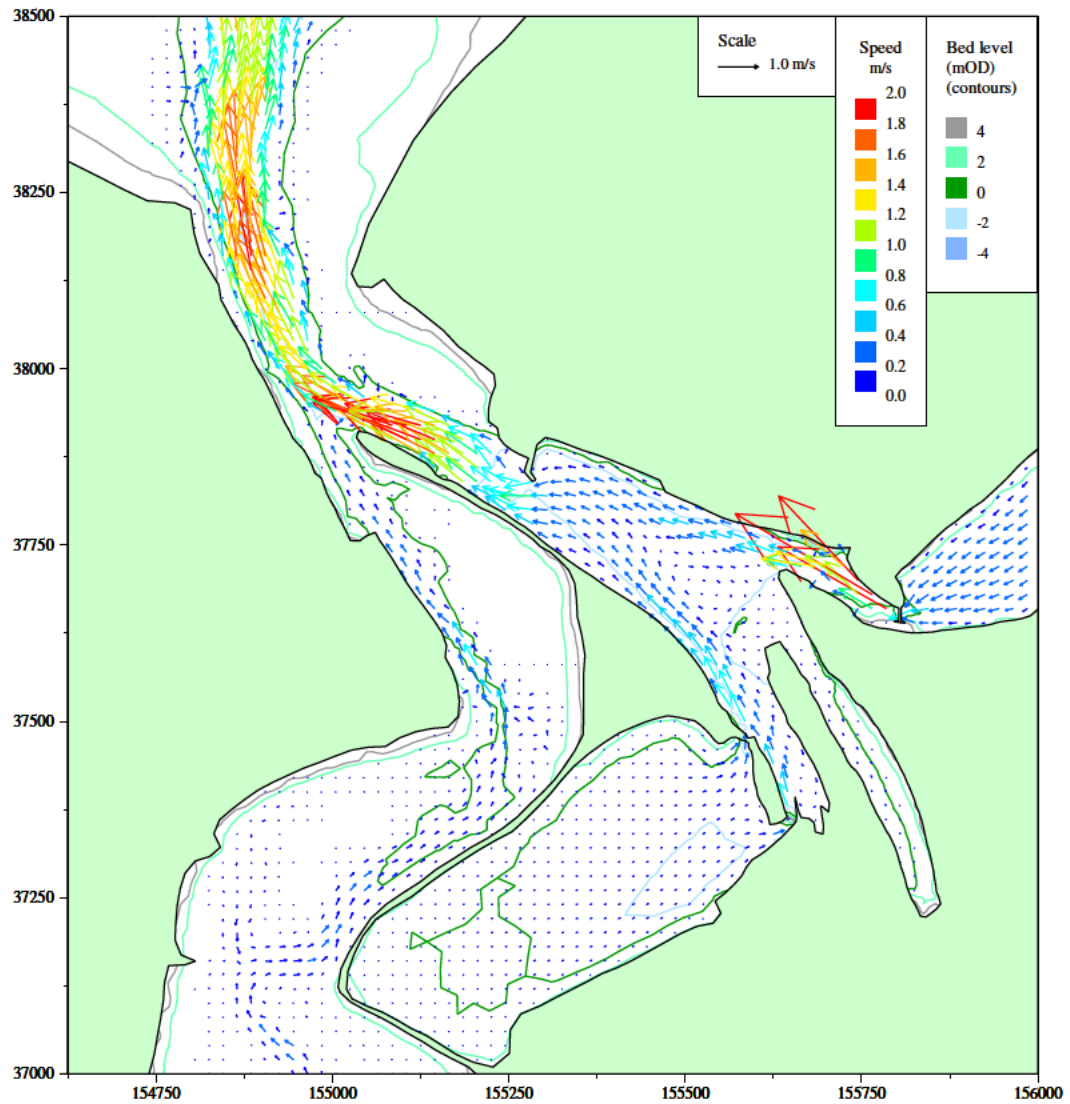
/HR_projects/ddr3839/model/SedimentTransport/report/Rubensp/flow_dev10b.RUB/fig3.80.i

Figure 3.80 Scheme 3 conditions spring tide ebb currents (HW+4.5 Hours), Copperhouse sluice open (summer condition), double sluice operation on Carnsew Pool



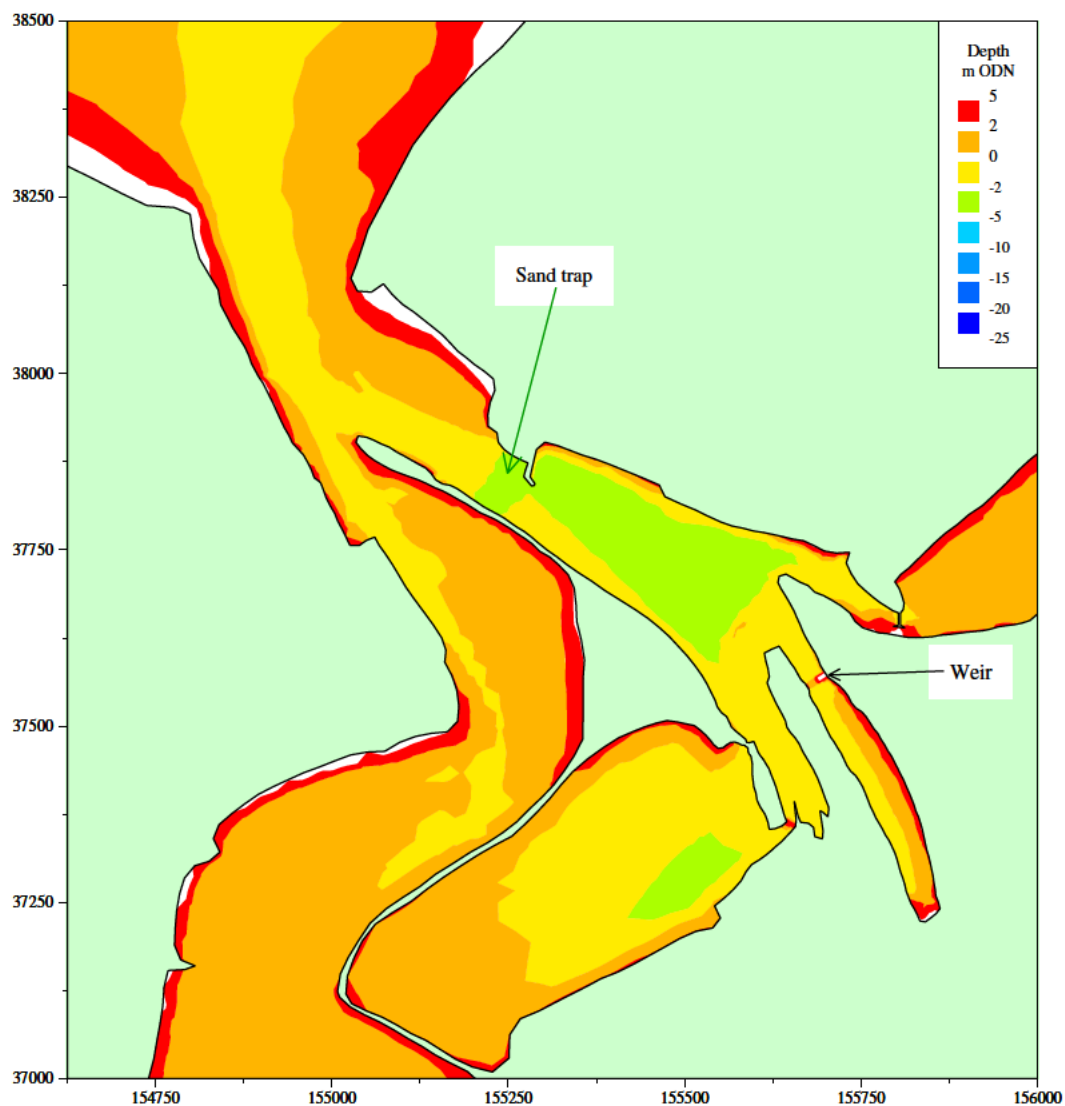
/HR_projects/ddr3839/model/SedimentTransport/report/Rubensp/flow_dev10d.RUB/fig3.81.i

Figure 3.81 Scheme 3 conditions spring tide peak flood currents with impounding in Carnsew and Copperhouse Pools to HW + 3 hours, double sluice operation on Carnsew Pool



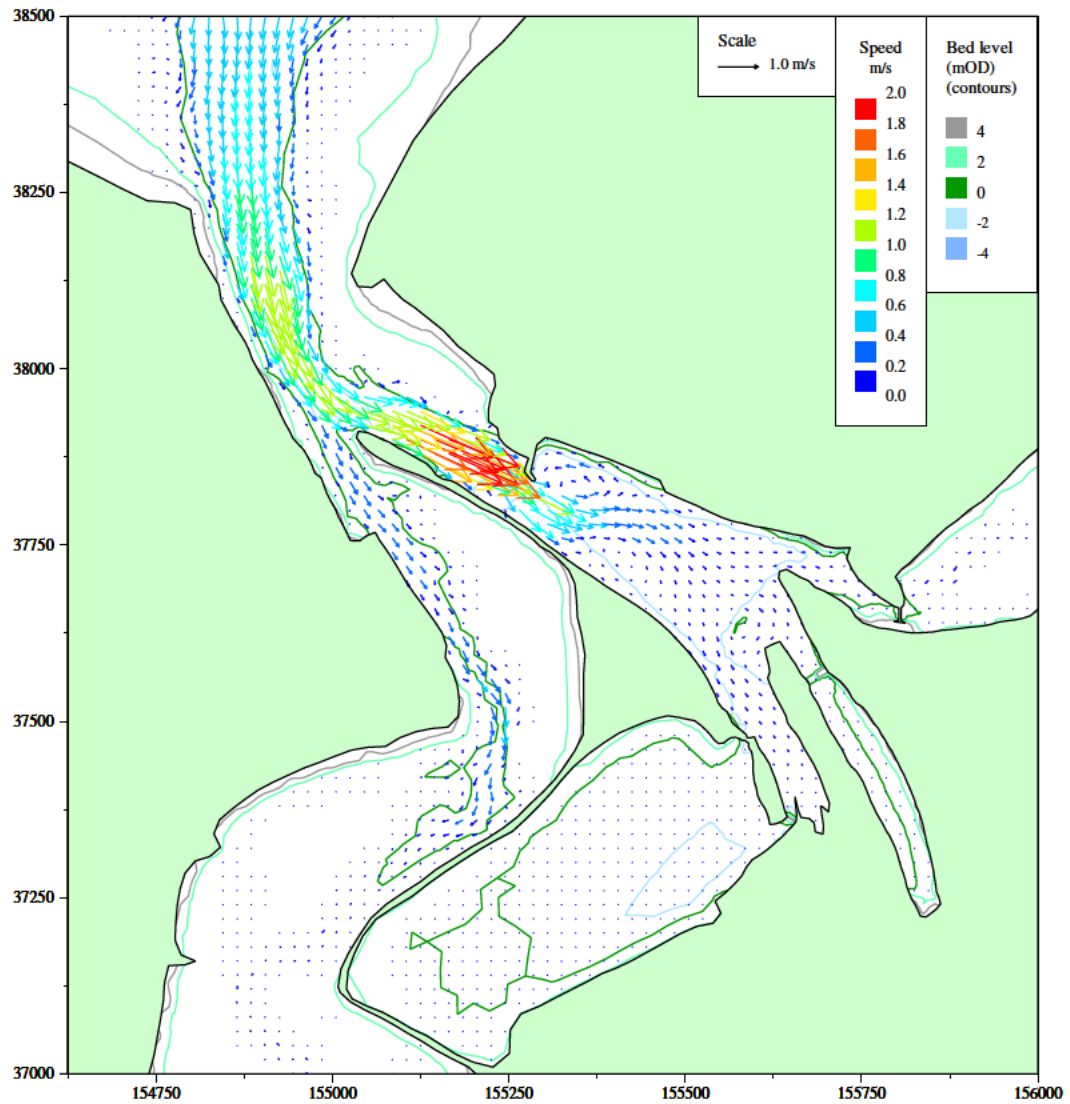
/HR_projects/ddr3839/model/SedimentTransport/report/Rubensp/flow_dev10d.RUB/fig3.82.i

Figure 3.82 Scheme 3 conditions spring tide peak ebb currents with impounding in Carnsew and Copperhouse Pools to HW + 3 hours, double sluice operation on Carnsew Pool



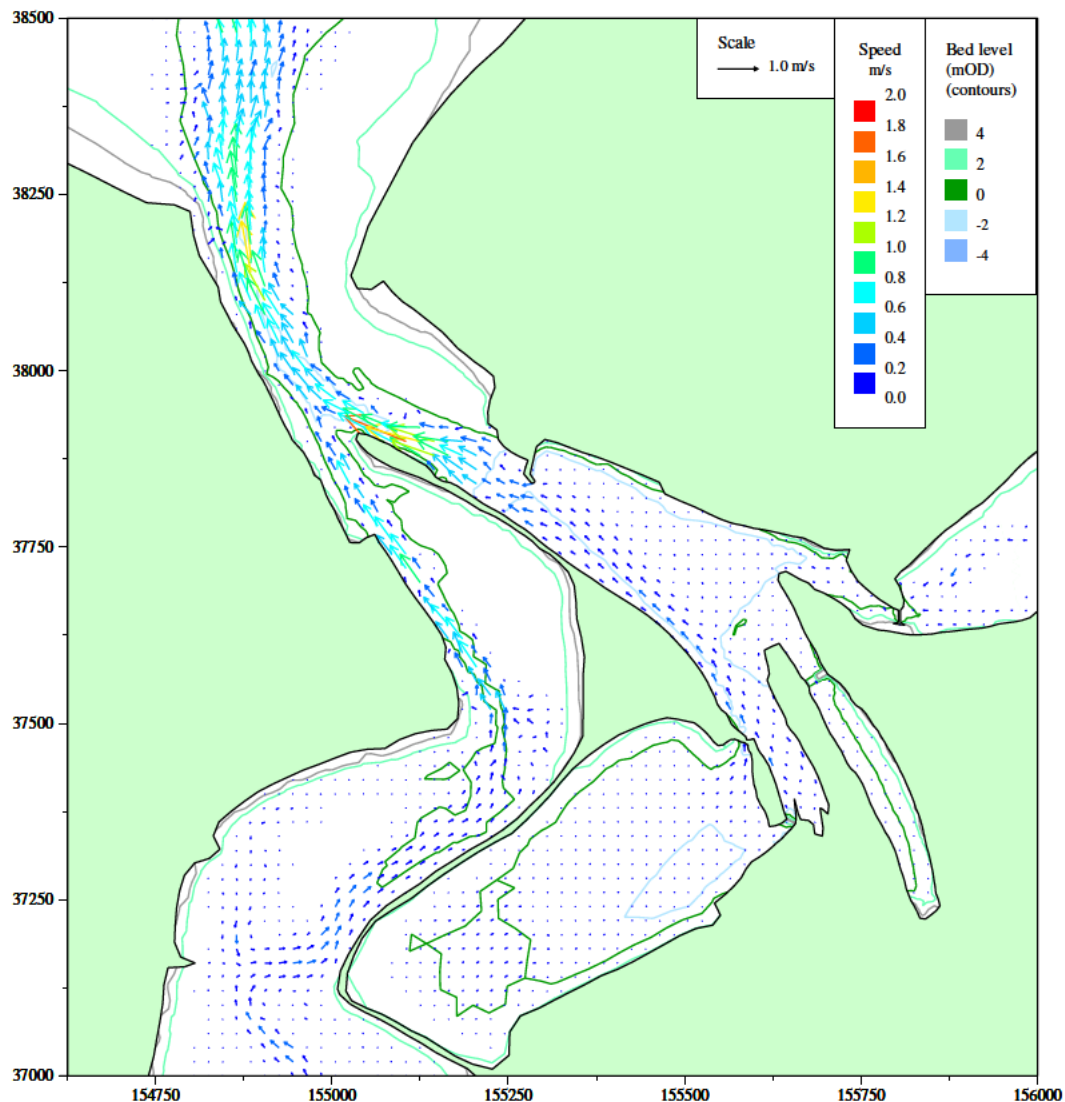
/HR_projects/ddr3839/model/SedimentTransport/report/Rubensp/flow_dev11b_sp.RUB/fig3.83.i

Figure 3.83 Model bathymetry, Scheme 3 with Penpol weir



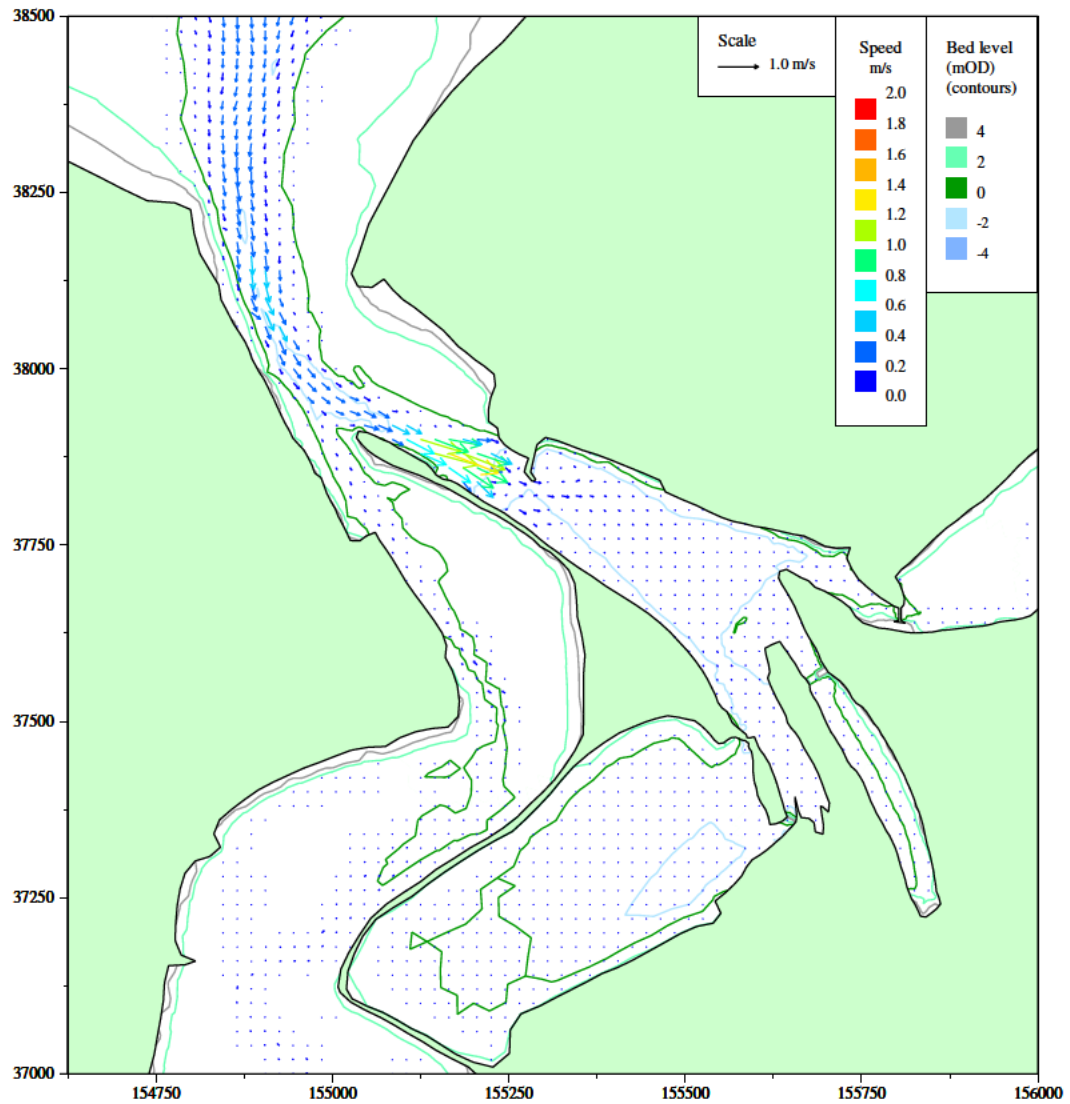
/HR_projects/ddr3839/model/SedimentTransport/report/Rubensp/flow_dev11b_sp.RUB/fig3.84.i

Figure 3.84 Scheme 3 with Penpol weir conditions spring tide peak flood currents (HW+9.5 Hours), Copperhouse sluice open (summer condition), double sluice operation on Carnsew Pool



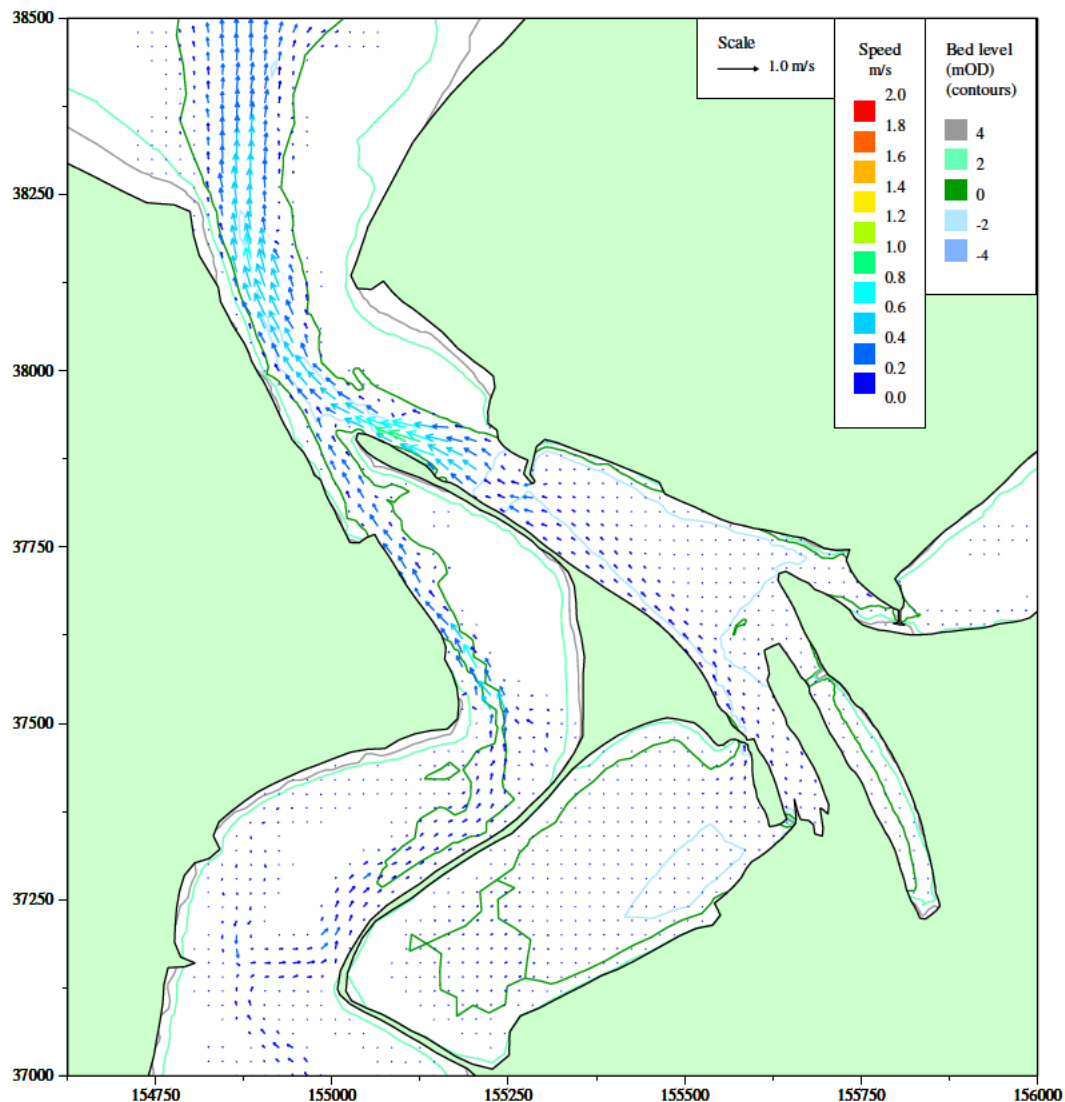
/HR_projects/ddr3839/model/SedimentTransport/report/Rubensp/flow_dev11b_sp.RUB/fig3.85.i

Figure 3.85 Scheme 3 with Penpol weir conditions spring tide peak ebb currents (HW+4.5 Hours), Copperhouse sluice open (summer condition), double sluice operation on Carnsew Pool



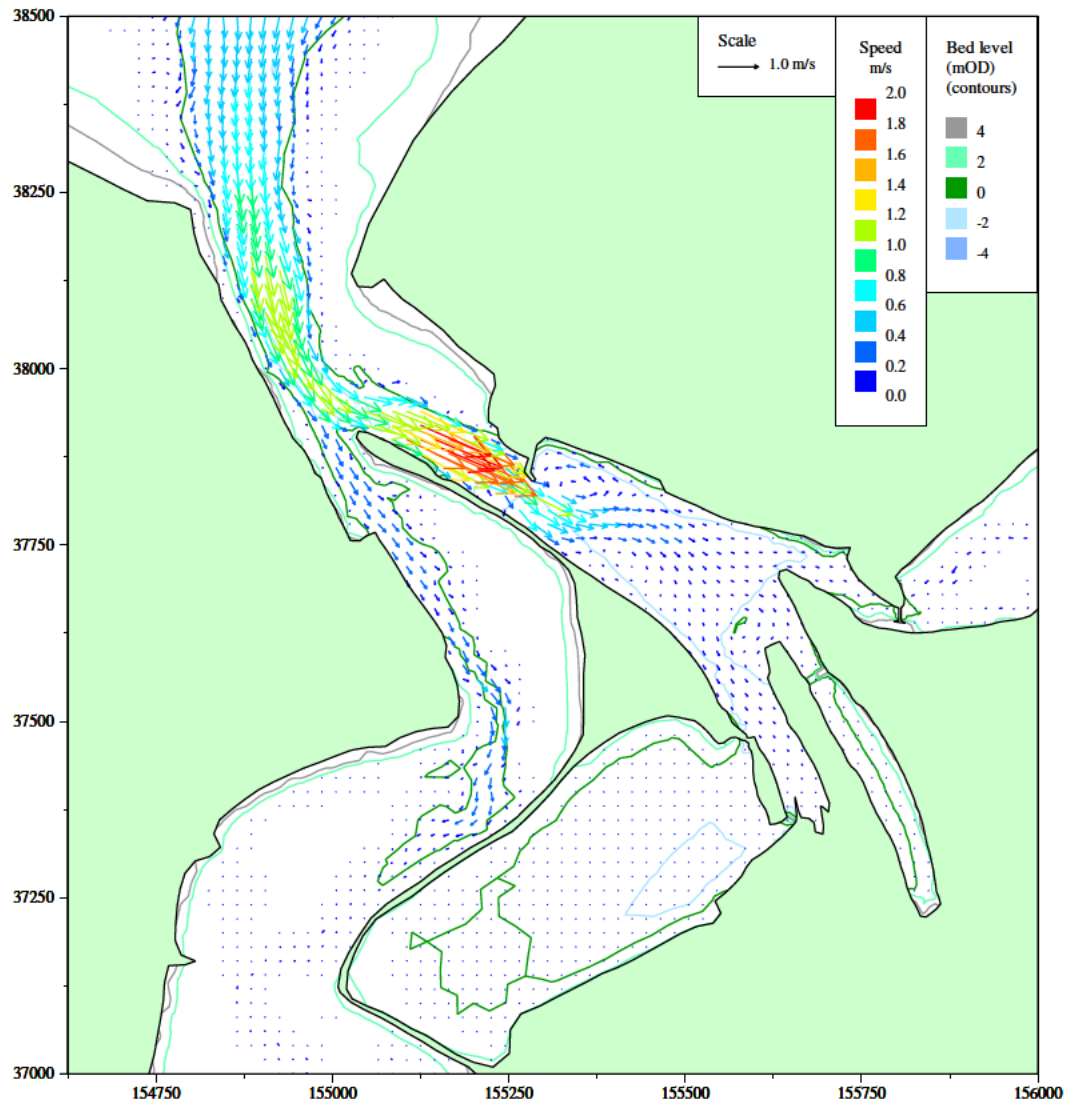
/HR_projects/ddr3839/model/SedimentTransport/report/Rubensp/flow_dev11b_np.RUB/fig3.86.i

Figure 3.86 Scheme 3 with Penpol weir conditions neap tide peak flood currents (HW+9.5 Hours), Copperhouse sluice open (summer condition), double sluice operation on Carnsew Pool



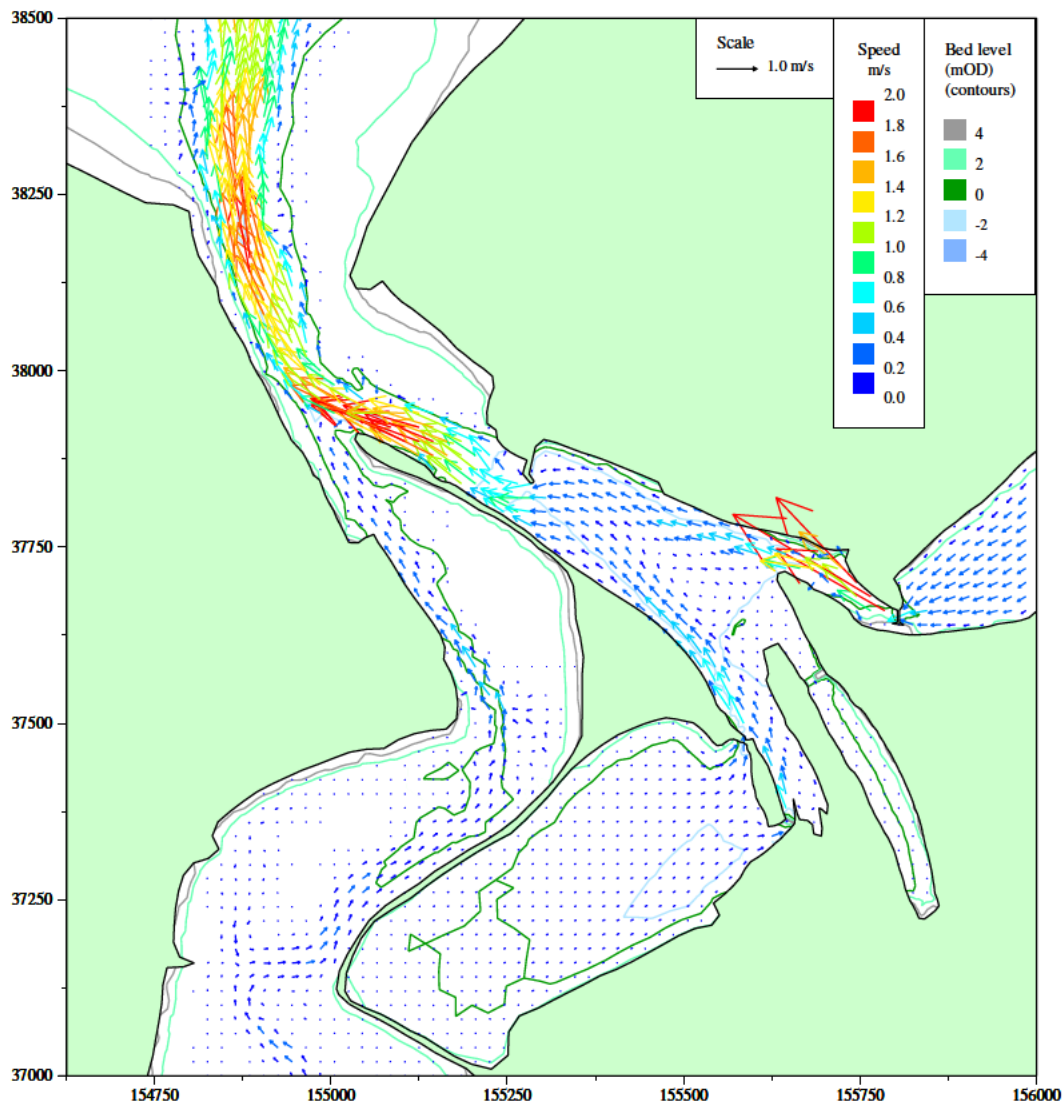
/HR_projects/ddr3839/model/SedimentTransport/report/Rubensp/flow_dev11b_np.RUB/fig3.87.i

Figure 3.87 Scheme 3 with Penpol weir conditions neap tide peak ebb currents (HW+4.5 Hours), Copperhouse sluice open (summer condition), double sluice operation on Carnsew Pool



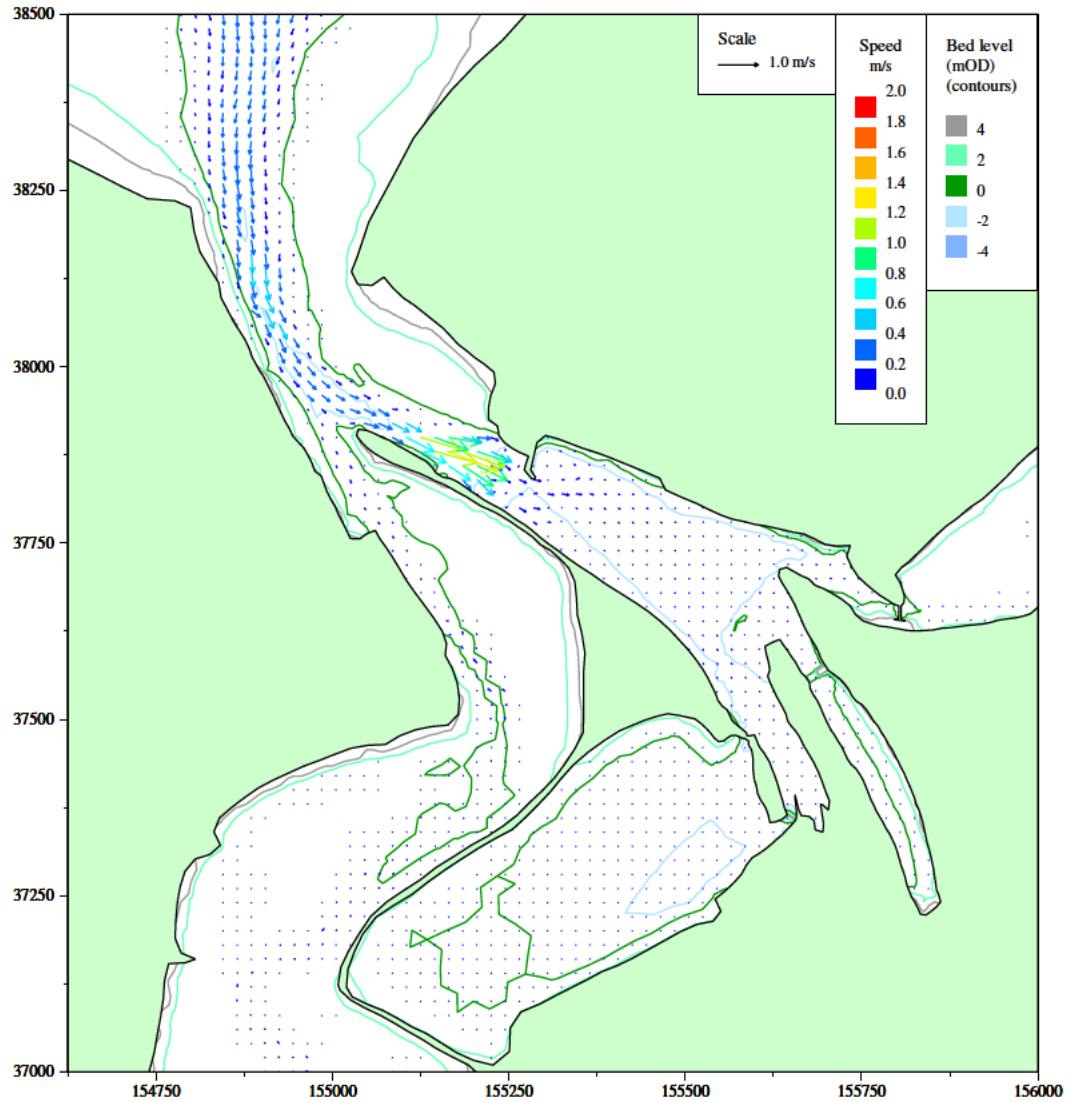
/HR_projects/ddr3839/model/SedimentTransport/report/Rubensp/flow_dev11d_sp.RUB/fig3.88.i

Figure 3.88 Scheme 3 with Penpol weir conditions spring tide peak flood currents (HW+9.5 Hours), with impounding in Carnsew and Copperhouse Pools to HW + 3 hours, double sluice operation on Carnsew Pool



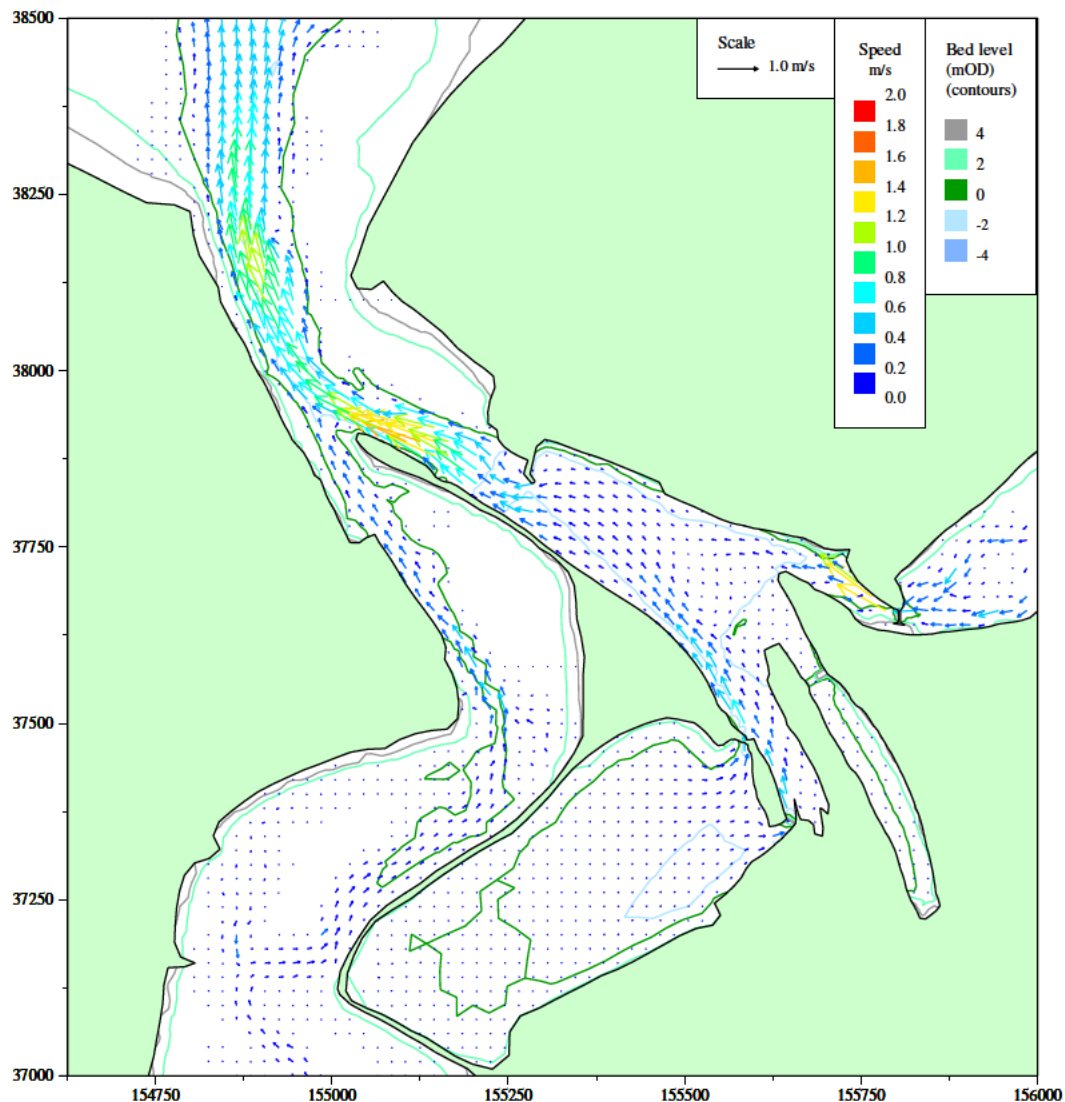
/HR_projects/ddr3839/model/SedimentTransport/report/Rubensp/flow_dev11d_sp.RUB/fig3.89.i

Figure 3.89 Scheme 3 with Penpol weir conditions spring tide peak ebb currents (HW+4.5 Hours), with impounding in Carnsew and Copperhouse Pools to HW + 3 hours, double sluice operation on Carnsew Pool



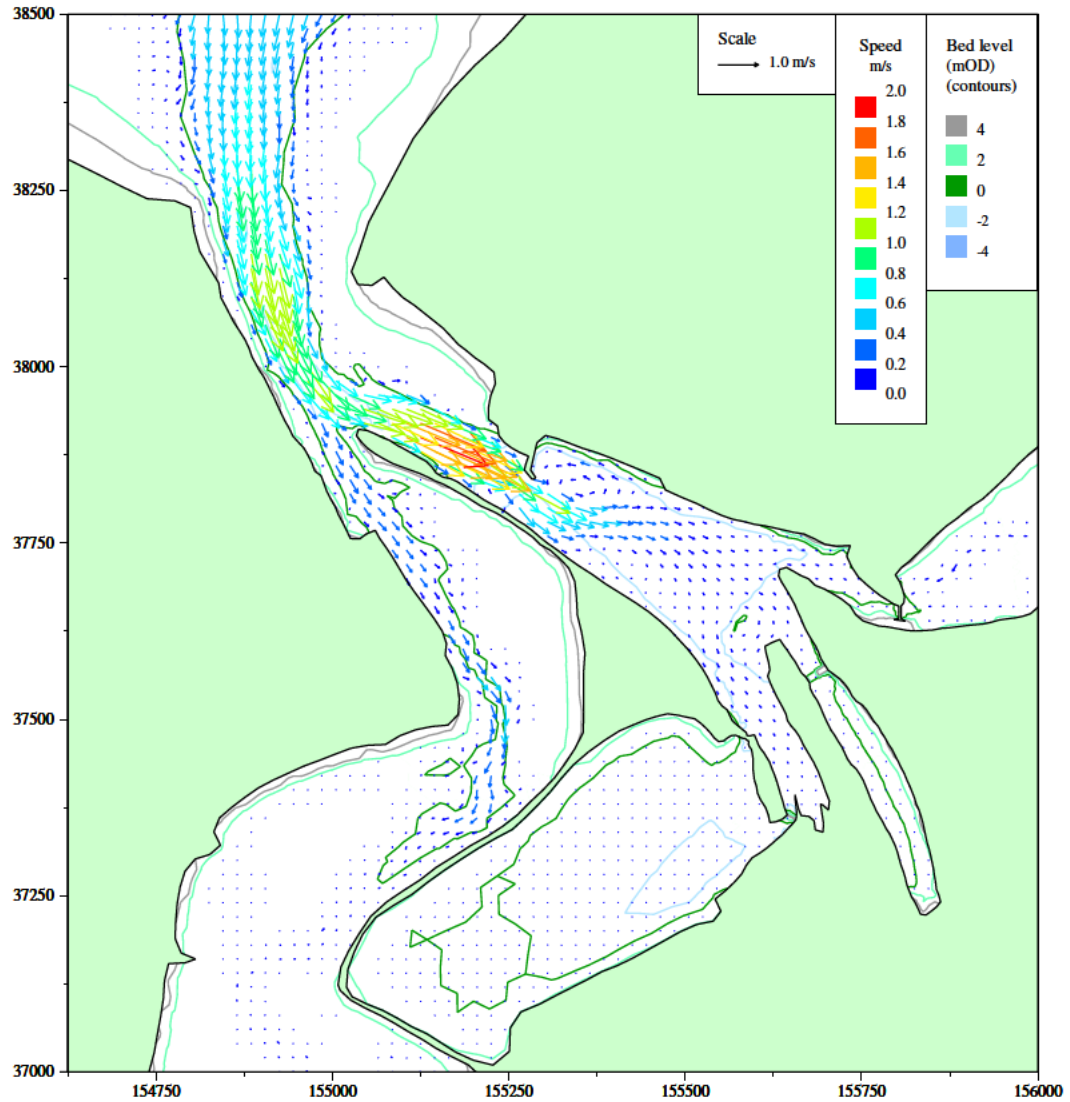
/HR_projects/ddr3839/model/SedimentTransport/report/Rubensp/flow_dev11d_np.RUB/fig3.90.i

Figure 3.90 Scheme 3 with Penpol weir conditions neap tide peak flood currents (HW+9.5 Hours), with impounding in Carnsew and Copperhouse Pools to HW + 3 hours, double sluice operation on Carnsew Pool



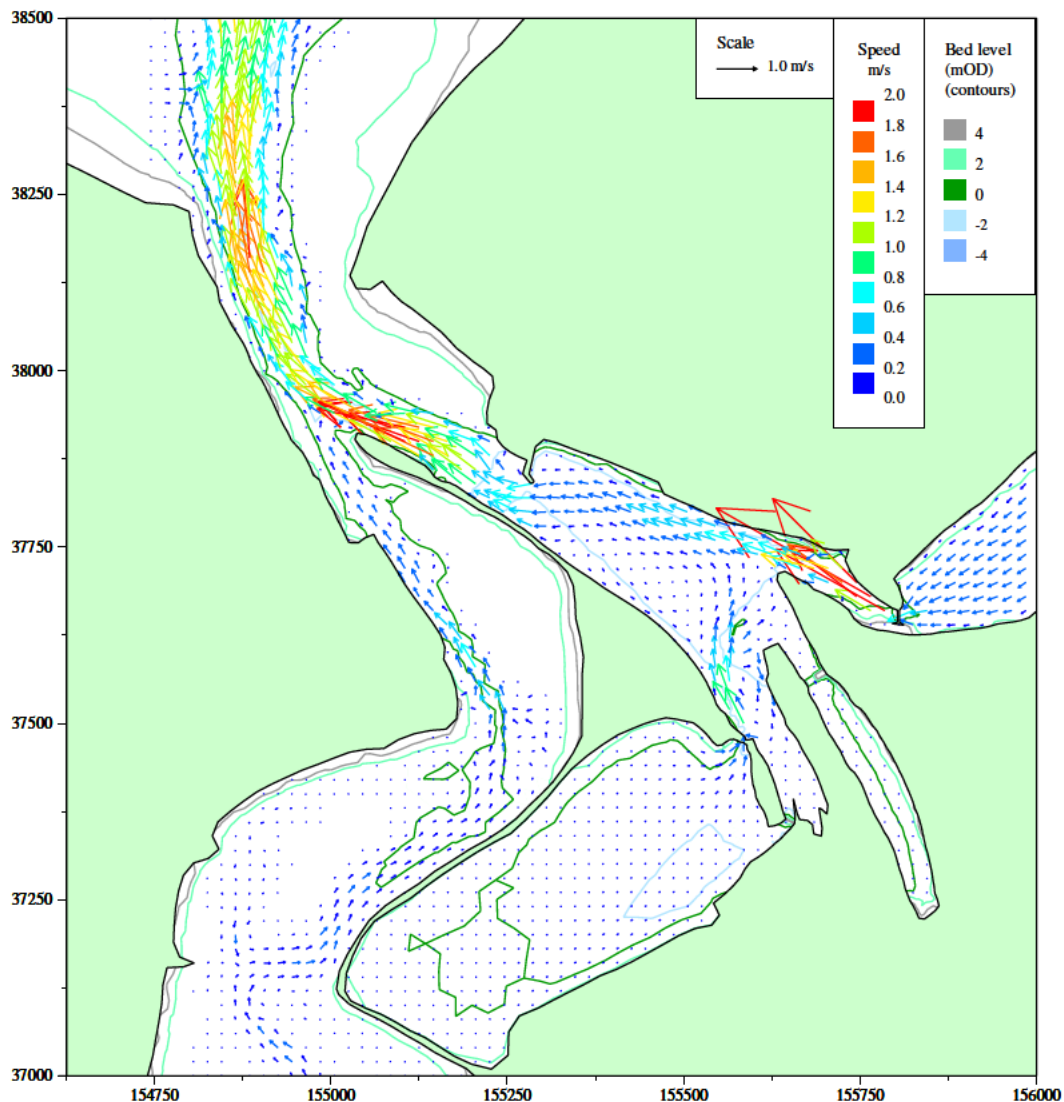
/HR_projects/ddr3839/model/SedimentTransport/report/Rubensp/flow_dev11d_np.RUB/fig3.91.i

Figure 3.91 Scheme 3 with Penpol weir conditions neap tide peak ebb currents (HW+4.5 Hours), with impounding in Carnsew and Copperhouse Pools to HW + 3 hours, double sluice operation on Carnsew Pool



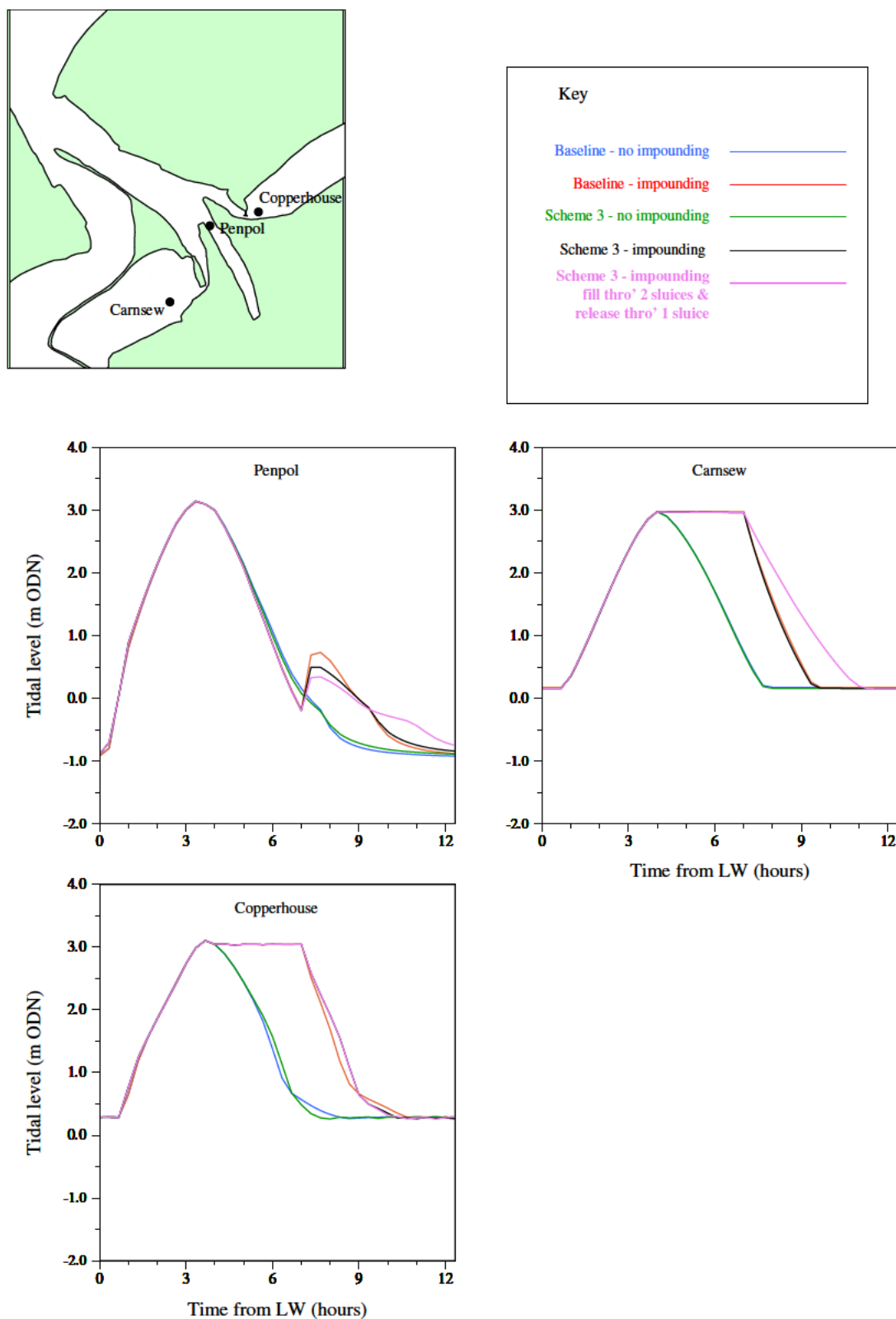
/HR_projects/ddr3839/model/SedimentTransport/report/Rubensp/flow_dev11e_sp.RUB/fig3.92.i

Figure 3.92 Scheme 3 with Penpol weir conditions spring tide peak flood currents (HW+9.5 Hours), with impounding in Carnsew and Copperhouse Pools to HW + 3 hours, double sluice fill, single sluice empty on Carnsew Pool



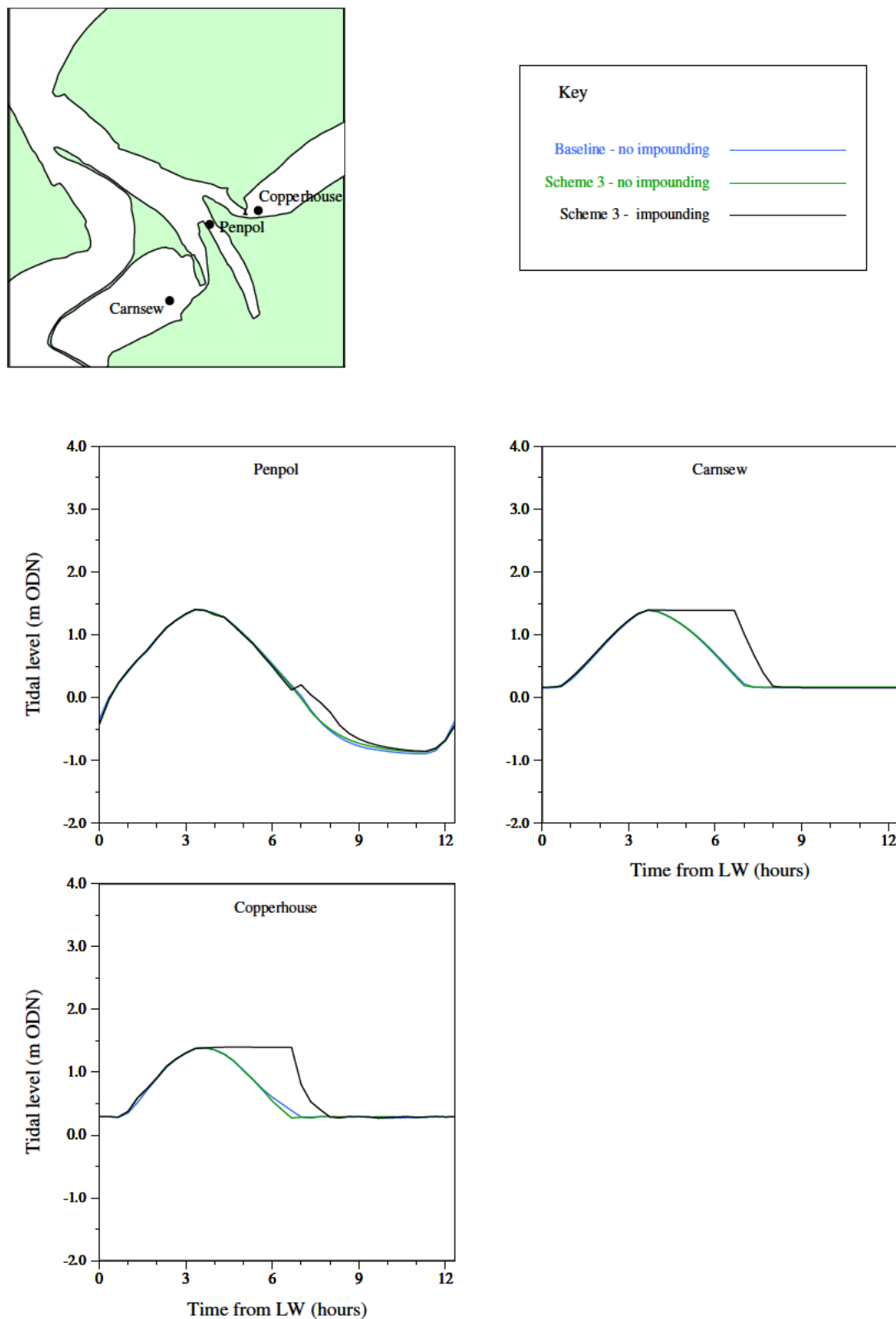
/HR_projects/ddr3839/mode/SedimentTransport/report/Rubensp/flow_dev11e_sp.RUB/fig3.93.i

Figure 3.93 Scheme 3 with Penpol weir conditions spring tide peak ebb currents (HW+4.5 Hours), with impounding in Carnsew and Copperhouse Pools to HW + 3 hours, double sluice fill, single sluice empty on Carnsew Pool



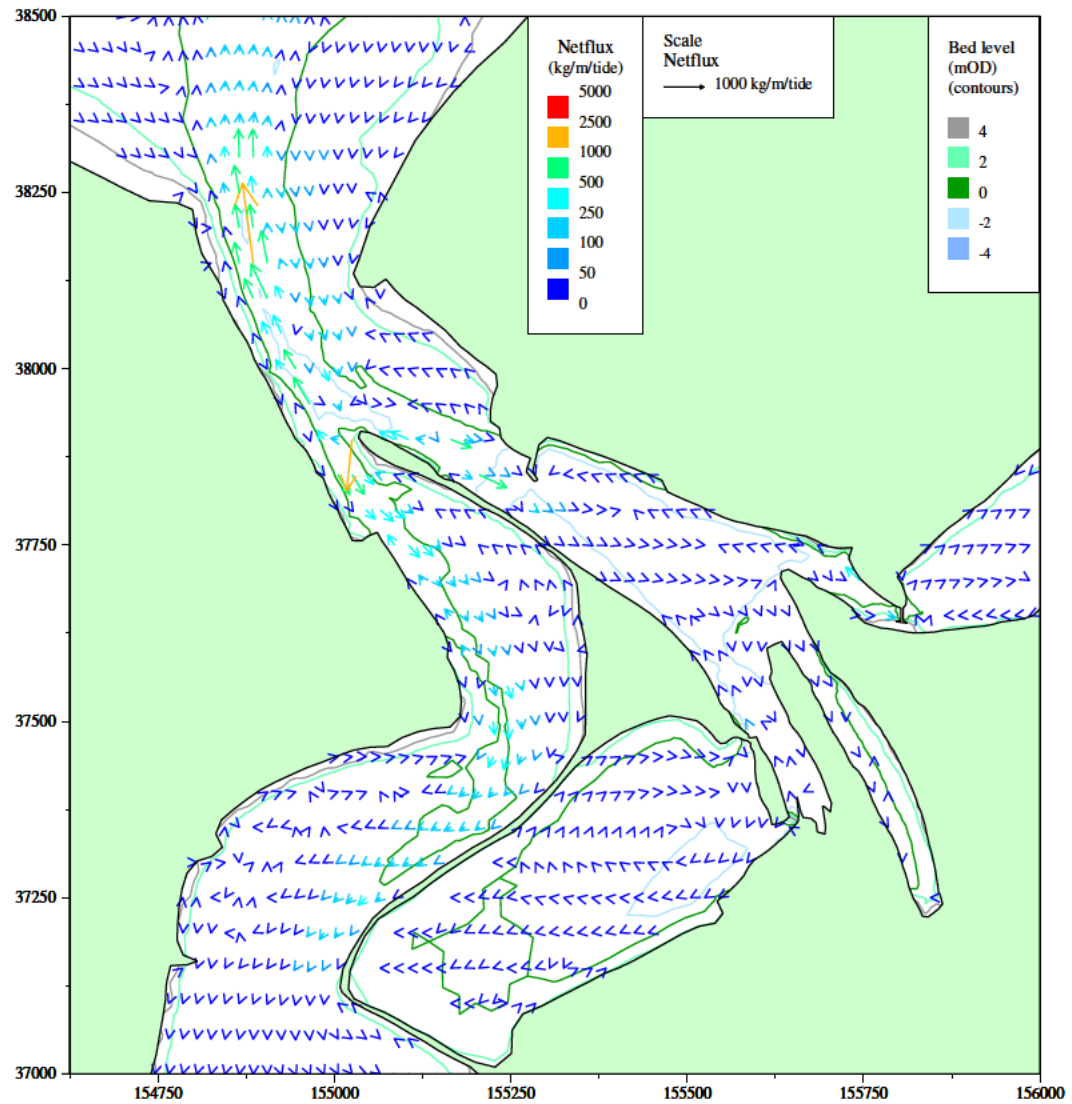
/HR_projects/ddr3839/model/SedimentTransport/report/Rubensp/flow_dev11e_sp.RUB/fig3.94.i

Figure 3.94 Comparison of modelled spring tide water levels with and without impounding, Scheme 3



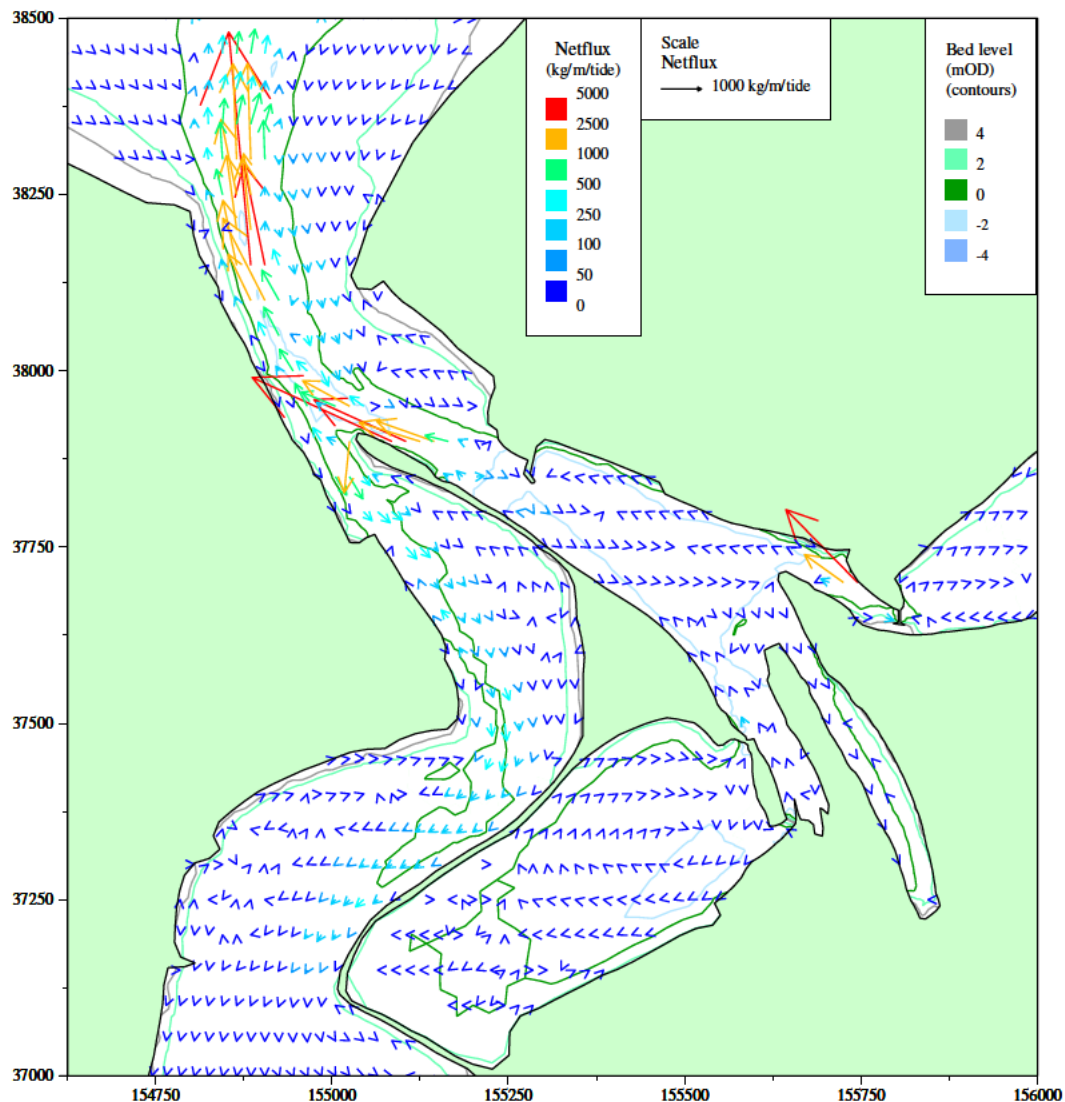
/HR_projects/ddr3839/model/SedimentTransport/report/Rubensp/flow_dev11d_np.RUB/fig3.95.i

Figure 3.95 Comparison of modelled neap tide water levels with and without impounding, Scheme 3



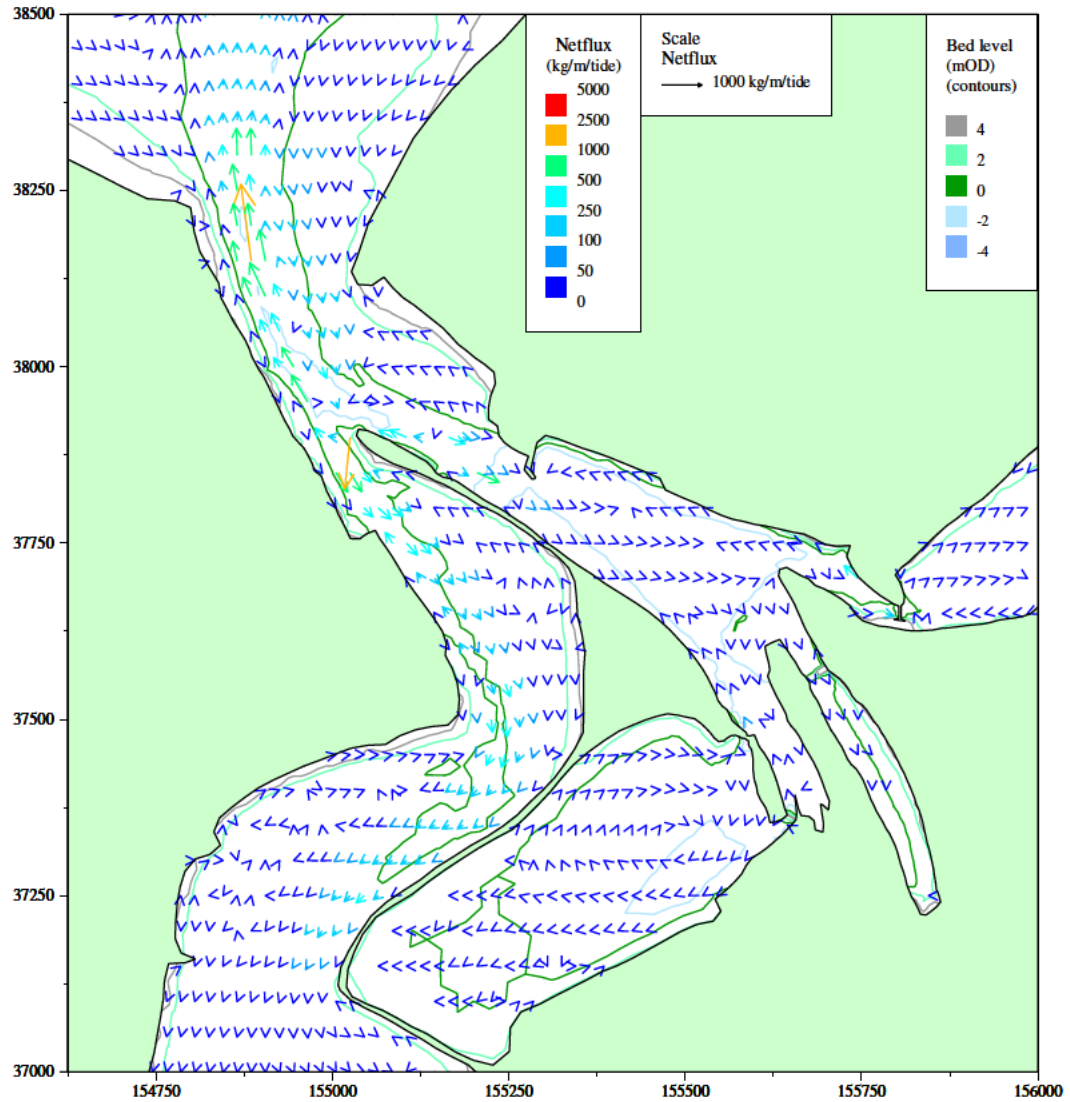
/HR_projects/ddr3839/model/SedimentTransport/report/Rubensp/sand_dev10b.RUB/fig3.96.i

Figure 3.96 Scheme 3 conditions net sand flux patterns, Copperhouse sluice open (summer condition), double sluice operation on Carnsew Pool



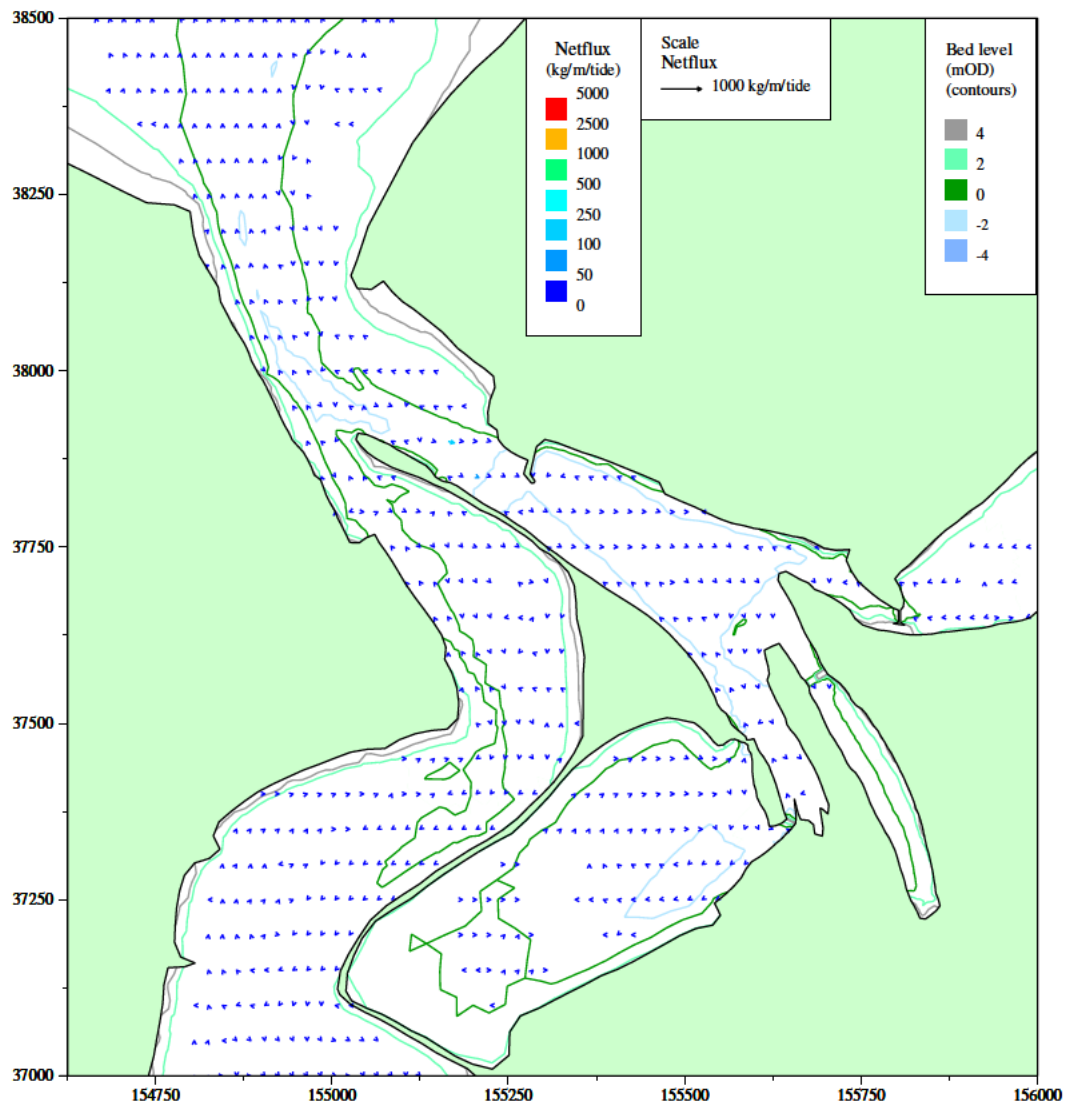
/HR_projects/ddr3839/model/SedimentTransport/report/Rubensp/sand_dev10d.RUB/fig3.97.i

Figure 3.97 Scheme 3 conditions net sand flux patterns with impounding in Carnsew and Copperhouse Pools to HW + 3 hours, double sluice operation on Carnsew Pool



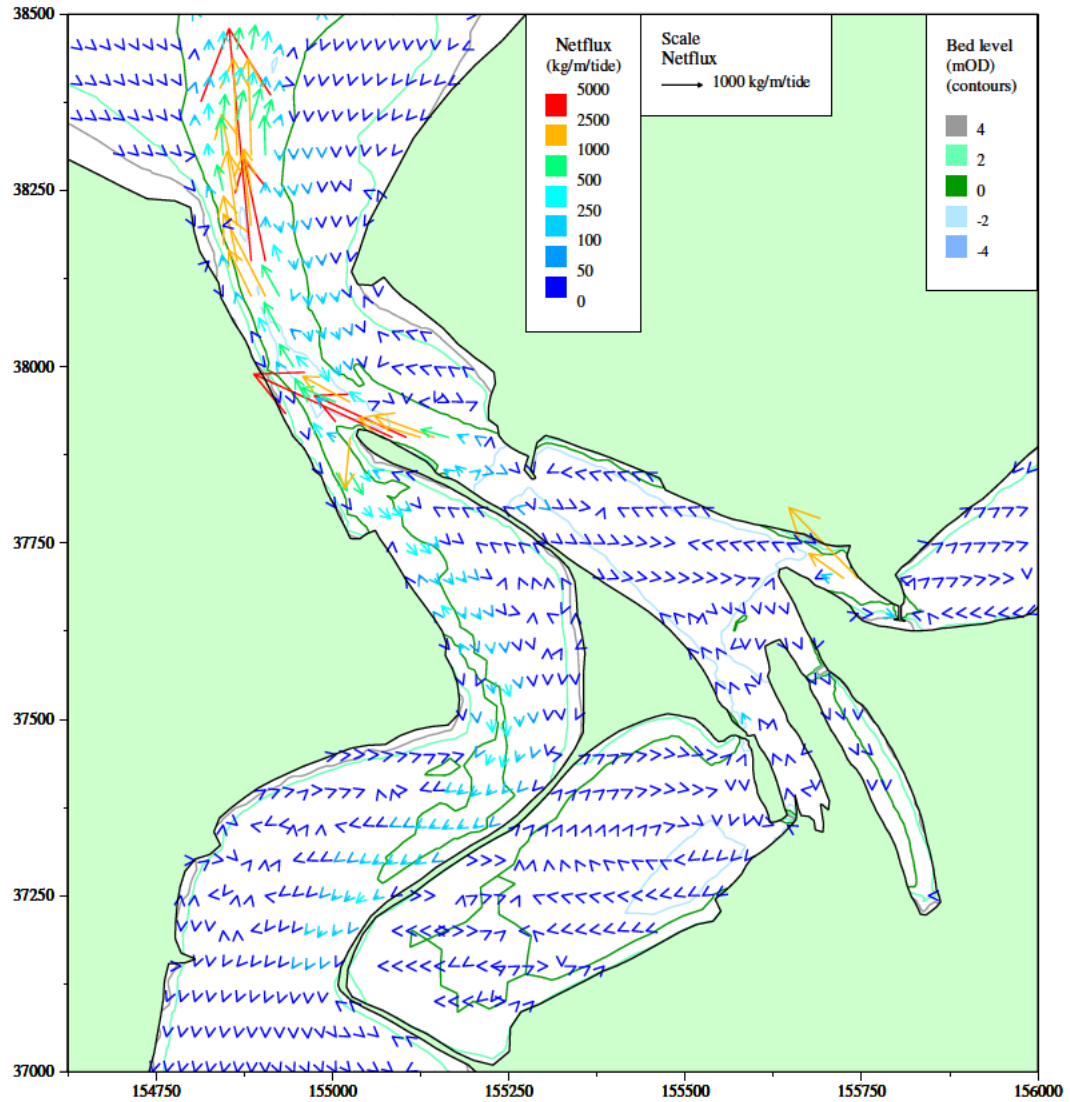
/HR_projects/ddr3839/model/SedimentTransport/report/Rubensp/sand_dev11_sp.RUB/fig3.98.i

Figure 3.98 Scheme 3 with Penpol weir conditions, spring tide net sand flux patterns, Copperhouse sluice open (summer condition), double sluice operation on Carnsew Pool



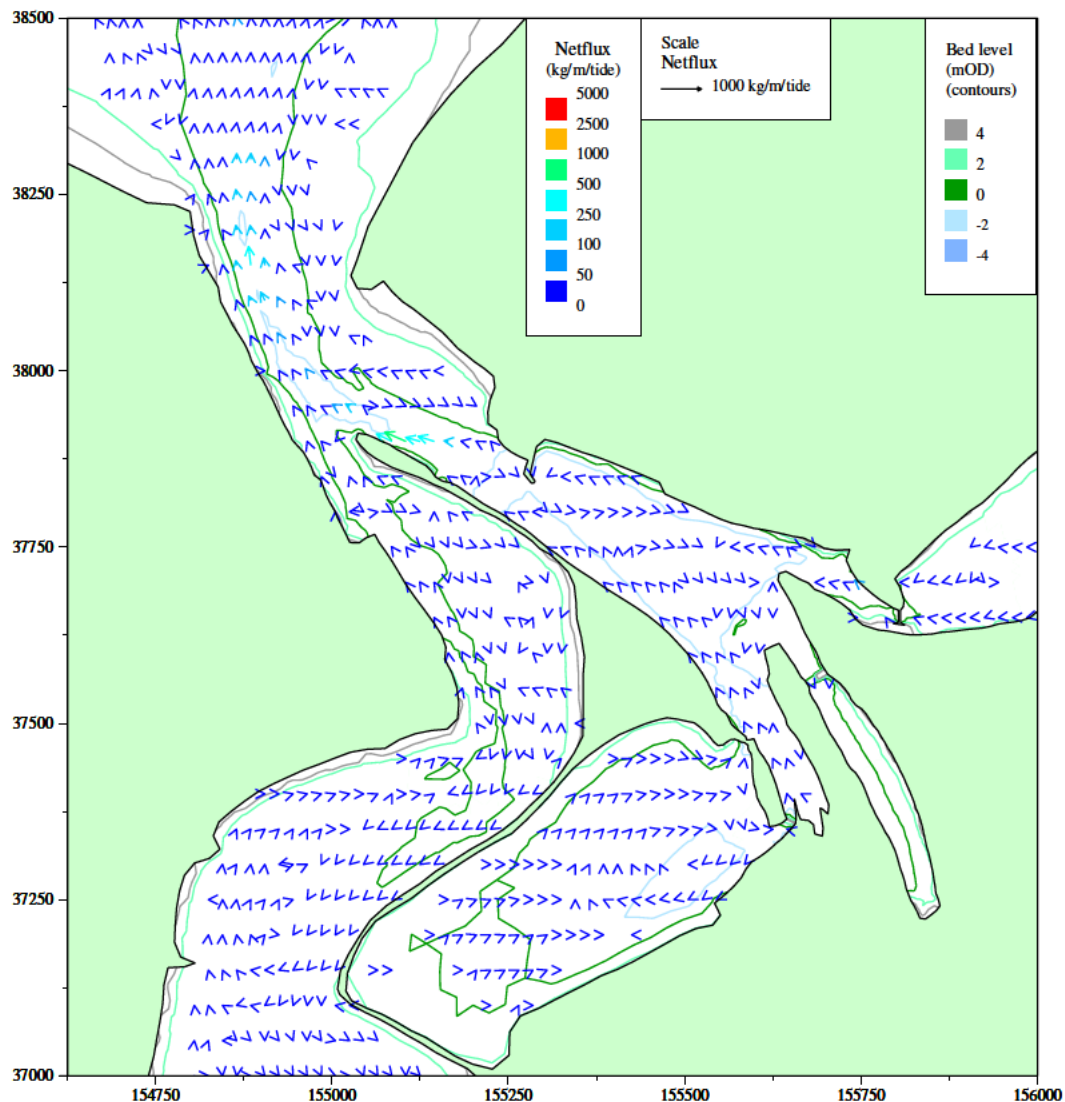
/HR_projects/ddr3839/model/SedimentTransport/report/Rubensp/sand_dev11_np.RUB/fig3.99.i

Figure 3.99 Scheme 3 with Penpol weir conditions, neap tide net sand flux patterns, Copperhouse sluice open (summer condition), double sluice operation on Carnsew Pool



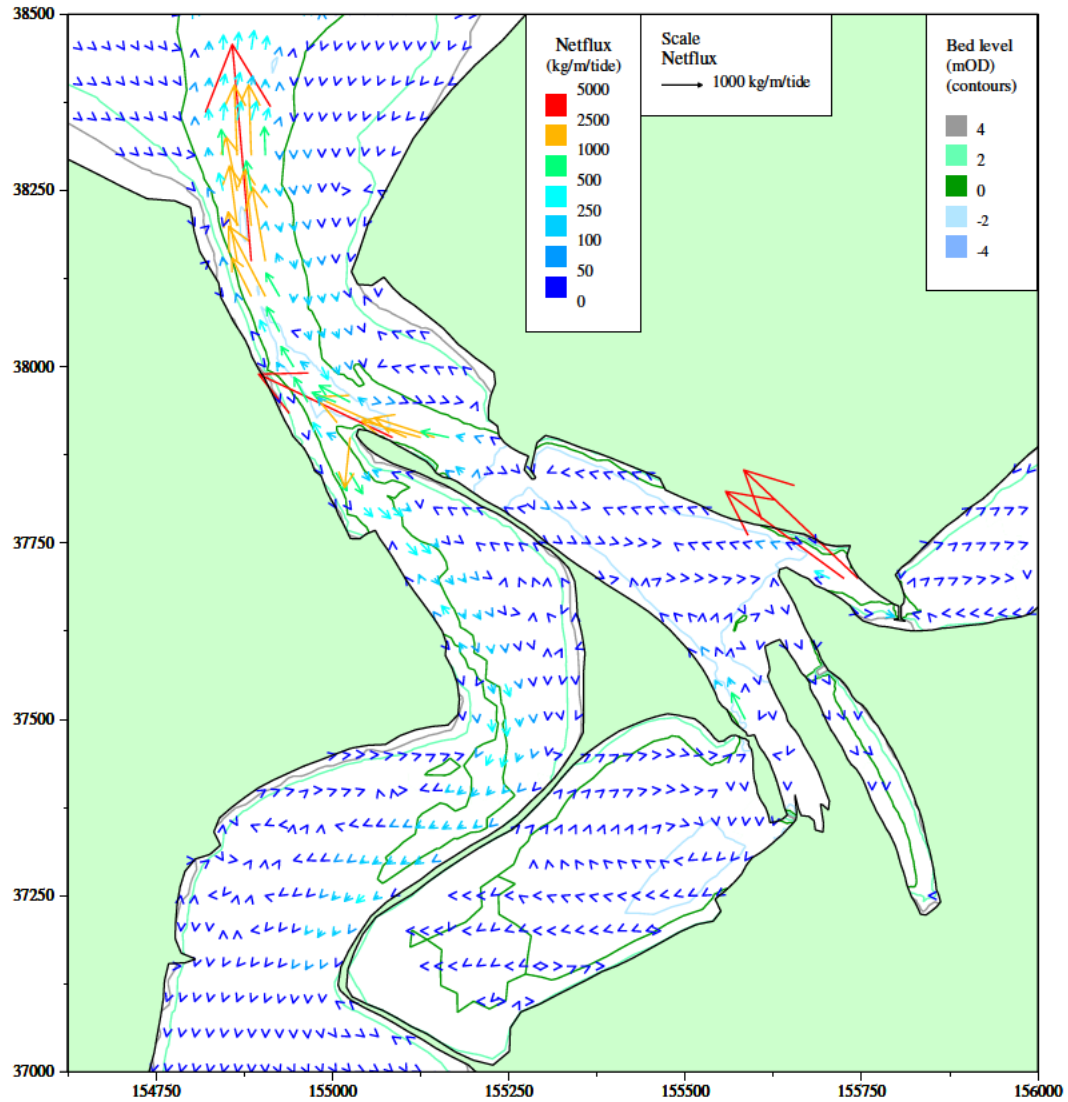
/HR_projects/ddr3839/model/SedimentTransport/report/Rubensp/sand_dev11d_sp.RUB/fig3.100.i

Figure 3.100 Scheme 3 with Penpol weir conditions, spring tide net sand flux patterns with impounding in Carnsew and Copperhouse Pools to HW + 3 hours, double sluice operation on Carnsew Pool



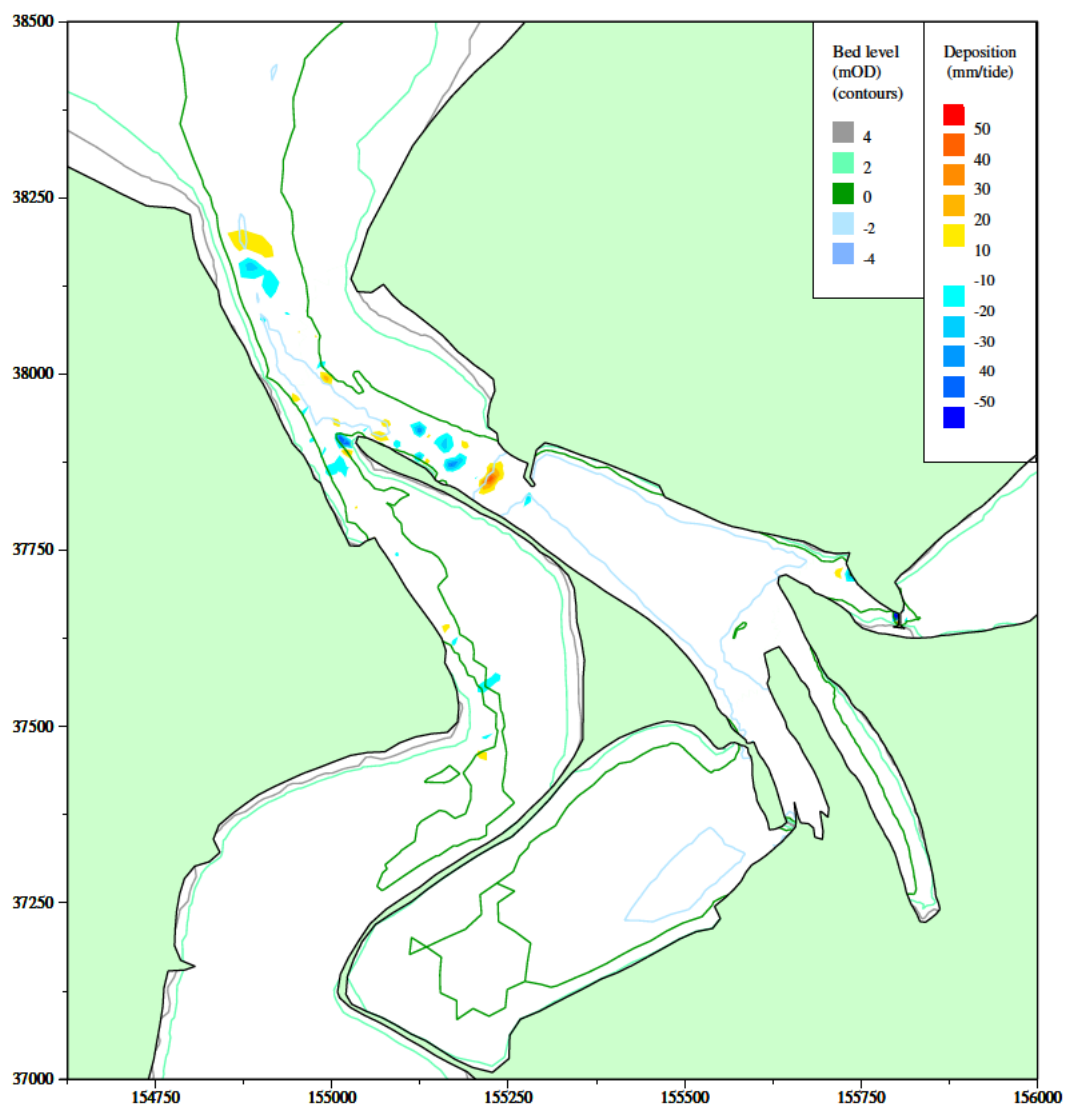
/HR_projects/ddr3839/model/SedimentTransport/report/Rubensp/sand_dev11d_np.RUB/fig3.101.i

Figure 3.101 Scheme 3 with Penpol weir conditions, neap tide net sand flux patterns with impounding in Carnsew and Copperhouse Pools to HW + 3 hours, double sluice operation on Carnsew Pool



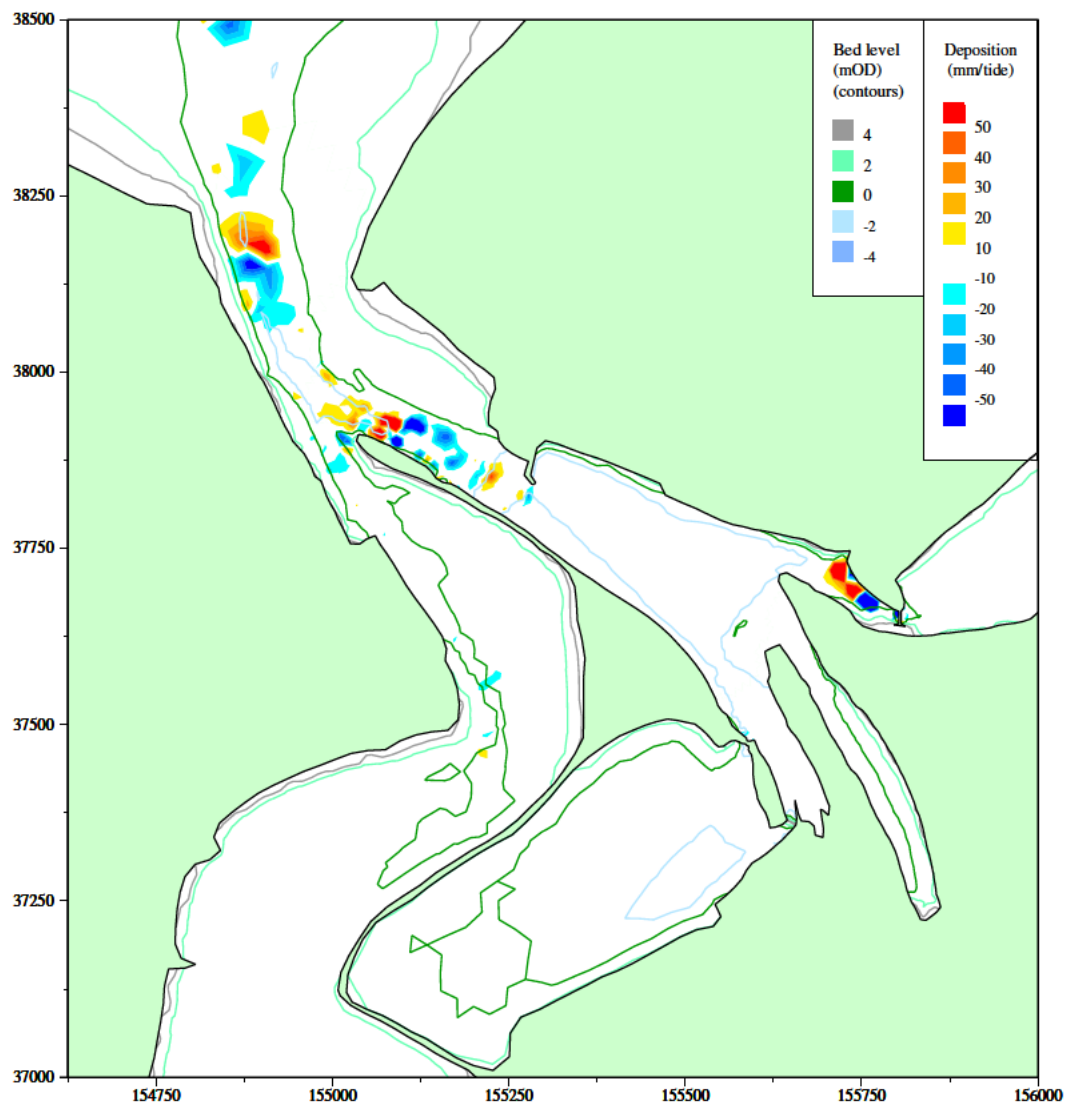
/HR_projects/ddr3839/model/SedimentTransport/report/Rubensp/sand_dev11e_sp.RUB/fig3.102.i

Figure 3.102 Scheme 3 with Penpol weir conditions, spring tide net sand flux patterns with impounding in Carnsew and Copperhouse Pools to HW + 3 hours, double sluice fill, single sluice empty on Carnsew Pool



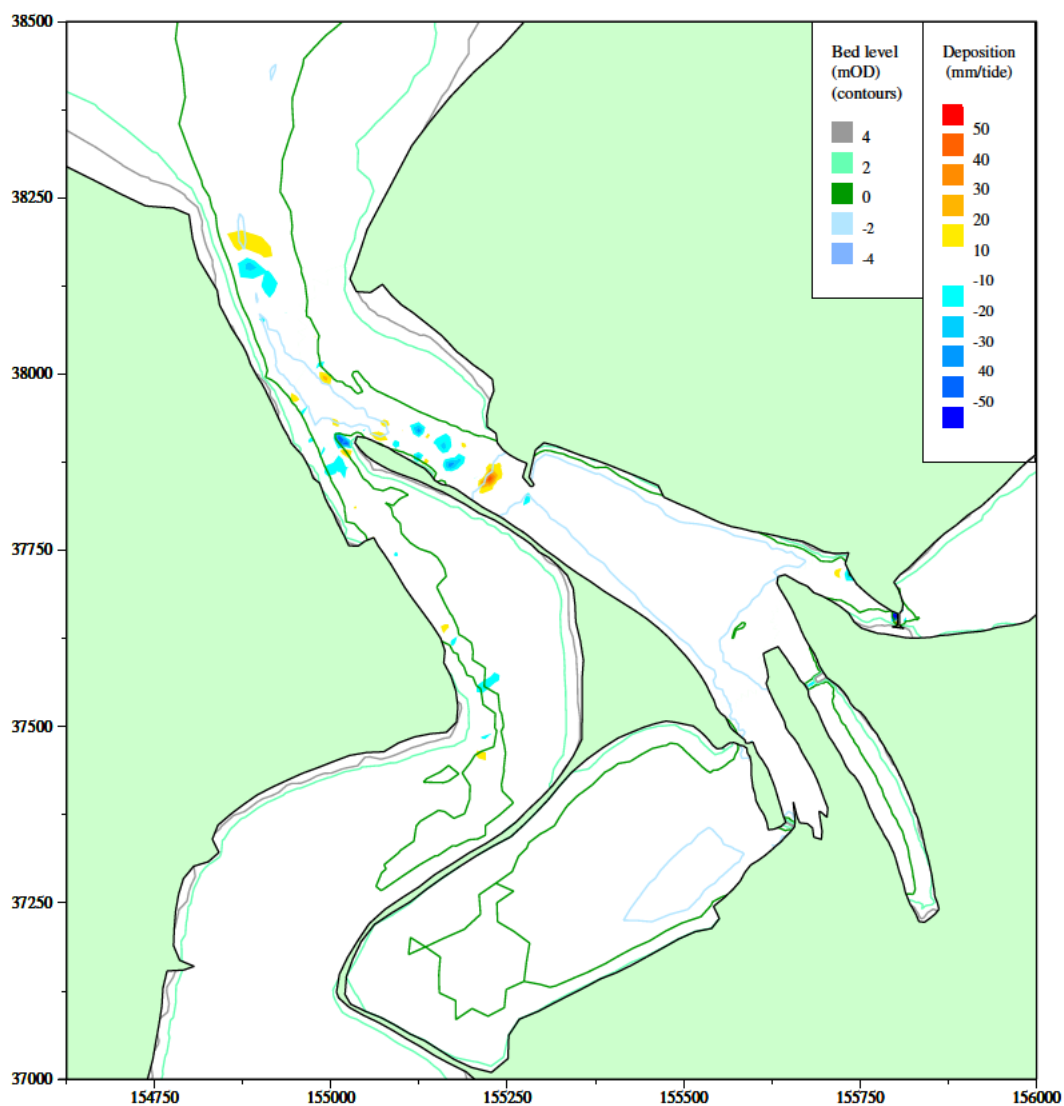
/HR_projects/ddr3839/model/SedimentTransport/report/Rubensp/sand_dev10b.RUB/fig3.103.i

Figure 3.103 Scheme 3 conditions patterns of erosion and deposition, Copperhouse sluice open (summer condition), double sluice operation on Carnsew Pool



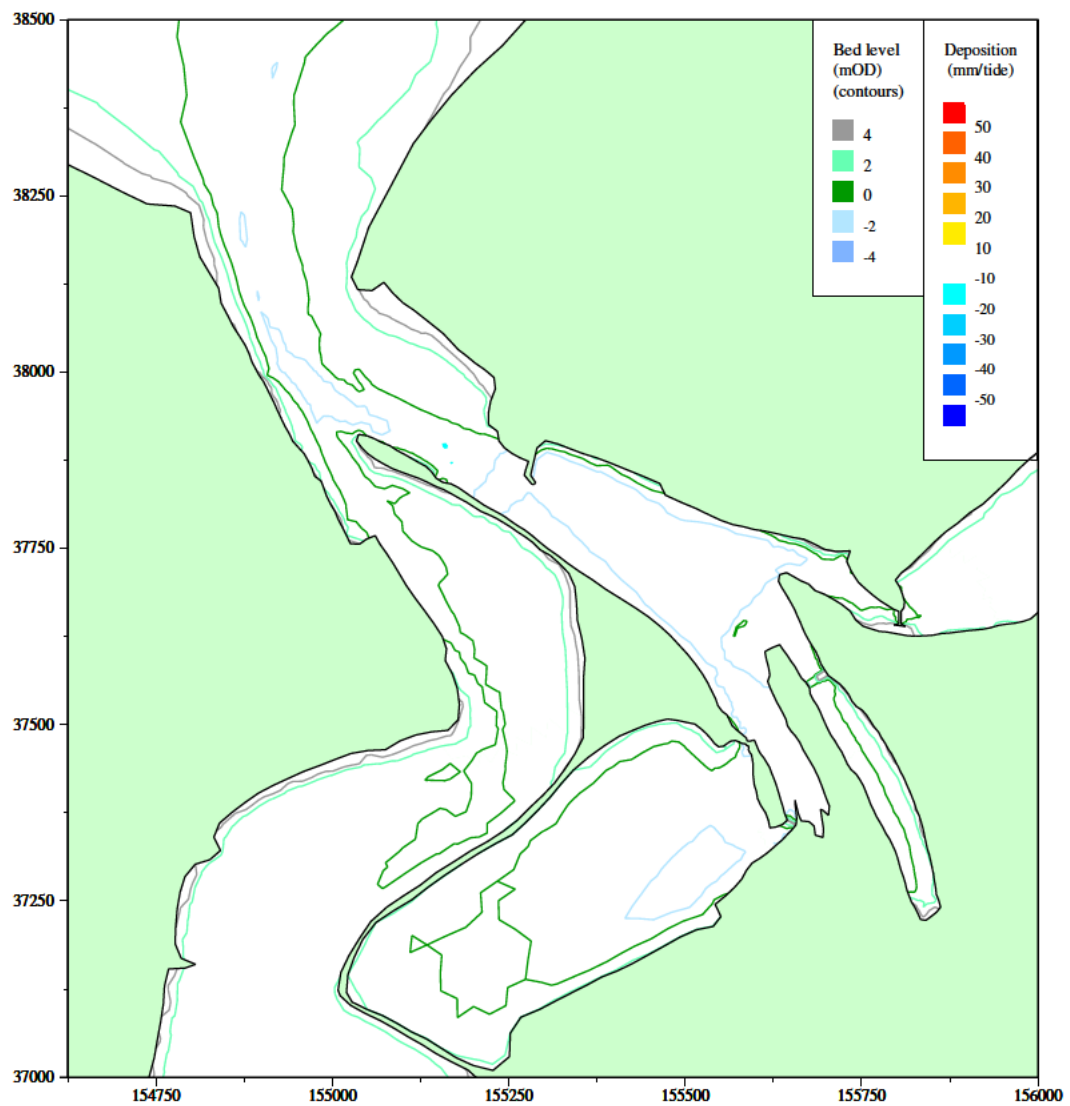
/HR_projects/ddr3839/model/SedimentTransport/report/Rubensp/sand_dev10d.RUB/fig3.104.i

Figure 3.104 Scheme 3 conditions patterns of erosion and deposition with impounding in Carnsew and Copperhouse Pools to HW + 3 hours, double sluice operation on Carnsew Pool



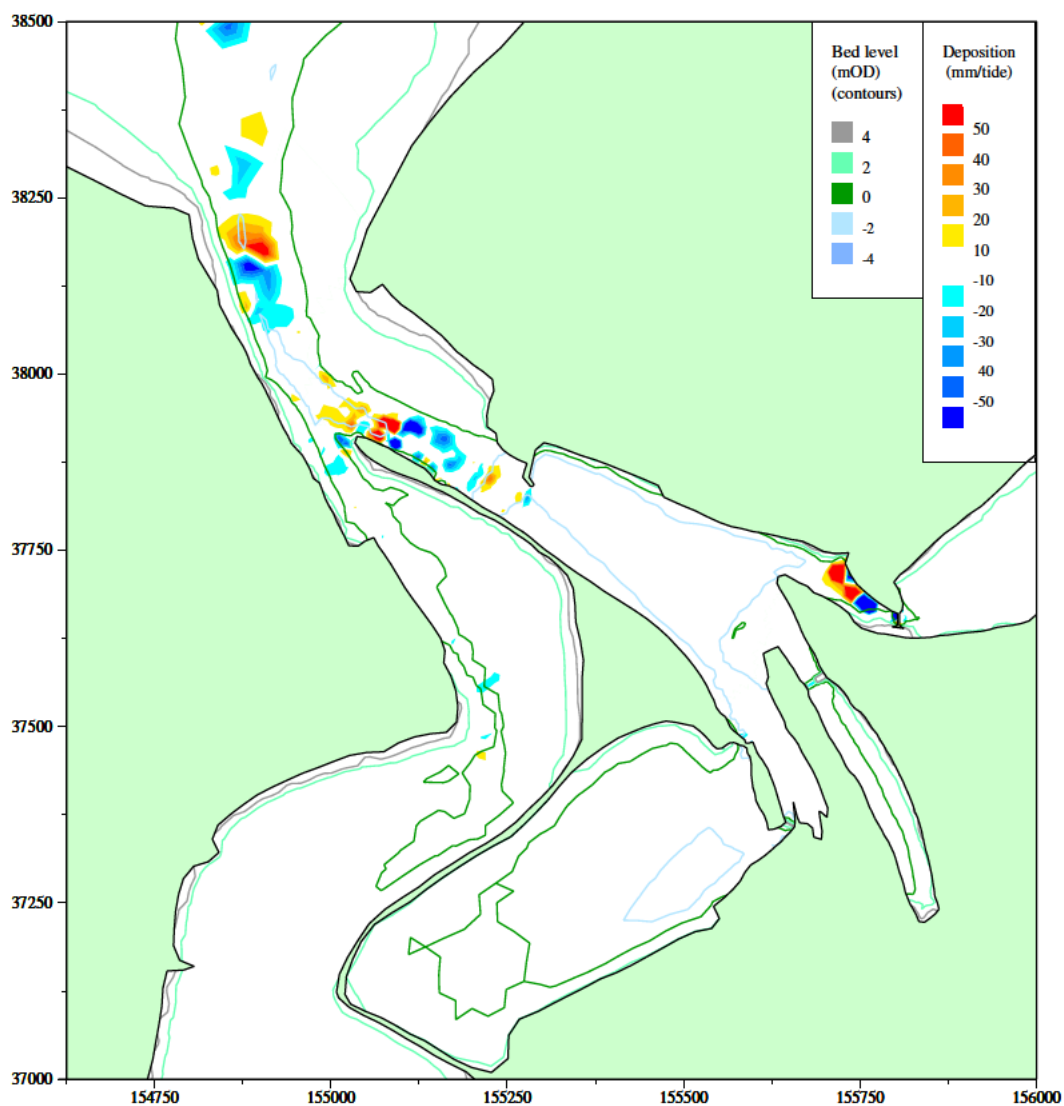
/HR_projects/ddr3839/model/SedimentTransport/report/Rubensp/sand_dev11_sp.RUB/fig3.105.i

Figure 3.105 Scheme 3 with Penpol weir conditions, spring tide patterns of erosion and deposition, Copperhouse sluice open (summer condition), double sluice operation on Carnsew Pool



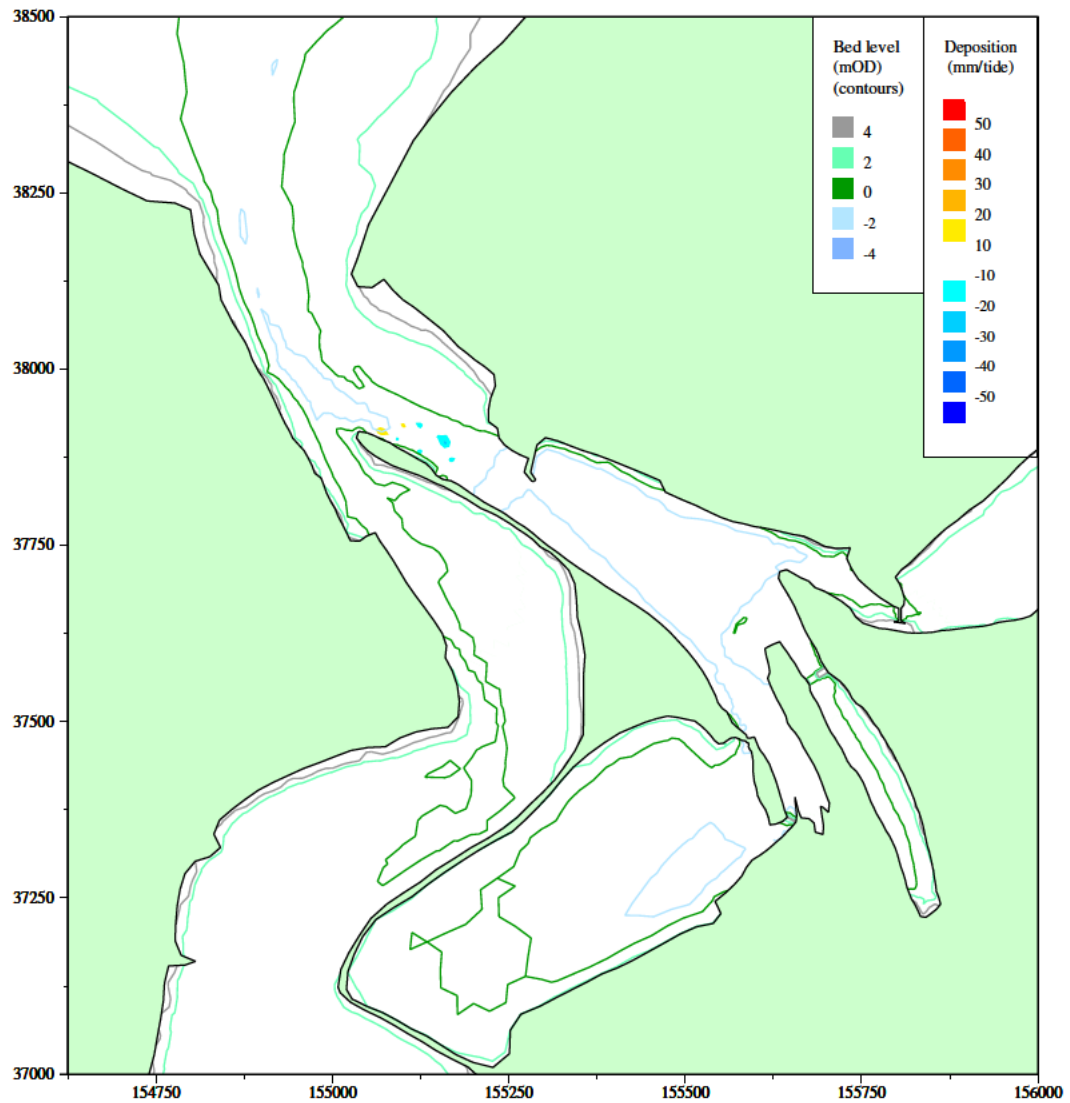
/HR_projects/ddr3839/model/SedimentTransport/report/Rubensp/sand_dev11_np.RUB/fig3.106.i

Figure 3.106 Scheme 3 with Penpol weir conditions, neap tide patterns of erosion and deposition, Copperhouse sluice open (summer condition), double sluice operation on Carnsew Pool



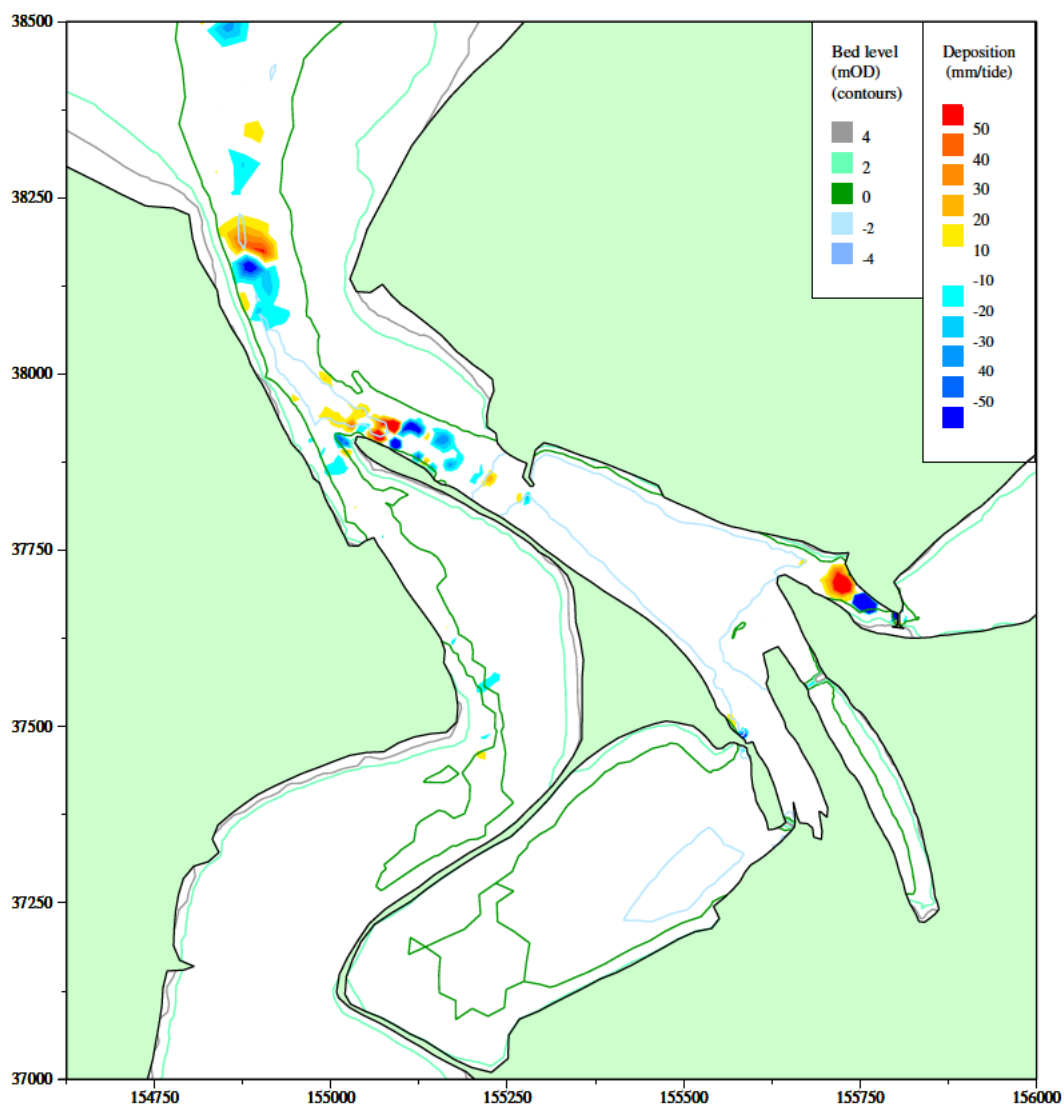
/HR_projects/ddr3839/model/SedimentTransport/report/Rubensp/sand_dev11d_sp.RUB/fig3.107.i

Figure 3.107 Scheme 3 with Penpol weir conditions, spring tide patterns of erosion and deposition with impounding in Carnsew and Copperhouse Pools to HW +3 hours, double sluice operation on Carnsew Pool



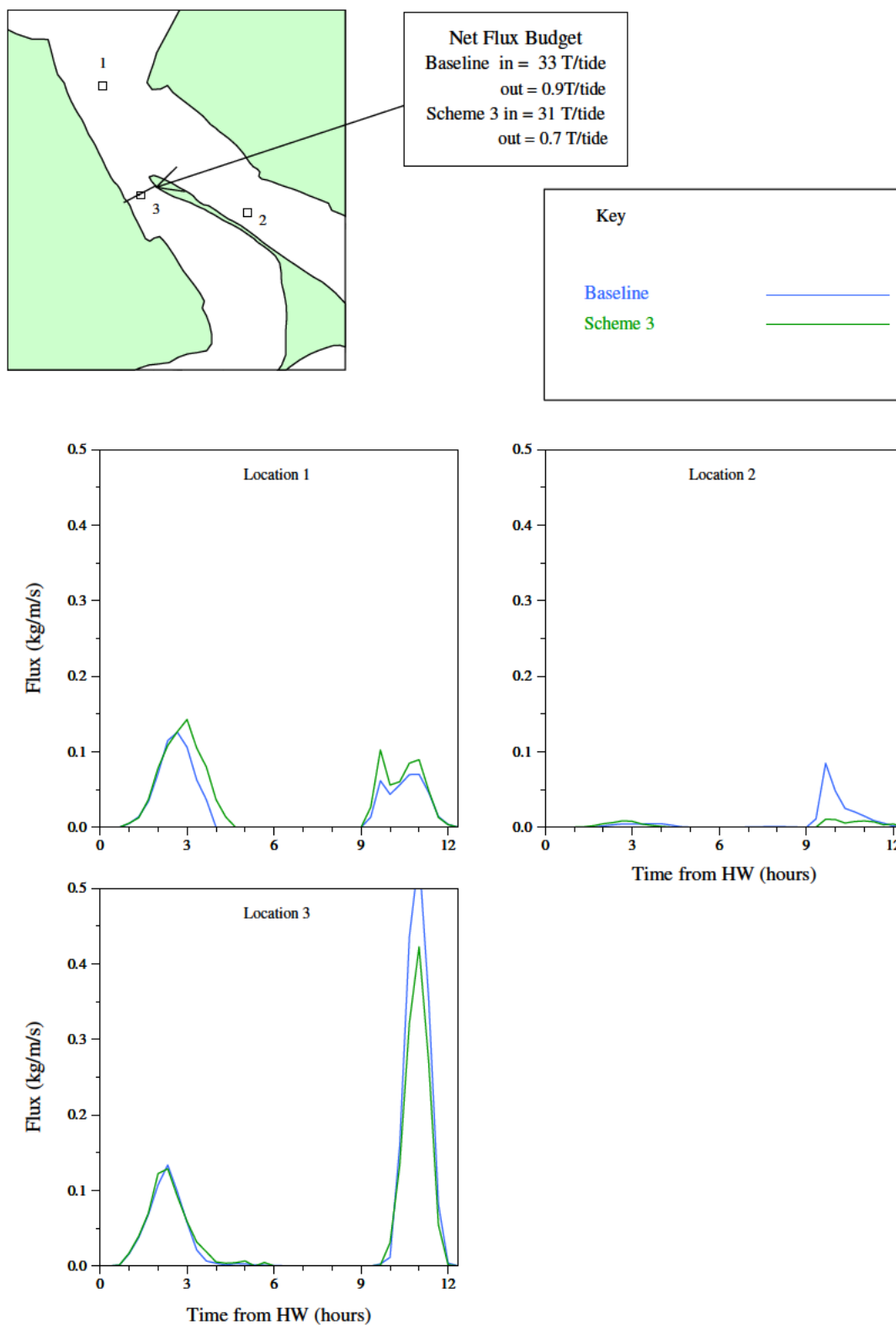
/HR_projects/ddr3839/model/SedimentTransport/report/Rubensp/sand_dev11d_np.RUB/fig3.108.i

Figure 3.108 Scheme 3 with Penpol weir conditions, neap tide patterns of erosion and deposition patterns with impounding in Carnsew and Copperhouse Pools to HW +3 hours, double sluice operation on Carnsew Pool



/HR_projects/ddr3839/model/SedimentTransport/report/Rubensp/sand_dev11e_sp.RUB/fig3.109.i

Figure 3.109 Scheme 3 with Penpol weir conditions, spring tide patterns of erosion and deposition with impounding in Carnsew and Copperhouse Pools to HW +3 hours, double sluice fill, single sluice empty on Carnsew Pool



/HR_projects/ddr3839/model/SedimentTransport/report/Rubensp/sand_dev11_sp.RUB/fig3.110.i

Figure 3.110 Comparison between baseline and Scheme 3 of sand flux at 3 locations in harbour

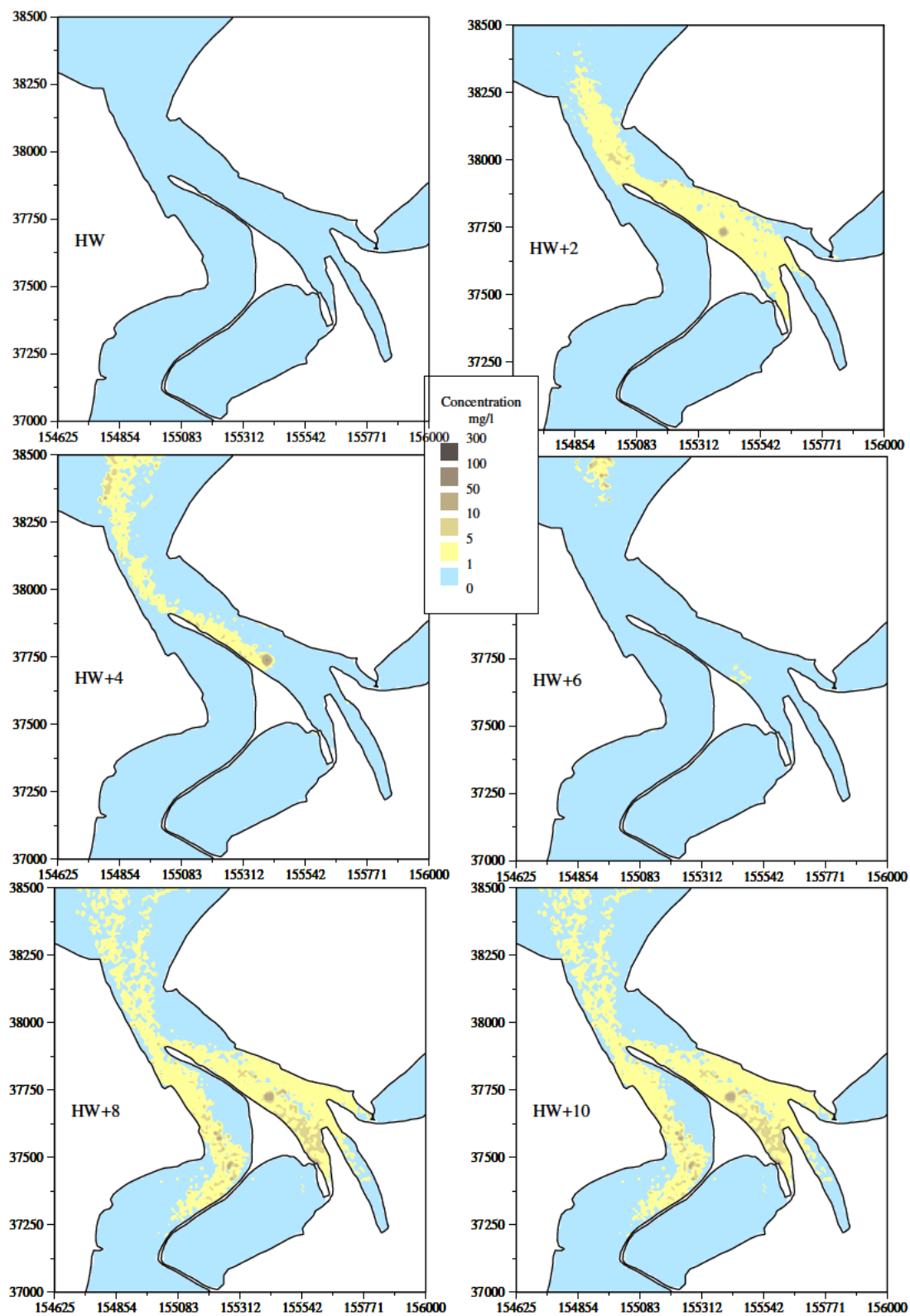


Figure 4.1a Sediment plume concentrations during the dredging operations, HW – HW+10hrs

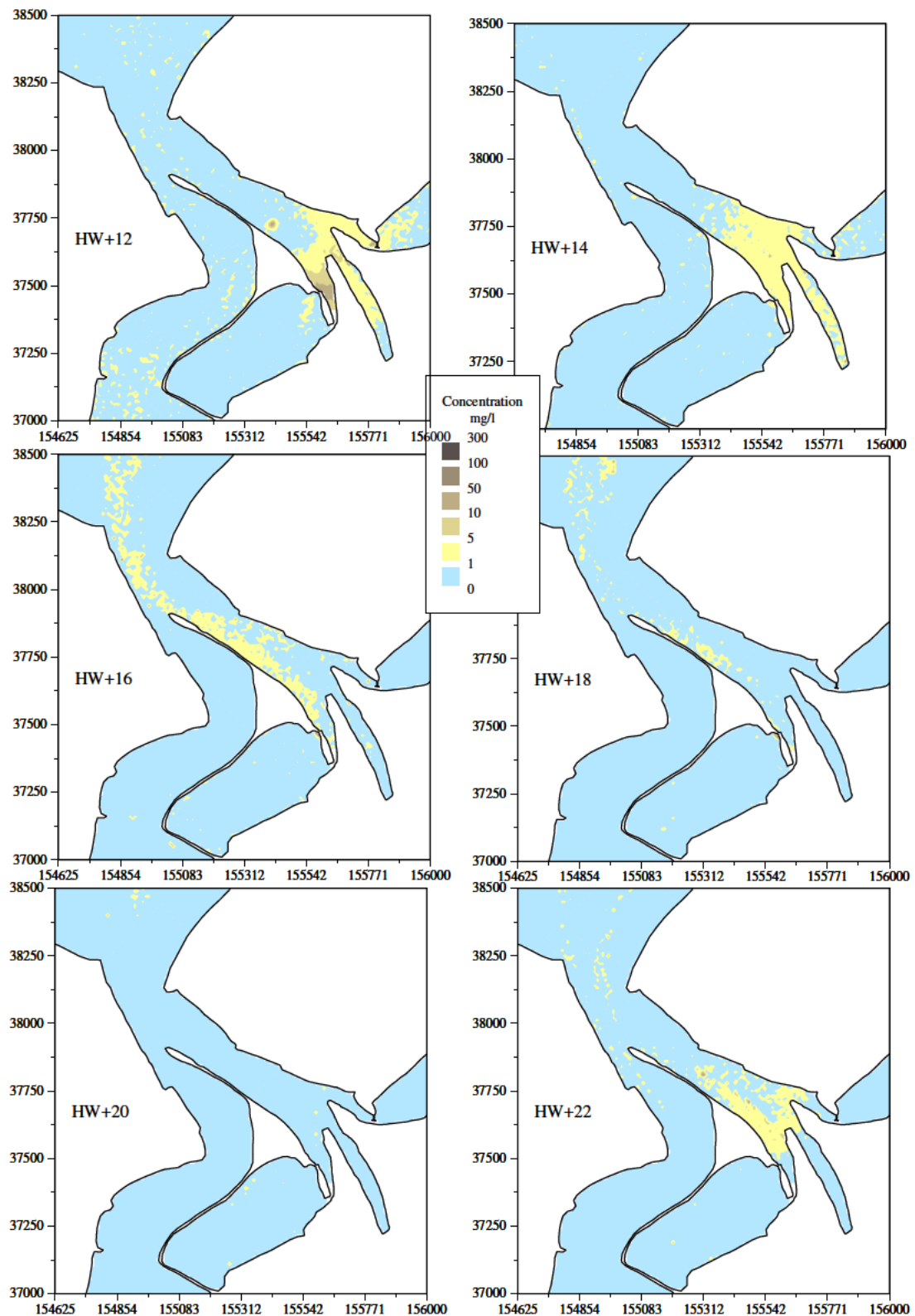


Figure 4.1b Sediment plume concentrations during the dredging operations, HW+12hrs – HW+22hrs

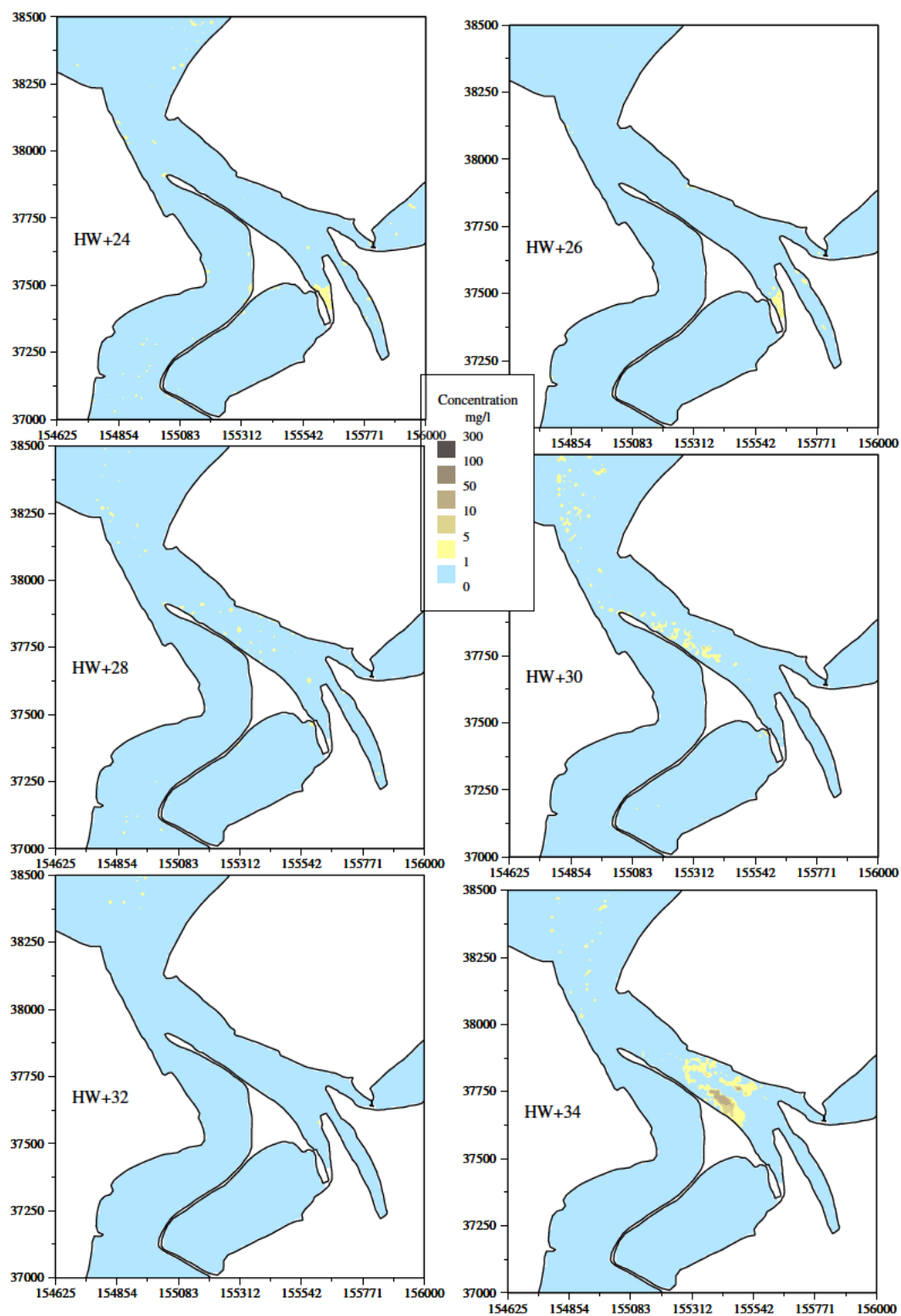


Figure 4.1c Sediment plume concentrations during the dredging operations, HW+24hrs – HW+34hrs

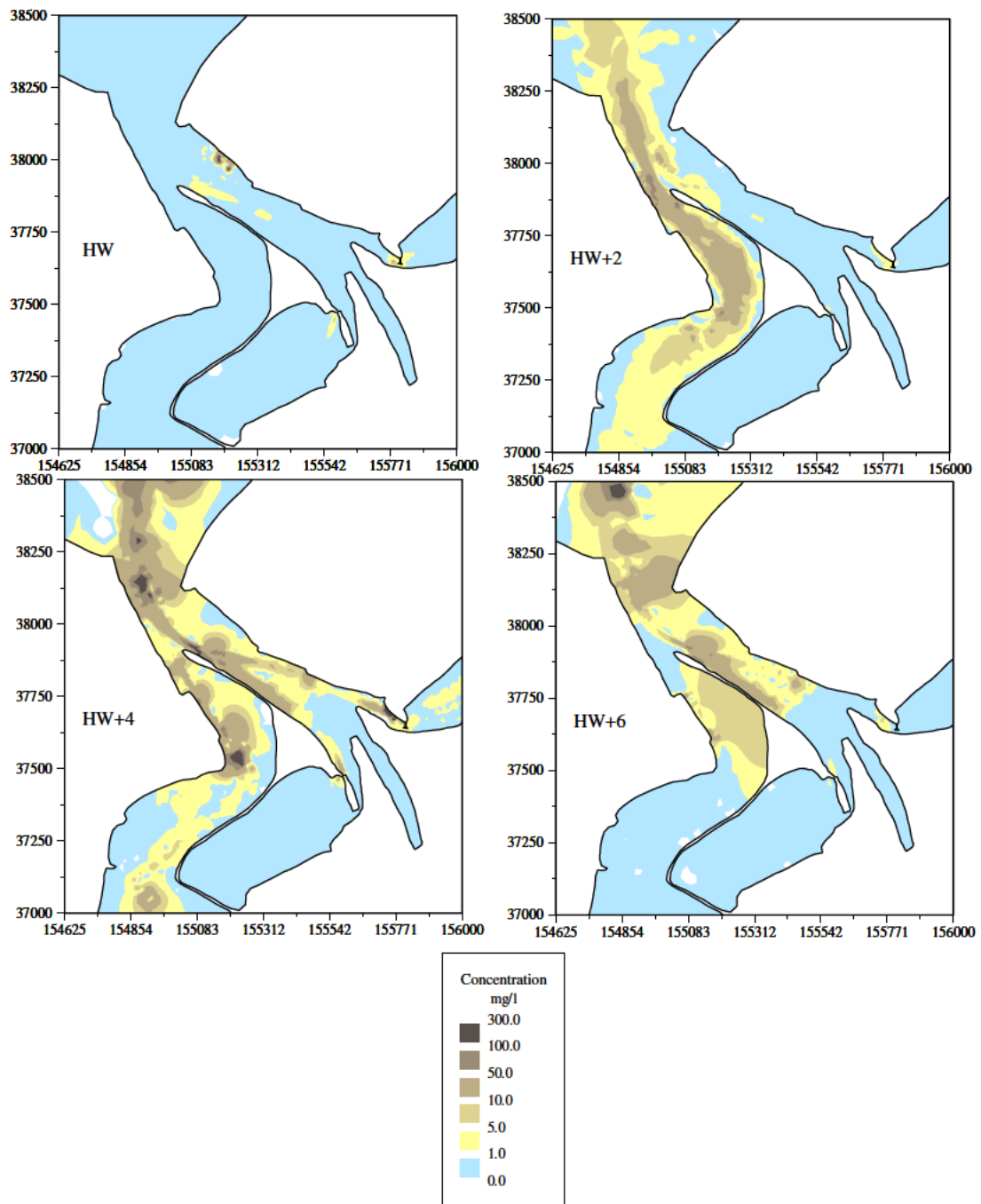


Figure 4.2a Spring tide background suspended sediment concentrations, HW – HW+6hrs

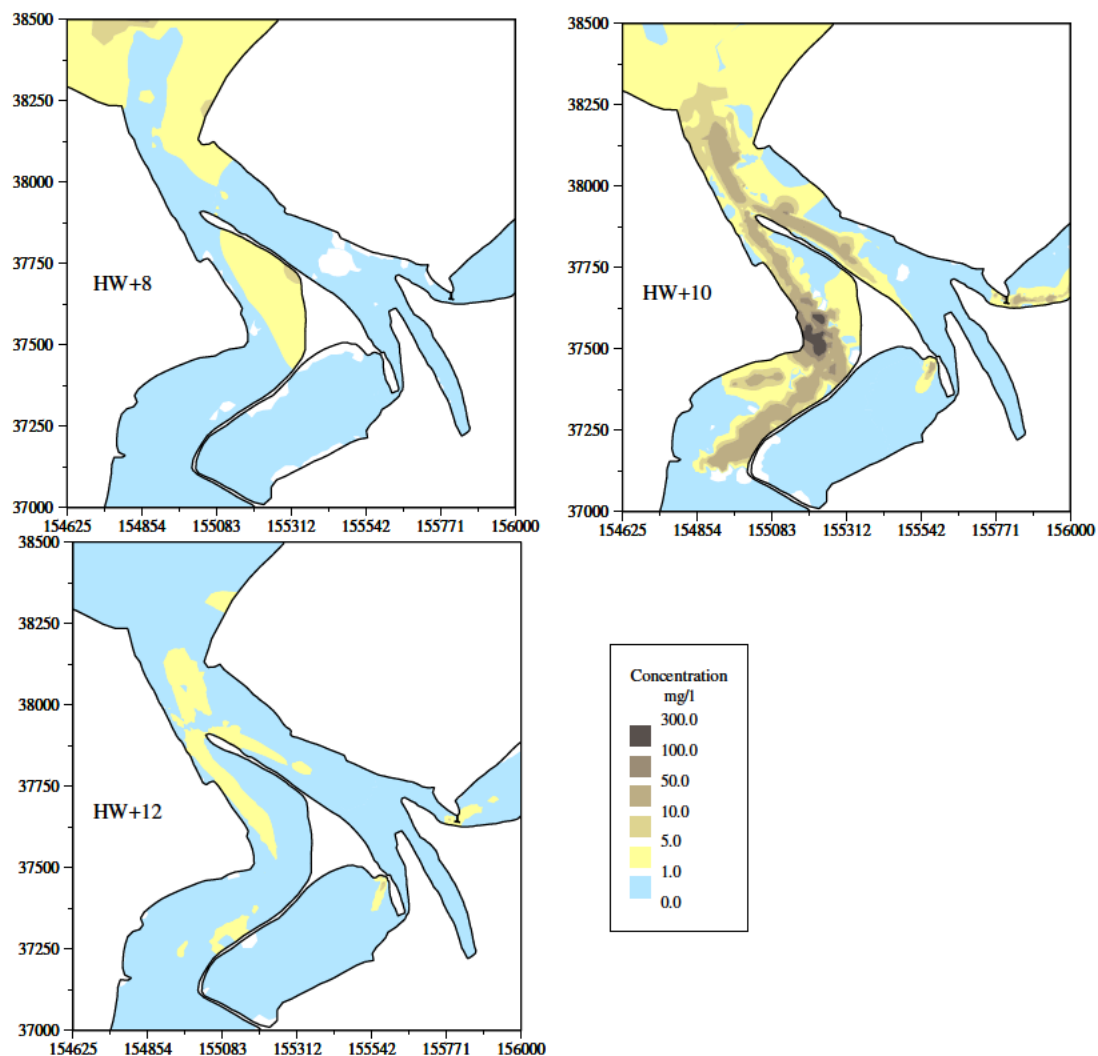
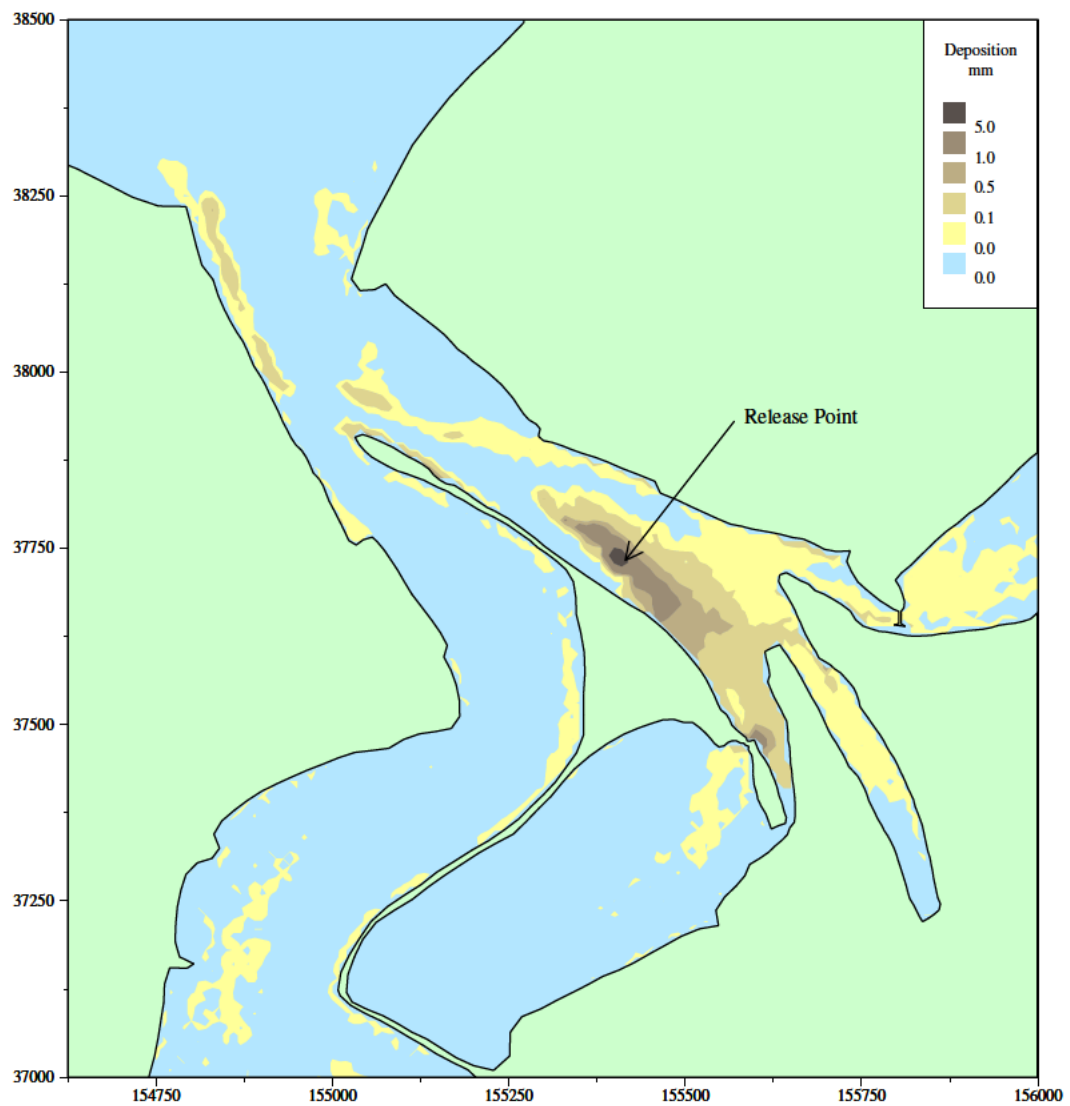
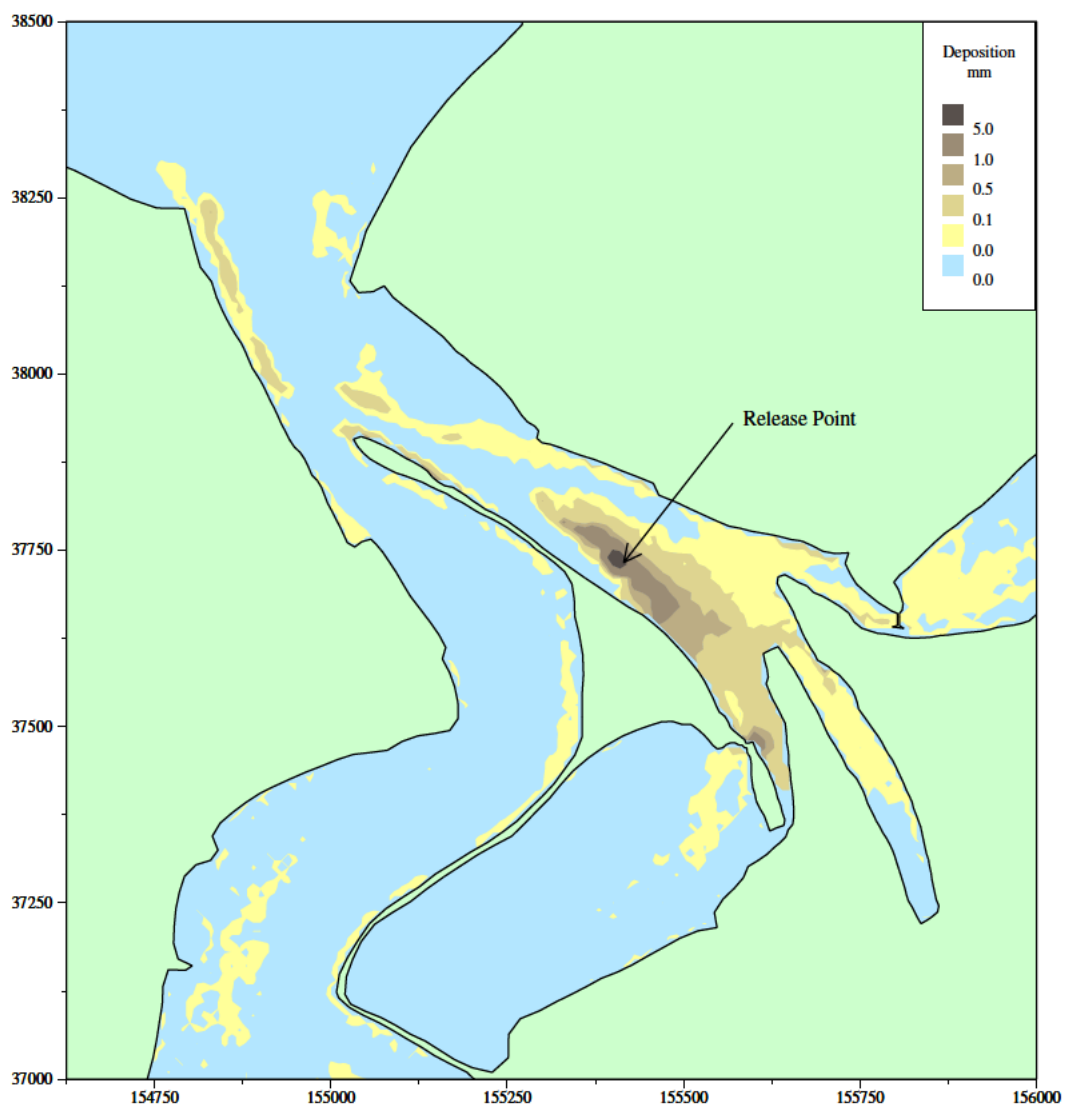


Figure 4.2b Spring tide background suspended sediment concentrations, HW+8hrs - HW+12hrs



/HR_projects/ddr3839/model/sedplume_modelling/Rubensprojects/run4_cul1.RUB/fig4.2n.i

Figure 4.3 Peak suspended sediment concentrations occurring at any stage during the three-tide dispersion simulation



/HR_projects/ddr3839/model/sedplume_modelling/Rubensprojects/run4_cul1.RUB/fig4.2n.i

Figure 4.4 Deposition patterns after three-tide simulation

Appendices

Appendix 1 Numerical model details

TELEMAC-2D model details

Description of model and main areas of application

TELEMAC-2D is a sophisticated flow model, which was originated by LNH in Paris, for free surface flows. It solves the 2D depth-integrated shallow water equations that are used to model flows in rivers, estuaries and seas. It uses finite element techniques so that very flexible, unstructured triangular grids can be used. It has been developed under a quality assurance system including the application of a standard set of validation tests.

The model can simulate depth integrated tidal flows in estuaries and seas including the presence of drying banks. It can also simulate flows in rivers including turbulence structures resulting from flow obstructions and transcritical flows.

The advantage of using finite elements lies primarily in the possibility of using a very flexible grid. This is superior to using an orthogonal curvilinear grid as the user has far more complete control over grid refinement with a finite element system.

The applications of TELEMAC have included studies of tidal flows, storm surges, floods in rivers, dam break simulations, cooling water dispersion and infill of navigation channels.

Theoretical background and solution methods

TELEMAC solves the shallow water equations on an unstructured finite element grid (usually with triangular elements). The various variables (bed elevation, water depth, free surface level, and the u and v velocity components) are defined at the nodes (vertices of triangles) and linear variation of the water and bed elevation and of the velocity within the triangles is assumed.

When the model is used a time-step is chosen and the computation is advanced for the required number of time-steps. There is no particular limit on the time-step for a stable computation but it is best to ensure that the Courant number based on propagation speed is less than about 10. It is found that if the solution is nearly steady then few computational iterations are required at each step to achieve the required level of accuracy, which in TELEMAC is computed according to the actual divergence from the accurate solution. The computation at each time-step is split into two stages, an advective step and a propagation-diffusion step.

The advective step

The advective step is computed using characteristics or stream-wise upwind Petrov-Galerkin. The characteristic step makes it possible for the code to handle such problems as flow over a bump giving rise to locally supercritical flow and eddies shedding behind flow obstructions.

The propagation/diffusion step

The finite element method used is based on a Galerkin variational formulation. The resulting equations for the nodal values at each time-step are solved using an iterative method based on pre-conditioned conjugate gradient (PCG) methods so that large problems are solved efficiently. Several PCG solvers are coded and a selection is available to the user. The complete matrix is not assembled. Instead an element by element method is used so that most of the operations are carried out on the element

matrices; this is computationally more efficient, both in speed of execution and in memory requirements. Rather than using Gauss quadrature exact analytical formulae are used for the computation of matrices. Symbolic software was used to draw up the formulae used. The software makes it possible to carry out a second iteration of the solution at each time-step in order to represent the non-linear terms in a time centred way, otherwise these terms are treated explicitly.

Boundary conditions

Boundary conditions are applied at solid boundaries where a "zero normal flow" and either a slip or non-slip boundary condition are applied. At open boundaries a selection of possibilities can be invoked depending on whether the flow is subcritical or supercritical or whether a wave absorbing boundary using a Riemann invariant is needed. A water discharge along a boundary segment can also be applied and the software distributes the flow along the segment chosen. This facility is valuable when running models of river reaches and the discharge in a cross section may be known rather than the velocity at each point in the cross-section.

Grid selection

The model can be run with a Cartesian grid for modelling rivers, estuaries and small areas of sea, with the possibility to apply a uniform Coriolis parameter, or on a spherical grid for larger areas of sea in which case the Coriolis parameter is computed from the latitude at each node. The effect of a wind blowing on the water surface and causing a set-up or wind induced current or of an atmospheric pressure variation causing an inverted barometer effect can be included, as can a k-epsilon model of turbulence if required.

Friction

The bed friction can be specified via a Chezy, Strickler or linear coefficient, or a Nikuradse roughness length. A variable friction coefficient over the model area is a possibility. Sidewall friction can also be included if wanted. Viscosity can be imposed as a given eddy viscosity value or a k-epsilon model can be used if needed.

Tracer calculation

TELEMAC-2D includes also the capability to simulate the transport of a tracer substance. The tracer is again computed using an advective step followed by a propagation/diffusion step. Tracer boundary conditions can be applied at model inflow boundaries. The tracer calculation has been used in order to simulate cooling water dispersion and mud transport. Sources of water and/or of tracer can be specified in terms of the discharge required and the x and y co-ordinates of the location.

INPUTS

TELEMAC requires as input a finite element grid of triangles covering the area to be modelled. Bathymetric data from which the bed elevation at each node can be computed is also required covering the area. A file of keyword values is used to steer the computation (supplies bed roughness, time-step, duration of run etc).

Methods of inputting the data

The finite element grid may be provided by a standard FE grid generator such as IDEAS or SIMAIL. The software STBTCL (part of the TELEMAC suite) is used to read the output file from the grid generation software. The bathymetry is input using a digitising tablet and the SINUSX software is used to capture the bathymetry data. The

data is stored in a form to be read into the TELEMAC system and depths interpolated to the model nodes.

Methods of checking and amending input data

SINUSX is a powerful interactive graphical software that can be used to check and amend the input data. Bathymetric curves can be duplicated, deleted, smoothed, moved etc.

Time to set up/calibrate/run/amend model

This depends on the form in which the data is supplied. Typically 1-2 days to digitise the chart data and 1-2 days to create the finite element grid. Boundary conditions may take a day to prepare. A run may take 1 to 5 hours to run a tide (for a 2000 cell model). The duration of the calibration process is hard to generalise as it depends entirely on particular circumstances.

OUTPUTS

Output parameters

The user can select from a range of output parameters including u and v velocity, u and v discharge, water level, bed level, water depth, tracer concentration and Froude number.

Output files

The TELEMAC output is contained in a single binary file which can be input to the graphics post-processor RUBENS. A listing file contains reflection of the input keywords and information on time-step reached, number of iterations to convergence etc. This file can be used to monitor the progress of a run.

Output plots

Results from the TELEMAC system are processed using the interactive graphics system RUBENS. This is a powerful and friendly environment in which figures can be produced interactively. By pointing and clicking time history plots, cross sections, vector plots and contour plots of any parameter at any position can be produced. Parameters other than those input can be calculated in RUBENS and plotted.

GENERAL

Interaction and compatibility of the model with other models

The main modules apart from TELEMAC-2D itself (the 2D flow model code) are SINUSX and RUBENS (described above).

The TELEMAC suite includes a bed load transport model (TSEF) and a suspended load model (SUBIEF). Also a wave model ARTEMIS that solves the mild slope equation.

The TELEMAC modelling suite also includes a quasi-3D random walk model for pollution transport modelling and a detailed water quality model with many water quality parameters including dissolved oxygen balance and particulates.

Quality Assurance

The software has been developed under the quality assurance procedures required by the French Electricity Industry. This has included the production of an extensive dossier of validation tests.

Validation

Validation tests on TELEMAC include:

- Simulation of eddies produced behind bridge piers. This test case includes the ability of the model to produce an unsteady solution from steady boundary conditions (von Karman vortex street).
- Drying on a beach.
- Simulation of the tides on the continental shelf including the Bay of Biscay. This model has been closely compared with the observed tides at coastal sites.
- Flow over a step in the bed with critical flow and a hydraulic jump. This solution is compared with the analytically known solution to this problem.

SANDFLOW model details

Description of model and main areas of application

SANDFLOW-2D is the sand transport modelling module of the TIDEWAY-2D system. SANDFLOW-2D uses the flows calculated by TIDEFLOW-2D to study the transport, deposition and erosion of non-cohesive (sandy) sediment and thereby identify areas of potential siltation and erosion. SANDFLOW-2D has also been adapted to use the flows produced by the TELEMAC flow model for sand transport calculation.

Theoretical background and solution methods

The sediments under consideration here are very fine and fine sands ($d_{50} \sim 0.06$ to 0.25 mm) which mainly move in suspension. The model can also be used to identify trends in the case of medium sand ($d_{50} \sim 0.25$ to 0.5 mm). If the sediment contains a high proportion of clay or silt particle sizes less than 0.06 mm, it would be more appropriate to use the MUDFLOW-2D (TIDEWAY) or SUBIEF (TELEMAC-2D) models.

The main factors controlling sand transport are:

- advection by currents
- settlement under gravity
- turbulent diffusion in all directions (but only the vertical component is of significance under most circumstances)
- exchange of sediment between the flow and the bed

The study of sand transport generally is very difficult but more so in the case of estuaries or coastal areas. This is because the water movements are continually changing, with the rise and fall of the tide, and there is usually a wide range of sediments on the bed and areas without mobile sediment, leading to unsaturated loads in the water.

Method

Although sand transport in estuaries is really an unsteady, 3D problem, it has been shown by HR Wallingford that it can be dealt with using a 2D, depth-averaged model provided special provision is made to account for the vertical profile effects of the sediment concentration. Under these circumstances the depth-averaged, suspended solids concentration $c(x, y, t)$ satisfies the conservation of mass equation.

$$\frac{\partial}{\partial t}(dc) + \alpha \left[\frac{\partial}{\partial x}(duc) + \frac{\partial}{\partial y}(dvc) \right] - \frac{\partial}{\partial s} \left(dD_s \frac{\partial c}{\partial s} \right) + \frac{\partial}{\partial n} \left(dD_n \frac{\partial c}{\partial n} \right) + S \quad (1)$$

where

(u,v)	=	depth-averaged components of velocity (m/s)
D_s	=	longitudinal (shear flow) dispersion coefficient (m^2/s)
D_n	=	lateral (turbulent) diffusivity (m^2/s)
(x,y)	=	Cartesian co-ordinates in horizontal plane (m)
(s,n)	=	natural co-ordinates (parallel with and normal to mean flow) (m)
t	=	time (sec)
d	=	water depth (m)
S	=	erosion from or deposition on the bed ($kg/m^2/s$)
α	=	advection factor to recover the true sediment flux from the product of depth-averaged quantities

Advection factor (α)

This is introduced to compensate for the omission of the vertical profile in the sediment flux terms.

$$\alpha = T/qcd \quad (2)$$

where

$$\begin{aligned} T &= \int_0^d q'c'dz \text{ is the sand transport (kg/m width/s)} \\ q &= \text{the depth-averaged water speed } (u^2 + v^2)^{1/2} \end{aligned}$$

and q',c' are the full three-dimensional velocity and concentration variables.

Since the highest concentrations occur near the bed it follows that $\alpha \leq 1$. Typical values of α can be obtained by evaluating equation (2) for sand transport profile observations or from the integration of theoretical solutions for suspended solids profiles. However, in practice, it is usually acceptable to take $\alpha = 1$ on the grounds that the external and internal sources of mobile sediment are not well enough known to justify a more precise formulation.

Bed exchange relations

The simplest formulation of the bed exchange relation is

$$S = \beta_s \omega_s (c_s - c) \quad (3)$$

where

$$\begin{aligned} c_s &\text{ is the depth-averaged concentration when the flow is saturated with sediment (kg/m}^3\text{)} \\ \omega_s &\text{ is the representative settling velocity (m/s)} \\ \beta_s &\text{ is a profile factor to compensate for integrating out the vertical profile of suspended sediment ie to correct for higher sediment concentrations near the bed.} \end{aligned}$$

Deposition or erosion takes place depending on whether the instantaneous sediment load (c) exceeds or is less than the saturated value (c_s). Pick up of sediment from the bed is prevented if there is no sediment available on the bed. A shortage of material on the bed is reflected in a low concentration of suspended solids being advected away by the flow.

Typical values of β_s could be obtained from actual observations of sediment profiles or from theoretical considerations. However, HR Wallingford has derived an analytical expression for this so that bed exchanges are performed automatically. This involves simplifying the vertical diffusivity relation and a profile mixing factor is introduced to enable the user to increase or decrease the effective mixing during calibration of the model.

Sediment transport relation

The evaluation of bed exchanges requires a depth-averaged sediment concentration (c_s). Sandflow-2D obtains this from a sediment transport relation specified by the user. Three sand transport relations are supplied in the package (Ackers-White, van Rijn and

a simple power law) and since the source code is provided other relationships can be added by the user if preferred.

The choice of sand transport relation needs care. It should be borne in mind that most relationships found in the literature are based on river or channel data where sediments are more narrowly graded than in estuaries. Also there is normally a small proportion of cohesive material in estuary sediments and this can alter the transport properties. If possible, sand fluxes should be measured at the study site, and if such data is available it may be best to use it to obtain the best-fit power law relation for the site.

Diffusion

The dispersion (D_s) and diffusion (D_n) coefficients are not well defined. When viewed in close enough detail the whole motion appears advective; but when viewed on a coarser grid the smallest motions appear diffusive. Thus selection of the appropriate diffusion or dispersion coefficients depends on the grid size of the model - one model will treat as advection what a coarser grid model will treat as diffusion or dispersion.

Fortunately, the solutions to the equation are not normally sensitive to D_s and D_n . As a first approximation, $D_n = Bdu$, where d and u are representative depths and velocities. It has been found that B is usually in the range 0.01 (for fairly uniform depths and smooth beds) to 0.1 (for irregular geometry and/or rougher beds).

D_s is automatically calculated by the program for each model cell depending on the local depth and velocity to give more diffusion in the direction of flow. The overall scale of D_s can be changed using the relative dispersion parameter (in keyword DIFFUSION). This normally has the value unity but it can be adjusted upwards or downwards during calibration to get agreement between the model results and any dispersion observations that may be available.

Numerical model

A simple, explicit, upstream finite difference technique is used to solve the advection - diffusion equation. Flux corrections are not considered to be necessary because the background concentrations of suspended sand are normally fairly uniform throughout the model in contrast to POLLFLOW-2D applications that have one or two point sources and correspondingly steeper concentration gradients.

The use of an explicit method introduces a stability constraint on the computing time step (Δt).

$$\Delta t < \Delta s / (\text{maximum flow velocity})$$

where Δs is the grid size (TIDEWAY) or separation between nodes (TELEMAC-2D) in metres.

Generally, this does not pose any problems in practice because the allowable Δt is usually much larger than the TIDEFLOW-2D time step and there is only a single equation to solve in the process model compared to three in TIDEFLOW-2D. Under these circumstances an explicit method is preferred because it enables the user to understand the code more easily and to modify the treatment of the physics of the processes being simulated. Note that where TELEMAC-2D is being used the values of Δs will vary and so the minimum value of Δs is the most important in terms of stability.

The treatment of the dispersion (D_s) and diffusion (D_n) terms introduces another stability constraint.

$$\Delta t < \Delta s^2 / 4 D_{\max}$$

where D_{\max} is the maximum of D_s and D_n .

This constraint is normally weaker than the advective stability limit but the user should be aware that a high value of diffusivity can lead to an instability. In the event of problems the possible violation of both limits should be checked.

Application of the model

The application of the model and interpretation of the results requires a good understanding of sand physics. Firstly it is important to choose representative values for the main parameters. Ideally these should be based on laboratory tests of actual sediment samples from the site. It is also important for the modeller to be aware of the limitations of this type of model when applied to real sites.

In addition it should be appreciated that sand transport is not an exact science. Accordingly, whatever model is used, and whatever parameter values are chosen it is essential that results are interpreted correctly. Provided this is done the model will be a valuable engineering tool.

Calibration/validation

Calibration of sediment models is difficult because bed changes are usually too slow or too variable to measure anything significant for comparison. Sometimes historical charts or dredging records may be available but even then it is unlikely that the sources of suspended sediment can be quantified for the relevant period. Sometimes it is possible to get scaling factors for model results in cases where information is available and use these to estimate siltation in the new situation, but in many cases one is forced to use the best available values for the parameters and to demonstrate that the siltation and erosion patterns produced by the model agree with the observed state of the estuary or coastal region being studied.

Some evidence to support the physical realism of the model is given by the following results of simulation of sand transport in a flume and of observations from the Thames estuary.

The computer model results were compared with the results of a laboratory experiment performed in a flume with a length of 30m, a width of 0.5m and a depth of 0.7m. The discharge was measured by a circular weir. The mean flow depth was 0.25m and the mean flow velocity was 0.67 m/s. The bed material had a $d_{50} = 230\mu\text{m}$ and a $d_{90} = 320\mu\text{m}$. The median diameter of the particles in suspension was estimated to be about 200 μm , resulting in a representative fall velocity of 0.022 m/s (water temperatures 9°C). The stream bed was covered with bed forms having a length of about 0.1m and a height of about 0.015m. Small Pitot tubes were used to determine the vertical distribution of flow velocity. Water samples were collected simultaneously by means of a siphon method at four locations to determine the spatial distribution of the sand concentrations. At each location (profile) five samples were collected at a height of about 0.015, 0.025, 0.05 and 0.22m above the average bed level and these were integrated to give the suspended load transport. The HR SANDFLOW-2D model was run for the same

conditions assuming the overall shear velocity was 0.0477 m/s and the results in Figure 1 shows that the model could be calibrated if suitable data is available.

The model was compared with some flume data to test its response to a change in the sediment load. It was shown that the model simulation could be calibrated by adjusting the settling velocity and vertical diffusivity parameters. This procedure is justified for practical applications because in nature these parameters are not well defined. For example, there is no unique settling velocity because the suspended load would contain a range of sediment sizes and the true nature of the vertical diffusivity is not yet fully understood.

The basic physics of the model was then checked against real field data from Foulness in the Thames Estuary. There was a wide range of sediment sizes in the data but the model was only used to simulate individual fractions. The saturation concentrations in the model were calculated using a cubic velocity relation derived from the observed sand fluxes.

Results from the model simulation of the 75 to 100 μm sand fraction are shown in Figures 2 and 3 plotted at half hourly intervals with a sequence number showing the progression through the tide. The model has a similar hysteresis effect to the observations on both stages of the tide. The systematic underestimation of concentrations during the ebb is probably due to a different availability of sediment sizes not allowed for in the simplified model. Nevertheless the demonstration confirms the general validity of the model in a natural situation.

An example of the agreement achieved during validation, between the SANDFLOW-2D model results and observed sediment distribution is shown in Figure 4. Note in particular the agreement between the areas of potential erosion predicted by the model and areas of rock bed, and also the areas of potential deposition and areas of sand bed observed.

INPUTS

Input data required

SANDFLOW-2D requires as input the elevation and flow results from a TIDEFLOW-2D run or a TELEMAT-2D run, together with information describing the initial distribution of sand on the bed. A boundary data file is also required to specify sediment concentrations at the model edges with respect to time. Other parameters required include the typical size of sand and its basic properties such as settling velocity and threshold stress for initiation of motion.

Methods of inputting the data

Data is input to SANDFLOW-2D using ASCII data and steering files and unformatted direct access results files from TIDEFLOW-2D or the TELEMAT-2D equivalent. The steering files are set up using the context sensitive editor included in the user interface.

User interface

A keyword driven interface controls all aspects of using SANDFLOW-2D from setting-up a model through to analysis of the results. The interface includes file management functions, graphical presentation of results and utilities for results analysis and file format conversion.

OUTPUTS

Output parameters

SANDFLOW-2D calculates concentrations of suspended sediment and distributions of erosion and deposition are stored at user selected intervals during the run. SANDFLOW-2D calculates suspended sediment concentration, erosion and deposition throughout the model area for each time step through the tide.

Output files

Each run of the SANDFLOW-2D model generates three output files. Two of these files contain the suspended concentrations and bed deposits. The third output file; the List File contains run information.

Output plots

The results from the SANDFLOW-2D may be represented using report quality-graphics utilities included in the TIDEWAY-2D system or, where TELEMAC-2D has been deployed, the RUBENS visualisation system. Contour plots of suspended concentrations and/or bed deposits at user selected times and concentration-time and deposit-time plots at selected locations can be produced.

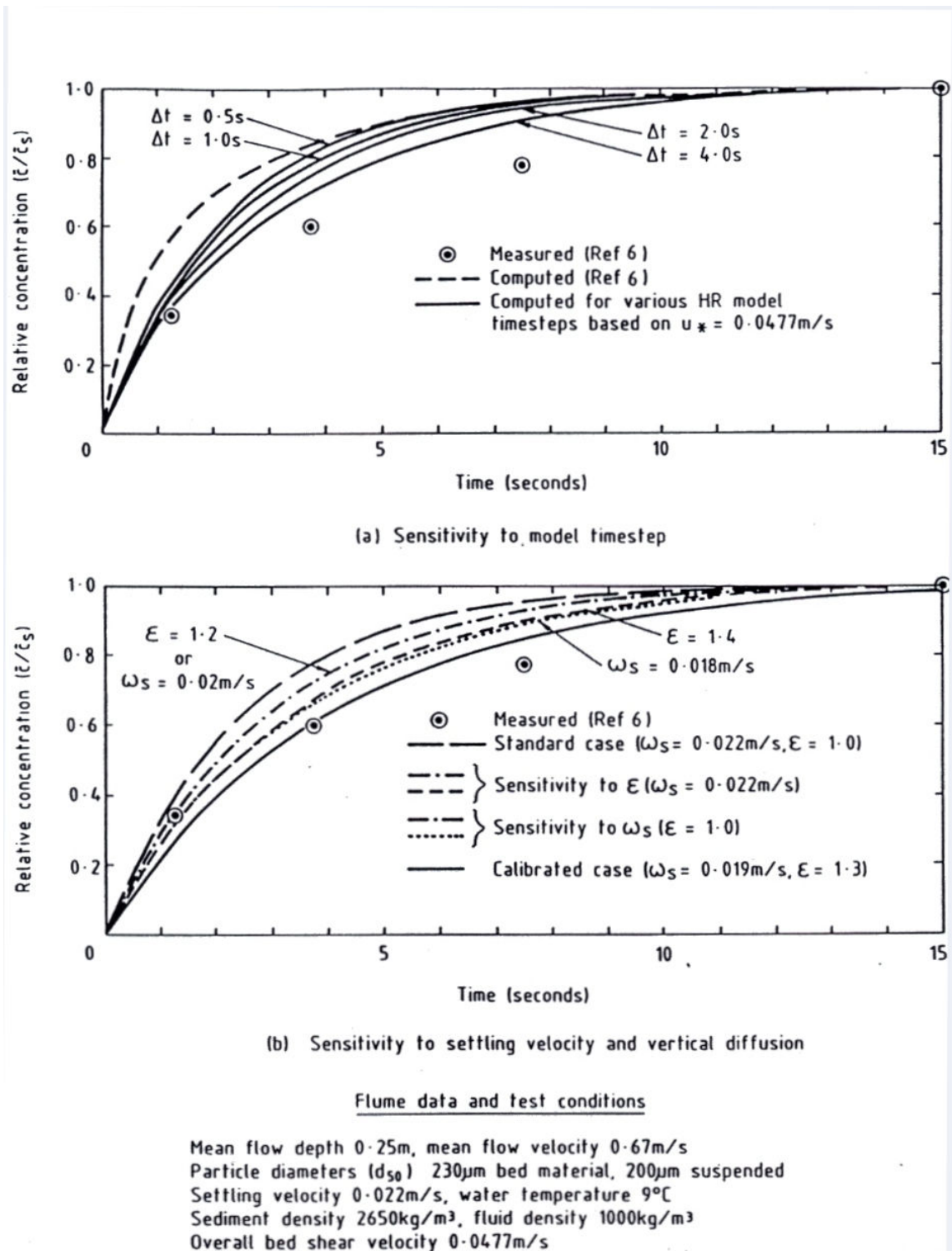


Figure 1 Computed and measured evolutions of sediment load

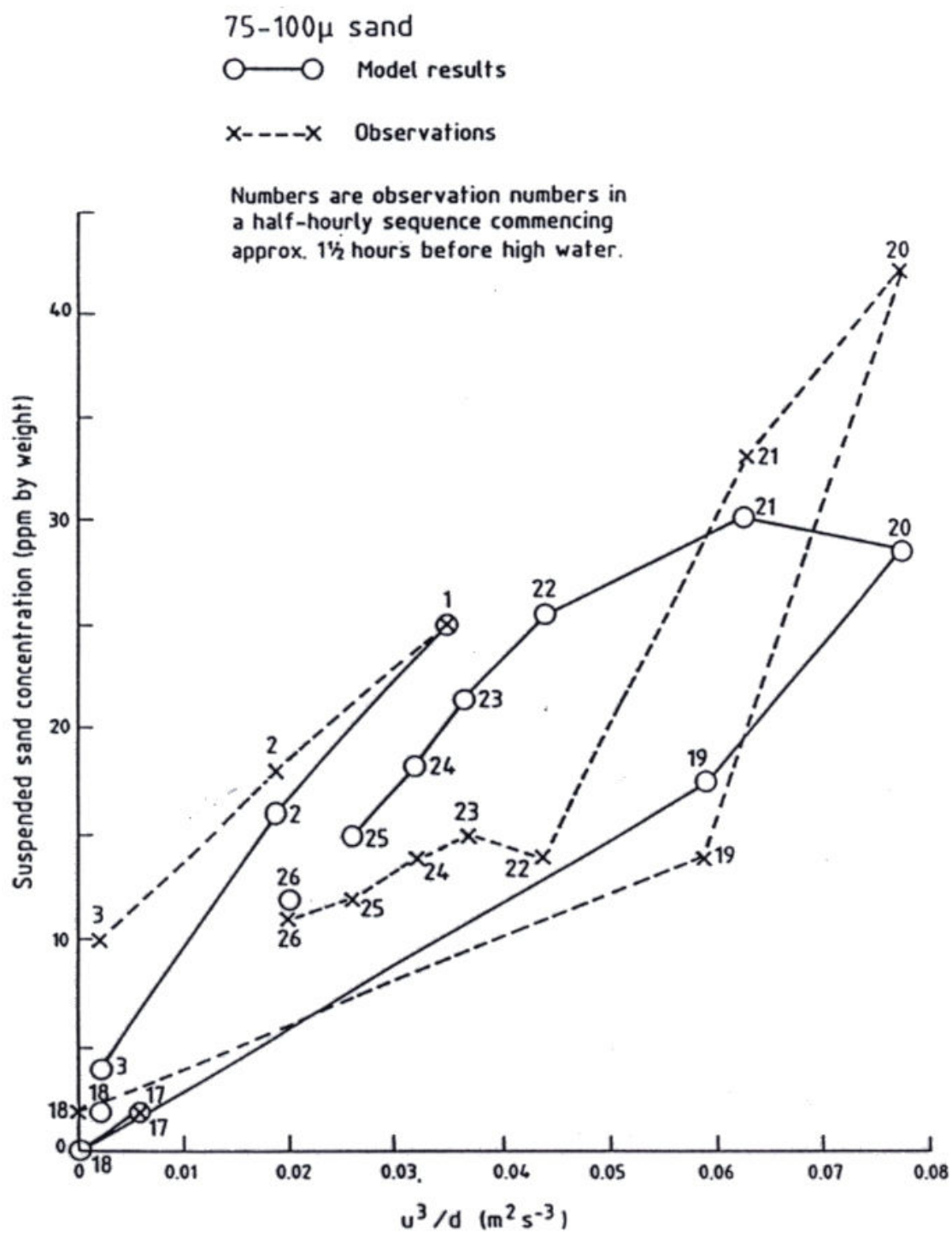


Figure 2 Simulation of Foulness position 1 flood tide

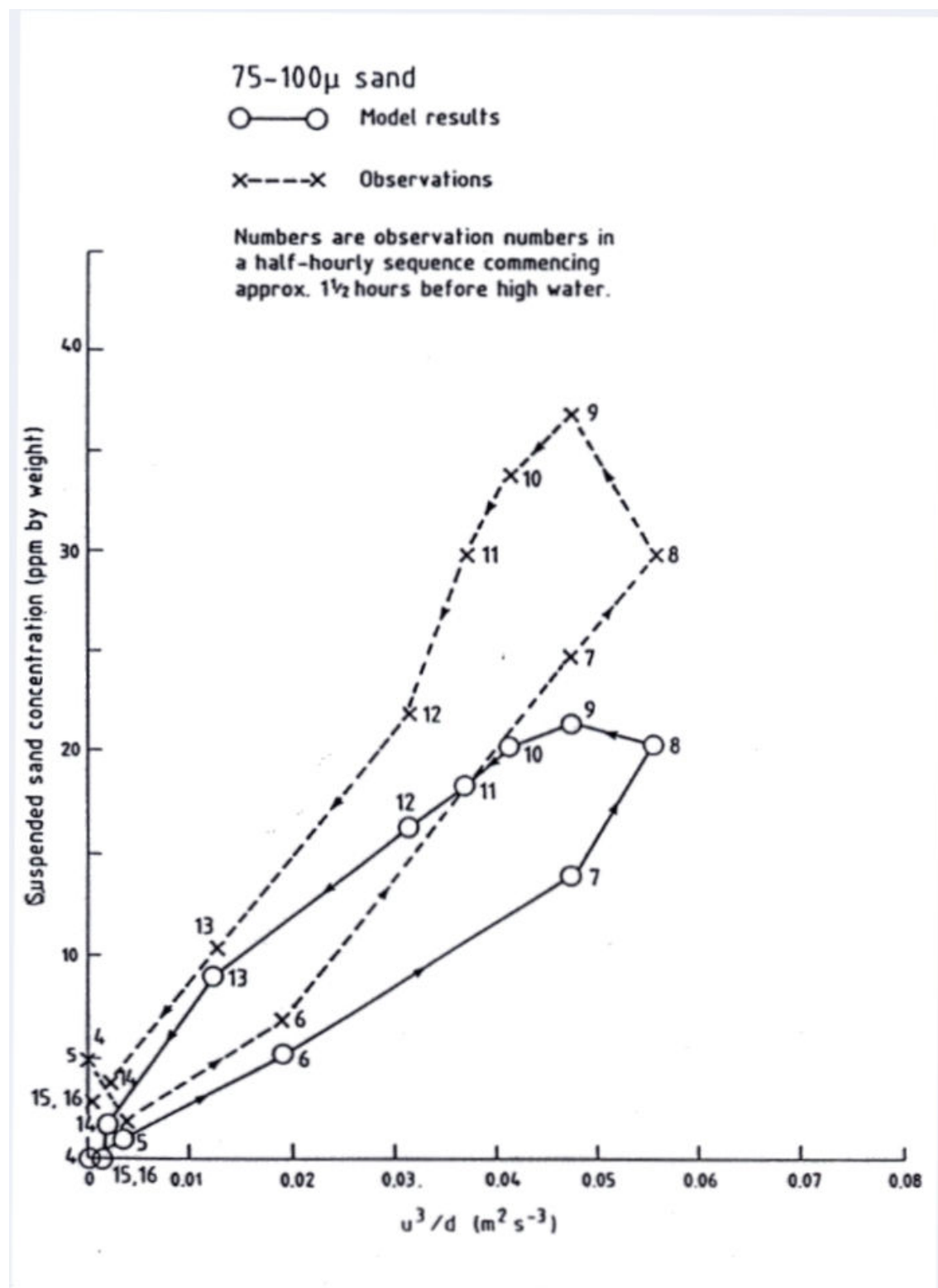
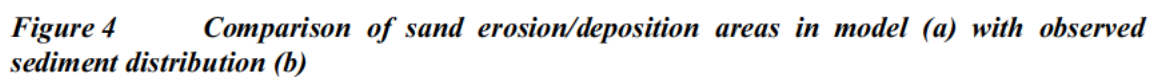


Figure 3 Simulation of Foulness position 1 ebb tide



SEDPLUME-RW model details

Flow in a coastal region consists of large-scale tidal motion, wind-driven currents and small-scale turbulent eddies. In order to model the dispersal of suspended mud in such a region, the effects of these flows on suspended mud plumes must be simulated. The random walk dispersal model, SEDPLUME, represents turbulent diffusion as random displacements from the purely advective motion described by the turbulent mean velocities computed by the depth-averaged free surface flow model, TELEMAC-2D.

Representation of mud disturbance

In SEDPLUME, the release of suspended mud in coastal waters is represented as a regular or intermittent discharge of discrete particles. Particles are released throughout a model run to simulate continuous mud disturbance or for part of the run to simulate mud disturbance over an interval during the tidal cycle, for instance to represent the resuspension of fine sediment during dredging operations. At specified sites a number of particles are released in each model time-step and, in order to simulate the release of suspended mud, the total mud released at each site during a given time interval is divided equally between the released particles. Particles can be released either at the precise coordinates of the specified sites, or distributed randomly, centred on the specified release sites. The particles can be released at the surface or evenly distributed through the water column. This allows the representation of the initial spreading of plumes of material released by a dredger, for example, but SEDPLUME results are generally fairly insensitive to the specified initial spreading radius.

Large scale advection

TELEMAC-2D simulates depth-averaged tidal flows in coastal waters. SEDPLUME converts the depth-averaged current TELEMAC-2D output into a 3D representation of tidal currents using the well-known logarithmic velocity profile:

$$U(z) = \frac{U_*}{K} \ln \left(\frac{30.1z}{k_s} \right) \quad 1$$

where

U	=	current speed (ms^{-1})
U_*	=	friction velocity for a tidal current (ms^{-1})
K	=	von Karman's constant
z	=	distance above sea bed (m)
k_s	=	roughness length (m)

Each particle is then advected by the local flow conditions. Because the three dimensional structure of the flow is calculated by SEDPLUME, effects such as shear dispersion of plumes are automatically represented.

In the case of wind-driven currents, SEDPLUME assumes that the surface wind-driven current is parallel to the wind vector with a speed given by:

$$S = \alpha w \quad 2$$

where

S	=	surface wind-driven current speed (ms^{-1})
-----	---	--

α = an empirical constant
 w = wind speed at 10m above the sea surface (ms^{-1})

SEDPLUME uses this information to establish a parabolic velocity profile through depth due to wind which is superimposed upon the tidal current profile.

Turbulent diffusion

In order to simulate the effects of turbulent eddies on suspended mud plumes in coastal waters, particles in SEDPLUME are subjected to random displacements in addition to the ordered movements which represent advection by mean currents. The motion of simulated plumes is, therefore, a random walk, being the resultant of ordered and random movements. Provided the lengths of the turbulent displacements are correctly chosen, the random step procedure is analogous to the use of turbulent diffusivity in depth-averaged mud transport models. This is discussed in more detail below.

(a) Lateral diffusion

The horizontal random movement of each particle during a time-step of SEDPLUME consists of a displacement derived from the parameters of the simulation. The displacement of the particle in each of the orthogonal horizontal directions is calculated from a Gaussian distribution, with zero mean and a variance determined from the specified lateral diffusivity. The relationship between the standard deviation of the displacement, the time-step and the diffusivity is defined in Reference 1 as:

$$\frac{\Delta^2}{\Delta t} = 2D \quad 3$$

where

Δ = standard deviation of the turbulent lateral displacement (m)
 Δt = time-step (s)
 D = lateral diffusivity (m^2s^{-1}).

In a SEDPLUME simulation, a lateral diffusivity is specified, which the model reduces to a turbulent displacement using Equation (3). No directional bias is required for the turbulent movements, as the effects of shear diffusion are effectively included through the calculated depth structure in the mean current profile.

(b) Vertical diffusion

Whilst lateral movements associated with turbulent eddies are satisfactorily represented by the specification of a constant diffusivity, vertical turbulent motions can vary significantly horizontally and over the water depth, so that vertical diffusivities must be computed from the characteristics of the mean flow field, rather than specified as constants. In neutral conditions, the vertical diffusivity, K_z , is given by:

$$K_z = 0.16 h^2 \left(1 - \frac{h}{d} \right) \frac{\partial u}{\partial z} \quad 4$$

where

h = height of particle above the bed

d = water depth
0.16 = (von Karman constant)²
u = current speed
z = vertical coordinate

The value of the vertical diffusivity is calculated at each particle position, then a vertical turbulent displacement is derived for each particle from its K_z value using an equation analogous to (3) for the lateral turbulent displacement.

(c) Drift velocities

A particle undergoes a random walk as follows:

$$x^n = x^{n-1} + A(x^{n-1}, t^{n-1})\Delta t + B(x^{n-1}, t^{n-1})\sqrt{\Delta t} \xi^n \quad 5$$

where x^n is the position of the particle at time t^n , A is the advection velocity at timestep $n-1$ and B is a matrix giving the diffusivity. ξ is a vector of three random numbers, each drawn from a normal distribution with unit variance and zero mean. In the case of SEDPLUME, B is diagonal, with the first two entries equal to $\sqrt{(2D)}$ (as introduced in the previous section) and the third diagonal entry being equal to the local value of $\sqrt{(2K_z)}$.

The movement of a particle undergoing a random walk as described in equation (5) can be described by the Fokker-Planck equation in the limit of a very large number of particles and a very short timestep, where we introduce subscripts i, j and k running over the three coordinate directions:

$$\frac{\partial f}{\partial t} + \frac{\partial}{\partial x_i} (A_i f) = \frac{\partial^2}{\partial x_i \partial x_j} \left(\frac{1}{2} B_{ik} B_{jk} f \right) \quad 6$$

The probability density function $f(x, t | x_0, t_0)$ is the probability of a particle which starts at position x_0 at time t_0 being at position x at time t .

Equation (6) can be compared with the advection-diffusion equation for the concentration of a pollutant, c :

$$\frac{\partial c}{\partial t} + \frac{\partial}{\partial x_i} (u_i c) = \frac{\partial}{\partial x_i} \left(K_{ik} \frac{\partial c}{\partial x_k} \right) \quad 7$$

where K_{ik} is the eddy diffusion matrix, diagonal in our case but not necessarily so. Thus identifying f with c , we can see that the two equations are equivalent provided that we take the advection velocity as:

$$A_i = u_i + \frac{\partial}{\partial x_k} K_{ik} \quad 8$$

In the case of SEDPLUME, the diffusivity varies only in the vertical and is constant in the horizontal, so the horizontal advection velocity is simply the flow velocity (assuming that the relatively small effects of changing water depth can be neglected). However, when considering the movement of particles in the vertical it is important to include the gradient of the diffusivity (often referred to as a drift velocity) in the advection step. If this term is

omitted then particles tend to accumulate in regions of low diffusivity, which in our case means at the surface and at the bed.

This subject is discussed in considerably more detail in References 2, 3, 4, and 5.

Sedimentation processes

(a) Settling

In SEDPLUME, the settling velocity (w_s) of suspended mud is assumed to be related to the mud concentration (c) through an equation of the form:

$$w_s = \max(w_{\min}, Pc^Q) \quad 9$$

where w_{\min} , P and Q are empirical constants. Having computed a suspended mud concentration field, as described subsequently in this section, a settling velocity can be computed in each output grid cell from Equation (7) and used to derive a downward displacement for each particle during each time-step of a model simulation. This displacement is added vectorially to the other computed ordered and random particle displacements. Note that there is a specified minimum value of w_s . This results in settling velocities being constant at low suspended mud concentrations, as indicated by recent research at HR. (Reference 6).

(b) Deposition

SEDPLUME computes bed shear stresses from the input tidal flow fields using the rough turbulent equation, based on a bed roughness length input by the user. If the effects of storm waves on mud deposition and erosion at the sea bed are to be included in a model simulation, a bed shear stress associated with wave orbital motions, computed from the results of mathematical wave model simulations, is added to that resulting from the simulated tidal currents (Reference 7). Where the computed bed stress, τ_b , falls below a specified critical value, τ_d , and the water is sufficiently deep, then deposition is assumed to occur. Mud deposition is represented in SEDPLUME by particles approaching the sea bed becoming inactive when τ_b is below τ_d . Whilst active particles in the water column contribute to the computed suspended mud concentration field, as described subsequently in this appendix, inactive particles contribute to the mud deposit field.

In shallow areas, where tidal currents are sufficiently weak to allow mud accretion, normal wave action can prevent mud deposition. This effect is included empirically in SEDPLUME, by specifying a minimum water depth below which deposition does not occur.

(c) Erosion

The erosion of mud deposits from the sea bed is represented in SEDPLUME by inactive particles returning to the water column (becoming active) when τ_b exceeds a specified erosional shear strength, τ_e . The number of particles which become re-suspended in each cell of the output grid in each time-step of a simulation is determined by the equation:

$$\frac{\partial m_e}{\partial t} = M(\tau_b - \tau_e) \quad 10$$

where

m_e is the mass eroded (kg)
 t is time (s)
 M is an empirical erosion constant.

Computation of suspended mud concentrations

In SEDPLUME, suspended mud concentrations are computed on the TELEMAC-2D grid which can be designed to resolve the essential features of relatively small-scale plumes. In each SEDPLUME grid cell a concentration is derived by dividing the total suspended mud represented by all the active particles in that cell by the volume of the cell.

Computation of mud deposit distributions

SEDPLUME computes mud deposit distributions by summing the mass of mud represented by the inactive particles in each cell of the output grid, and assuming that the resulting mass is evenly distributed over the cell area.

The model is usually used to simulate the dispersal of mud released by dredging-related activity in one of the following three ways:

- (a) Dredging in shallow areas releases small quantities of mud into the water column close to the sea bed.
- (b) When dredging for marine fill, the coarse sediment content of dredged material may be increased by over-filling of the receiving barge; with coarse material settling rapidly in the barge and the fine mud component remaining in suspension and re-entering the water column.
- (c) The disposal of dredged spoil in deep water results in a dense column of sediment descending rapidly to the sea bed. Entrainment of water into this column results in some of the fine mud component entering the water column.

The model is most suited to simulating detailed distributions of suspended mud and mud deposits near areas of dredging-related activity over a few tidal cycles. The far-field effects of dredging-related activity can be simulated using other models in use at HR Wallingford.

References

- 1 H B Fischer, E J List, R C Y Koh, J Imberger and N H Brooks, 1979. Mixing in Inland and Coastal Waters. New York : Academic. 483 pp.
- 2 A S Monin and A M Yaglom. "Statistical Fluid Mechanics". MIT Press, Cambridge, Massachusetts, 1971.
- 3 A F B Thompson and L W Gelhar. "Numerical simulation of solute transport in three-dimensional randomly heterogeneous porous media". Water Resources Research, Vol 26 pp2541-2562, October 1990.
- 4 K N Dimou and E E Adams. "A random-walk particle tracking model for well-mixed estuaries and coastal waters". Estuarine, Coastal and Shelf Science, Vol 37, pp99-110, 1993.

- 5 B J Legg and M R Raupach. "Markov-chain simulation of particle dispersion in inhomogeneous flows: the mean drift velocity induced in a gradient in Eulerian velocity variance". Boundary Layer Meteorology Vol 24, pp3-13, 1982.
- 6 HR Wallingford. Port and Airport Development Strategy - Enhancement of the WAHMO Mathematical Models. Calibration of the North West New Territories Coastal Waters Mud Transport Model for Normal Wet and Dry Season Conditions. Report EX 2266, January 1991.
- 7 HR Wallingford. Port and Airport Development Strategy - Enhancement of the WAHMO Mathematical Models. Testing of the North West New Territories Coastal Waters Mud Transport Model for Storm Wave Conditions in the Wet Season. Report EX 2267, January 1991.